Isolation and characterization of Phanerochaete chrysosporium mutants resistant to antifungal compounds

Duy Vuong Nguyen

Ecole Doctorale SIReNa

(Sciences et Ingénierie des Ressources Naturelles)

Thèse

Présentée et soutenue publiquement pour l'obtention du titre de

DOCTEUR DE l'UNIVERSITE DE LORRAINE

Mention « Biologie et écologie des forêts et des agrosystèmes »

Par **Duy Vuong NGUYEN**

Isolation et caractérisation de mutants de *Phanerochaete chrysosporium* résistants à différents composés antifongiques

Soutenance le 3 Juin 2020

Membres du jury :

Rapporteurs :

Mme. Catherine RAFIN	MCF, Université du Littoral Côte d'Opale
M. Christian MEYER	DR, INRAE, Versailles

Examinateurs :

Mme. Harivony RAKOTOARIVONINA	MCF, Université de Reims
M. Philippe GÉRARDIN	Pr, Université de Lorraine
M. Éric GELHAYE	DR, INRAE Nancy, Directeur de thèse
M. Rodnay SORMANI	MCF, Université de Lorraine, Co-directeur de thèse

Invités :

Mme. Nadine AMUSANT	Chargée de Recherche, CIRAD

ACKNOWLEGEMENTS

First of all, I would like to thank the members of the thesis committee, Catherine Rafin, Christian Meyer, Harivony Rakotoarivonina, Nadine Amusant, and Philippe Gérardin for agreeing to read this manuscript and evaluate my thesis work.

The research was carried out at the team Stress Response and Redox Regulation (Redox team), UMR 1136 laboratory at the University of Lorraine where my work was supported by Laboratory of Interactions between Plants and Microorganisms (IAM). This support is warmly acknowledged. I would like to sincerely thank the Vietnam Ministry of Agriculture and Rural Development, Vietnam Ministry of Education and Training, France embassy at Hanoi, and Campus France for the scholarship and supports during my studies in France. I would also like to thank the Lab of Excellence ARBRE for funding to the project ANR-11-LABX-0002-01 that provides materials for my studies.

I am very grateful to my supervisors, Professor Eric Gelhaye and co-supervisor A. Professor Rodnay Sormani, for your valuable guidance and supports during my study and for me a chance and freedom to explore the physiology of filamentous fungi (regulatory and signaling proteins) due to I only studied biochemistry as a branch of physical science in previously. Thank both for reading, providing critical comments, and giving me ideas to improve my thesis manuscript, that is a very big work, and I know that it took so much time of yours. Thank Eric so much for your financial support to my travel to the ECFG14th in Israel, a very big international congress on fungal biology. I consider myself very lucky to work with you as my thesis supervisor. Sincerely, thank Eric and Rodnay for everything.

I warmly thank Professor Jean-Pierre who read carefully my thesis and give me useful comments and suggestions, and also for supporting me English improvement as other PhD students of Redox team during our working time at here. I also wish to thank Professors Nicolas Rouhier and Mélanie Rouhier, leaders of Redox team who keep weekly seminars. I have obtained not only so much knowledge on plant biochemistry and fungal physiology but also slides preparation and presentation skills from those seminars. Thank Nicolas also for reminding all people to organize workspace of the laboratory as cultural space, it is not easy to find a space as here.

Special thanks to Elena, who always motivates me through your bits of help in both work and life. I always remember images we talked on the way coming back home together in many times, they will be importantly memorable of mine.

Special thanks also to Mélanie and Flavian, who started PhD course with me. Both always have paid attention so much to my work, especially during writing the thesis manuscript, which was a very difficult period. Your supportive attitude towards my work is very important. Thanks to your sincere inspirations, I had got more motivation for working.

I would like to thank many colleagues and friends who I have had the pleasure of working during the years for the very open and friendly space in the laboratory. Those include Jérémy, Arnaud, Tiphaine, Benjamin Petre, Benjamin Selles, Jean-Michel, Julien, Muriel, Alexis, Raphael, Fanny, Elodie, Nicolas Valette, Anna, Jonathan, Thomas, Antonio, Delphine, Damien, Loïck, Marion, Kevin, Corrine, and Martine.

I also would like to warmly thank all the administrative staff of the Doctoral Register office, the School of RP2E and SIReNa, for the information necessary for my study activities and also for their aides when I have several issues.

Warm thanks are sent to all my Vietnamese friends for helping me to keep spirits and motivation, also to find a solution for the difficulties and problems I met.

Finally, I feel especially lucky to have such a wonderful family. My parents, my wife Anh Thu, and my daughter Minh Thai always inspire me to have confident thoughts. Thank you all for your love and support. I know that all of the achievements I have obtained here belongs to you.

TABLE OF CONTENTS

List of Figures

RÉSUMÉ

Isolation et caractérisation de mutants de *Phanerochaete chrysosporium* résistants à différents composés antifongiques

Contexte de mes études

Les champignons lignivores, responsables de la dégradation du bois et de la litière, suscitent un intérêt croissant ces dernières années, principalement en raison (i) de leur utilisation potentielle dans la **valorisation de la** biomasse pour la production de biocarburants, (ii) de leur fonction importante dans **le cycle global du carbone** et (iii) des dommages qu'ils peuvent causer au **matériau bois**.

Ces champignons, et en particulier les basidiomycètes, sont des organismes capables de dégrader et d'utiliser la cellulose, les hémicelluloses et la lignine comme sources de carbone et d'énergie. Cependant, **les processus oxydatifs utilisés par ces champignons pour décomposer le bois** génèrent une myriade de molécules potentiellement toxiques et augmentent la biodisponibilité de molécules de faibles masses moléculaires non liées de façon covalente aux polymères : les substances extractibles. Les extractibles sont des composants non structurels du bois qui peuvent être éliminés avec un solvant neutre à polaire. La composition de ces substances extractibles peut varier en fonction du tissu, des conditions de culture et est spécifique à l'espèce (Kebbi-Benkeder et al., 2015). **Les extractibles sont responsables des propriétés du bois** telles que sa couleur et sa durabilité, car elles font partie du système de défense de l'arbre.

Pour s'adapter à cet environnement toxique, les champignons responsables de la décomposition du bois ont développé diverses **stratégies de détoxication** (Morel et al., 2013). Les approches de génomique comparative ont permis de montrer la présence d'extensions de familles de gènes codant pour les systèmes de détoxication chez les champignons décomposeurs du bois par rapport à d'autres champignons (principalement les cytochromes P450 monooxygénases et les glutathion transférases (GST)). L'analyse du transcriptome de *Phanerochaete chrysosporium* cultivé en présence d'extractibles de chêne a révélé une induction de l'expression de certains de ces gènes impliqués dans la détoxication (Thuillier et al., 2014). Enfin, au niveau fonctionnel, des résultats intéressants concernant la caractérisation biochimique de GST et leur interaction avec les extractibles ont été obtenus (Mathieu et al., 2012; Perrot et al., 2018). Cependant, bien que très informatives, ces données ne sont pas suffisantes pour **déterminer le rôle physiologique de ces protéines dans les cellules fongiques lors de la dégradation du bois**. Une approche sans *a pr*iori est donc essentielle pour identifier les acteurs impliqués dans le processus de détoxication.

Le manque de données physiologiques concernant les voies de détoxication chez les champignons est principalement dû à l'**absence d'outils génétiques disponibles pour ces organismes**. Pour contourner ce problème, nous avons développé **une stratégie de génétique directe chez *P. chrysosporium***, champignon dégradeur de bois, choisi par la communauté comme modèle pour ces études. La première partie du projet que j'ai développé visait à prouver la faisabilité et la pertinence d'une telle approche. Deux études prouvant le concept ont été réalisées, la première utilisant un antifongique appelé itraconazole, la deuxième utilisant la rapamycine.

Description de la stratégie de génétique directe mise en œuvre:

1. Identification d'une molécule toxique.
2. Production de mutants de *P. chrysosporium.*
3. Identification parmi ces mutants de ceux capables de résister à la molécule toxique.
4. Identification des mutations chez les mutants résistants.
5. Comprendre comment la mutation permet la résistance.

Deux études: preuves de concept

Avant de nous lancer dans l'étude de la réponse des champignons aux molécules toxiques contenus dans le bois (les extractibles), nous avons choisi de tester la faisabilité de cette approche en travaillant avec des molécules dont les mécanismes d'actions sont connus au moins chez d'autres organismes.

Preuve de concept 1, l'itraconazole

L'itraconazole est un antifongique appartenant à la famille des triazoles qui inhibe la biosynthèse de l'ergostérol en agissant sur la lanostérol 14α déméthylase (CYP51A) (Bowyer and Denning, 2014). Il y a une décennie, des résistances aux triazoles ont été rapportées dans des isolats d'*Aspergillus fumigatus* prélevés chez des patients atteints d'aspergillose invasive. La propagation de la résistance a été étudiée en analysant les isolats d'*A. fumigatus* provenant de patients de 7 pays différents. Les mutations du gène *CYP51A* se sont avérées être le mécanisme de résistance dominant (Snelders et al., 2008). L'homologue de CYP51A chez *P. chrysosporium* se trouve sur le scaffold 16 entre les positions 46319 et 47911 (http://genome.jgi.doe.gov/programs/fungi/index.jsf) du génome de ce champignon. La séquence protéique correspondante présente une identité de séquence de 54,1% avec celle d'*A. fumigatus* (Warrilow et al., 2008).

Lors de notre étude, les conidies de *P. chrysosporium* ont été soumises à U.V. afin de produire des mutations de façon aléatoire dans le génome de ces cellules. Un crible de résistance génétique a été réalisé à l'aide d'une dose létale d'itraconazole. Quarante mutants ont été isolés et appelés ***rit* pour résistant à l'itraconazole**. Des lignées de descendance ont été produites pour chacun des 40 mutants identifiés. Tous ces mutants sont résistants à l'itraconazole (Fig. 1).

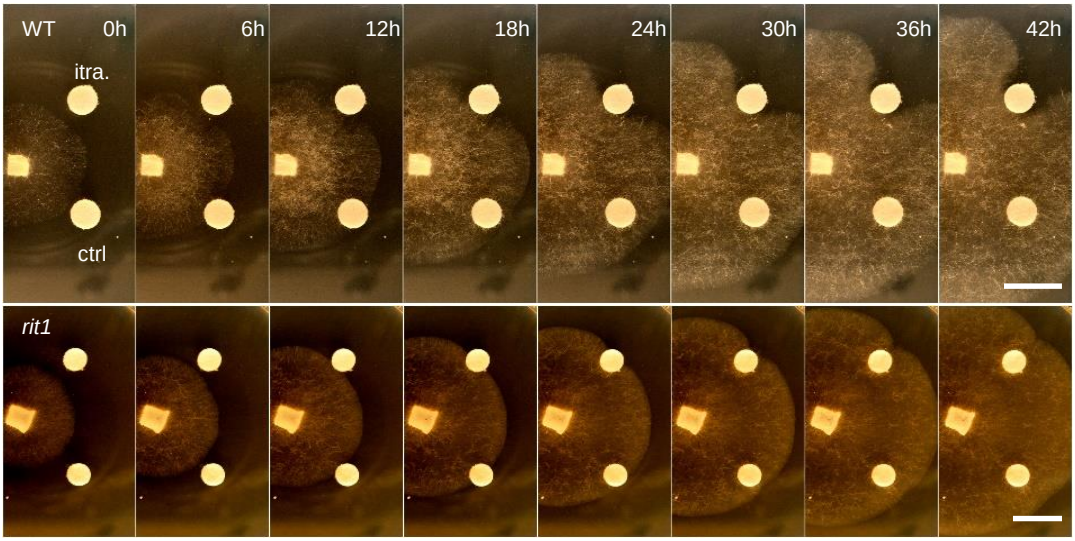

Figure 1. Effet de l'itraconazole sur la croissance de *P. chrysosporium*.

Panneau supérieur WT et panneau inférieur rit1 mutant.

8 µg d'itraconazole (itra) ou de DMSO (ctrl) ont été déposés sur le disque en papier.

Barre d'échelle : 1 cm.

Les 40 mutants *rit* obtenus lors de notre expérience portent tous des **mutations dans le gène *PcCYP51A***. Parmi ces 40 mutants, seuls deux allèles ont été trouvés et ils conduisent à la même substitution d'acide aminé : l'alanine 290 est remplacée par une valine dans la protéine. Dans 34 séquences, nous avons trouvé GTT à la place de GCT et dans les autres cas GTC à la place de GTT. Pour comprendre le phénotype de résistance observé, une modélisation structurelle du PcCYP51 a été effectuée (Fig. 2).

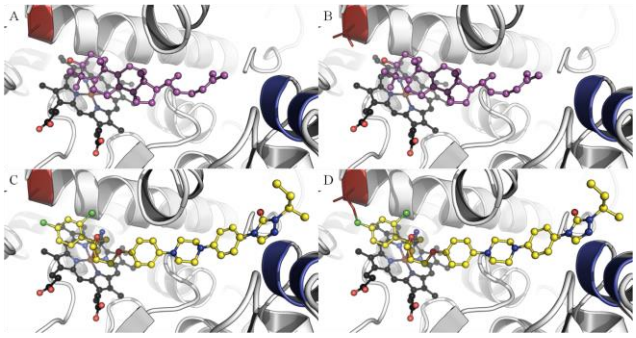

Figure 2. Prédiction des sites de liaison du lanostérol et de l'itraconazole par modélisation de la 14-α-déméthylase de *P. chrysosporium* (PcCYP51). Zoom sur les sites actifs PcCYP51 et PcCYP51 A290V en présence de lanostérol (respectivement en A et B) ou d'itraconazole (en C et D respectivement). Dans chaque cas, les molécules de l'hème, du lanostérol et de l'itraconazole sont colorées respectivement en noir, violet et jaune. La position Ala290 (Ala ou Val) est également indiquée en rouge.

La structure cristalline du CYP51 (identité de 54,1%) du champignon filamenteux pathogène *A. fumigatus* (entrée pdb 4UYL) a été utilisée comme matrice pour le modèle structural de la protéine PcCYP51A et les sites de liaison du lanostérol et de l'itraconazole ont été obtenus par modélisation à partir de la structure cristalline obtenue en rayons X de la 14-alpha déméthylase de *Saccharomyces cerevisiae* lanostérol (entrées pdb 4LXJ et 5EQB, respectivement). À partir de cette analyse, la substitution de Ala290 par des acides aminés plus importants (tels que la valine dans notre cas) ne devrait pas gêner l'activité enzymatique du lanostérol (Fig. 2A et 2B), mais entraverait probablement le positionnement de l'itraconazole en raison d'un voisinage trop proche (Fig. 2C & 2D). Ces résultats expliquent le phénotype de résistance à l'itraconazole sans aucun défaut de croissance des mutants *rit* (Fig. 1).

Nous avons donc produit et criblé des **mutants résistants à l'itraconazole** pour lesquels le gène cible a bien été décrit et nous avons confirmé que le phénotype observé était lié à des mutations dans ce gène cible (Sormani et al. à paraitre). Ces mutants sont actuellement utilisés dans le cadre du projet ANR woodwaste (Porteur Pr. Mélanie Rouhier). En effet, les bois de construction et d'ameublement sont traités à l'aide de molécule de la classe des triazoles (classe à laquelle appartient l'itraconazole) pour assurer leur imputrescibilité. Le retraitement des déchets bois traités est un problème écologique que nous tentons d'étudier en utilisant les mutants *rit* insensibles à l'itraconazole et par nature, dégradeurs de bois.

Preuve de concept 2, la rapamycine

La voie de signalisation cible de la rapamycine (**Taget Of Rapamycin, TOR**) est très conservée chez les eucaryotes et régule les processus cellulaires essentiels, notamment la synthèse des protéines, la biogenèse des ribosomes, l'autophagie et l'organisation du cytosquelette. Chez les champignons, la voie de TOR est impliquée dans la réponse à la disponibilité des ressources en

éléments nutritifs, en particulier le sucre et l'azote. TOR intervient également dans les réponses aux stress, tels que les stress osmotiques et oxydatifs. Mais cette voie restait inconnu chez les basidiomycètes et en particulier, chez *P. chrysosporium*.

Parmi les basidiomycètes, les champignons responsables de la pourriture blanche sont des modèles écologiques très intéressants en raison de leur capacité à se développer sur du bois mort et à le minéraliser. **Le bois est considéré comme une niche écologique très spécifique** : en effet, il contient des sources de carbone récalcitrantes à la dégradation, une faible teneur en azote et un environnement hautement toxique en raison de la présence de substances extractibles du bois (Valette et al. 2017). En conséquence, étudier la voie de TOR chez *P. chrysosporium* en utilisant la rapamycine et notre stratégie de génétique directe nous est apparu pertinent.

Nous avons testé l'effet de la rapamycine sur la croissance et la composition en sécrétomes de *P. chrysosporium*. En combinant l'analyse génomique à une approche de modélisation des structures tridimensionnelles des domaines protéiques impliqués, nous avons identifié dans cette étude **la voie de signalisation TOR de *P. chrysosporium*** et mis en évidence son rôle dans la régulation du sécrétome (Nguyen et al., 2020).

Suivant la même stratégie que précédemment, les conidies de *P. chrysosporium* ont été soumises aux U.V. afin de générer aléatoirement des mutations dans leur génome. Un crible de résistance génétique a été réalisé à l'aide d'une dose létale de rapamycine. Dix mutants ont été isolés et appelés ***rap* pour résistant à la rapamycine**. Les descendances ont été obtenues pour chacun des mutants identifiés. Toutes ces lignées mutantes sont résistantes à la rapamycine comparés au sauvage (Fig. 3).

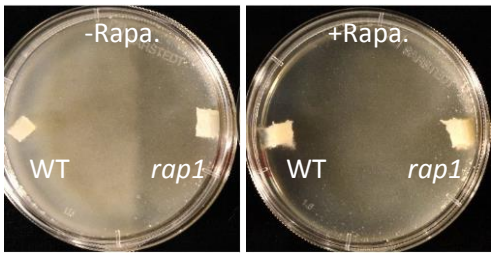

Figure 3. Effet de la rapamycine sur la croissance de *P. chrysosporium* sauvage et mutant *rap1*. A droite, en l'absence de rapamycine, les deux champignons se développent. A gauche en présence de rapamycine, seul rap1 se développe.

La collection de mutants *rap* est composée de 10 mutants capables de croître et de produire des conidies sur des milieux contenant de la rapamycine. Dans cette collection, des mutations ont été identifiées dans 3 gènes TOR1, TOR2 et FKBP12. Chez d'autres espèces, le complexe TOR-rapamcyine-FKBP12 a déjà été caractérisé. La rapamycine est prise en étau entre le domaine FRB de TOR (domaine de liaison FK506-Rapamycine) et FKBP12 (Fig. 4). À partir de la modélisation, il est facile de comprendre comment les mutations trouvées dans les mutants *rap* peuvent affecter

l'interaction avec la rapamycine et conduire au phénotype de résistance (Nguyen et al., manuscrit en préparation).

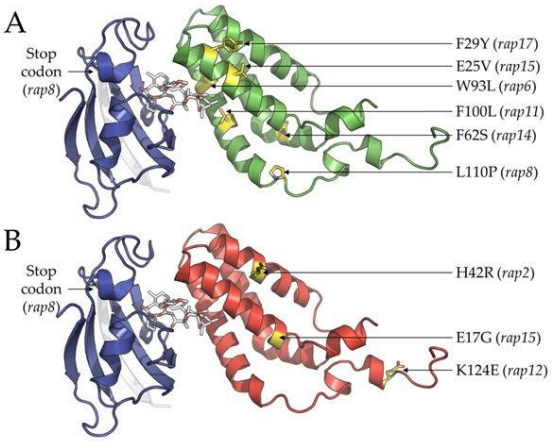

Figure 4. Mutations identifiées dans les complexes FKBP12-rapamycine-FRB de *P. chrysosporium*. Modèles 3D du domaine prédit FKBP12-rapamycine-FRB1 de *P. chrysosporium* de TOR1 (A) et du domaine FKBP12-rapamycine-FRB2 de TOR2 (B). FKBP12, FRB1, FRB2 et la rapamycine sont colorés en bleu, vert, rouge et blanc, respectivement. Les structures secondaires sont représentées sous forme de ruban et la rapamycine sous forme de bâtons. Les mutations ponctuelles survenant sur FRB1 et FRB2 en fonction de la souche fongique sont mises en évidence par des bâtons jaunes. Le codon d'arrêt trouvé dans FKBP12 (*rap8*) est également pointé.

Production de mutants résistants aux extractibles (rex) de bois

La première étape à consisté en l'identification de composés toxiques issus de bois. Pour rappel, le bois contient un certain nombre de composés toxiques dénommés extractibles permettant, entre autre, sa durabilité. Une première série d'extractibles a été fournie grâce à une collaboration avec le LERMAB (EA 4370). Cette collection d'extractibles a été obtenue à partir des bois provenant d'arbres présents dans les forêts de l'est de la France (Kebbi-Benkeder et al., 2015). Sur 95 extraits différents fournis, les extraits acétoniques de cerisier ont été les plus efficaces pour retarder la croissance de *P. chrysosporium* (Fig. 5).

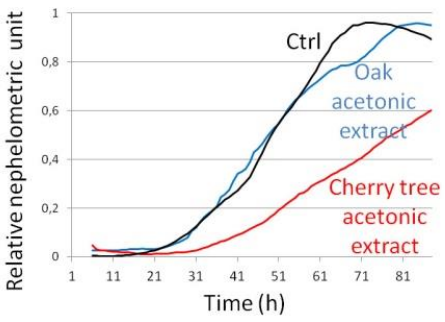

Figure 5. Cinétique de croissance de *P. chrysosporium* déterminée par néphélométrie dans des conditions standard ou en présence de substances extractibles du bois de chêne, de substances extractives du bois de cerisier à une concentration finale de 1 µg / ml (n = 3).

Ensuite, une collection d'extractibles provenant de la forêt tropicale de Guyane française a été produite (en collaboration avec l'UMR EcoFoG). L'effet de ces extractibles sur la croissance des champignons et leur capacité à interagir avec des protéines impliquées dans la détoxication chez les champignons de pourriture du bois ont été testés (Perrot et al., 2018). Ces études nous ont conduit à choisir les extraits de deux essences de bois : la bagasse et le saint martin rouge pour leur toxicité vis-à-vis du champignon modèle pour nos études, *P. chrysosporium*.

La seconde étape a consisté en la production de collection de mutants résistants aux extractibles *(rex)* de bois. Suivant la même stratégie que décrite dans les études préliminaires, les conidies de *P. chrysosporium* ont été soumises aux U.V. afin de générer aléatoirement des mutations dans leur génome. Un crible de résistance génétique a été réalisé à l'aide d'une dose létale des différents extractibles. Trois collections d'une quarantaine de mutants ont été isolées et les mutants sont appelés ***chy* pour résistant aux extrait de bois de cerisier (cherry tree), *bag* pour résistant aux extrait de bois de bagasse, et *sam* pour résistant aux extrait de bois de saint Martin rouge.**

Perspectives

À partir de nos études précédentes, nous avons généré plus d'une centaine de lignées mutantes résistantes aux composés toxiques de trois différentes essences de bois. Le séquençage du génome a été effectué pour les collections de mutants *chy*, *bag* et *sam*, et un séquençage de génome individuel a été effectué pour 2 mutants de *bag* et un mutant *chy*. La suite de ce travail sera de réaliser la caractérisation de ces mutants et d'identifier la mutation causale responsable des phénotypes de résistances observés. Ceci devrait nous permettre :

i/ d'identifier les cibles des molécules antifongiques contenues dans les extractibles de bois .

ii/ de mieux comprendre les mécanismes de détoxication mis en œuvre par les champignons dégradeurs de bois.

Références

Bowyer, P., Denning, D.W., 2014. Environmental fungicides and triazole resistance in Aspergillus. Pest Management Science 70, 173–178. https://doi.org/10.1002/ps.3567

Kebbi-Benkeder, Z., Colin, F., Dumarçay, S., Gérardin, P., 2015. Quantification and characterization of knotwood extractives of 12 European softwood and hardwood species. Annals of Forest Science 72, 277–284. https://doi.org/10.1007/s13595-014-0428-7

Mathieu, Y., Prosper, P., Buée, M., Dumarçay, S., Favier, F., Gelhaye, E., Gérardin, P., Harvengt, L., Jacquot, J.-P., Lamant, T., Meux, E., Mathiot, S., Didierjean, C., Morel, M., 2012. Characterization of a *Phanerochaete chrysosporium* Glutathione Transferase Reveals a Novel Structural and

Functional Class with Ligandin Properties. J. Biol. Chem. 287, 39001–39011. https://doi.org/10.1074/jbc.M112.402776

Morel, M., Meux, E., Mathieu, Y., Thuillier, A., Chibani, K., Harvengt, L., Jacquot, J.-P., Gelhaye, E., 2013. Xenomic networks variability and adaptation traits in wood decaying fungi. Microbial Biotechnology 6, 248–263. https://doi.org/10.1111/1751-7915.12015

Nguyen, D.V., Roret, T., Fernandez-Gonzalez, A., Kohler, A., Morel-Rouhier, M., Gelhaye, E., Sormani, R., 2020. Target Of Rapamycin pathway in the white-rot fungus *Phanerochaete chrysosporium*. PLOS ONE 15, e0224776. https://doi.org/10.1371/journal.pone.0224776

Nguyen Duy V, Fernandez-Gonzalez A, Roret T, Morel-Rouhier M, Gelhaye E, Sormani R. Generation and characterization of mutants resistant to rapamycin in Target Of Rapamycin pathway in the white_rot fungus *Phanerochaete chrysosporium*. En préparation.

Perrot, T., Schwartz, M., Saiag, F., Salzet, G., Dumarçay, S., Favier, F., Gérardin, P., Girardet, J.-M., Sormani, R., Morel-Rouhier, M., Amusant, N., Didierjean, C., Gelhaye, E., 2018. Fungal Glutathione Transferases as Tools to Explore the Chemical Diversity of Amazonian Wood Extractives. ACS Sustainable Chemistry & Engineering. https://doi.org/10.1021/acssuschemeng.8b02636

Snelders, E., Lee, H.A.L. van der, Kuijpers, J., Rijs, A.J.M.M., Varga, J., Samson, R.A., Mellado, E., Donders, A.R.T., Melchers, W.J.G., Verweij, P.E., 2008. Emergence of Azole Resistance in *Aspergillus fumigatus* and Spread of a Single Resistance Mechanism. PLOS Medicine 5, e219. https://doi.org/10.1371/journal.pmed.0050219

Thuillier, A., Chibani, K., Belli, G., Herrero, E., Dumarçay, S., Gérardin, P., Kohler, A., Deroy, A., Dhalleine, T., Bchini, R., Jacquot, J.-P., Gelhaye, E., Morel-Rouhier, M., 2014. Transcriptomic Responses of *Phanerochaete chrysosporium* to Oak Acetonic Extracts: Focus on a New Glutathione Transferase. Appl. Environ. Microbiol. 80, 6316–6327. https://doi.org/10.1128/AEM.02103-14

Warrilow, A., Ugochukwu, C., Lamb, D., Kelly, D., Kelly, S., 2008. Expression and Characterization of CYP51, the Ancient Sterol 14-demethylase Activity for Cytochromes P450 (CYP), in the White-Rot Fungus *Phanerochaete chrysosporium*. Lipids 43, 1143. https://doi.org/10.1007/s11745-008-3239-5

INTRODUCTION

I. Fungal adaptation to environment

As other organisms, fungi are always confronted with many chemicals in their natural habitats. These chemicals include nutritional and signaling molecules, which could influence fungal growth and development. Detection of these signals and appropriate coordinated responses are then essential for the survival of fungi. **This process can be separated into three main steps: signal perception, signal transduction, and response** (Bahn et al., 2007; van der Does and Rep, 2017; Martín et al., 2019)**.** Molecular mechanisms involved in those three steps are often designated as response signaling pathways. Advances in molecular techniques have led to a better understanding of the involved cellular mechanisms. As multicellular eukaryotic organisms characterized by a rapid growth, fungi are ideal models for studies of environmental sensing and cellular responses. In the first part of this manuscript, molecular mechanisms allowing fungi to sense and respond to environmental cues including nutrients and stress, are discussed.

I.1 Fungi have to adapt to their environment

Fungi are known to be the largest group of eukaryotic organisms on the planet, with an estimate of 3.5 to 5.1 million species, most of them being unknown (O'Brien et al., 2005). **The most basic feature of fungal growth and development is the production of spores**, which can be distributed in the air or mobilized to all parts of the planet by water (Bayram and Braus, 2012). Therefore, the ability to adapt to new ecological niches is the most important dynamic for their evolution.

Yeasts are fungi that exist mainly as unicellular organisms. They account for approximately 1% of the described fungal species. They have been evolved into several taxonomic groups (Kurtzman and Piškur, 2015), as shown in Fig. 1A. The fundamental feature of the yeast's developmental program is the transition from the round single-cell yeast form to the filamentous growth mode. The switch between these two modes is known as fungal dimorphism and depends on environmental conditions. The dimorphism can generate pseudohyphae and true hyphae (Fig. 1A). Pseudohyphae are the form with interconnected cellular units produced from adhesion of elongated cells. They are typical forms of diploid budding yeasts.

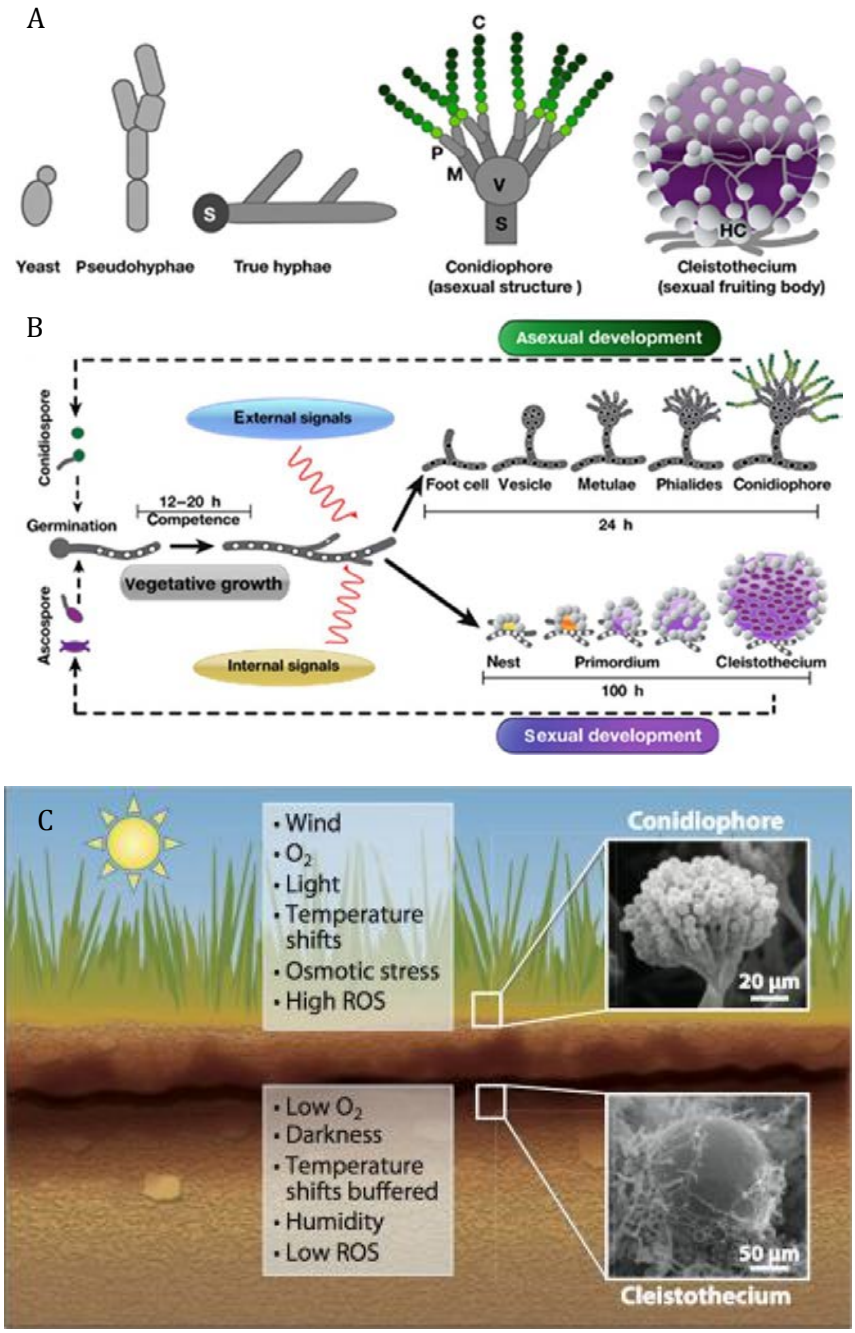

Figure 1. Fungi have to adapt to their environment.

A-C. Cellular forms and life cycle of the filamentous model fungus *Aspergillus nidulans*. A. Yeast form: unicellular fungal growth mode; pseudohyphae: filamentous growth form with individual cells; true hyphae: filaments, often separated by permeable septae; conidiophore: composed asexual structure; cleistothecium: spherical closed sexual fruiting body (common in *Aspergillus* species). S, stalk; V, vesicle; M, metulae; P, phialides; C, conidia; HC, Hülle cells. **B**. Life cycle from vegetative growth to asexual or sexual alternatives of development (Bayram and Braus, 2012). **C.** Environmental factors in soil and at the surface. A conidiophore and a cleistothecium of *A. nidulans* are produced on the surface and in the substrate, respectively. ROS represents for reactive oxygen species (Rodríguez-Romero et al., 2010).

The specific fungal growth mode is the formation of multicellular hyphae, as described in Fig. 1A. **Hyphae have a tube-like structures that are formed from the germination of a fungal spore**. They are the basic growth units of most filamentous fungi and expand at the apex of the tip cell. Polar tip growth is due to plasma membrane expansion combined with the biosynthesis of cell wall components (Steinberg, 2007).

Filamentous fungi comprise fungi without dimorphic forms. The fundamental feature of their developmental program is the formation of vegetative hyphae before moving on to other development programs. Vegetative growth starts from spore germination with the production of a fungal hypha. The differentiation capability of the latter is determined by its susceptibility to environmental signals, as shown in Fig. 1B. The range of time from spore germination to the fungal hypha, depends on the considered fungal species and is called the competent time, which is linked to the growth rate. For example, the competent time of *Aspergillus nidulans* is from 12 to 20 hours (Fig. 1B).

For filamentous fungi, developmental programs include the transition to asexual spore formation and to sexual fruiting bodies, as described in Fig. 1B. **The transition from asexual to sexual development programs depends on environmental interactions and signals sensing,** including nutrients, fungal pheromones, stressors, surface, oxygen, or light (Bayram and Braus, 2012). These interactions also modify the production of secondary metabolites that could play a role in fungal protection against competitive interactions in their ecosystems (Rohlfs et al., 2007).

To adapt to their environment, fungi have to sense their chemical environment and react appropriately. Saprophytic fungi use organic matters as nutritional resources. *A. nidulans*, a soil-living organism, has for instance to adapt to the low oxygen concentration in underground conditions. Such anoxic environment can induce the generation of cleistothecia resulting from the sexual reproductive system (Fig. 1C). At the soil surface or above the ground, environmental conditions change rapidly and drastically. For instance, *A. nidulans* can be confronted to a large range of temperature, humidity, and light in a short period of daytime (night-day cycle for instance). In these conditions, the fungal mycelium may desiccate quickly leading to osmotic stress. Besides, light exposure through ultraviolet irradiation could induce damages to fungal DNA or production of harmful reactive oxygen species (ROS) (Fig. 1C). Light affects the fungal metabolism and possibly induce the production of secondary metabolites either potentially toxic for human or animals or industrially valuable (Rodríguez-Romero et al., 2010).

In the case of pathogenic fungi, these latter have to sense the specific physicochemical environment of their host. They have to deal in particular with oxidative stress, chemokines,

immune mediators, serum factors, hormones, and host-microbiota. The oxidative environment could be due to reactive oxygen species production by the host in response to infection (Braunsdorf et al., 2016).

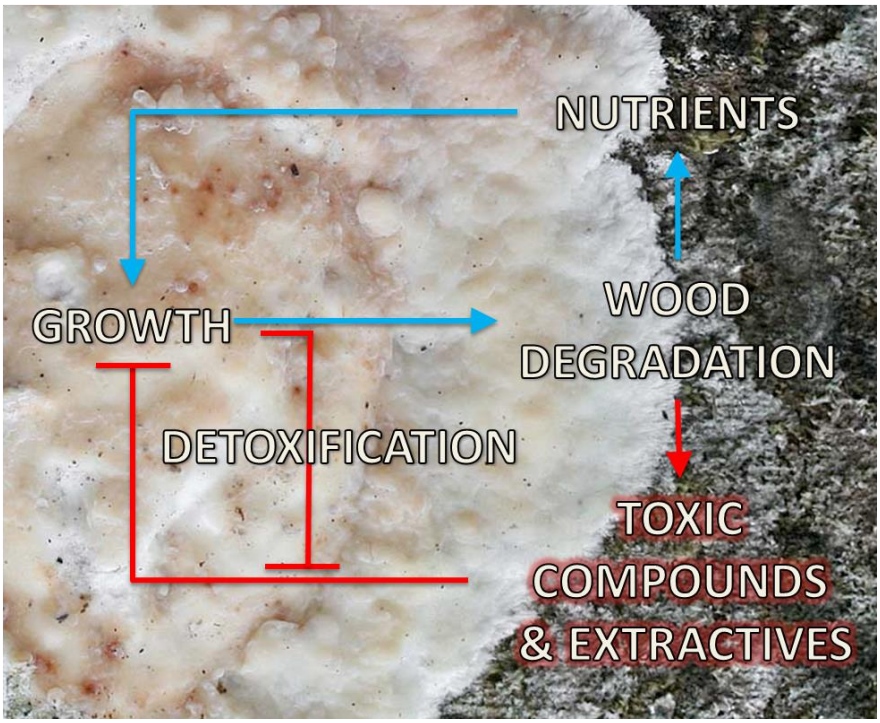

Figure 2. Wood decaying fungi have to adapt to a specific environment.

Picture of *Phanerochaete carnosa* growing on wood bark (copyright creative commons CC3). Fungal growth leads to wood degradation, and wood degradation releases nutrients which sustain fungal growth. Wood degradation also releases toxic compounds such as lignin degradation products and plant cell secondary metabolites found in wood known as extractives. Those compounds inhibit fungal growth and fungi have to detoxify those compounds to develop on wood.

In a similar way, **wood decaying fungi are also adapted to wood or lignocellulosic materials**. Those materials are specific: rich in carbon and poor in nitrogen. In addition, fungi have to sense and detoxify factors that could be harmful or toxic for fungi including metabolites from lignin transformations, reactive oxygen species (ROS), and wood extractives (Fig. 2). ROS can be produced during the fungal degradation process. Therefore, sensing of the environment will be discussed in this thesis with a focus on carbon, nitrogen, and stress sensing.

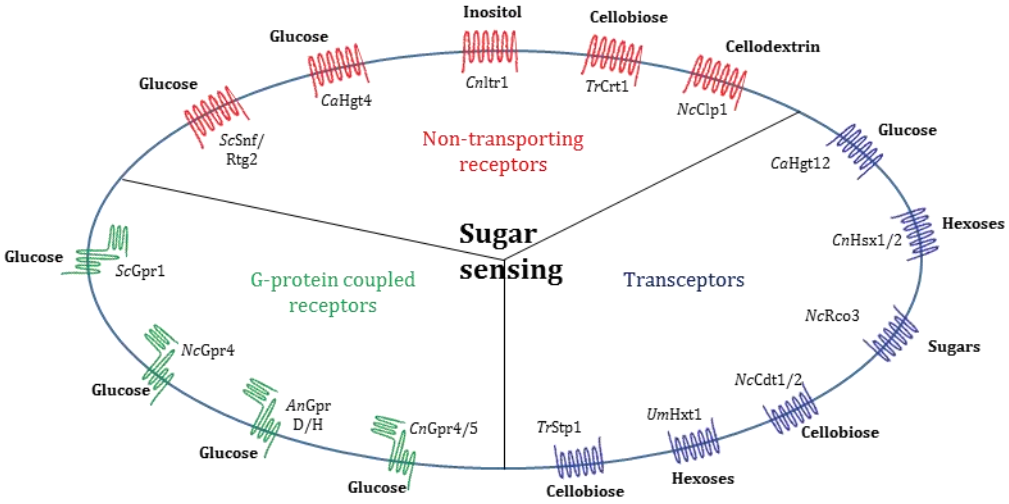

Figure 3. Sugar-sensing membrane proteins of fungal cells.

Sugar GPCRs include the *Saccharomyces cerevisiae* (Sc) glucose sensors Gpr1, the *Neurospora crassa* (Nc) glucose sensor Gpr4, the *Aspergillus nidulans* (An) glucose sensors GprD/H, and the *Cryptococcus neoformans* (Cn) glucose sensors Gpr4/5. Nontransporting sugar receptors include the Sc glucose sensors Snf3/Rgt2, the *Candida albicans* (Ca) glucose sensor Hgt4, the *Cryptococcus neoformans* (Cn) inositol sensor Itr1, the *Trichoderma reesei* (Tr) cellobiose sensor Crt1, and the Cn cellodextrin sensor Clp1. Sugar transceptors include the Ca glucose sensor Hgt12, the Cn hexose sensors Hxs1/2, the Nc sugar sensor Rco3, the Nc cellobiose sensors Cdt1/2, the *Ustilago maydis* (Um) hexose sensor Hxt1, and the Tc cellobiose sensor Stp1. From Dijck et al, with modifications (Dijck et al., 2017).

I.2 Fungal sensing of the environment

The knowledge of nutrient sensing and responses in fungi is mostly due to studies using the model yeast *Saccharomyces cerevisiae*. The identified regulatory components are often conserved in filamentous fungi, however, their functions and regulation are poorly known (Martín et al., 2019). Nutrient sensing and response of filamentous fungi, especially lignocellulose-decomposing fungi will be then discussed in comparison with *S. cerevisiae* in the following chapters.

Nutrient sensing is usually mediated by membrane proteins that activate downstream signaling pathways (Dijck et al., 2017). They are clustered into three classes: non-transporting receptors, transceptors, and G–protein-coupled receptors. Non-transporting receptors are proteins that have a similar structure to that of transport proteins but without transport capacity. They could function as receptors. Transceptors function as both transporters and receptors. All types of receptors are involved in the regulation of transporters involved in nutrient uptake (Dijck et al., 2017). Among those, G–protein-coupled receptors (GPCRs) are the best-studied receptors. They sense extracellular signals and transmit them to intracellular G-proteins allowing the activation of signaling pathways for the coordination of appropriate responses (Dijck et al.,

2017). G-proteins are cytosolic proteins that could be associated with cell membrane receptors as well as receptors found in intracellular membranes such as the endoplasmic reticulum, Golgi apparatus, vesicle membranes, and late endosomes. These proteins possess GTPase activity and require GTP in their active state (Martín et al., 2019; Ramanujam et al., 2013).

I.2.1 Nutrient sensing

Carbon sensing

Carbon nutrients include simple sugars and cleaved polysaccharides from the external biomass that can be imported through the cellular membrane to provide energy and matters for fungal biosynthesis and catabolism. They also have regulatory roles in fungi. Glucose is considered the most abundant nutrient for both yeast and filamentous fungi (Bahn et al., 2007; Brown et al., 2014). Besides, other sugars derived from hemicelluloses such as xylose, also play an important role in the growth of filamentous fungi. Lignocellulose mineralization requires the ability to utilize many carbon nutrients, leading to complex and flexible detection mechanisms. However, these sensing mechanisms in filamentous fungi remain largely to be unraveled.

Non-transporting receptors:

In yeast *S. cerevisiae*, glucose uptake is done by hexose transporters (*HXT* family) whose expression depends on the availability of extracellular glucose. Glucose uptake is also controlled by sensing the internal/external ratio of glucose via the regulation of the receptors ScSnf3 and ScRgt2 (Fig. 3). ScSnf3 and ScRgt2 are members of *HXT* family without transport activity. They regulate the expression of other *HXT* genes through the Hxt suppressor ScRgt1 (Polish et al., 2005).

Due to the diversity of sugars and saccharides derived from the biomass during the degradation process, **in lignocellulolytic filamentous fungi, the sensing mechanisms are distinct from those of yeast *S. cerevisiae***. For example, in the early stage of biomass degradation, the release of saccharidic inducers such as cellobiose induces the secretion of CAZymes by the fungus *Trichoderma reesei* (Brown et al., 2014). Additionally, few non-transporting receptors have been reported in filamentous fungi, and none of them is homologous to ScSnf3 and ScRgt2 found in *S. cerevisiae*. Crt1 in *A. nidulans* and in *Neurospora crassa* (Zhang et al., 2013) and the cellodextrin transporter-like protein NcClp1 in *N. crassa* (Cai et al., 2015) have been functionally identified as non-transporting receptors. These receptors have no role in the transport of cellulose, cellobiose, and cellodextrin. They function as inducers or repressors of the cellulolytic expression machinery (Cai et al., 2015; Zhang et al., 2013).

Transceptors:

In *S. cerevisiae*, hexose transporters functioning as plasma membrane transceptors implicated in activating the downstream signaling pathways are not present. In contrast, they were identified in *Candida albicans* and *Cryptococcus neoformans* but poorly characterized (Dijck et al., 2017).

In filamentous fungi, transceptors have been identified and functionally characterized in several lignocellulolytic fungi such as *N. crassa*, *T. reesei*, and also in phytopathogenic fungi *Ustilago maydis* (Fig. 3). In these fungi, they could play roles in the detection and uptake of polysaccharides, and then affect the interactions of those fungi with their environment (Dijck et al., 2017). For example, in *N. crassa*, NcCdt1/2 are cellodextrins (cellulose breakdown products) transporters, and they were proposed to sense cellulose leading to the induction of cellulases in response to crystalline cellulose (Znameroski et al., 2014). In *T. reesei*, TrStp1 was identified as a cellobiose transporter. It is essential in sensing and transmitting the cellulose signal (Zhang et al., 2013).

G–protein-coupled receptors (GPCRs)

GPCRs activate the signaling pathways for responses through heterotrimeric G-proteins. Heterotrimeric G-proteins comprises three units: α, β, and γ, that are associated with the plasma membrane. In the heterotrimeric state, a GDP molecule binds to the Gα-subunit and G-proteins are inactive. They become active when Gα-subunit dissociated from Gβ-Gγ dimer by guanine nucleotide exchange as a result of binding between extracellular ligands and GPCRs. These Gα-subunit and a Gβ-Gγ dimer interact with downstream proteins to transmit the stimulus signal (Li et al., 2007b; Martín et al., 2019).

GPCRs are classified into five main categories including pheromone, carbon, nitrogen, cAMP, and microbial opsin receptors (Li et al., 2007b). Despite the high conservation of the GPCR-signaling mechanism in eukaryotes, there are significant differences between yeast and filamentous fungi (Dijck et al., 2017).

In yeast *S. cerevisiae*, extracellular glucose is sensed by GPCR named ScGpr1, leading to the activation of the Gα-protein ScGpa2 which, in turn, activates the adenylate cyclase ScCyr1 (Fig. 4). Besides, ScCyr1 activation is also mediated through ScRas1/2 proteins which are stimulated by intracellular glucose (Fig. 4). This activation results in a cAMP increase, which directly causes PKA activation by docking to the binding pockets of the PKA regulatory subunits releasing the catalytic domain (Yun et al., 1998). These active subunits migrate to the nucleus where they phosphorylate a wide spectrum of target proteins associated with rapid cell growth. PKA is the protein kinase A

mediating a large range of cAMP-depending processes in fungi including nutrient sensing and stress response (Casado et al., 2011; Thevelein et al., 2005). Nutrient control of PKA pathway in *S. cerevisiae* has been considered to be an outstanding model for studying nutrient sensing mechanisms.

Filamentous fungi are able to utilize diverse sugars derived from the biomass including hexoses, pentoses, and complex saccharides. This ability may be reached through the presence of additional Gα-proteins. Indeed, most characterized filamentous fungi contain three Gα-proteins, whereas yeasts only possess two (Li et al., 2007b).

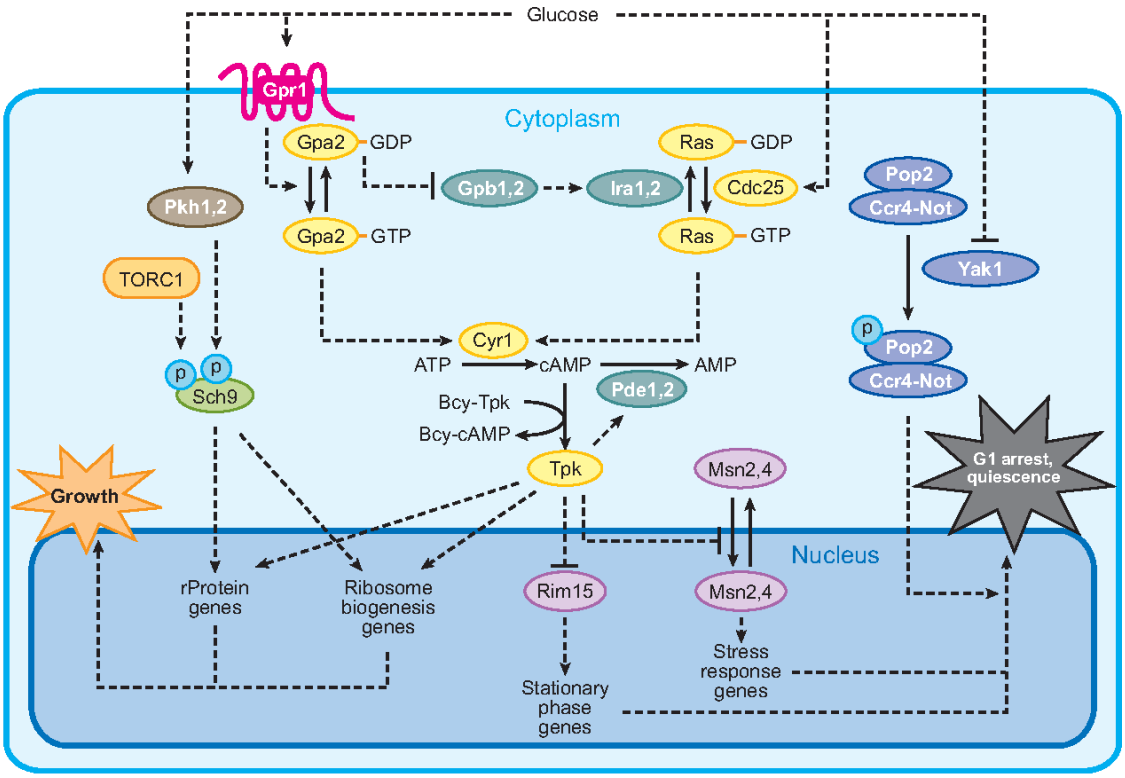

Figure 4. Glucose sensing pathways through G-protein in *S. cerevisiae*.

Induction of ribosome biogenesis via protein kinase A (PKA), which regulates glucose signaling mediated by G-protein Gpa2. Dashed lines represent regulatory interactions, which may not be direct and in some cases are only surmised (Zaman et al., 2008).

In filamentous fungi, glucose sensed by GPCRs also activates protein effectors involved in fungal growth and development via stimulation of the cAMP/PKA signaling pathway. For example, in *N. crassa*, NcGpr4 (Fig .3) interacts with NcGna1 as an orthologue of Gpa2 in *S. cerevisiae* (Fig. 4) to trigger cAMP production and asexual development in response to the carbon nutrient composition (Li and Borkovich, 2006). The deletion of NcGpr4 causes a reduction in growth on glycerol, mannitol, and arabinose (Li and Borkovich, 2006). Similarly, in *A. nidulans*, the putative protein AnGprD, affects hyphal growth, sexual development, metabolic pathways, and stress responses (Souza et al., 2013). When growing on a 1% glucose containing medium, a deletion mutant for GprD exhibits a critical reduction in PKA activity (Souza et al., 2013). Recently, AnGprH, a GPCR highly expressed in *A. nidulans* under carbon starvation, has been shown to function as an upstream sensor of the cAMP-PKA pathway affecting primary metabolism and hyphal growth and repressing sexual development (Brown et al., 2015). In summary, the cAMP/PKA signaling pathway is a major pathway responding to glucose which controls the growth of filamentous fungi.

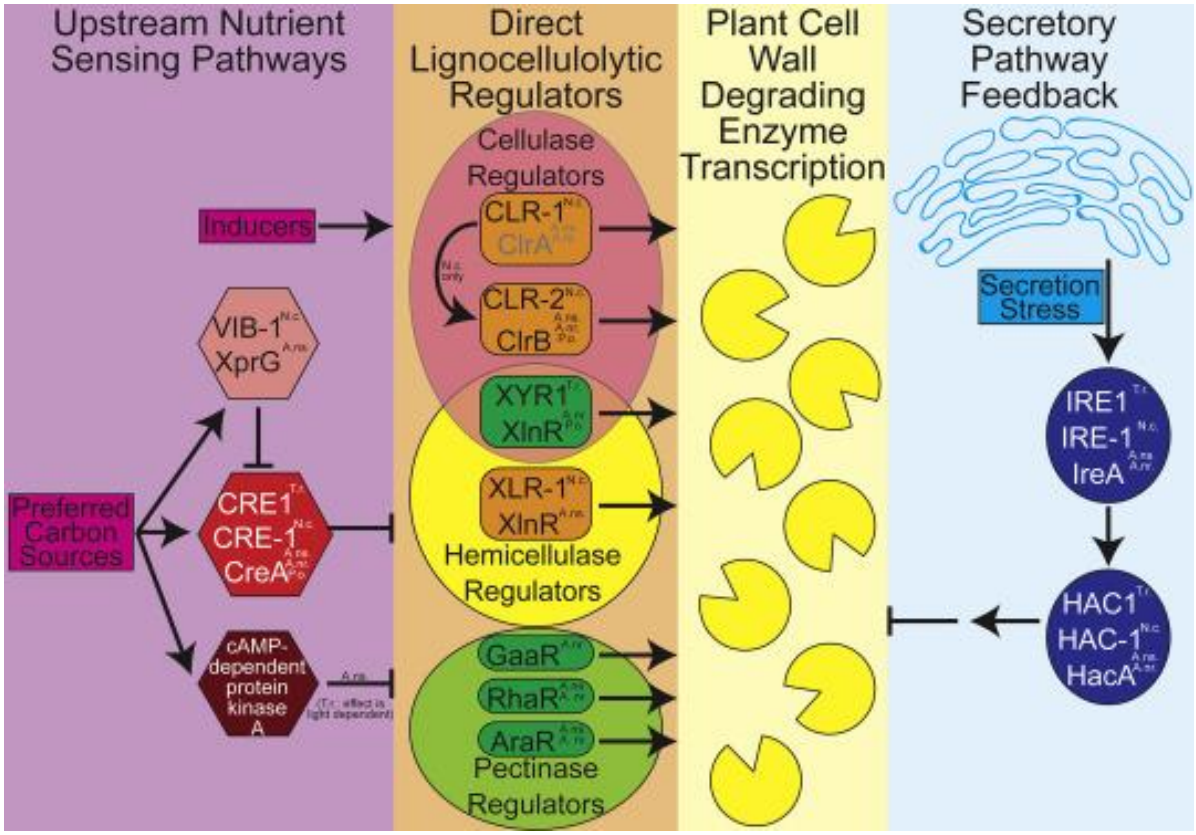

Figure 5. Regulation of lignocellulolytic CAZymes in filamentous fungi.

Upstream nutrient sensing pathways: The transcription factor Cre1/CreA, regulated by VIB-1/XprG, controls the utilization of preferred carbon sources. Under activation, it represses transcription of both direct lignocellulolytic regulators and plant cell wall degrading enzymes. Besides, the cAMP-dependent protein kinase A (PKA) have a role in nutrient sensing in the manner depending on species. Inducers derived from the carbohydrates of biomass cell walls activate lignocellulolytic regulators. **Direct lignocellulolytic regulators**: XYR1/XLnR activates transcription of both cellulases and hemicelluloses in *T. reesei*, *A. niger*, and *P.oxalicum*, but only hemicellulases in *N. crassa* and *A. nidulans*. In *N. crassa*, CLR-1 activates transcription of genes required for cellulose utilization and CLR-2 known as the main transcriptional activator of cellulase transcription. The CLR-1 homolog, ClrA has been found to have a small role in the regulation of cellulase transcription in *A. nidulans* and *A. niger*, but not control ClrB, the CLR-2 homolog which is involved in cellulase transcription in *A. nidulans*, *A. niger*, and *P. oxalicum*. **Secretory pathway feedback**: Under secretion stress, IRE1/IRE-1/IreA activates HAC1/HAC-1/HacA via direct cleavage a non-canonical intron from the transcription factor. In turn, HAC1/HAC-1/HacA activates the unfolded protein response, which may downregulate the transcription of plant cell wall degrading enzymes. (A.nr. = *A. niger*, A.ns. = *A. nidulans*, N.C. = *N. crassa*, P.o. = *Penicillium oxalicum*, T.r. = *T. reesei*). From Huberman et al. (Huberman et al., 2016).

Carbon nutrient sensing and responses in lignocellulose degradation

The lignocellulose degrading process is mainly mediated by extracellular enzymes involved in the cleavage of polysaccharides. Nutrient sensing pathways, especially pathways enabling the use of preferred carbon sources are very important for the survival strategy used of the fungi. In filamentous fungi, those pathways function as the upstream of the direct activation of genes encoding CAZymes (Fig. 5). This activation results in the inhibition of the energy-consuming production of lignocellulose degrading enzymes (Huberman et al., 2016). Up to date, the best-studied pathway is carbon catabolite repression (CCR).

The utilization of a diverse array of carbon sources derived from lignocellulose degradation requires the coordination of the cellular metabolism and the preferential consumption of glucose prior to other carbon sources, a phenomenon known as carbon catabolite repression (CCR). CCR mechanism represses transcription of secreted and intracellular metabolic enzymes and has been described in both yeasts and filamentous fungi (Brown et al., 2014). The transcription of these genes is tightly regulated by a Cys2-His2 type DNA-binding zinc finger factor, named Mig1 in *S. cerevisiae*, and CreA/Cre1 in filamentous fungi (Fig. 5, 6).

In *S. cerevisiae*, the repressor protein ScMig1 is imported into the nucleus when glucose is added to derepressed cells (Fig. 6A). In the nucleus, ScMig1 binds to upstream regulatory elements (URE) of genes coding for transcription factors. This leads to inhibit the expression of those transcription factors which transcriptionally regulate alternative carbon usage. In addition to ScMig1, CCR is also regulated by nuclear chromatin structure which can be linked to intrinsic cellular program and environmental factors (Brosch et al., 2008). In yeast, ScMig1 reacts with the corepressors ScTup1 and ScSsn6 (Fig. 6A). The obtained complex binds to promoters of alternative carbon usage genes leading to their repression through the modulation of nucleosome positioning (Li et al., 2007a; Treitel and Carlson, 1995).

In filamentous fungi, the carbon nutrient-dependent nuclear localization of CreA/Cre1 (Fig. 6B) is similar to ScMig1 in *S. cerevisiae*. However, this repressor is not only regulated by glucose but also by other sugars resulting from carbon nutrient sources (Brown et al., 2013; Sun and Glass, 2011). The role of CreA nuclear localization in regulation of CCR has been confirmed in *A. nidulans*, and *N. crassa* by use of GFP fusions (Brown et al., 2013; Sun and Glass, 2011).

Orthologues of the *S. cerevisiae* corepressors ScTup1 and ScSsn6 have also been widely identified in filamentous fungi (García et al., 2008). In *A. nidulans*, the homolog of ScTup1 is AnRcoA (Fig. 6B). This corepressor is dispensable for CCR and affects the repressed chromatin structures in the alcR promoter during repression (García et al., 2008). alcR is a *trans*-acting gene containing a

specific site allowing the binding of the repressor CreA (Kulmburg et al., 1993). In comparison with *S. cerevisiae*, the regulatory role of the CreA/Cre1 complex to CCR is less well-known in detail in filamentous fungi. The role of CreA in nucleosome positioning has been only shown in *T. reesei*. In particular, TrCreA is essential for correct nucleosome positioning in the cellulase promoter *cbh2* under repressing and inducing conditions (Zeilinger et al., 2003).

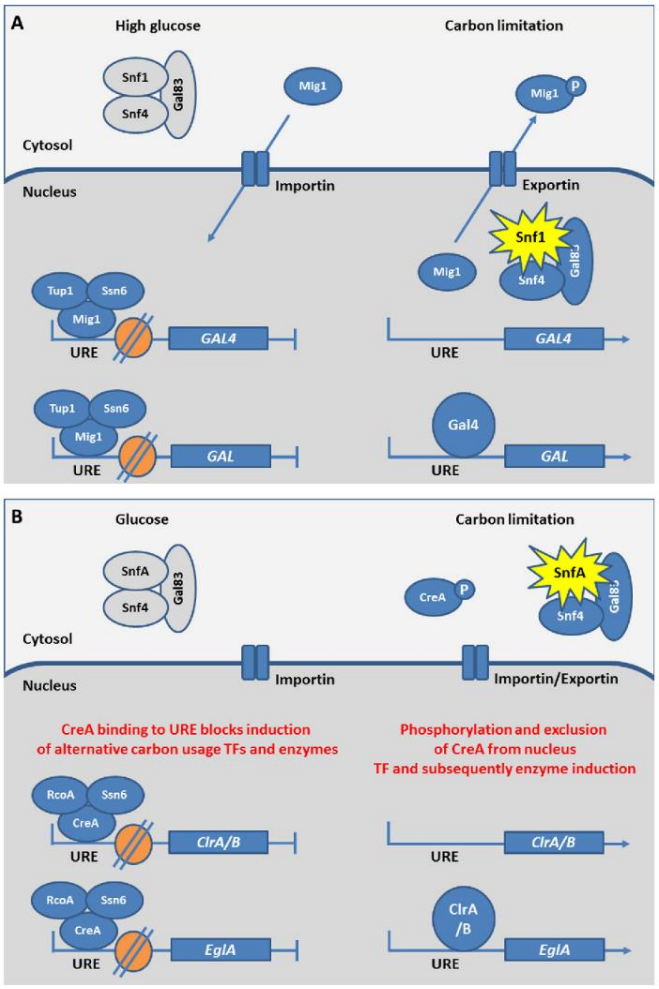

Figure 6. The molecular mechanism of carbon catabolite repression in *S. cerevisiae* (A), and filamentous fungi (B).

In presence of glucose, *S. cerevisiae* and filamentous fungi repress the expression of alternative carbon utilization genes via binding of a repressor protein to upstream regulatory elements (URE), which inhibit the expression of the transcription factors (TF) and metabolic enzymes necessary for alternative carbon utilization. Besides, chromatin structure hampers transcription. In the condition of limited carbon nutrient, Snf1/SnfA mediates phosphorylation and relocalisation of the repressor protein leading to depression, while local modifications to chromatin structure enable transcription. (Grey Snf1/SnfA complex = unactive; yellow star = activate Snf1/SnfA complex; P = phosphorylation; orange circle = nucleosome). From Brown et al (Brown et al., 2014).

In addition to CreA/Cre1 considered as a crucial regulator in CCR, the protein kinase Sucrose non-fermenting complex (Snf1/SnfA) (Fig. 6A, B) and the protein kinase A (PKA) play also a regulatory role for CCR and for the expression of lignocellulolytic enzymes (Fig. 5). In *S. cerevisiae*, ScSnf1 phosphorylates the repressor ScMig1 under carbon limitation and promotes the expression of glucose-repressed genes (Fig. 6A) (García-Salcedo et al., 2014). ScSnf1, therefore, releases the CCR in glucose depleted conditions. When present at high levels, glucose is imported into the cell and the intracellular production of phosphorylated glucose lead to the inactivation of ScSnf1, which in turn inhibits ScMig1 phosphorylation. As a result, ScMig1 is localized in the nucleus (Fig. 6A). In filamentous fungi as *A. nidulans*, a similar function for SnfA (Fig. 6B) to phosphorylate CreA was confirmed (Brown et al., 2013; Ries et al., 2016).

Besides the cAMP/PKA pathway, the TOR (Target of Rapamycin) pathway has also been proposed possibly having an important role in regulating the expression of cell wall degrading enzymes in response to lignocellulosic material (Brown et al., 2013; Xiong et al., 2014). The TOR signaling pathway is a highly conserved nutrient sensing pathway in eukaryotes, and is found to work in parallel with the cAMP/PKA pathway to regulate common targets relating to growth in *S. cerevisiae* (Zurita-Martinez and Cardenas, 2005). The roles of TOR signaling in filamentous fungi will be separately discussed in detail in one following part.

In summary, there are several carbon sensing pathways having a role in regulation of growth of filamentous fungi in response to the lignocellulosic material. Among those, CCR and cAMP/PKA appear to be the major pathways. However, the regulatory role of other nutrient sensing pathways, for instance, the TOR pathway, remains to be unraveled and may provide novel solutions to enhance the extracellular enzyme productivity.

Nitrogen sensing

Fungi are able to use many nitrogen sources such as amino acids, ammonium ions, and other sources such as nucleotidic bases (Bahn et al., 2007; Dijck et al., 2017). Sensing and uptake of these nutrients are essential for the synthesis of many cellular components. However, the number of described nitrogen sensing receptors is smaller than carbon sensing receptors. To date, there are no non-transporting receptors for ammonium sensing described in yeasts. That observation is also true for amino acid sensing with the absence of described transceptors that mediate amino acid sensing in filamentous fungi. For ammonium sensing, transceptors have been found only in the ectomycorrhizal fungus *Hebeloma cylindrosporum* (Javelle et al., 2003) and in the phytopathogenic fungi *Fusarium fujikuroi* and *Colletotrichum gloeosporioides* (Shnaiderman et al., 2013; Teichert et al., 2008).

Non-transporting receptor Ssy1 for amino acid sensing in *S. cerevisiae*

In *S. cerevisiae*, extracellular amino acids are detected by a multiprotein complex composed of ScSsy1-ScPtr3-ScSsy5 (SPS). This detection induces the transcriptional expression of amino acid transporters genes and other genes encoding nitrogen-metabolizing enzymes (Kodama et al., 2002). ScSsy1 is an amino acid permease (AAP) and functions as a receptor in the SPS complex (Klasson et al., 1999). ScPtr3 is a linker between ScSsy1 and ScSsy5. ScSsy5 contains an inhibitory domain that dissociates in response to extracellular amino acids, freeing a catalytic domain to activate the transcription factor ScStp1p (Pfirrmann et al., 2010).

The receptor induction by binding of amino acids to ScSsy1 results in activating the endoproteolytic cleavage of transcription factors Stp1/2 in a process called receptor-activated proteolysis (RAP) in which Stp1/2 functions as latent cytoplasmic precursors (Pfirrmann et al., 2010). Stp1/2, in turn, induces the expression of genes encoding amino acid–metabolizing enzymes and amino acid permeases. In *S. cerevisiae*, Stp1 is regulated by the TOR signaling pathway (Fig. 4). Indeed, in presence of amino acids, activated Stp1 localizes in nucleus and induces expression of its target genes. In contrast, in absence of amino acids or in presence of rapamycin at a concentration at which TOR kinase activity is inhibited (TOR pathway will be discussed later), Stp1 is degraded in a manner dependent on the activity of a protein phosphatase 2A (PP2A)-like phosphatase, and Sit4, which have been known as effectors of TOR. This degradation results in the disappearance of Sit4 from the nucleus (Shin et al., 2009).

Transceptors in *S. cerevisiae*

In the model yeast *S. cerevisiae*, all identified transceptors belong to the AAP family. The best-studied receptor for amino acid sensing is Gap1, which transports all L-amino acids, several D-amino acids, and polyamines (Uemura et al., 2005). The role as an amino acid receptor of Gap1 was found when studying the amino acid induced rapid activation of the PKA pathway, which has been known to be activated in a cAMP dependent reaction (Fig. 4). In this pathway, Gap1 is involved in the downstream relay of the signal according to an unknown mechanism (Donaton et al., 2003).

In *S. cerevisiae*, three genes encoding for ammonium transporters have been identified, but only one is a transceptor named ScMep2. ScMep2 acts as a regulator of pseudohyphal growth and PKA activation when ammonium is added to nitrogen-starved cells (Boeckstaens et al., 2007). ScMep2 in controlled by the ScNpr1, a kinase that is the target of ScTORC1 (Fig. 4). Under nitrogen starvation or ScTOR inactivation, ScNpr1 is activated by dephosphorylation. In presence of sufficient ammonium, ScNpr1 is phosphorylated and inactive (Boeckstaens et al., 2007).

G – protein-coupled receptors (GPCRs) in nitrogen sensing of yeast and filamentous fungi

There are no GPCRs established as nitrogen receptors in *S. cerevisiae* while orthologues of ScGpr1 known as glucose sensor (Fig. 4) were reported to sense methionine in pathogenic *C. albicans* and *C. neoformans* (Maidan et al., 2005; Xue et al., 2005). Methionine sensing is important for the hyphal transition of *C. albicans* on agar medium, and it can induce a transient cAMP production, as well as mating hyphal elongation in *C. neoformans* (Maidan et al., 2005; Xue et al., 2005).

In filamentous fungi, amino acids appear to be sensed by the cAMP receptor-like GPCR named GprH which is the glucose sensor in *A. nidulans* (Fig. 3) (Li et al., 2007b). Orthologues of GprH have been found in other filamentous fungi such as NcGpr4 in *N. crassa*, and AfGprC/D in *Aspergillus flavus* (Fig. 3) (Affeldt et al., 2014; Li and Borkovich, 2006). Additionally, the function of cAMP receptor-like GPCRs in the regulation of sexual development is conserved in fungi. GPCRs therefore may have a dual role in sensing both sugars and amino acids.

There is very little literature dealing with GPCRs requirement in ammonium sensing of filamentous fungi. To date, ammonium sensing via GPCRs has been only shown in *Aspergillus flavus* (Affeldt et al., 2014). In this fungus, mutations in GprC/D receptors impair growth on ammonium chloride and proline (Affeldt et al., 2014).

In summary, in addition to cAMP/PKA signaling pathways, the TOR signaling pathway may play an important role in regulating a wide range of functions in response to both carbon and nitrogen nutrient sources in the filamentous fungi. In the next part, TOR signaling will be described and discussed in these fungi.

Target Of Rapamycin (TOR) signaling as a key regulator of growth in the adaptation of filamentous fungi

All living organisms sense and respond to nutrient signals by regulating growth and developmental programs for survival. In eukaryotic organisms, a role for the TOR signaling pathway has emerged as a global regulator of cell growth. The central component of this signaling pathway is **Target Of Rapamycin (TOR), a conserved serine/threonine kinase** which belongs to the family of phosphatidylinositol kinase-related kinases (PIKK) (Wullschleger et al., 2006).

TOR was first found in *S. cerevisiae* via the characterization of strains resistant to rapamycin. Rapamycin is a metabolite produced by *Streptomyces hygroscopicus* (Heitman et al., 1991). **Rapamycin binds to the intracellular receptor FKBP12 (FK506 binding protein 12) to form a complex which then inhibits TOR kinase activity** resulting in cellular toxicity (Wullschleger

et al., 2006). In *S. cerevisiae*, two genes encoding two proteins named TOR1 and TOR2 are present. The resulting proteins are the main components of two complexes named TORC1 and TORC2. Up to date, TOR characterization in fungi has been mainly carried out in *S. cerevisiae* wherein TOR has been demonstrated as the central controller of growth, proliferation, and survival in response to nutrients and stress (Loewith and Hall, 2011). Up to date, TOR has been identified in all tested eukaryotes, controlling cellular processes via regulating networks named TOR signaling pathways.

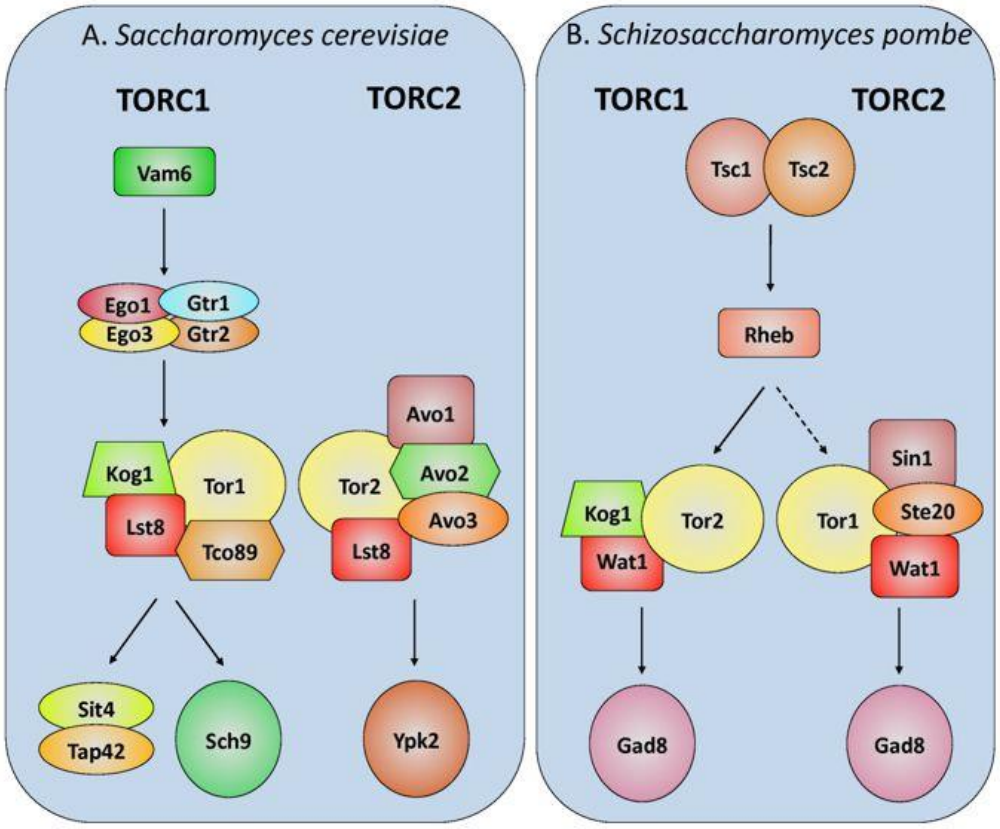

Figure 7. TOR signaling pathway in the model yeasts.

The TOR pathway components in *S. cerevisiae* (A) and *S. pombe* (B). The functional homologs between the two species are shown in the same shape and color (Shertz et al., 2010).

In the fungal kingdom, TOR signaling pathways have been best-characterized in model yeasts *S. cerevisiae* and *S. pombe* as presented in Fig. 7 (Shertz et al., 2010). In *S. cerevisiae*, only ScTORC1 is sensitive to rapamycin. It comprises ScTOR1 or ScTOR2, ScKog1, ScTco89, and ScLst8 (Fig. 7A). ScTORC1 controls protein synthesis, mRNA synthesis and degradation, ribosome biogenesis and autophagy. ScTORC2 is composed of ScTOR2, ScLst8, ScAvo1, ScAvo2, ScAvo3 (Fig. 7A), it is insensitive to rapamycin and is involved in the control of actin polarization and cell wall integrity (Loewith and Hall, 2011). The downstream effectors of ScTORC1 are the ScSit4, one PP2A-like phosphatase, and the AGC kinase ScSch9. ScSch9 has been deeply studied due to its involvement in stress response. Under stress conditions including nutrient starvation, high salt, redox stress, temperature, ScSch9 phosphorylation is strongly reduced (Urban et al., 2007). Due to this property, ScSch9 has been used to quantify ScTORC1 activity through its phosphorylation in various nutrient and stress conditions (González et al., 2015). In comparison to *S. cerevisiae*, there is an extension or expansion in upstream components of the TOR pathway in *S. pombe*, with the presence of ScTsc1 and ScTsc2 (Fig. 7B). In this fungus, the TOR pathway has functional roles in nutrient and stress signaling, cell growth and differentiation, and sexual development (Alvarez and Moreno, 2006; Otsubo and Yamamoto, 2010; Weisman and Choder, 2001).

In addition to *S. cerevisiae* and *S. pombe*, TOR signaling has been also well-studied in human pathogenic yeasts such as *C. albicans* and *C. neoformans* (Rutherford et al., 2019). *C. albicans* is the first fungus found to be inhibited by rapamycin in 1975 which opened the story of TOR signaling researches (Sehgal et al., 1975). In contrast to yeasts, TOR signaling pathways have been less investigated in filamentous fungi. In these organisms, TOR and TOR signaling pathways have been only identified and partially functionally characterized (focusing on genetics, development, and pathogenicity) in several fungal models such as *A. nidulans* (Fitzgibbon et al., 2005), *N. crassa* (Park et al., 2011), *Podospora anserina* (Pinan-Lucarré et al., 2006), *A. fumigatus* (Castro et al., 2016), *C. neoformans* (Lee et al., 2012), *Fusarium fujikuroi* (Teichert et al., 2006), *Fusarium graminearum* (Yu et al., 2014), *Fusarium oxysporum* (López-Berges et al., 2010), *Magnaporthe oryzae* (Qian et al., 2018), and *Verticillium dahliae* (Li et al., 2019). In all these fungi, TOR signaling is functionally conserved and involved in the regulation of cellular growth, metabolism, virulence and vegetative development. In addition to the TOR identification, the components of the TOR signaling pathway have also been identified in the focus on downstream effectors of TOR. Indeed, homologs of ScSit4 (AnSit4) and ScSch9 (AnSchA and NcSch9) were identified in *A. nidulans* (Fitzgibbon et al., 2005) and in *N. crassa* (Park et al., 2011). Functional characterization of these components showed similar roles in response to stress and in autophagy regulation under rapamycin treatment or nutrient-starvation. For these fungi, to date, only one upstream component of TOR signaling pathways has been identified in *N. crassa*: the protein VTA for

Vacuolar TOR-Associated protein (Ratnayake et al., 2018). This is the homolog of ScEgo1 in *S. cerevisiae* (Fig. 6) and Lamtor1 in mammals. In *N crassa*, it has a role in maintaining circadian daily rhythmicity (Ratnayake et al., 2018).

Similar to the model fungi and mammalian pathogenic fungi mentioned above, almost of plant pathogenic fungi also have a single gene encoding TOR, with the exception of *F. oxysporum* which contains two genes of TOR (López-Berges et al., 2010). In these fungi, TOR has an important role in the virulence regulation via control traits which are similar to those described for the human pathogenic yeasts. For example, the key role of TOR signaling as a virulent regulator has been well studied in *M. oryzae*. In this fungus, TOR signaling inhibits appressorium formation in a GATA transcription factor-depending manner (Marroquin-Guzman and Wilson, 2015). In phytopathogenic fungi, the downstream effectors of TOR including homologs of ScSit4 and ScSch9 (Fig. 7A) have been also characterized with regard to their role in virulence. Indeed, two of these effectors (FgSit4 and FgSch9) were identified and characterized in *F. graminearum* (Chen et al., 2014; Yu et al., 2014). In this fungus, FgSit4 is necessary for hyphal development, virulence and sexual reproduction. It also exhibits different roles in conidiation regulation, the mycotoxin [deoxynivalenol (DON)] biosynthesis as well as involvement in cell wall integrity (Yu et al., 2014). FgSch9 is a key protein in stress response, DON biosynthesis, and pathogenesis (Chen et al., 2014).

Recently, TOR was studied in *Ganoderma lucidum*, a basidiomycete model with the aim to characterize the regulatory mechanisms of growth, development, and metabolism in response to environmental cues (Chen et al., 2019). This is the first report on TOR functional characterization in basidiomycetes. In this fungus, TOR regulates the synthesis of cell wall components including chitin and β-1,3-glucan through the Slt2-MAPK pathway. Studies carried out on Slt2-silenced strains suggested a potential connection between TOR signaling and cell wall integrity (CWI) signaling (Chen et al., 2019).

I.2.2 Stress sensing and responses for adaptation to environment

In various ecosystems, fungi have to deal with many stresses including hypoxia, osmotic stress, cell wall stress, oxidative stress, pH stress, etc... In fact, all stresses, in the end, lead to oxidative stress. Sensing and adaptation to stress are one of the essential strategies for survival, and it also is an important mechanism involved in detoxification and resistance against environmental antifungal agents including reactive species molecules and fungicides.

Stress adaptation is dependent on three fundamental principles: (i) the ability to detect and change environmental signals, (ii) the ability to transduce these signals in order to regulate cellular processes mediating stress adaptation, and (iii) initiating responses that allow cells to

survive. These processes either counteract or detoxify the initial stress and repair or remove the molecular damages caused by that stress (Brown et al., 2017).

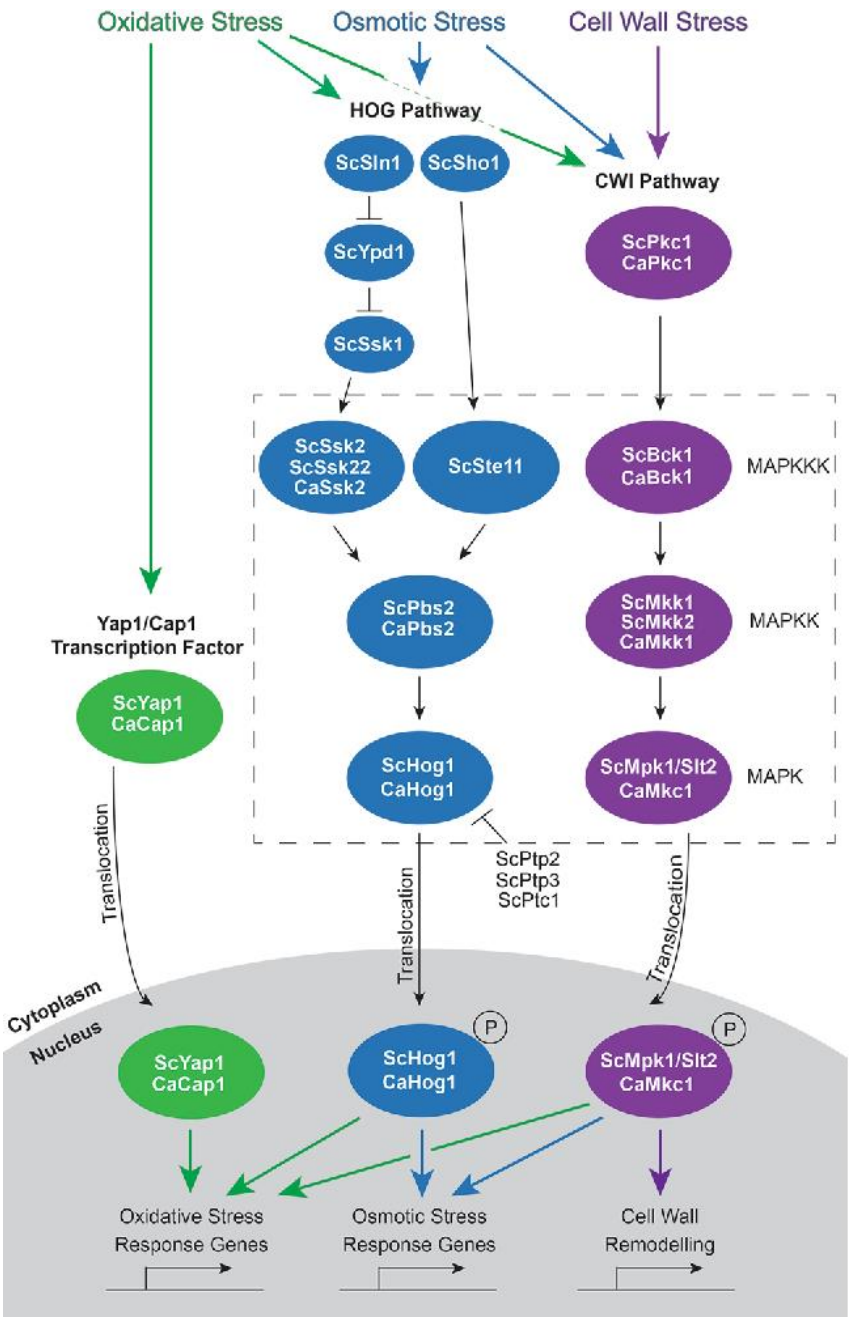

Figure 8. Stress signaling pathways in *S. cerevisiae* and *C. albicans*.

Green, blue and purple arrows represent oxidative stress, osmotic stress, and cell wall stress. Sc, *Saccharomyces cerevisiae*; Ca, *Candida albicans* (Hayes et al., 2014).

In fungi, the most extensively studied pathway is the HOG pathway which activates the mitogen-activated protein kinase (MAPK) pathways (Fig. 8) (Smith et al., 2010). These pathways signal through cascades of phosphorylation catalyzed by protein kinases. It starts from the detection of an upstream signal, a MAP kinase kinase kinase (MAP-KKK) then phosphorylates and activates a MAP kinase kinase (MAPKK), which in turn phosphorylates the MAP kinase (MAPK). This activated MAPK then moves to the nucleus and induces several changes including activation of transcription factors, cell cycle regulation, and kinase activation, which produce an adaptive response to the stress. Transcription factors are also activated directly by stress. For example, in *S. cerevisiae* and *C. albicans*, the transcription factor Yap1/Cap1 which resides in the cytoplasm under normal physiological conditions is activated by oxidative stress and moves to the nucleus where it regulates gene expression (Hayes et al., 2014). Yap1/Cap1 is a bZip transcription factor and plays a key role in cellular protection from oxidative stress. In *C. albicans*, mutants lacking CaCap1 (ΔCaCap1) are more sensitive to reactive oxygen species (ROS), the obtained data suggesting that CaCap1 is required for cell survival under conditions of both low and high levels of reactive oxygen species (Alarco and Raymond, 1999; Enjalbert et al., 2005).

Concerning lignocellulose-interacting fungi, MAPK pathways have been mainly studied in *N. crassa*, and *A. nidulans*. In *N. crassa*, this pathway is named OS-MAPK pathway due to the identification of NsOS-2, a homolog of Hog1-MAPK in *S. cerevisiae*, involved in the response to osmotic stress. The targets of this kinase are similar to those found in *S. cerevisiae*. The NsOS-2 phosphorylation is essential for adaptation in response to fludioxonil and osmotic stress (Irmler et al., 2006; Noguchi et al., 2007). Recently, the OS-MAPK pathway has been shown to regulate the sensing of carbon nutrients from cell wall components deriving from plant biomass (Huberman et al., 2017). In *A. nidulans*, the MAPK pathways are highly conserved in comparison with *S. cerevisiae* and the role of these pathways in stress response has been mostly clarified in comparison to other pathways (Hagiwara et al., 2016). In this fungus, HogA-MAPK is the homolog of ScHog1. This kinase also moves to the nucleus for the activation of bZip transcriptional factors. One of them is AnAtfA, an ortholog of *S. cerevisiae* Sko1p and *S. pombe* Atf1. This factor is strongly expressed in response to fludioxonil and osmotic stress (Hagiwara et al., 2009). AnAtfA was also identified as interacting with the MAPK SakA to regulate general stress responses, development, and spore functions. Nevertheless, AnAtfA could play only a minor role in adaptation to osmotic and oxidative stresses since the AnAtfA-deleted mutant did not exhibit a clear phenotype under strong osmotic and oxidative stresses (Hagiwara et al., 2008, 2009). Up to date, no signaling pathway has been identified for wood decaying basidiomycetes in response to stress, although proteins known for their involvement in oxidative stress protection have been described in the model fungus *P. chrysosporium* (Morel et al., 2009a).

Besides the HOG pathway, the nutrient-sensing TOR and cAMP-PKA pathways (Fig. 4, 5, 7) play also significant roles in controlling stress responses. In *S. cerevisiae*, inhibition of TOR by rapamycin or reduced PKA activity is strongly related to the transcriptional induction of genes containing stress-regulated elements (STREs). TOR controls the cellular localization of ScMsn2/4 by preventing them from moving to the nucleus (Fig. 4). TOR inhibition leads to the nuclear localization of ScRim15 (Fig. 4) which activates the expression of ScMsn2/4. Those three proteins are transcription factors involved in the transcriptional activation of genes in response to several stress conditions such as heat shock or H_2O_2 treatment. As mentioned above, TOR signaling regulates stress response from yeasts to filamentous fungi via Sch9 (Fig. 4)/SchA, the direct effector of TOR, and also via Sit4/sitA.

In summary, environmental sensing of nutrient and stress, combined with the coordinated response is essential for the survival of both yeasts and filamentous fungi. One of the key pathways activated by this process is the TOR signaling pathway. The understanding of the TOR signaling pathway role in regulation of cellular detoxification responses of wood decaying fungi is one of this thesis's objectives. Therefore, the next part of this introduction will describe their substrate, wood, focusing on the presence of potential toxic molecules (wood extractives).

II. Wood and wood degrading fungi

II.1 Wood components

Wood components are generally divided into two main groups: structural and extractive components. The structural components are polymers, mainly cellulose, hemicelluloses, and lignin that form the structure of the cell wall and are involved in the physical and chemical properties of wood (Fig. 9). Extractive components are non-structural components that can be found in cell lumina and cellular channels. They consist of a wide variety of organic compounds mainly of low molecular weight and a small proportion of inorganic compounds (Pereira H et al., 2009).

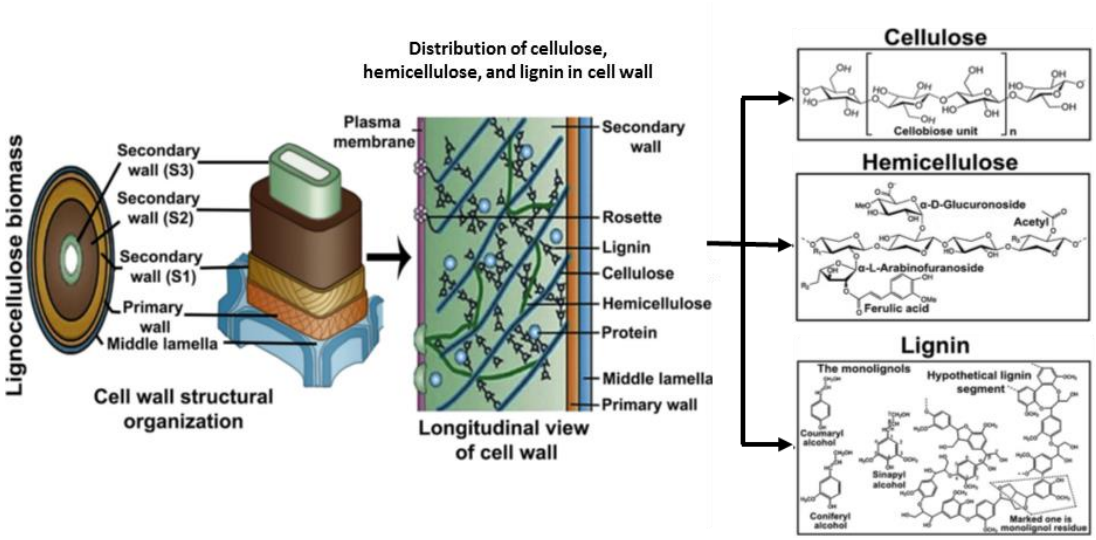

Figure 9. Structural and chemical composition of ligno-cellulose biomass.

Plant cell walls contain three main layers. The first is the middle lamella formed during cell division. The primary wall, formed after middle lamella, comprises of cellulose microfibrils. The final layer named the secondary wall is a thick layer composed of cellulose, hemicellulose, and lignin that is produced inside the primary cell wall and provides compression strength. From Manavalan et al. with modifications (Manavalan et al., 2015).

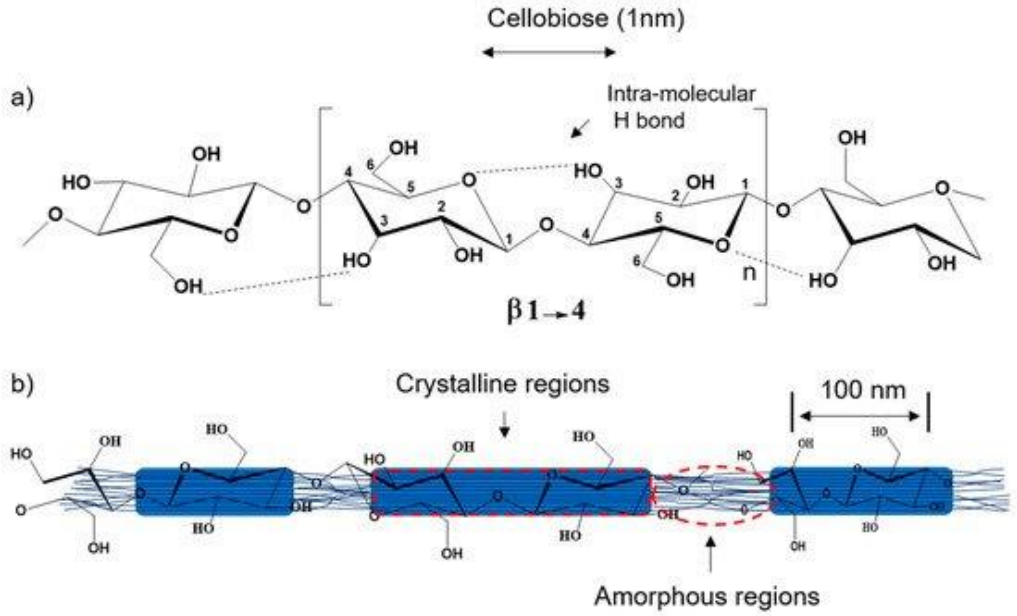

Figure 10. A chemical chain of cellulose composed of glucose units attached with β-1,4 linkages and organization of cellulose in a microfibril (Tayeb et al., 2018).

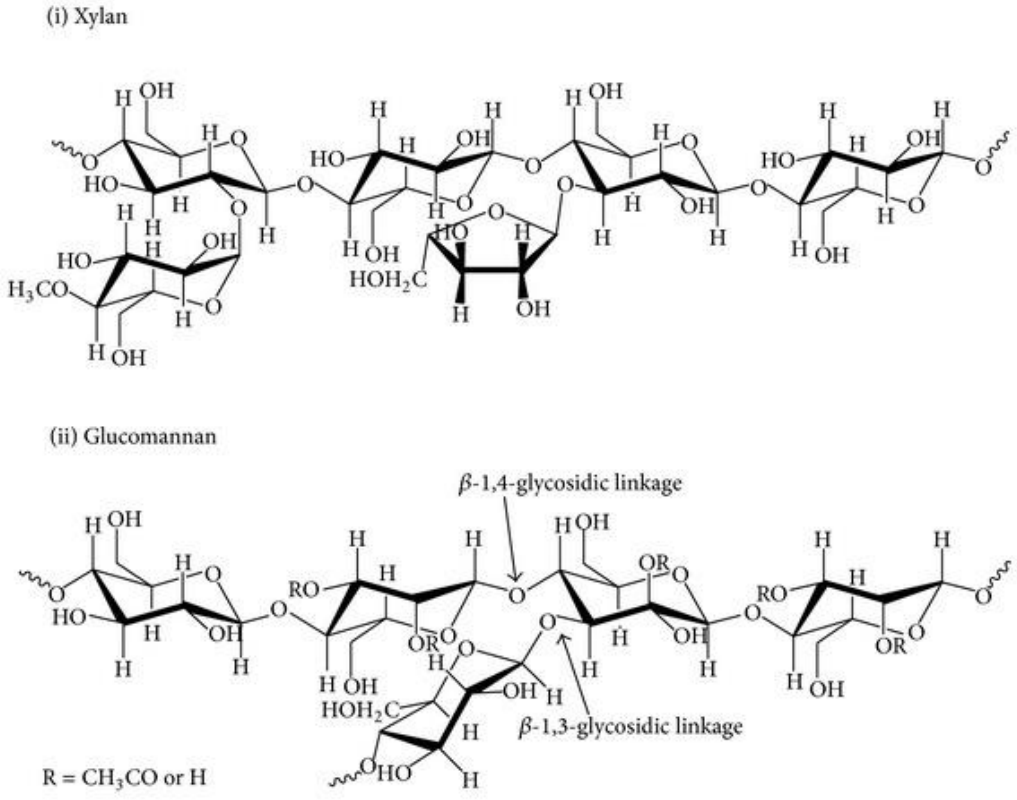

Figure 11. Chemical composition of hemicellulose compounds. (i) Xylan, and (ii) Glucomannan (Lee et al., 2014).

II.1.1 Structural compositions

II.1.1 Cellulose

Cellulose is the most abundant polysaccharide in wood (40% to 50% of dry weight). It is located in both the primary and secondary cell walls (S2 layer) and is involved in the mechanical strength of cell wall structure. Homo-polysaccharide cellulose chains include repeats of D-glucose units, which are linked together by β-1,4-glucosidic bonds. Organization of these chains with intermolecular hydrogen bonds form linear crystalline structures of microfibrils and amorphous regions (Fig. 10), which can be distinguished in the wood cell wall.

II.1.2 Hemicellulose

Hemicelluloses are the branched hetero-polysaccharides, occurring from 20% to 30% of the dry weight of wood cell walls. They support the cell wall structure through hydrogen bonding to cellulose microfibrils and covalent linkages to lignin. Hemicelluloses of hardwood differ from those of softwood. In hardwood, glucuronoxylans containing side groups of D-xylose backbone and (4-o-methyl-)-D-galactoturonic acid are common hemicelluloses (Fig. 11(i)). In softwood, galactoglucomannans, with a backbone of randomly distributed D-mannose and D-glucose residues, supplemented with α-1,4-linked D-galactose residues or acetyl groups, are major hemicelluloses (Fig. 11(ii)) (Jacobs et al., 2002).

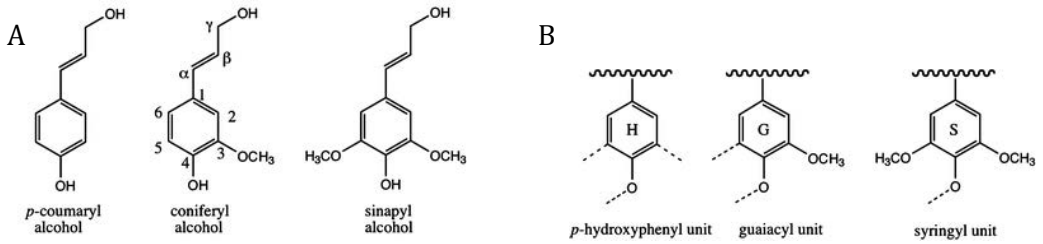

Figure 12. Structure of primary lignin monomers and three corresponding lignin units.

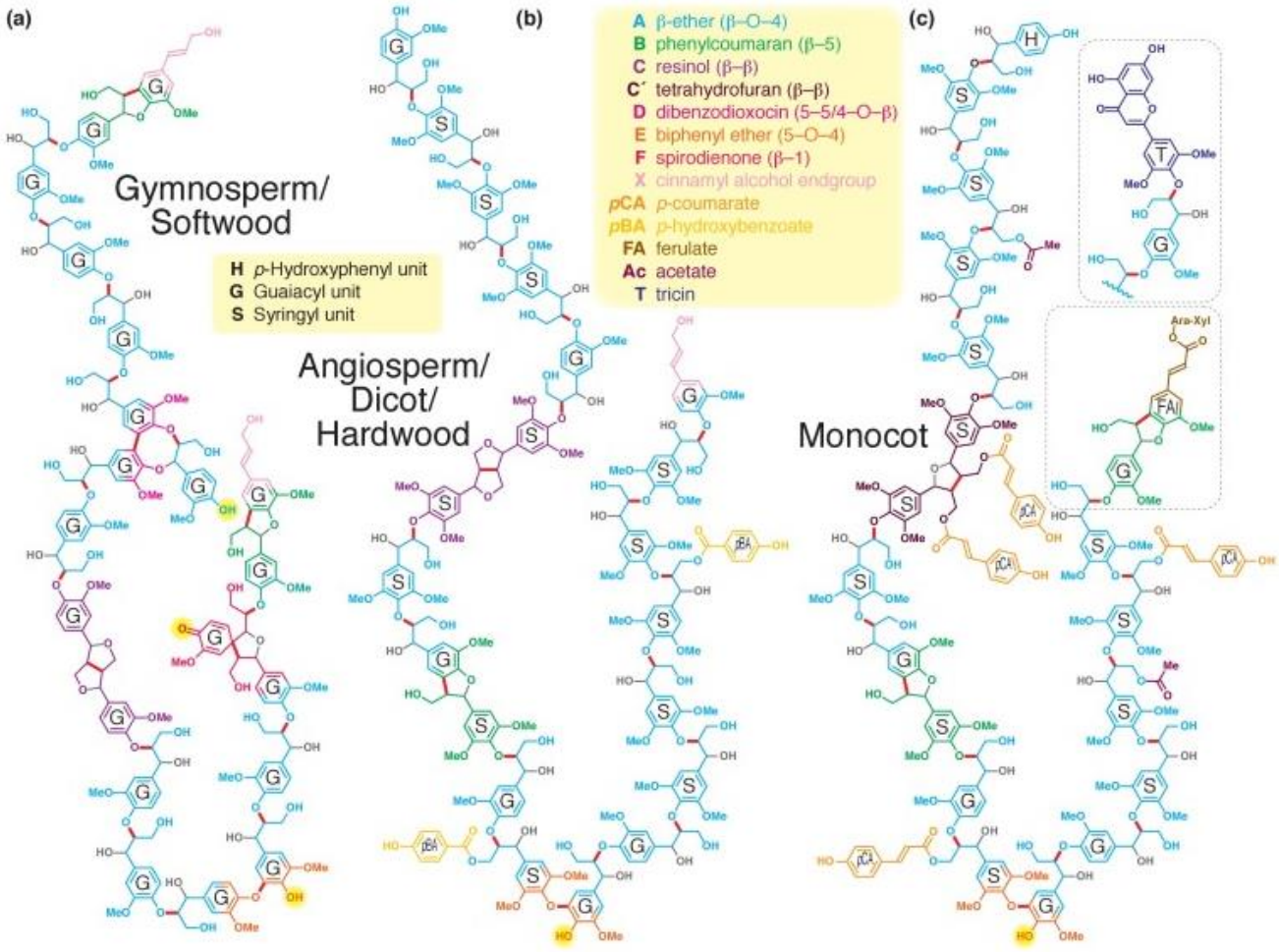

Figure 13. Model structures of lignin (Ralph et al., 2019). Lignin 20-mers models stand for: (a) A gymnosperm/softwood, (b) An angiosperm/hardwood, and (c) A monocot.

II.1.3 Lignin

Lignin is a polyphenolic and amorphous polymer found in all layers of wood cell walls. It represents the most abundant aromatic polymer source in nature. As a structural component of wood, lignin strengthens the cell walls by adhesion to the cellulose microfibrils, and additionally, it is extremely recalcitrant to microbial degradation. In plant, lignin is composed of guaiacyl (G), syringyl (S) and hydoxyphenyl (H) type subunits which are formed through oxidative polymerization of three phenylpropanoid precursors including coniferyl alcohol, sinapyl alcohol, and p-coumaryl alcohol, in presence of free radicals (Fig. 12) (Marriott et al., 2016). During lignification, three subunits are linked together with various types of carbon-carbon and ether carbon bonds to form a large array of structural units that can be found in the polymeric products (Wong, 2009).

The composition and amounts of lignin differ in softwood and hardwood (Fig. 13). Softwood lignin comprises mostly of guiaiacyl (G) subunits and forms 25%-33% of the cell wall dry weight. Hardwood lignin contains both guaiacyl (G) and syringyl (S) subunits at similar levels with traces of hydoxyphenyl (H) units, and accounts for 20%-25% of the cell wall dry weight (Vanholme et al., 2010).

II.I.2 Wood extractives

Wood extractives are the non-structural components of wood, occurring mainly in the heartwood. Their synthesis is often induced in response to environmental stresses. They could modify wood properties including natural durability, mechanical and dimensional stability. Their most important and interesting function is their involvement in wood natural durability. Some of extractives are very toxic for wood-destroying organisms (Kirker et al., 2013). Their antimicrobial activity has been also successfully tested against human and plant pathogens. The chemical compositions, quantity, and distribution of wood extractives have also been studied in several woody species (Belt et al., 2017), in particular for the exploration of new wood preservatives (Singh and Singh, 2012).

From their chemical composition, **wood extractives are classified into three main groups: phenolic compounds, terpenoids, and other extractives** (Pereira et al., 2009). The third group components cluster fats, waxes, and sugars. These compounds having probably a very little role in wood durability will be not discussed here. The next paragraphs will be then devoted to phenolic compounds and terpenoids.

II.I.2.1 Phenolic compounds

Phenolic compounds are secondary metabolites derived from either phenyl-propanoids of shikimate pathway or simple phenols of the polyketide acetate/malonate pathway. Plant phenolics possess a very large structural diversity gathering thousands of identified structures. For wood extractives, phenolic compounds include several subgroups: Flavonoids, tannins, stilbenes, lignans, and quinones (Fig. 14). In the following part, some structural and biological properties of these subgroups are discussed.

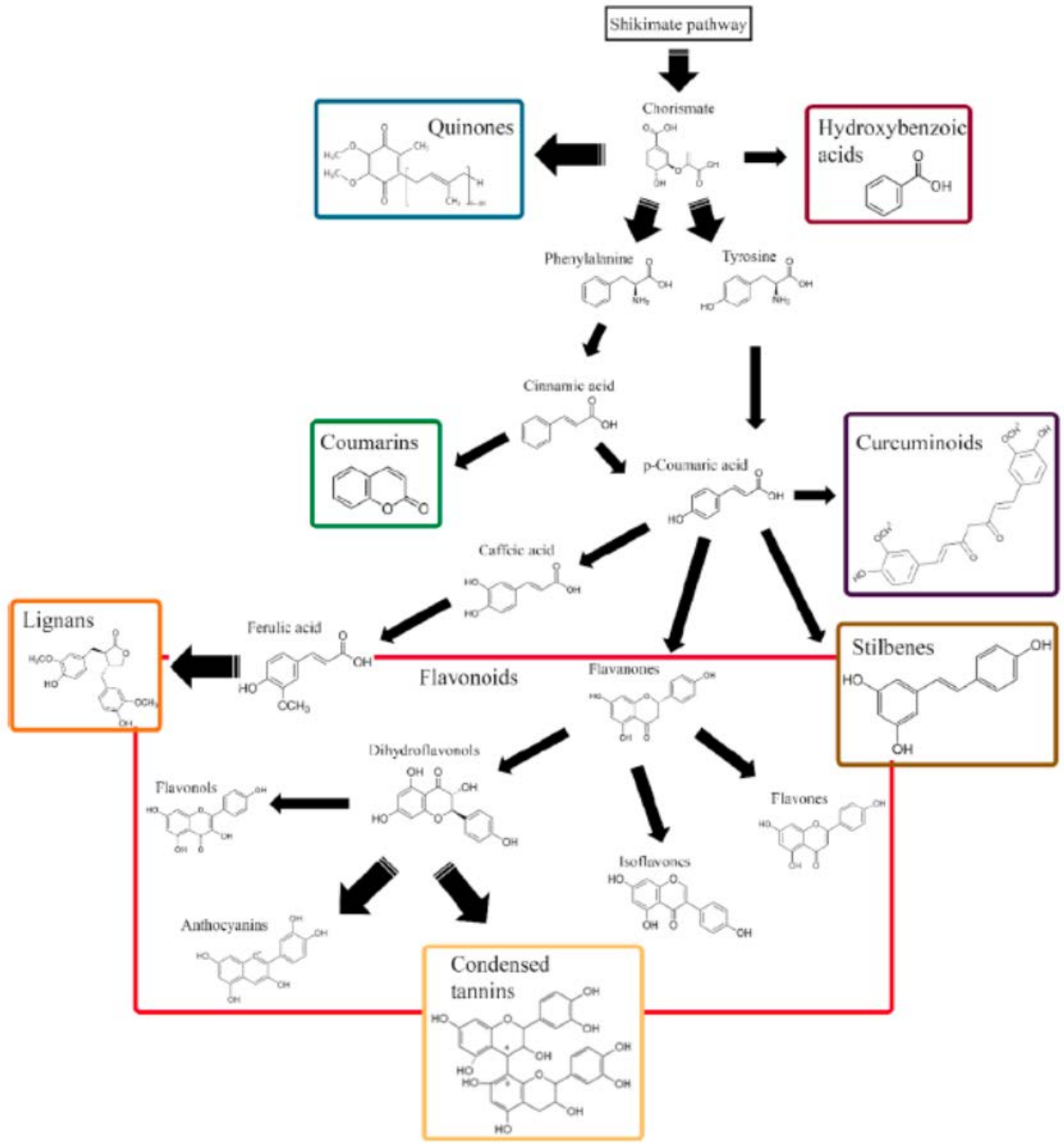

Figure 14. Biosynthetic pathways of phenolic compounds based on their carbon skeleton (Mark et al., 2019).

II.I.2.1.1 Flavonoids

Flavonoids are secondary metabolites, derivatives of 2-phenyl-benzyl-γ-pyrone, and are ubiquitous in plants. There are over 9000 identified flavonoids. In plants, the main biological function of flavonoids is protection against ultraviolet radiation, pathogens, signaling in microbes-plants interactions, male fertility, auxin transport and the coloration of flowers (Winkel-Shirley, 2001; Falcone Ferreyra et al., 2012).

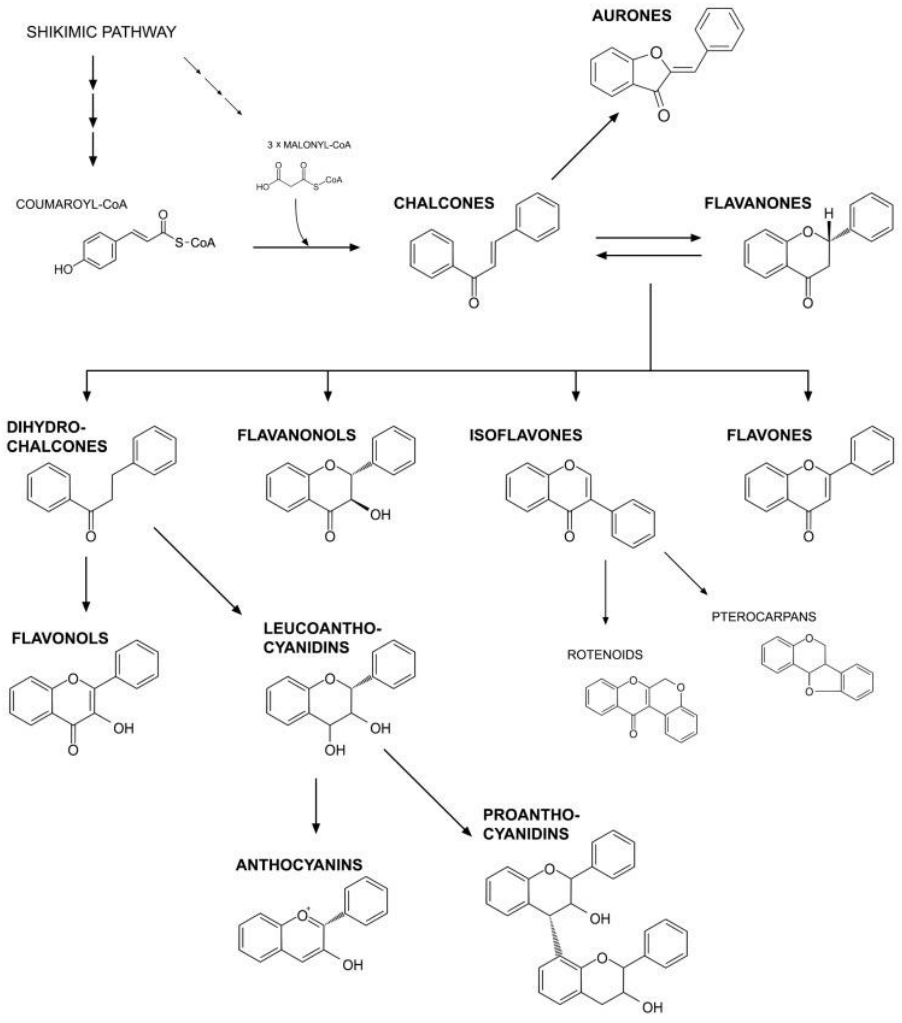

Figure 15. Chemical structure of main groups of flavonoids (Mierziak et al., 2014).

Based on their chemical structure, flavonoids include six major groups: chalcones, flavones, flavonols, flavandiols, anthocyanins, and proanthocyanidins or condensed tannins (Fig. 15) (Falcone Ferreyra et al., 2012).

As wood components, flavonoids have an important role in natural durability against fungi and insects. For fungal resistance, the proposed mechanism for these compounds is their ability to prevent wood colonization through the combination of antifungal and antioxidant activities

(Schultz and Nicholas, 2000). Polyphenolic molecules could indeed scavenge free radicals which are produced by both white and brown-rot fungi to promote wood degradation (Schultz and Nicholas, 2000). For instance, several flavonoids isolated from durable heartwoods such as (+)-catechin, (-)-epicatechin have no antifungal activity but exhibit high antioxidant activity. They could contribute to wood durability through their radical scavenging activity besides antifungal activity of other compounds present in wood extractives (Anouhe et al., 2018). Another example is wood of aspen species which are known as a rich source of bioactive flavonoids causing the deposit problems in the papermaking process (Pietarinen et al., 2006). Teak (*Tectona grandis* Linn. f.), one highly valuable wood in wood industry, contains also high contents of flavonoids. One of them, the 4, 5-dihydroxyepiisocatalponol, a derivative of napthoquinone, exhibits strong fungicidal activity against the white rot *T. versicolor* and was proposed as a chemical marker for durability of teak wood (Niamké et al., 2012). Teak heartwood extractives have been also proposed previously as potential wood preservatives against brown, white, and soft-rot fungi (Brocco et al., 2017).

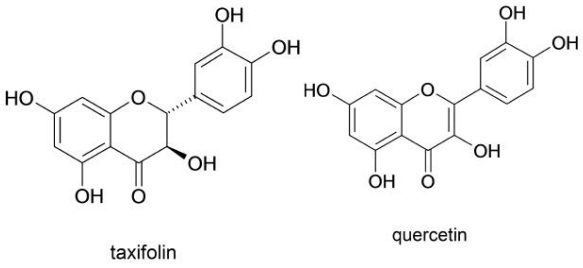

Figure 16. Structures of taxifolin and quercetin, two flavonoids found in the heartwood of *Larix leptolepis* (Ohmura et al., 2000).

Wood flavonoids play also a role in resistance against insects, especially termites which strongly attack wood in tropical countries. The suggested main mechanism is an antifeedant activity as proposed for quercetin and taxifolin (Fig. 16) which are present in *Larix leptolepis* wood and exhibit a protective activity against *Coptotermes formosanus* Shiraki (Ohmura et al., 2000). Another example is the termiticidal and antifeedant activities of latifolin, which is present in the heartwood of *Dalbergia latifolia*, this latter being highly resistant to *Reticulitermes speratus* (Sekine et al., 2009).

With regard to their strong antioxidant activity, many researches have been performed to find wood flavonoids for health care. For example, flavonoids isolated from French maritime pine (*Pinus pinaster*) and radiata pine (*Pinus radiata*) barks are used in nutritional supplements products with the commercial name of pycnogenol and enzogenol respectively (Yazaki, 2015).

Recently, robinetinidol-(4α,8)-catechin, one compound isolated from *Acacia mearnsii* heartwood which is able to reduce carbohydrate absorption and limit the rise of blood glucose in human, has been commercialized for dietary supplement products named ACAPOLIA® and ACAPOLIA PLUS in Japan (Ogawa et al., 2018).

II.I.2.1.2 Tannins

Tannins are polyphenolic compounds exhibiting a molecular size from 500 to more than 20000 Da. They are among the most important compounds with defensive functions in plants due to their higher antimicrobial activities in comparison to smaller phenols (Scalbert, 1992). They differ from other phenolic compounds in their ability to precipitate proteins such as gelatin (Spencer et al., 1988).

Based on structural characteristics, tannins are classified into three main groups according to their chemical structures (Fig. 17): hydrolyzable tannins including gallotannins and ellagitannins, condensed tannins or proanthrocyanidins, and complex tannins (Arbenz and Avérous, 2015; Khanbabaee and Ree, 2001).

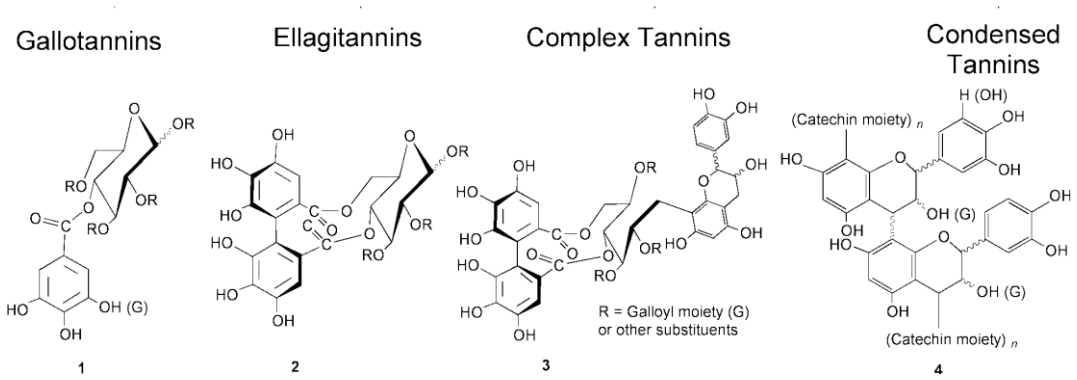

Figure 17. Classification of the tannins (Khanbabaee and Ree, 2001).

Hydrolysable tannins are esters of glucose as polyol and garlic acid, or phenolic acids deriving from the oxidation of gallic acid, present in plants at very low concentrations. They consist of two subgroups: the gallotannins, which produce gallic acid and its derivatives after hydrolysis; and the ellagitannins, which produce ellagic acid after hydrolysis (Arbenz and Avérous, 2015). These tannins have been identified in numerous plants used in traditional medicine. They exhibit antiviral, antibacterial, and antitumoral activities (Jourdes et al., 2013).

Condensed tannins are the most popular phenolic compounds in plants, present mostly in barks and heartwood. They have also been found in fruits, leaves, and roots. These tannins are usually formed from 3 to 8 flavanoid repetition units or associated precursors of carbohydrates as well

as amino and imino acid traces (Arbenz and Avérous, 2015). They have been found at high concentrations (more than 10% dry weight) in woody tissues and possess antimicrobial activities against filamentous fungi, yeasts, and bacteria. They have been therefore considered as natural preservatives, and many of them have been studied in the context of eco-friendly wood preservation (Scalbert, 1991; Anttila et al., 2013).

Antimicrobial activities of tannins have been studied for a long time and were reviewed (Scalbert, 1991). The proposed inhibitory mechanisms include inhibition of extracellular enzymes, the competition to polysaccharides or nutrient substrates required for growth of microorganisms, direct inhibition of oxidative phosphorylation in metabolism, the formation of complexes with metal ions and cell membrane leading to morphological changes of cell wall and increasing permeability (Scalbert, 1991; Liu et al., 2013).

II.I.2.1.3 Stilbenes

Stilbenes are plant polyphenols characterized by the presence of a 1, 2 diphenylethylene nucleus. They are divided into two groups: oligomeric and polymeric stilbenes (Shen et al., 2009). Stilbenes are considered to be synthesized in response to mechanical wounds, fungal infection, and insect infestations (Shen et al., 2009).

Stilbenes play an important role in contributing to heartwood natural durability against brown-rot fungi (Venäläinen et al., 2004). Indeed, based on the chemical analysis of phenolics of wood samples of Scots pine from two distinct groups of trees including one resistant and the another susceptible to decay, that was classified based on one previously screening of the brown-rot fungus *Coniophora puteana* resistance (Harju and Venäläinen, 2002), results showed that there was a significant difference in the average content of pinosylvins including three individual stilbenes of pinosylvin, pinosylvin monomethyl ether, and pinosyvin dimethyl ether, between these two groups of trees, thereby there was a suggestion that stilbenes made a contribution to the differences in the decay rate of natural wood substrate, nevertheless, stilbenes alone are not involved in variation in the rate of decay between heartwood and sapwood (Venäläinen et al., 2004). The decay resistance role of stilbenes have been recently confirmed by an experiment of impregnation of Scots pine with stilbenes including pinosylvin and pinosylvin-monomethyl-ether as preservatives, that showed that they have the ability to resist to the common brown rot fungi (Lu et al., 2015).

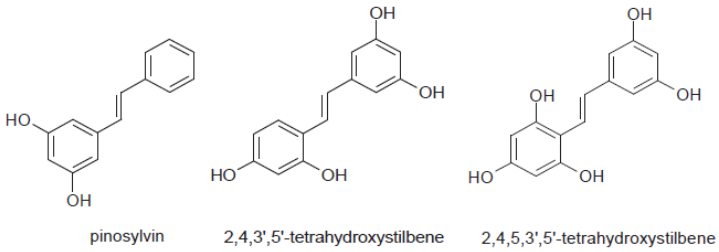

Figure 18. Structure of pinosylvin and derivatives.

Wood decaying fungi resistance mechanism of stilbenes therefore could be explained via studies on pinosylvin (Fig. 18). Pinosylvin is present in *pinus* species heartwood. The antifungal activity of this compound and of its monomethyl ether derivatives could be due to their action on -SH group found in active sites of several fungal enzymes (Celimene et al., 2005). To evaluate this hypothesis, the antifungal activity of a mixture of pinosylvin, pinosylvin-monomethyl-ether, and pinosylvin-dimethyl-ether was examined against white-rot and brown-rot fungi. The different antifungal assays indicated that these compounds were only active against brown-rot but not against white-rot fungi. The resistance of white-rot fungi was explained by their production of laccases and pectinases which have not -SH groups in their catalytic sites (Lyr, 1962). Furthermore, the antioxidant stilbenes could be also able to scavenge radicals required for wood degradation at the initial stages of infection by brown-rot fungi (Celimene et al., 2005; Schultz and Nicholas, 2000).

Some structure-function studies have also highlighted the mechanisms underlying the activity of stilbenes against wood decaying fungi (Schultz et al., 1990). Biological assays, involving a number of (E)-4 hydroxy-3'- and/or 4'-substituted stilbenes and related analogues, were performed on agar plates using the white rot fungus *T. versicolor* and two brown-rot fungi: *G. trabeum* and *Postia placenta*. The obtained results showed that the tested stilbenes have no or little activity against *T. versicolor*, while all compounds have fungicidal activity for both brown rot fungi. Furthermore, this study showed a linear relationship between the fungicidal activity and the hydrophobicity of the tested compounds. Combining these results with prior results, the authors proposed that stilbene compounds may be modified *in vivo* through partial methylation to enhance their activity (Schultz et al., 1990).

II.I.2.1.4 Lignans

Lignans are polyphenolic compounds widely distributed in the plant kingdom and are synthesized from the shikimic acid biosynthetic pathway. These compounds are dimeric with a β, β'-linkage between two phenyl propane units comprising various degrees of oxidation in the side-chains and a different substitution patterns in the aromatic moieties (Bertrand Teponno et al., 2016; MacRae and Towers, 1984).

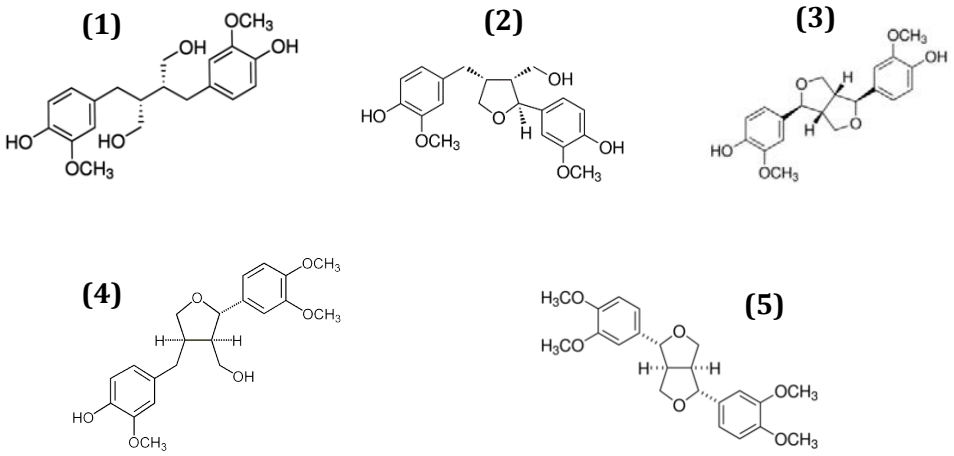

Figure 19. Chemical structures of lignans identified in methanol extractives of heartwood of *Araucaria araucana* (Mol.) K. Koch.: Secoisolariciresinol (1), lariciresinol (2), pinoresinol (3), 4-methoxy-pinoresinol (4) and eudesmin (5). From Céspedes et al. With modifications (Céspedes et al., 2014).

In plant, lignans have been isolated from all parts of the tree including root neck (Latva-Mäenpää et al., 2013), heartwood (Kawamura et al., 2005), and knots (Willför et al., 2005). They have antimicrobial and insecticidal activities, these properties explaining their defensive functions against pathogens and pests. For example, lignans including pinoresinol and secoisolariciresinol were shown to inhibit the growth and the production of the trichothecene of mycotoxin by *F. graminearum* (Kulik et al., 2014). In addition, some lignans possess antiviral, antifungal, antioxidant, antitumor, or immunosupression activities (Pan et al., 2009). The mechanisms of these biological activities have ever been previously described (MacRae and Towers, 1984). In addition to secoisolariciresinol, other lignans such as pinoresinol, eudesmin, lariciresinol, and lariciresinol-4- methyl ether, which were isolated from methanol extractives of *Araucaria araucana* (Mol.) K. Koch heartwood (Fig. 19), were also tested against a wide range of microbial agents including human and plant pathogens, white-rot, and wood-staining fungi. All compounds have activity against selected Gram positive bacteria, but not against Gram negative, the most active compound being pinoresinol. Secoisolariciresinol and total methanol extracts were able to completely inhibit growth of the wood decaying fungus *T. versicolor*. For pathogenic fungi, only

total methanol extracts were tested, and results showed inhibitory effects at concentrations of extract ranging from 2500 to 4000 µg/mL. From analyzed compositions of total extract, the authors proposed that the inhibition was related to the antioxidant properties of lignans (Céspedes et al., 2014).

II.1. 2.1.5 Quinones

Quinones have been isolated from the heartwood of both softwoods and hardwoods. Based on plant families, three groups of quinones could be identified in wood, as described in Fig. 20 (Leistner, 1985).

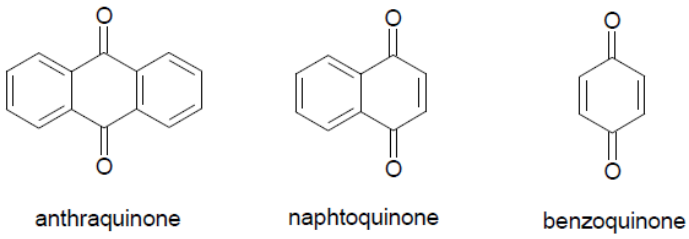

Figure 20. Classification of quinones.

Quinones are involved in the natural durability of wood. 4,5-Dihydroxy-epiisocatalponol and 2-methylanthraquinone were identified in Teak heartwood (*Tectona grandis* Linn. f.) and found at least in part to be responsible for the resistance against *T. versicolor*. They were proposed as chemical markers for rapid evaluation of teak natural durability (Niamké et al., 2012). Besides, another derivative, 2-(hydroxymethyl)anthraquinone, also exhibits antifungal activity (Niamké et al., 2011). Recently, quinones from plantation-grown Teak have been repeatedly shown to have important roles in resistance against both white-rot and brown-rot fungi including *T. versicolor*, *P. chrysosporium*, and *G. trabeum* (Rodríguez et al., 2019).

II.1.2.2 Terpenoids

Terpenoids or isoprenoids are terpenes attached to functional groups. All terpenoids are built with units of five carbon atoms. They range in size from volatile monomers (isoprene) to the polymer rubber. Terpenoids constitute the largest class of compounds produced by plants. They have been widely used in food, pharmaceutical, and chemical industries. In the plant kingdom, the production of terpenoids is essential for growth and development, and also for the plant interactions with abiotic and biotic environmental conditions, and therefore they play very important roles in ecology (Singh and Sharma, 2015; Tholl, 2015).

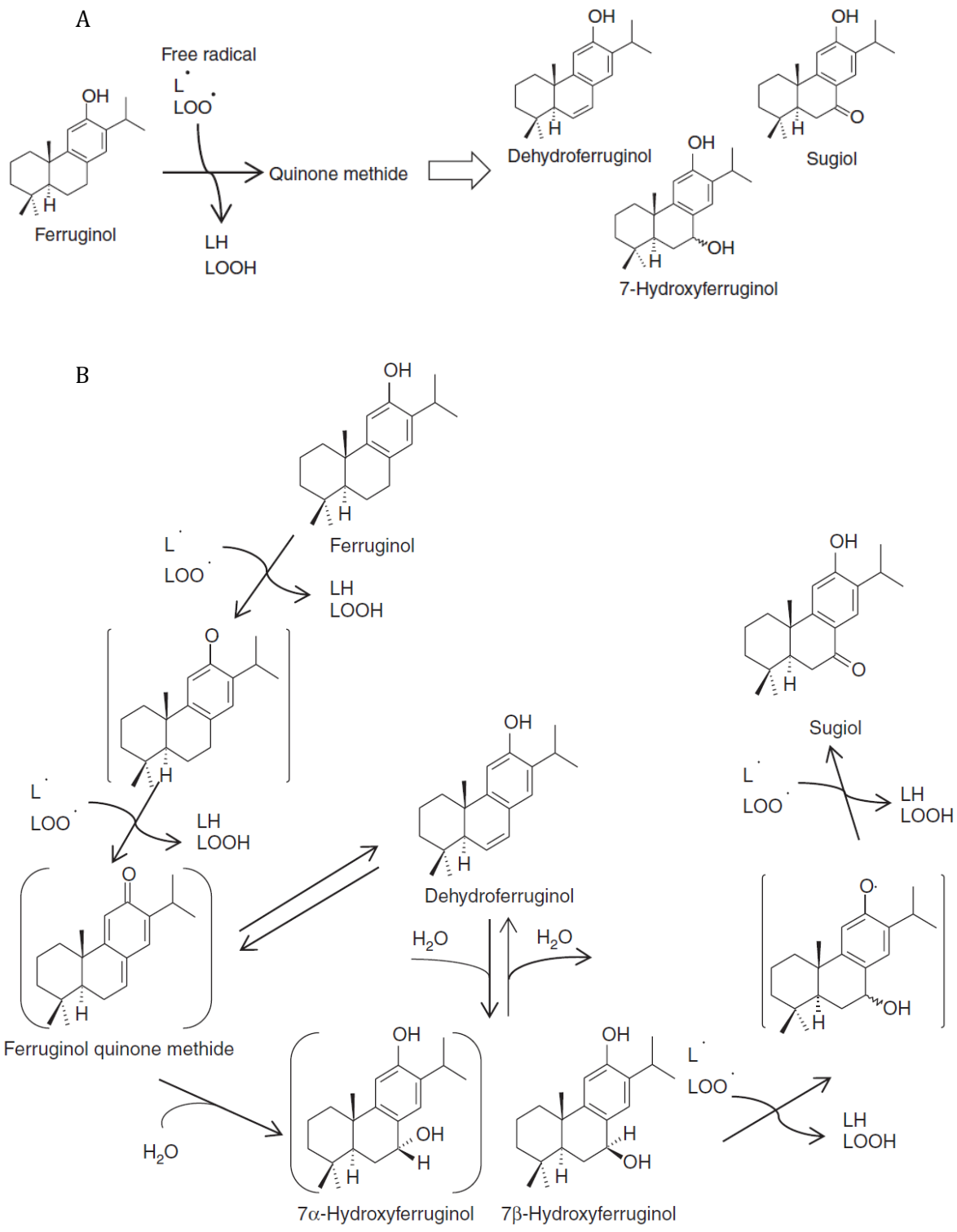

Figure 21. Antioxidant activity of ferruginol.

Antioxidant reaction of ferruginol (A), Proposed antioxidant mechanism of ferruginol against methyl linoleate oxidation (B). From Saijo et al. (Saijo et al., 2015).

In comparison with phenolic compounds, the effects of wood terpenoids against fungi and insects have been less studied. Investigation of defensive function has been restricted to terpenoids isolated from the heartwood of several species including Scots pine (Nerg et al., 2004), *Taiwania cryptomerioides* Hayata (Wang et al., 2005), *Cryptomeria japonica* D. Don (Kusuma and Tachibana, 2008). In these species, terpenoids exhibit antifungal and antioxidant activities (Kusumoto et al., 2010). For instance, among twelve terpenoids, ten of them belonging to abietane type components, isolated from cones of *Taxodium distichum* Rich, were examined for their antifungal activity against *T. versicolor* and *F. palustris*. The results showed potential relationships between the position and the number of hydroxyl groups in abietane type structures and antifungal activity (Kusumoto et al., 2010).

One of the best-studied wood terpenoids is ferruginol, a phenolic diterpene identified in the resin and heartwood of plants such as *Cryptomeria japonica* D. Don (Kusuma and Tachibana, 2008), *Taiwania cryptomerioides* Hayata (Wang et al., 2005). This compound was reported to have antifungal activity against basidiomycetes, in particular against *T. versicolor* tested on agar plates (Chang et al., 2005). Proteomic analyses have demonstrated that ferruginol induced a downregulation of cytoskeleton tubulin, multiple drug transporters, peroxiredoxin TSA1, polypeptide sorting, and DNA repair while upregulating heat shock proteins and autophagy-related protein 7. Ferruginol was then considered to cause cellular dysfunction and generate damages leading to growth inhibition and autophagic death cell (Chen et al., 2015). Previously, this compound was also reported to have antioxidant activities, (Fig. 21) (Saijo et al., 2015).

II.2 Wood decaying fungi

Wood degrading fungi of basidiomycetes are traditionally classified into two functional groups : brown rot and white rot fungi, according to their decaying mechanism and the visual appearance of the decomposed wood material. They are mainly polypore, gilled pleurotoid basidiomycota species of the class agaricomycetes. In nature, they are common inhabitants of forest litter or wood where they have an important role in the carbon cycle process.

Generally, wood-rotting fungi are not phytopathogenic, excepting some species from the genera *Heterobasidion*, *Fomitopsis,* and *Ganoderma* (Kües et al., 2015; Lundell et al., 2014). Besides, some species belonging to Boletales such as *Serpula lacrymans*, *Phlebiopsis gigantea, Phlebia centrifuga*, and *Hypholoma fasciculare*, are related to mycorrhizal fungi (Eastwood et al., 2011; Vasiliauskas et al., 2007).

II.2.1 Brown-rot fungi

Brown rot fungi belonging to wood-rotting basidiomycetes account for less than 10% of the lignocellulose degrading basidiomycetes. In the coniferous ecosystem, brown-rot fungi are considered to be the most important agents involved in the biodegradation of structural wood products as well as the dead-wood (Arantes and Goodell, 2014).

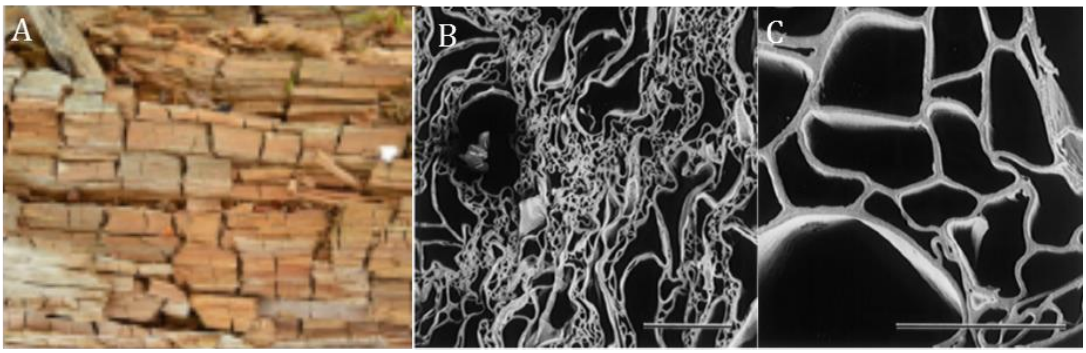

Figure 22. Decay of wood by brown rot fungi.

(A) Macroscopic image of degraded wood, show cubic (B) cellulose degradation in woody cell walls leaves a residual network of lignin, (C) Degraded cells exhibit porous and fragile walls. (Blanchette, 2000; Krah et al., 2018).

During the wood degradation, hemicelluloses are firstly attacked and rapidly depolymerized before degrading the celluloses resulting in cell wall carbohydrates degradation to leave lignin residues (Fig. 22B, C). Brown rotters have not the capability to mineralize lignin completely to form CO_2 and H_2O but they modify lignin to form polymeric residues, leading to a brown or rust color of the system. The degraded wood thus becomes dark in color, breaks into cubical fragments (Fig. 22A). Wood can easily turn into brown powders in the later stages (Martínez et al., 2005; Yelle et al., 2008). The main mechanism for wood destruction by brown rotter is non-enzymatic and oxidation via Fenton reaction which generates highly reactive free radicals. This statement is from an intensive analysis of chemical components of lignin from wood decayed by brown-rot fungus (Hammel et al., 2002; Kirk, 1975).

II.2.2 White rot fungi

White rot fungi are the group of wood-decaying fungi that are able to degrade all structural components of wood including cellulose, hemicellulose, and lignin. To degrade cellulose and hemicellulose, these fungi produce an array of extracellular hydrolases while for attacking lignin, they use a system with oxidative enzymes including the well-characterized peroxides, laccases and H_2O_2 generating enzymes.

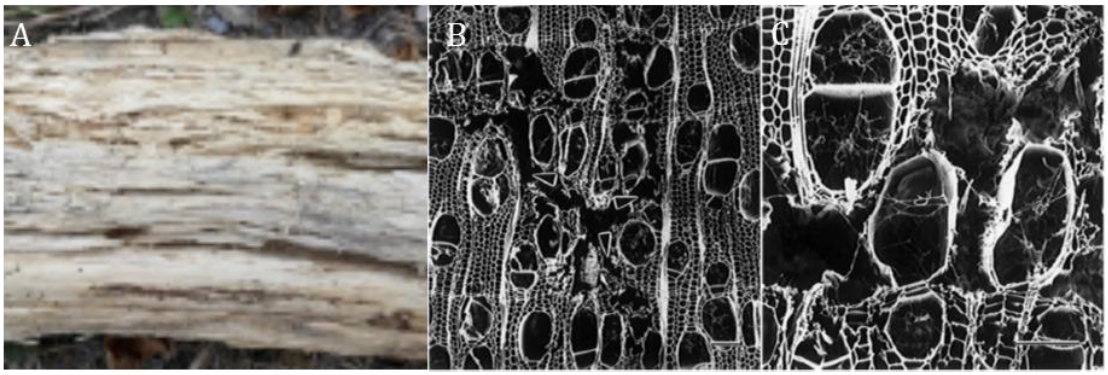

Figure 23. Decay of wood by white rot fungi.

(A) macroscopic image of wood degraded by white rot fungi, (B and C) microscopic image of transverse sections show nonselective attack, all cell wall components are degraded to form voids within degraded wood. Bar = 100 μm in B and C. (Blanchette, 2000; Krah et al., 2018).

Fungi of this group mainly belong to Basidiomycetes and account for over 90% of wood-decaying basidiomycete species. They colonize rather the wood of angiosperms than that of gymnosperms (Hatakka and Hammel, 2011). The decomposition of wood starts with quick attacks of hyphae to the cells of the wood, to create the condition for its development by secretion of the degradation systems. Upon degradation, wood fades gradually into white or yellow in color. Degraded wood is soft and fibrous (Fig. 23A). After the colonization of the cell's lumina and erosion of cell wall, progressive decay generates large voids filled with mycelium, referred to non-selective or simultaneous decay (Fig. 23B, C) (Blanchette, 2000).

II.2. 3 General biological characteristics of *Phanerochaete chrysosporium*

The genus of *Phanerochaete* belongs to the Polyporales, an order of saprophytic homobasidiomycetes growing on woody materials, with more than 90 identified morphologically heterogeneous species (De Koker et al., 2003). Due to its ability to degrade lignin selectively, *P. chrysosporium* is the most intensively studied white-rot basidiomycete. Similar to other species of *Phanerochaete,* this fungus is able to produce extracellular enzymes that degrade completely wood components. Extracellular oxidative components have also been shown to degrade a variety of persistent environmental pollutants, including polycyclic and chlorinated aromatic compounds, synthetic polymers, pesticides, munitions and dyes (Cameron et al., 2000).

P. chrysosporium was first named in 1974 after a description of a new species isolated from wood while collecting wood-rotting fungi in the Sonoran Desert, Arizona, in 1971. In nature, fruit bodies of this fungus can be collected from the undersides of decaying log-wood (Fig. 24) as well as from wood chip piles (Burdsall and Eslyn, 1974). This fungus generates simple crust-like fruiting bodies bearing basidia on the surface of a smooth hymenium and also produces ample conidia in

culture. The asexual form was previously described as a separate anamorphic genus. Because of the production of basidiocarps and basidiospores by strains derived from single basidiospores, the mating system of *P. chrysosporium* was considered to be homothallic. But analysis of putative mating-type genes showed evidence for a bipolar heterothallic mating system (Fig. 25) while not rejecting homothallism (James et al., 2011).

Figure 24. Wood degradation by *P. chrysosporium* in nature (Fulekar et al., 2013).

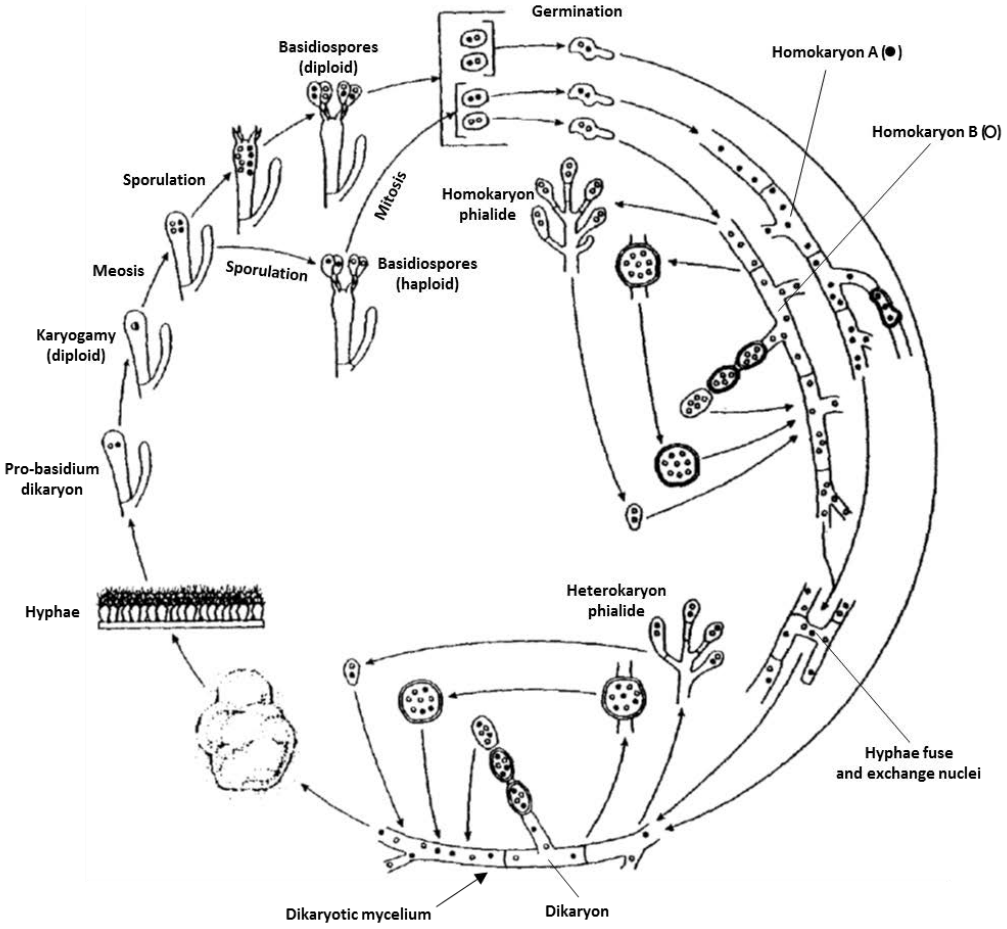

Figure 25. Life cycle of *P. chrysosporium*.

The nuclear status shown in each state gives assumption of a heterothallic incompatibility system, which is possessed by nearly all white rot fungi. From Young and Akhtar with the detail description for stages of the life cycle (Young and Akhtar, 1998).

Before 2000, there were three wild type strains commonly used including ME-466, BKM-F-1767, and OGC101, which is a derivative of ME-446 (MacDonald et al., 2012). Of those, BKM-1767 was the best-studied strain. However, using this strain with its dikaryotic nucleus hampered analysis of complex gene families. Furthermore, there were several limitations when using single-basidiospore strains for allelic variants from closely related genes. To solve these issues, a homokaryotic strain derived from BKM-1767, with the name *P. chrysosporium* RP78, was generated in 2000. This new strain contains identical nuclei (homokaryon) and under standard nitrogen-limited conditions, the activity of lignin-degrading enzymes is similar to that of the parental dikaryon. From 2000 on, this strain is usually used in studies for characterization of lignin and xenobiotic degradation with *P. chrysosporium*, especially after its genome was completely sequenced and reported in 2004 (Stewart et al., 2000; Martinez et al., 2004).

The genome of *P. chrysosporium* RP78 was the first sequenced genome of *Basidiomycota* and white-rot fungi. Analysis of its 29.9 Mb genome revealed a large array of genes encoding for lignocellulose degrading enzymes. In details, for extracellular oxidative enzymes in lignin degradation, the numbers of identified genes include: 10 lignin peroxidases (LiP), 5 manganese peroxidases (MnP), 7 copper radical oxidases or glyoxal oxidases (GLX), 4 multicopper oxidases (MCO) and one cellobiose dehydrogenase (CDH) (Kersten and Cullen, 2007). Interestingly, no sequences encoding laccases were found in the genome of *P. chrysosporium*. Laccase is the highly efficient phenol-degrading enzyme found commonly in other white-rot fungi. Concerning to the extracellular carbohydrate-active enzymes, in the version 2.2 of the annotated genome of fungus, there are 440 putative carbohydrate degrading enzymes among which there are 181 glycoside hydrolases, 89 auxiliary activity enzymes, 65 carbohydrate-binding modules, 20 carbohydrate esterases, 70 glycosyl transferases, and 6 polysaccharide lyases (Kameshwar and Qin, 2017). For the intracellular enzymes related to lignocellulose degradation, known as intracellular detoxification system, 149 genes of cytochrome P450 (Syed and Yadav, 2012) and 27 genes of glutathione S transferases were identified (Morel et al., 2009b).

II. 3 Antifungal mechanisms of wood extractives and fungal adaptation

Some antifungal compounds are popularly used in medicine. They are known to target fungal cell wall, membrane phospholipid bilayer, endoplasmic reticulum, DNA and RNA synthesis organelle, protein synthesis organelle and microtubule assembly (Odds et al., 2003). In this part, interactions between wood extractives and identified targets will be described and suggested mechanisms of detoxification will be discussed.

Extractives are involved in the heartwood natural durability. That role has been proven with resistance tests against wood decay fungi and insects after the removal of extractives from wood.

For example, a research was performed to examine the protective role of extractives in species with high durable wood from north America (Kirker et al., 2013). The obtained results showed a relationship between extractives content and resistance against wood decaying fungi but not with the quantity of extractives. The authors proposed that individual components of wood extractives confer the durability and also the discovery of active compounds could give wood preservatives (Kirker et al., 2013). This proposal was also consistent with previously obtained results (Taylor et al., 2007).

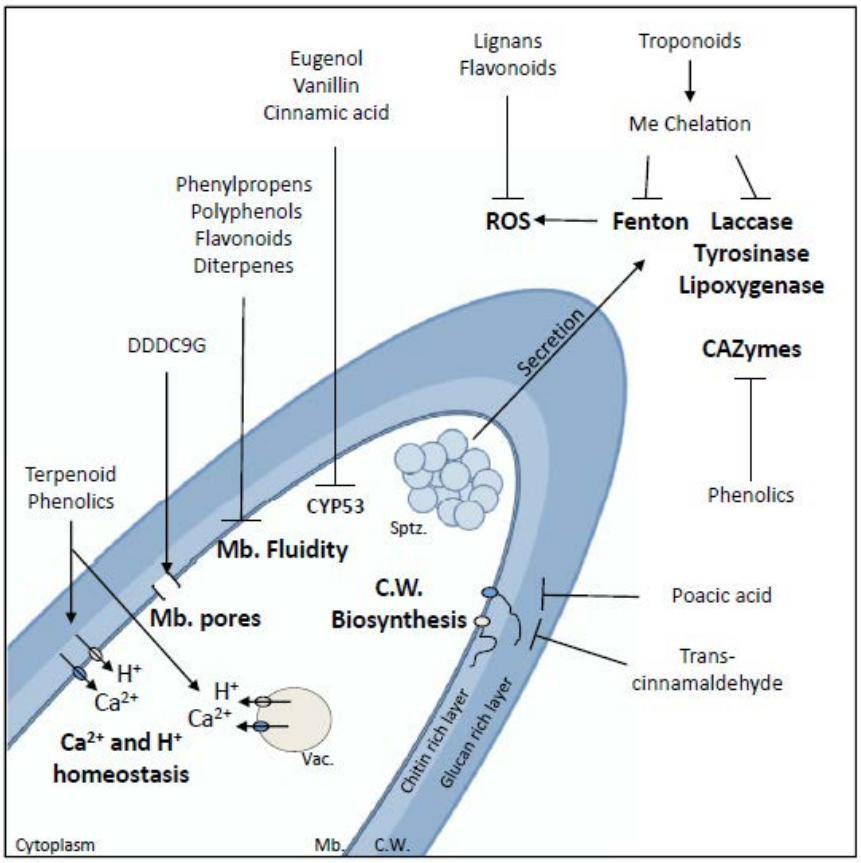

Figure 26. Effect of compounds derived from wood extractives at the tip of a fungal hypha. Different molecules from a mentioned family share the same effect. C.W.: cell wall, Mb.: plasma membrane, Vac.: vacuole, Sptz.: Spitzenkörper, ROS: reactive oxygen species, Me: metallic ions, DDDC9G: dihydro-dehydro-diconiferyl alcohol 9'-O-3-D-glucoside. From Valette et al. (Valette et al., 2017).

The progress of chemical analysis systems has led to the characterization of extractives in correlation with their biological activities. Those works have provided information concerning the most active isolated compounds and also revealed synergy between others. For example, a synergistic activity of moracins identified in *Bagassa guianensis* heartwood was proposed (Royer et al., 2012). Besides, the location and distribution of extractives could be also important for their activities (Royer et al., 2012). The synergy between wood extractives properties, involving fungicidal activity, free radical scavenging, and metal-chelating properties could also explain their involvement in natural durability (Schultz and Nicholas, 2000, 2002). By classifying these compounds according to their targets, four main mechanisms for fungal cell inhibition have been proposed including: metal and free radical scavenging; direct binding on wood-degrading enzymes; disruption of cell-wall and plasma membrane; perturbation homeostasis, chaotropic activity (Fig. 26) (Valette et al., 2017).

To cope with these compounds, fungi have developed different detoxification or protection strategies. Three main strategies were identified: stress responses; extracellular degradation and intracellular detoxification (Valette et al., 2017).

In the presence of wood extractives, intracellular stress is generated inducing a response, which leads in particular to the production of protective proteins. For example, in presence of oak wood extractives which are toxic for the white-rot fungus *P. chrysosporium*, the first response of this fungus is a transcriptional up-regulation of genes encoding for antioxidant systems including methionine sulfoxide reductase, catalase, peroxiredoxins or glutathione reductase (Thuillier et al., 2014).

In wood decaying fungi, extracellular oxidative enzymes are also very important for degradation not only of lignin but also of toxic compounds. In the presence of wood extractives, transcription of genes encoding for manganese and lignin peroxidases are strongly induced. For example, genes encoding for these enzymes are induced when cultivating *P. chrysosporium* in presence of oak wood extractives (Thuillier et al., 2014). Laccases, important extracellular enzymes for lignin degradation, were also shown to play a role in extractives detoxification. For instance, in the first stage of colonization of *T. versicolor* on *Fagus sylvatica* wood, there was a correlation of induction of these enzymes and extractives degradation. This result highlighted the role of laccases in removal of wood extractives (Lekounougou et al., 2008). Besides ligninolytic enzymes, the recent studies exploring the early response of *P. chrysosporium* to oak extractives have suggested that small secreted proteins (SSP) could also have important roles in cell protection and signaling (Fernández-González et al., 2018).

In addition to the extracellular system, the intracellular system also plays a crucial role in detoxifying toxic compounds of wood extractives. Intracellular detoxification pathways involved three main steps: an activation step through oxidation, the second with conjugation, and the third with either excretion or storage of the eliminated molecule. Multigenic families involved in these detoxification pathways and mainly studied in the context of wood degradation include the cytochrome P450 monooxygenases (CytP450ome) (Doddapaneni and Yadav, 2005; Syed and Yadav, 2012) and the Glutathione transferases (GSTome) (Morel et al., 2013; Valette et al., 2017). As an example, when *P. chrysosporium* was cultivated in presence of oak wood extractives, 12 CytP450 - encoding genes were induced (Thuillier et al., 2014). CytP450s of *P. chrysosporium* were also shown to transform compounds derived from wood extractives such as 7-ethoxycoumarin, flavone, and naringenin (Hirosue et al., 2011; Kasai et al., 2009, 2010). Concerning glutathione S transferases (GSTs), interactions between several compounds isolated from wood and GSTs from several classes have been investigated (Deroy et al., 2015; Mathieu et al., 2012, 2013; Meux et al., 2013). PcGSTFuAs are able to bind coniferaldehyde, vanillin, syringaldehyde, and catechin hydrate, this binding preventing their conjugating activity (Mathieu et al., 2012, 2013). PcGSTO3 and PcGSTO4 interact with antifungal terpenes from *F. sylvatica* and biochemical investigations suggested that catalytic cysteinyl residues could be involved in these reactions. (Meux et al., 2013). Results carried out with GSTOs of *T. versicolor* showed the binding of extractives such as gallic acid, epicatechin, and quercetin at the active site (Deroy et al., 2015).

In conclusion, wood extractives with antifungal activity can be used as a tool for functional characterization of the detoxification systems in wood decaying fungi (Morel et al., 2013). The next tasks, in line with the objectives of this thesis, are the identification of unknown components of those networks in addition to characterizing more in detail known components.

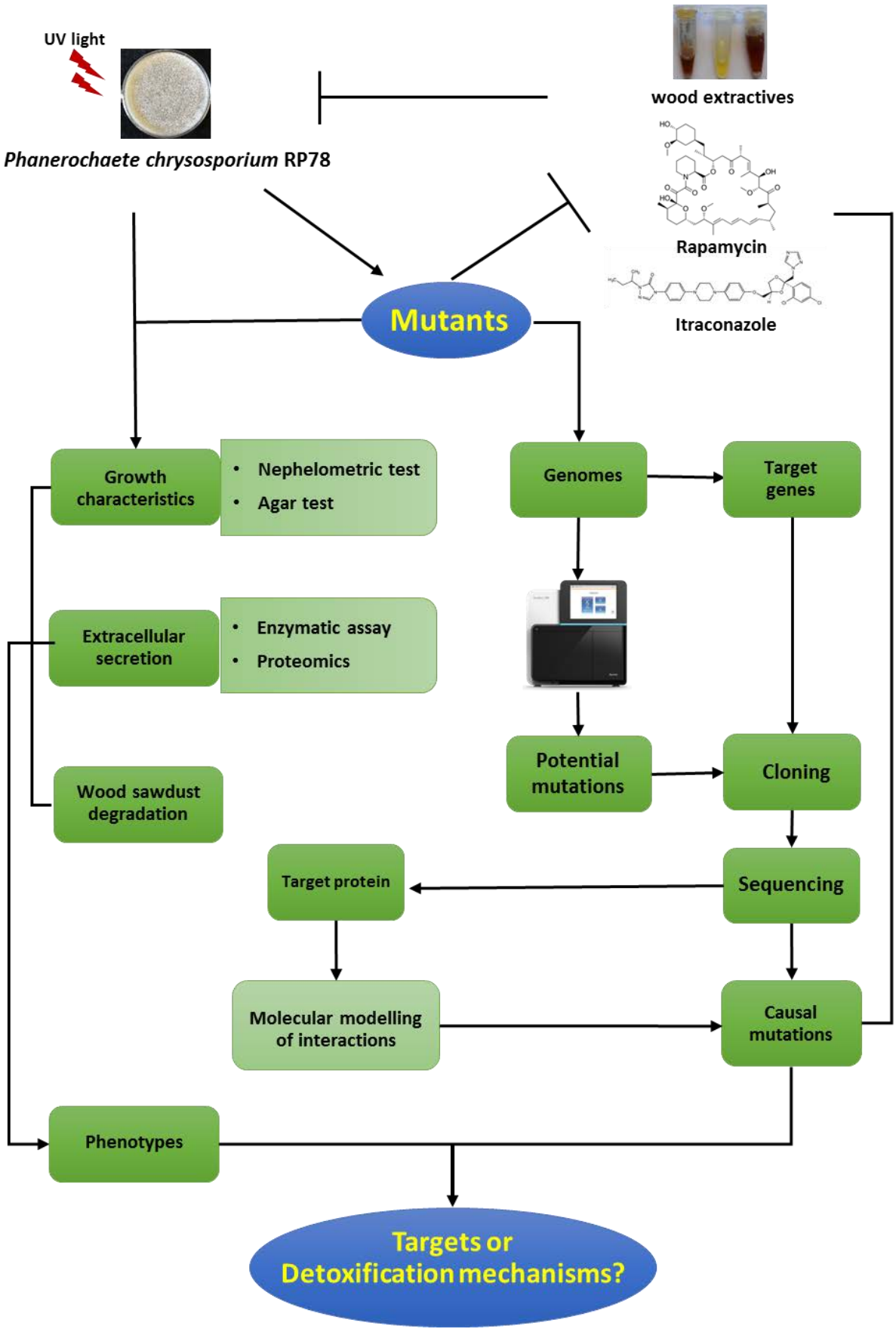

Figure 27. Scheme represents the main approach used in the thesis.

Objectives

As discussed in the introduction part, the wood decaying fungi possess the extracellular and intracellular detoxification systems enabling them to adapt to and bypass efficiently their toxic environment in the lignin or xenobiotic degrading process. Major proteins of these systems, especially, extracellular peroxidases, have been intensively biochemically characterized. In addition, several candidates of the intracellular system have also been described in recent years. However, **how these systems and their components coordinate is still unknown**. In fact, this point has been very little studied in the fungal kingdom as indicated in the discussion on the regulation of intracellular detoxification.

One of the major difficulties in characterizing the detoxification systems is the lack of genetic tools for basidiomycetes. Therefore, **a forward genetic approach was developed using *Phanerochaete chrysosporium* RP78.** Modules of the selected framework are described in Fig. 27.

The first work is generating mutant strains using classical techniques with the utilization of ultraviolet radiation as the mutation-causing agent. Mutation-containing spores were screened to obtain mutants resistant to antifungal compounds. WGS technology was planned to serve for the approach of the project. **The first objective of this project was to examine if WGS could be used to find candidate genes associated with resistance phenotypes in *P. chrysosporium*.** Therefore, the first selected compound was itraconazole which targets the cytochrome P450 monooxygenase Cyp51. Cyp51 is involved in the synthesis of ergosterol. Mining results obtained from WGS of the genomic background of mutants resistant to itraconazole showed that this technology has been highly reliable and could be used for the forward genetic approach in *P. chrysosporium*.

In a second step, rapamycin, which inhibits Target Of Rapamycin (TOR), one highly conserved protein in eukaryotic cells, was used. TOR has been intensively characterized in model yeasts where it is the central regulator of the cell. TOR has been identified in several important filamentous fungi, but not in *P. chrysosporium*. Therefore, **the second objective was to identify and characterize TOR in this fungus before generating mutants resistant to rapamycin.** In this project, TOR identification was done, and by mining genomic data, TOR signaling pathway also was identified in this fungus. Importantly, TOR has been found to have a key role in regulating the extracellular secretion system in *P. chrysosporium*. For mutants resistant to rapamycin, classical genetic techniques including sequencing directly target genes or indirectly through cloning were performed. The identified mutations enabled building a hypothesis linking a given

mutation on TOR genes in *P. chrysosporium* to quantified phenotypes belong to TOR genes in *P. chrysosporium*. The WGS is required to be performed individually for each mutant to confirm this hypothesis.

The WGS, that was confirmed as a reliable technique serving for the forward genetic approach in *P. chrysosporium*, was continuously used to find high potential targets in mutants resistant to wood extractives previously used for screening them. **The next objective of our project was to identify the candidate genes related to the phenotypes that exhibit *Bagassa guianensis* wood extractives resistance.** Data mining of the genomic background of two selected mutants showed the same mutation of one gene with high frequency (> 0.75). The classical cloning technique was used to confirm the mutation. The sequence analysis combined with molecular modeling results in several hypotheses explaining the toxic activity of extractives but also to the link of this target to the extracellular secretion system. Mining supplementary data to identify the causative elements linked to *Prunus avium* wood extractives resistance phenotype gave more one uncharacterized target in *P. chrysosporium*. Analysis of possible relationships among identified targets from the works of this thesis and integration with available data of this fungus enabled to propose a new potential detoxification pathway. Therefore, it is possible that a new emerging detoxification pathway necessary in *P. chrysosporium* is yet to be discovered.

RESULTS

Article I

Whole-genome sequencing as an efficiently-applicable technique for the forward genetic approach in characterizing the fungus *Phanerochaete chrysosporium*

(This paper was submitted to the journal *Genes, Genomes, Genetics*, and under revisions for publication)

Introduction: *Phanerochaete chrysosporium* is a model of wood decaying fungi. This fungus exhibits well-characterized extracellular wood degrading enzymes and also possesses various intracellular detoxification enzymes that give it the very high capability of degrading a variety of xenobiotic compounds in environment. Understanding how these complex networks are regulated and correlated required more studies, which are restricted due to the absence of genetic tools. Nevertheless, the recent advances in genome sequencing technology suggest that a forward genetic approach could be used based on whole-genome sequencing (WGS). Here we report a strategy of mapping by sequencing and of candidate gene identification within the same genetic background using only mutagen-induced changes as marker with the simple itraconazole resistance phenotype. Itraconazole was selected because its target, the cytochrome P450 monooxygenase (Cyp51) that catalyzes ergosterol biosynthesis, has been intensively characterized in several fungi.

Results: Mutants of *P. chrysosporium* resistant to itraconazole (*rit* mutants) were generated by UV light and their genomic DNA have been sequenced. Mutations leading to amino acid substitution have been identified in the itraconazole target (CYP51) encoding gene. Those mutations limit the inhibitory effect of itraconazole and allow *rit* mutants to have ergosterol production in the presence of itraconazole. The obtained results confirm that such an approach could be used to investigate the detoxification system of *P. chrysosporium*.

Isolation of mutants resistant to itraconazole in the lignin-degrading basidiomycete *Phanerochaete chrysosporium* RP78 leads to identification of allele in *CYP51*/ *ERG11*

Authors: Sormani Rodnay[1], Fernandez-Gonzalez Antonio[1], Roret Thomas[1, 3], Hego Elena[1], Nguyen Duy Vuong[1], Valière Sophie[2], Morel-Rouhier Mélanie[1], Gelhaye Eric[1].

[1] Université de Lorraine, INRAE, IAM, F-54000 Nancy, France

[2] US1426, GeT-PlaGe, Genotoul, Castanet-Tolosan, France

[3] Present address: CNRS, LBI2M, Sorbonne Universités, Roscoff, France

Short title:

rit mutants in *P. chrysosporium*

Key words:

Phanerochaete chrysosporium, itraconazole resistance, UV mutagenesis

Corresponding author:

Rodnay Sormani

Mail: rodnay.sormani@univ-lorraine.fr

Tel: + 33 3 72 74 51 59

Unité Mixte de Recherches 1136 Université de Lorraine/INRA

Interactions Arbres / Micro-organismes

Faculté des sciences, entrée 1B, 3éme étage

Bd des aiguillettes

54500 VANDOEUVRE-Lès-NANCY

France

Abstract

Phanerochaete chrysosporium is a model of white-rot fungus able to degrade all components of wood. Since we have access to the genome sequence of the strain *P. chrysosporium* RP78, forward genetic strategy using next-generation sequencing can be a powerful tool to decipher the molecular basis of white-rot fungi physiology. As a proof of concept of whole-genome sequencing of pool of individual mutants strategy in the white-rot *P. chrysosporium*, we choose to analyze the resistance to itraconazole. Itraconazole is a well-known antifungal drug belonging to the triazole family compounds inhibiting ergosterol biosynthesis by acting on lanosterol 14-alpha-demethylase CYP51 in other fungal species. Random mutagenesis has been done and mutants with *resistant to itraconazole* phenotype have been selected and their genomic DNA have been sequenced. Mutations leading to amino acid substitution have been identified in *CYP51* encoding gene. Those mutations limit the inhibitory effect of itraconazole and it allows *rit* mutants to have ergosterol production in presence of itraconazole. From this work, another interesting point is the possibility to produce and characterize mutants in *P. chrysosporium* RP78, these open further studies to better understand the molecular basis of the white-rot fungus living model.

Introduction

Wood biodegradation is a complex phenomenon involving a consortium of organisms. In forest ecosystems, the main microbial drivers of this process are fungi. Among these latter, white-rot fungi are able to degrade and mineralize all wood components and in particular the recalcitrant lignin. This unique feature has been extensively investigated starting with the extracellular enzymes involved in the breakdown of lignocellulosic materials in the model *Phanerochaete chrysosporium* (Kersten and Cullen, 2007; Tien and Kirk, 1983, 1984; Wariishi et al., 1991). The development of genomic and proteomic tools coupled to the industrial aim to produce energy from lignocellulosic biomass have led to a better understanding of the key enzymatic networks involved in the lignocellulose breakdown and in the catabolism of the decay byproducts (Eastwood et al., 2011; Floudas et al., 2012; Riley et al.,

2014). Recent phylogenomic analysis has proposed that the adaptation of white-rot fungi to their way of life concerns mainly the evolution of both extracellular decay systems and intracellular transport and detoxification systems (Nagy et al., 2017). However, a better understanding of thess complex phenomena is still restricted due to the lack of efficient genetic approaches for the transformation of agaricomycetes. Several attempts to transform *P. chrysosporium* have nevertheless been successful (for example (Alic et al., 1991; Li et al., 2000; Ma et al., 2001; Sharma and Kuhad, 2010). However, efficient genetic tools for studying basidiomycetes remain to be developed. In this context, forward genetic strategy using next-generation sequencing (NGS) could be a powerful tool to identify genes of interest in these fungi. This approach is based on several steps. First, organisms with well-defined genetic backgrounds are mutagenized using DNA damaging agents, which yields random mutations. The population of mutants is then screened for interesting phenotypes. At the last step, NGS could be used to identify the involved mutated genes from the mutants population (Schneeberger, 2014). The mapping-by-sequencing strategy is now widely used to map and identify phenotype-causing mutations in various species (Besnard et al., 2017; Laothanachareon et al., 2018; Schlötterer et al., 2014; Schneeberger, 2014), but at the best of our knowledge it has never been applied to rot fungi.

In order to demonstrate the feasibility of such approach in the model white-rot *P. chrysosporium*, we have chosen to identify gene(s) potentially involved in the resistance of itraconazole in this fungus. Itraconazole is a well-known antifungal drug belonging to the triazole family compounds inhibiting ergosterol biosynthesis by acting on ERG11/CYP51. That protein belongs to the family of cytochrome P450 monooxygenase and exhibits lanosterol 14α demethylase activity. Pathogenic fungal strains resistant to azoles have been identified in *Aspergillus fumigatus* (Diaz-Guerra et al., 2004), *Cryptococcus neoformans* (Sionov et al., 2012), *Candida albicans* (Flowers et al., 2015) and the most common mechanism of resistance is due to mutations causing alterations in the *ERG11/CYP51* gene. *P. chrysosporium* possesses a large number of genes (around 150) encoding cytochrome P450 (Syed and Yadav, 2012; Syed et al., 2014) and as expected a gene encoding CYP51 from this fungus has been shown to interact with triazoles (Warrilow et al., 2008).

Here we report a strategy mapping by sequencing and candidate gene identification within the same genetic background using only mutagen-induced changes as marker and the simple resistant to itraconazole phenotype. The causal link between mutations found and the phenotype has also been investigated.

Material and methods

Fungal strain

Fungal strain used in this study is *Phanerochaete chrysosporium* RP78, the homokaryotic strain isolated from dikaryotic strain *P. chrysosporium* BKM F-1767 through generation of protoplast (Stewart et al., 2000). All the cultures were maintained on solid Malt Agar medium (20 $g.L^{-1}$ and 30 $g.L^{-1}$ respectively).

Mutagenesis and screening of conidia from *P. chrysosporium*.

Conidia of wild type strain *P. chrysosporium* RP78 were obtained by cultivation on sporulation medium (Glucose (10 $g.L^{-1}$), malt extract (10 $g.L^{-1}$), peptone from potato (2 $g.L^{-1}$); yeast extract (2 $g.L^{-1}$), asparagine (1 $g.L^{-1}$), KH_2PO_4 (2 $g.L^{-1}$), $MgSO_4.7H_2O$ (1 $g.L^{-1}$), thiamine HCl (1 $mg.L^{-1}$), Agar (30 $g.L^{-1}$), all chemicals used were purchased from Sigma Aldrich. Mycelia were cultivated at 37°C for 5 days. These conidia were exposed in UV light for 30 s. Mutated spores were continuously suspended in water and filtered with Miracloth. A volume of suspension with 10.000 spores were used and plated on the Petri dish containing Malt-Agar medium (20 $g.L^{-1}$, 30 $g.L^{-1}$ respectively) mixed with 8 $mg.L^{-1}$ of itraconazole (Sigma Aldrich R51211). Petri dishes were incubated at 25°C until appearance of individual mycelium on medium surface. Appeared mycelia were harvested and cultivated on sporulation medium mixed with 8mg. L^{-1} of itraconazole. 10,000 conidia developed on that medium were moved into a Falcon tube containing 10 ml of liquid medium of 1% Malt in presence of 8 $mg.L^{-1}$ of itraconazole. Single spore progenies growing in liquid medium were fished and grown on sporulation medium mixed with itraconazole. Spores from this medium were used to establish mutant lines called *rit* mutants for further experiments.

DNA extraction

Genomic DNA from the different mutants and WT strains were individually extracted using Qiagen DNeasy Plant Mini Kit according to manufacturer protocol. DNA concentration was estimated using Qbit measurement.

Sequencing procedure

DNAseq was performed at the GeT-PlaGe core facility, INRA Toulouse. DNA-seq libraries were prepared according to Illumina's protocols using the Illumina TruSeq DNA PCR-free HT Library Prep Kit. Briefly, DNA was fragmented by sonication, size selection was performed using SPB beads (kit beads) and adaptors were ligated to be sequenced. Library quality was assessed using an Advanced Analytical Fragment Analyzer and libraries were quantified by qPCR using the Kapa Library Quantification Kit. DNA-seq experiments were performed on an Illumina HiSeq3000 using a paired-end read length of 2x150 pb with the Illumina HiSeq3000 Reagent Kits.

SNP identification

Firstly, the reads belonging to the sequenced mutants coming from high-throughput sequencing with BWA (Li and Durbin, 2009) were mapped to the reference genome of *P. chrysosporium* RP78 v2.2 (Martinez et al., 2004; Ohm et al., 2014). Secondly, the VCF file containing the called SNPs was performed with SAMtools (Li, 2011). Finally, the SNPs filtering, frequencies calculation and visualization were made with SHOREmap v3.5 (Sun and Schneeberger, 2015).

PCR validation

PCRs were performed at an annealing temperature of 57°C using iProof High-Fidelity DNA polymerase from BioRad with primers 47003f (TTCCCCAACCTTCCTCTCG) and 48216r (CTAGGGCCTCCTCTGTTGTG). PCR products were purified using kit and then sequenced.

Modeling

Firstly, the 3D structure of *P. chrysosporium* lanosterol 14-alpha-demethylase (CYP51) was generated by the SWISS-MODEL web server (Biasini et al., 2014). Among the various solutions, the crystal structure of CYP51B (51% identity) from a pathogenic filamentous fungus *A. fumigatus* pdb entry 4UYL (Hargrove et al., 2015) was used as template. Thus, for the PcERG11 structural model, a global model quality estimation (GMQE) score of 0.69 was obtained indicating a high reliability between the target and the template. Secondly, the resulting structure was improved by energy minimization in explicit water using the YAMBER force field of the YASARA server (Krieger Elmar et al., 2009). The same procedure was used to determine CYP51 A290V structure.

In each case (CYP51 and CYP51 A290V), the lanosterol and the itraconazole binding sites were obtained by homology modelling from the X-ray crystal structures of *Saccharomyces cerevisiae* lanosterol 14-alpha demethylase ERG11 (pdb entries 4LXJ and 5ESG, respectively) (Monk et al., 2014).

Ergosterol measurement

Ergosterol extraction was adapted from (Gong et al., 2001). Fungal biomass was placed in a 15 mL falcon tube, with 3.5 g of acid-washed glass beads and 6 mL of methanol. After been vortexed for 15 s, tubes were shaken for 1 h at 300 rpm protected from light with aluminum. The mixture was then let to precipitate for 15 min in the dark. An aliquot of 1.8 mL was transferred in a 2 mL Eppendorf tube and centrifuged 10 min at 11000 rpm at 4°C. Supernatant was filtered using sterile syringes and 0.45µm filter then stored in a brown vial at 4°C. 50 µL were loaded for the HPLC analysis.

Ergosterol analysis was performed on a Shimadzu HPLC equipped with a Kinetex C18 (2.6 µm 100x4.6mm) reverse-phase column and using a mix of methanol (95%) MetOH, 5% H_2O as mobile phase (flow rate of 1.6 $mL.min^{-1}$). Ergosterol quantification was then performed using a standard curve of ergosterol (Sigma, purity ≥ 95%) dissolved in methanol.

To estimate the effect of itraconazole treatment on fungal ergosterol production of the three strains (WT, *rit1* and *rit16*), a two factors ANOVA was performed and followed by a Tukey HSD test to estimate the differences between each experimental conditions. Statistical analyses were conducted on R v2.11.1 (R Foundation for Statistical Computing; Vienna, Austria).

Results

Isolation and characterization of *rit* mutants

First of all, *P. chrysosporium* RP78 was tested for its sensitivity to itraconazole. Fungal cultures have been done on malt-agar plates and exposed to itraconazole dropped on Whatman paper dots. Several amounts of itraconazole were tested and growth was affected (Fig. S1 and file S1). From this point we could performed the mutagenesis and screening for mutant using itraconazole.

To produce mutations in *P. chrysosporium* RP78, conidia were exposed to UV light for 30 s then plated on malt-agar plate supplemented with the selective agent itraconazole at 8 $mg.L^{-1}$ which is the threshold used in *A. fumigatus* to identify strains resistant to itraconazole (Diaz-Guerra et al., 2003). This concentration is 8 times the lowest dose tested which inhibit WT *P. chrysosporium* RP78 to grow (Fig. 1 and Fig. S1). After 5 days of culture at 27°C, appearance of small colonies was observed on the selective plates. Forty individual colonies were picked up and sub-cultured on fresh new sporulation medium containing itraconazole for one week; those are the original 40 *resistant to itraconazole* mutants (*rit*). For each mutant, conidia were harvested from those plates and around 10,000 of them were placed in 10 mL of 1% Malt medium with 8µg. mL^{-1} of itraconazole. After 48h of culture germinated conidia were fished individually and plated. Only 31 of the 40 mutant strains were able to be developed under this culture procedure. This is probably due to mutations, caused by UV exposure, in genes involved in asexual reproduction cycle. A second round of conidia production and isolation was done and lines established from that point were considered as “one spore progeny”. As expected, in contrast to the wild type, the obtained mutated fungal lines are able to grow on itraconazole containing medium (Fig. 1, file S2).

Identification of the causal mutation in *CYP51/ ERG11*

To gain insight about the molecular mechanism leading to this *rit* phenotype, a whole-genome sequencing of pool of individual mutant strategy was used. The first step was to extract individually genomic DNA (gDNA) from each of the identified *rit* mutant. Same amount of DNA from each individual mutant was pooled, and then gDNA from WT have been added in a ¼ ratio of the total amount of DNA. This gDNA mix was sequenced using HiSeq3000 technology.

The obtained sequences were aligned with the reference genome from the JGI (Ohm et al., 2014) revealing a unique list of mutations (Table S1). All those mutations could be mapped to the reference genome and a frequency value was calculated for each of them (Fig. 2A and Table S1). This value reflects the number of sequenced reads having a mutation in a specific position, in comparison to the total number of sequenced reads for the same position. Due to the design of our experiment, a frequency value higher than 75% indicated the presence of mutations in the genome of the used WT strain when compared to the reference genome. Even if the used strain of *P. chrysosporium* RP78 was the one that has been sequenced in 2004 (Martinez et al., 2004), years of subculture can indeed lead to mutations. This phenomenon has already been observed in other fungi (Jeon et al., 2013).

From our results, 11649 SNPs have been highlighted in the collection, 5344 are non-intergenic and 22 mutations occurred with a frequency value of 100%, one of them is in an intronic region the others are in the coding sequences (Fig. 2A and Table S1).

To pursue the analysis and identify the potential mutation(s) responsible for the *rit* phenotype, SNP possessing a frequency score of 75% have been searched. We identified a SNP with a frequency score of 75% located on Scaffold 16 at the 47253 position. This SNP is due to a C to T substitution. Interestingly a SNP (also a substitution: T to C, occurring at a frequency of 19%) for the next nucleotide (Scaffold 16 position 47254) was also detected, however with a lower frequency. Both mutations are located in the fifth exon of the AGR57_13091 gene (Fig. 2B). This gene encode the *P.chrysosporium*'s lanosterol 14-alpha-demethylase CYP51 which is known to interact with itraconazole (Warrilow et al., 2008).

To confirm these results, this part of the genome has been amplified in each tested mutants from gDNA and the resulting PCR products have been sequenced individually. All the mutants share the same mutation on Scaffold 16 at the 47253 position. The mutation at the next position is observed in 13% of them. Both mutations are not observed in the itraconazole sensitive WT. Interestingly, both substitutions affect the same triplet of nucleotide leading to the same amino acid substitution in the protein sequence. The alanine in position 290 is indeed substituted by a valine in the *rit* mutants (Fig. 2B).

Docking experiments of itraconazole in CYP51 A290V

The sequence homology between AGR57_13091 gene product and CYP51B from *A. fumigatus* (51%) allowed us to carry out modeling experiments (Figure 3). In the built model, itraconazole can fit in the active site of AGR57_13091 encoding protein identified as a target in previous step (Fig. 3A). Focusing on the lanosterol and the itraconazole binding pockets, 13 residues could be involved in the stabilization of one or both molecules (Ala48, Tyr51, Gly52, Thr106, Tyr116, Phe216, Phe221, Ala290, Ala294, Ile363, His364, Ser365 and Tyr504). Only 4 of the 13 residues are in close proximity (distance less than 3.5Å) to the itraconazole molecule and are far (distance greater than 3.5 Å) from the lanosterol molecule (Fig. 3B and 3C). Three of them (Ala48, Tyr51 and Gly52) are located at the entrance of the binding pocket and the last one (Ala290) is in the core active site close to the heme molecule. Thus, a mutation of Ala290 by bigger amino acids (such as valine in this case) should not interfere in the enzyme activity but will probably hinder the itraconazole binding (Fig. 3D and 3E).

Ergosterol biosynthesis in *rit* mutants

Since itraconazole leads to the inhibition of ergosterol biosynthesis, ergosterol content of *rit1* and *rit16* and WT strains has been measured. Those two mutant strains have been chosen because they are, respectively, the first strain identified with the single substitution and the first strain identified with the double mutation in their sequences. The design of the experiments is described in the materials and methods section. In liquid medium, in absence of itraconazole, a similar amount of ergosterol has been measured in WT and *rit16*, whereas this amount is slightly decreased (1 $\mu g.mg^{-1}$ on a total of 5.6 $\mu g.mg^{-1}$) in *rit1* (Fig. 4). These results suggest strongly that the UV induced mutations have not or few effects

on the efficiency of ergosterol biosynthetic pathways in the selected mutants. In contrast, in presence of itraconazole, the amount of ergosterol is strongly altered in WT and in both mutants. In the WT, after itraconazole treatment, the ergosterol amount represented around 34% of that one measured in the control experiment (1.9 *vs*. 5.6 $\mu g.mg^{-1}$). In contrast, for the both tested *rit* mutants, the amount of ergosterol remained around 50% of the amount found in absence of itraconazole (2.6 *vs*. 4.6 $\mu g.mg^{-1}$ for *rit1* and 2.9 *vs*. 5.2 $\mu g.mg^{-1}$ for *rit16*).

Discussion

In many ecosystems and in particular in forest ecosystems, agaricomycetes are involved in many fundamental processes. As symbiotic or pathogenic organisms, some of them are major actors of the tree growth whereas other such as wood decaying fungi are involved in the organic matter recycling. The study of the molecular mechanisms governing these fundamental processes is limited by the lack of genetic tools for basidiomycetes due particularly to the technical difficulties encountered to transform these organisms. The aim of this study was to propose a strategy to identify genes of interest in these organisms. It was based on random mutations induced by UV treatment, followed by a whole genome sequencing of the selected mutants. To validate the approach, the resistance of the white rot *P. chrysosporium* to itraconazole (a well-known inhibitor of the ergosterol biosynthesis) was used. As expected, *P. chrysosporium* was found to be sensitive to itraconazole allowing us to use it for the proposed strategy. After UV treatment and selection of mutants able to grow on 8 $\mu g.mL^{-1}$ of itraconazole in the tested conditions, genomic DNAs of these mutants were pooled and sequenced in a single round. Analysis of SNPs frequency allowed the identification of mutation inducing an amino acid change in the AGR57_13091 gene. This gene mutation is relevant in this study, since AGR57_13091 is predicted to encode the lanosterol 14-alpha-demethylase CYP51 known to be the target of itraconazole (Warrilow et al., 2008). The observed mutation causes the following substitution: A290V. From modeling experiments, it appears that the lateral chain of V290 could be responsible for a steric hindrance of the itraconazole binding, without altering the substrate binding pocket. This hypothesis is in agreement with higher amount of the ergosterol amount measured in the tested mutants in presence of itraconazole compared to wilt type, suggesting that the inhibitory efficiency of

itraconazole on the mutated protein is decreased. Substitutions in CYP51 sequence leading to itraconazole resistance have already been described in *A. fumigatus, C. neoformans, C. albicans* however involving other amino-acid residues (Diaz-Guerra et al., 2004; Flowers et al., 2015; Sionov et al., 2012).

Taking together, these data support the used strategy that has allowed to identify candidate gene involved in the itraconazole inhibition in *P. chrysosporium*. Using *P. chrysosporium* and the resistance to itraconazole as proofs of concept, we propose that the strategy developed in this study could be useful to detect candidate genes involved in many fundamental processes involving agaricomycetes. Nevertheless, this strategy is still restricted to an efficient selection of the obtained mutants. The *rit* mutants obtained in this study could be the first step to develop efficient genetic tools for at least the white-rot model *P. chrysosporium*.

Funding

This work was supported by a grant overseen by the French National Research Agency (ANR) as part of the "Investissements d'Avenir" program (ANR-11-LABX-0002-01, Lab of Excellence ARBRE). FGA was supported by a postdoctoral grant from Region Grand Est. NDV was supported by a Doctoral Fellowship from the Ministry of Agriculture and Rural Development, Vietnam (Agricultural and Fisheries Biotechnology Program) and support from French ministry of foreign affair (program Campus France).

References

Alic, M., M. B. Mayfield, L. Akileswaran, and M. H. Gold, 1991 Homologous transformation of the lignin-degrading basidiomycete *Phanerochaete chrysosporium*. Curr Genet 19: 491–494.

Besnard, F., G. Koutsovoulos, S. Dieudonné, M. Blaxter, and M.-A. Félix, 2017 Toward Universal Forward Genetics: Using a Draft Genome Sequence of the Nematode *Oscheius tipulae* To Identify Mutations Affecting Vulva Development. Genetics 206: 1747–1761.

Biasini, M., S. Bienert, A. Waterhouse, K. Arnold, G. Studer et al., 2014 SWISS-MODEL: modelling protein tertiary and quaternary structure using evolutionary information. Nucleic Acids Res 42: W252–W258.

Diaz-Guerra, T. M., E. Mellado, M. Cuenca-Estrella, and J. L. Rodriguez-Tudela, 2004 A Point Mutation in the 14α-Sterol Demethylase Gene cyp51A Contributes to Itraconazole Resistance in *Aspergillus fumigatus*. Antimicrobial Agents and Chemotherapy 48: 1071–1071.

Eastwood, D. C., D. Floudas, M. Binder, A. Majcherczyk, P. Schneider et al., 2011 The Plant Cell Wall–Decomposing Machinery Underlies the Functional Diversity of Forest Fungi. Science 333: 762–765.

Floudas, D., M. Binder, R. Riley, K. Barry, R. A. Blanchette et al., 2012 The Paleozoic Origin of Enzymatic Lignin Decomposition Reconstructed from 31 Fungal Genomes. Science 336: 1715–1719.

Flowers, S. A., B. Colón, S. G. Whaley, M. A. Schuler, and P. D. Rogers, 2015 Contribution of Clinically Derived Mutations in ERG11 to Azole Resistance in *Candida albicans*. Antimicrobial Agents and Chemotherapy 59: 450–460.

Gong, P., X. Guan, and E. Witter, 2001 A rapid method to extract ergosterol from soil by physical disruption. Applied Soil Ecology 17: 285–289.

Hargrove, T. Y., Z. Wawrzak, D. C. Lamb, F. P. Guengerich, and G. I. Lepesheva, 2015 Structure-Functional Characterization of Cytochrome P450 Sterol 14α-Demethylase (CYP51B) from *Aspergillus fumigatus* and Molecular Basis for the Development of Antifungal Drugs. J. Biol. Chem. 290: 23916–23934.

Jeon, J., J. Choi, G.-W. Lee, R. A. Dean, and Y.-H. Lee, 2013 Experimental Evolution Reveals Genome-Wide Spectrum and Dynamics of Mutations in the Rice Blast Fungus, *Magnaporthe oryzae*. PLOS ONE 8: e65416.

Kersten, P., and D. Cullen, 2007 Extracellular oxidative systems of the lignin-degrading Basidiomycete *Phanerochaete chrysosporium*. Fungal Genetics and Biology 44: 77–87.

Krieger Elmar, Joo Keehyoung, Lee Jinwoo, Lee Jooyoung, Raman Srivatsan et al., 2009 Improving physical realism, stereochemistry, and side-chain accuracy in homology modeling: Four approaches that performed well in CASP8. Proteins: Structure, Function, and Bioinformatics 77: 114–122.

Laothanachareon, T., J. A. Tamayo-Ramos, B. Nijsse, and P. J. Schaap, 2018 Forward Genetics by Genome Sequencing Uncovers the Central Role of the *Aspergillus niger* goxB Locus in Hydrogen Peroxide Induced Glucose Oxidase Expression. Front Microbiol 9:.

Li, H., 2011 A statistical framework for SNP calling, mutation discovery, association mapping and population genetical parameter estimation from sequencing data. Bioinformatics 27: 2987–2993.

Li, H., and R. Durbin, 2009 Fast and accurate short read alignment with Burrows–Wheeler transform. Bioinformatics 25: 1754–1760.

Li, B., F. A. J. Rotsaert, M. H. Gold, and V. Renganathan, 2000 Homologous Expression of Recombinant Cellobiose Dehydrogenase in *Phanerochaete chrysosporium*. Biochemical and Biophysical Research Communications 270: 141–146.

Ma, B., M. B. Mayfield, and M. H. Gold, 2001 The Green Fluorescent Protein Gene Functions as a Reporter of Gene Expression in *Phanerochaete chrysosporium*. Appl. Environ. Microbiol. 67: 948–955.

Martinez, D., L. F. Larrondo, N. Putnam, M. D. S. Gelpke, K. Huang et al., 2004 Genome sequence of the lignocellulose degrading fungus *Phanerochaete chrysosporium* strain RP78. Nature Biotechnology 22: 695–700.

Monk, B. C., T. M. Tomasiak, M. V. Keniya, F. U. Huschmann, J. D. A. Tyndall et al., 2014 Architecture of a single membrane spanning cytochrome P450 suggests constraints that orient the catalytic domain relative to a bilayer. PNAS 111: 3865–3870.

Nagy, L. G., R. Riley, P. J. Bergmann, K. Krizsán, F. M. Martin et al., 2017 Genetic Bases of Fungal White Rot Wood Decay Predicted by Phylogenomic Analysis of Correlated Gene-Phenotype Evolution. Mol Biol Evol 34: 35–44.

Ohm, R. A., R. Riley, A. Salamov, B. Min, I.-G. Choi et al., 2014 Genomics of wood-degrading fungi. Fungal Genetics and Biology 72: 82–90.

Riley, R., A. A. Salamov, D. W. Brown, L. G. Nagy, D. Floudas et al., 2014 Extensive sampling of basidiomycete genomes demonstrates inadequacy of the white-rot/brown-rot paradigm for wood decay fungi. PNAS 111: 9923–9928.

Schlötterer, C., R. Tobler, R. Kofler, and V. Nolte, 2014 Sequencing pools of individuals mining genome-wide polymorphism data without big funding. Nature Reviews Genetics 15: 749–763.

Schneeberger, K., 2014 Using next-generation sequencing to isolate mutant genes from forward genetic screens. Nature Reviews Genetics 15: 662–676.

Sharma, K. K., and R. C. Kuhad, 2010 Genetic transformation of lignin degrading fungi facilitated by Agrobacterium tumefaciens. BMC Biotechnology 10: 67.

Sionov, E., Y. C. Chang, H. M. Garraffo, M. A. Dolan, M. A. Ghannoum et al., 2012 Identification of a Cryptococcus neoformans Cytochrome P450 Lanosterol 14α-Demethylase (Erg11) Residue Critical for Differential Susceptibility between Fluconazole/Voriconazole and Itraconazole/Posaconazole. Antimicrobial Agents and Chemotherapy 56: 1162–1169.

Sun, H., and K. Schneeberger, 2015 SHOREmap v3.0: Fast and Accurate Identification of Causal Mutations from Forward Genetic Screens, pp. 381–395 in Plant Functional Genomics: Methods and Protocols, edited by J. M. Alonso and A. N. Stepanova. Methods in Molecular Biology, Springer New York, New York, NY.

Syed, K., K. Shale, N. S. Pagadala, and J. Tuszynski, 2014 Systematic Identification and Evolutionary Analysis of Catalytically Versatile Cytochrome P450 Monooxygenase Families Enriched in Model Basidiomycete Fungi. PLOS ONE 9: e86683.

Syed, K., and J. S. Yadav, 2012 P450monooxygenases (P450ome) of the model white rot fungus *Phanerochaete chrysosporium*. Crit Rev Microbiol 38: 339–363.

Tien, M., and T. K. Kirk, 1984 Lignin-degrading enzyme from *Phanerochaete chrysosporium*: Purification, characterization, and catalytic properties of a unique H2O2-requiring oxygenase. PNAS 81: 2280–2284.

Tien, M., and T. K. Kirk, 1983 Lignin-Degrading Enzyme from the Hymenomycete *Phanerochaete chrysosporium* Burds. Science 221: 661–663.

Wariishi, H., K. Valli, and M. H. Gold, 1991 In vitro depolymerization of lignin by manganese peroxidase of *Phanerochaete chrysosporium*. Biochemical and Biophysical Research Communications 176: 269–275.

Warrilow, A., C. Ugochukwu, D. Lamb, D. Kelly, and S. Kelly, 2008 Expression and Characterization of CYP51, the Ancient Sterol 14-demethylase Activity for Cytochromes P450 (CYP), in the White-Rot Fungus *Phanerochaete chrysosporium*. Lipids 43: 1143.

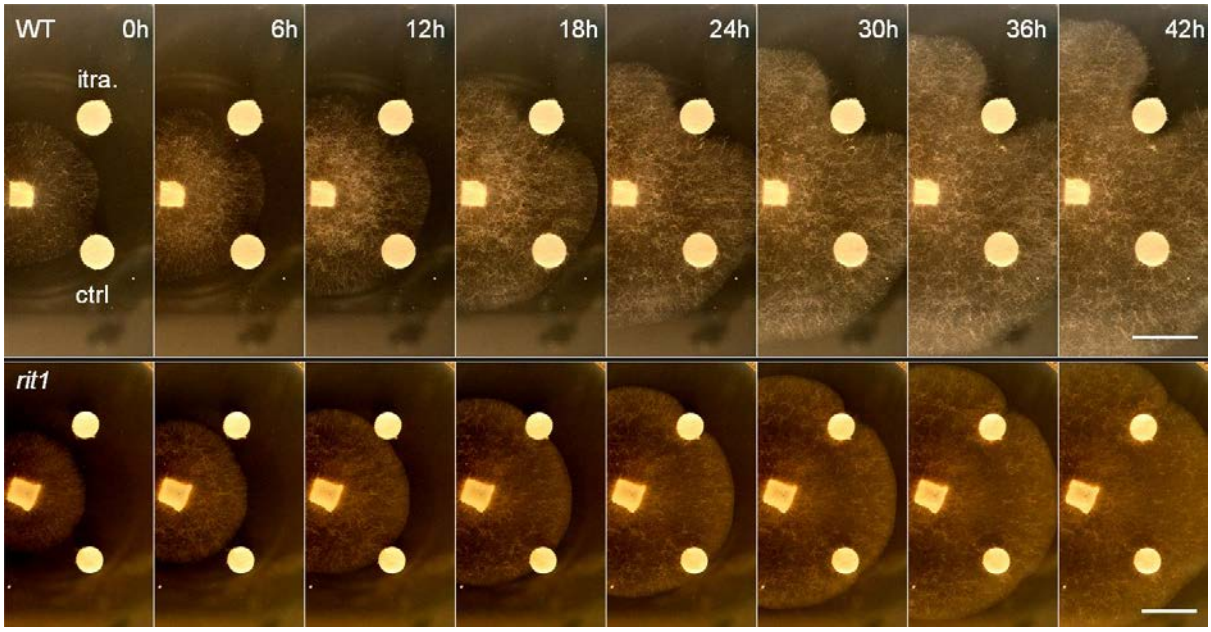

Figure 1. Effect of itraconazole on growth of *P. chrysosporium* RP78 WT and *rit1* mutant.

Fungi were cultivated on Malt-agar medium at 27 °C and disk diffusion test as been done with 8 µg of itraconazole or DMSO as control. Pictures represented in this figure show evolution of cultures every 6 h and corresponding movies are available as file S1 and S2. Scale bars represent 1cm.

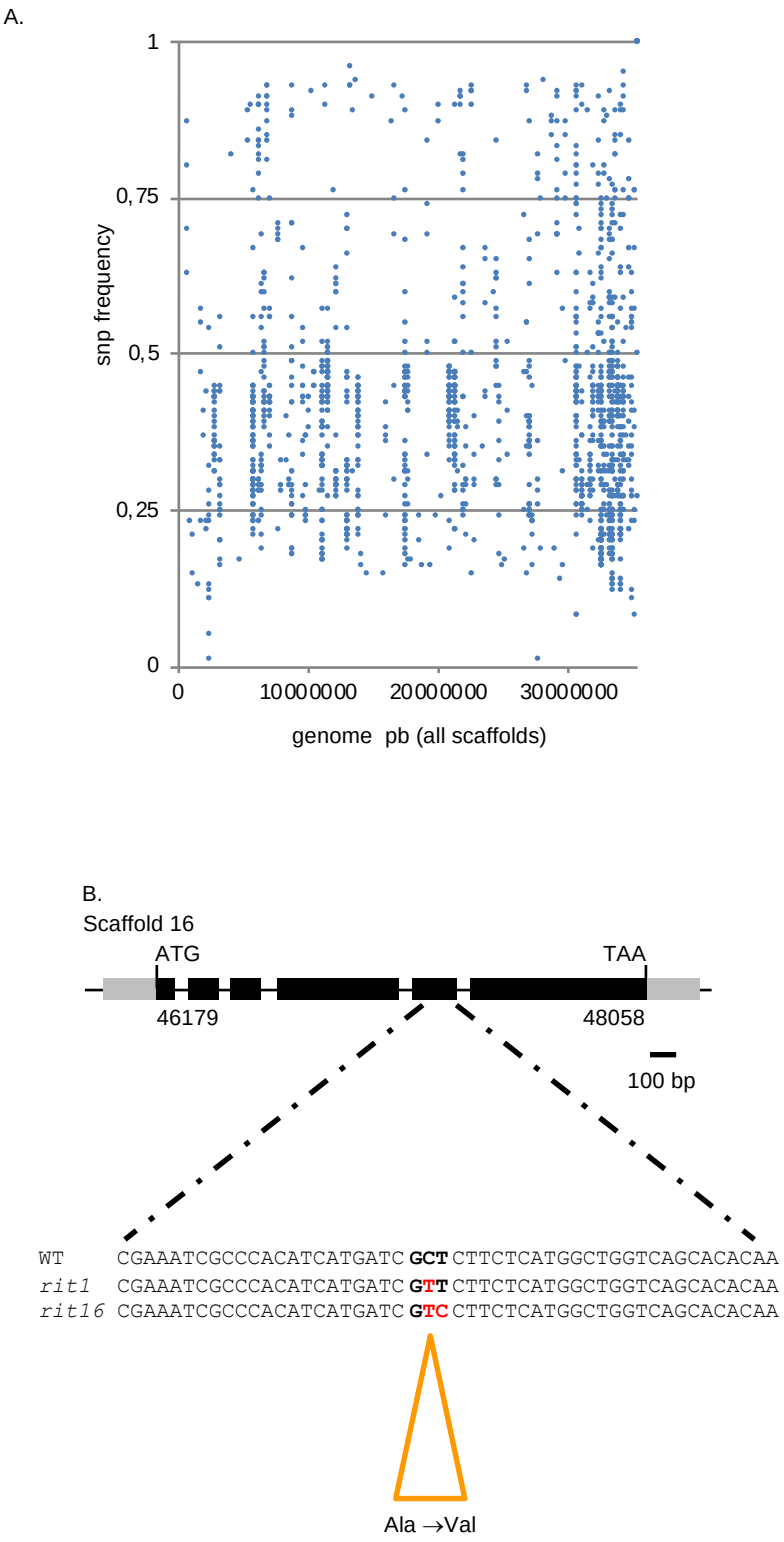

Figure 2. Identification of the causal mutation in *rit* mutants.

A. Graphical map of the SNPs list with their frequency. The SNPs list and frequency were obtained as output of shore map (Sun and Schneeberger, 2015); table is provided as Table S1. The x axis represents the scaffolds: Scaffold 1 cover the position from 1 to 3273479;

Figure 2. continued.

Scaffold 2 cover the position from 3273480 to 6317450 and so on until Scaffold 412 which cover the position from 35148491 to 35149519. The y axis is a direct output of shore map and represents the frequency of each SNP.

B. From the top to the bottom of this panel: i) Graphical representation of the *CYP51* locus on Scaffold 16 from position 46179 to 48058. ii) Highlight is done on the fifty nucleotide were the causal SNP have been detected, the sequence is given for WT, *rit1* and *rit16* has illustration of the different alleles detected. Substitutions are in red and the triplet of nucleotide altered is in bold and boxed. iii) The resulting amino acid substitution is also provided.

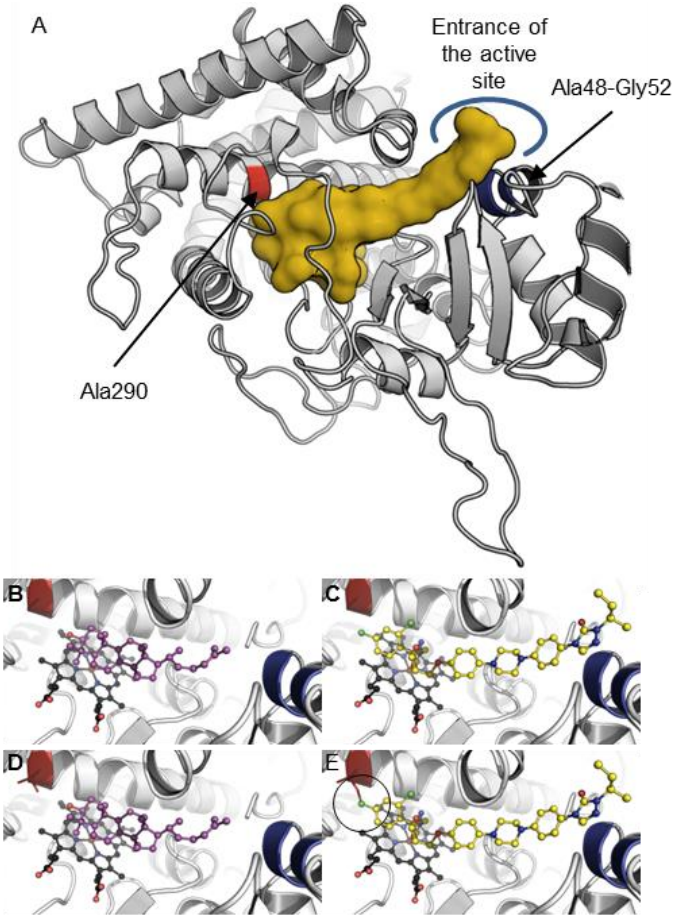

Figure 3. Lanosterol and Itraconazole binding sites prediction through homology modelling of *P. chrysosporium* lanosterol 14-alpha-demethylase (CYP51).

A. CYP51 structure with its active site pocket colored in yellow. The Ala290 residue near the heme binding site is colored in red and residues Ala48, Tyr51 and Gly52 near the entrance of the active site are colored in blue. B-E. Zoom of the CYP51 and CYP51 A290V active sites in the presence of lanosterol (B and C, respectively) or itraconazole (D and E, respectively). In each case, the molecules of heme, lanosterol and itraconazole are shown in ball-and-stick representation and colored in black, purple and yellow, respectively. The Ala290 position (Ala or Val), colored in red, is also shown in sticks.

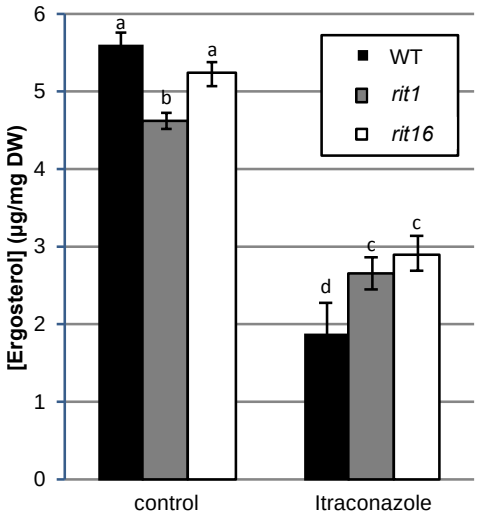

Figure 4. Ergosterol content of *P. chrysosporium* RP78 WT, *rit1* and *rit16* in response to itraconazole treatment.

The three different strains have been cultivated for 48h in liquid minimum medium with or without 8 µg.mL^{-1} of itraconazole (representative pictures of those cultures are provided in Fig. S2). Represented value are means ±SD, n=4, comparisons between values has been done using a two factors ANOVA followed by a Tukey test.

List of supplementary materials

Figure S1. Growth of *P. chrysosporium* RP78 in presence of itraconazole. Fungus was cultured on malt-agar Petri dish and Wattman paper disk soaked with itraconazole dissolve in DMSO were added in front of the tips of hyphae.

Figure S2. Representative pictures of *P. chrysosporium* RP78 WT, *rit1* and *rit16* cultivated in static liquid culture used for ergosterol content determination.

File S1. Movie illustrating the effect of itraconazole on *P. chrysosporium* RP78 growth. Fungus has been cultivated on malt-agar medium at 27°C, 8 µg of Itraconazole or DMSO have been dropped on Whatman paper dots. Pictures were taken every 5 min and the movie has been produced at 60 fps i.e. one second represent 5h.

File S2. Movie illustrating the resistance phenotype of *P. chrysosporium rit1* mutant. Fungus has been cultivated on malt-agar medium at 27°C, 8 µg of itraconazole or DMSO have been dropped on Whatman paper dots. Pictures were taken every 5 min and the movie has been produced at 60 fps i.e. one second represent 5h.

Table S1. List of SNPs found in the collection of *rit* mutants.

Article II

Target Of Rapamycin (PcTOR) signaling pathway plays an important role in the regulation of secretome in white-rot fungus *Phanerochaete chrysosporium*

(This paper has been available in the journal *Plos one*:

https://journals.plos.org/plosone/article?id=10.1371/journal.pone.0224776)

Introduction: Target Of Rapamycin (TOR) has been known as the central controller of eukaryotic cells in response to nutrient and various stresses. TOR has been functionally characterized intensively in model yeasts. To date, TOR has been still known little in filamentous fungi, and only in Ascomycetes. With the aim to characterize the detoxification systems of *P. chrysosporium*, the hypothesis that there are several functional links between them and TOR was tested.

Results: Two distinct genes encoding for PcTORs were identified and validated by sequencing clones of their FRB domain. This is an interesting result since almost filamentous fungi possess only one gene encoding TOR. Based on available genomic databases, components of PcTOR signaling pathway including PcTOR complexes, their upstream and downstream, were also identified through their homologies with *S. cerevisiae* and *S. pombe* orthologues. The obtained results suggest the presence of TSC1 and TSC2 in *P. chrysosporium* suggesting a higher similarity of PcTOR signaling pathway to that of *S. pombe* than that of *S. cerevisiae*. In addition to PcTOR signaling pathway identification, an experiment was designed to evaluate effects of rapamycin on extracellular proteins production by *P. chrysosporium*. The presence of rapamycin inhibits production of secreted proteins in ligninolytic conditions. Proteomic analysis demonstrated that FKBP12 known as an intracellular receptor essential for toxicity of rapamycin was found in secretome in presence of rapamycin. This is the first experimental report on the appearance of this protein in extracellular environment.

Using the previously described forward genetic approach, a screening of mutants resistant to rapamycin was carried out. Mutations in target genes including PcFKBP12 and PcTORs were identified and confirmed by a classical genetic technique. These preliminary experiments suggested a role of PcTOR in controlling secretome.

Title: Target Of Rapamycin pathway in the white-rot fungus *Phanerochaete chrysosporium*

Authors:

Nguyen Duy Vuong[a], Roret Thomas[a1], Fernandez-Gonzalez Antonio[a], Kohler Annegret[a], Morel-Rouhier Mélanie[a], Gelhaye Eric[a], Sormani Rodnay[a*]

[a] Université de Lorraine, INRAE, IAM, F-54000 Nancy, France

[1]Present address: CNRS, LBI2M, Sorbonne Universités, Roscoff, France

*Corresponding author

E-mail: rodnay.sormani@univ-lorraine.fr

Abstract

The Target Of Rapamycin (TOR) signaling pathway is known to regulate growth in response to nutrient availability and stress in eukaryotic cells. In the present study, we have investigated the TOR pathway in the white-rot fungus *Phanerochaete chrysosporium*. Inhibition of TOR activity by rapamycin affects conidia germination and hyphal growth highlighting the conserved mechanism of susceptibility to rapamycin. Interestingly, the secreted protein content is also affected by the rapamycin treatment. Finally, homologs of the components of TOR pathway can be identified in *P. chrysosporium*. Altogether, those results indicate that the TOR pathway of *P. chrysosporium* plays a central role in this fungus.

Key words:

Phanerochaete chrysosporium; Target of Rapamycin; rapamycin

Introduction

The Target Of Rapamycin (TOR) signaling pathway is highly conserved among eukaryotes and regulates essential cellular processes including protein synthesis, ribosome biogenesis, autophagy, and cytoskeleton organization [1]. In fungi, the TOR pathway is involved in the response to nutrient resources availability, this being true for carbon and especially sugar and nitrogen [2,3]. TOR is also involved in the stress responses, such as osmotic and oxidative stresses [4–6].

The serine/threonine-protein kinase TOR, firstly identified in *Saccharomyces cerevisiae* [7] is the central component of the TOR signaling pathway. This kinase interacts with other partners to form two multiprotein complexes named TORC1 and TORC2. Both complexes regulate their targets by phosphorylation. Of these two complexes, only TORC1 is sensitive to rapamycin [8,9]. Rapamycin binds to FK506 Binding Protein 12 (FKBP12) and the FK506 Rapamycin Binding (FRB) domain of TOR resulting in the inhibition of the TOR kinase activity and cell growth arrest. The sensitivity to rapamycin has permitted to decipher the TOR signaling pathway in numerous organisms. In fungi, the yeast models *S. cerevisiae* and *Schizosaccharomyces pombe* have been extensively studied even if the first report of the antifungal activity of rapamycin has been obtained with the human pathogenic fungus *Candida albicans* [10]. Since, rapamycin has been successfully tested either with pathogenic fungi such as *Cryptococcus neoformans* [11], Botrytis cinerea [12], *Mucor circinelloides* [13], *Fusarium graminearum* [14], or soft rot fungi [15]. Sensitivity to rapamycin has been observed in all fungal

lineages tested underlying conservation of the targets: TOR complexes and the mechanism of action, the TOR signaling pathway [16].

Most studies on fungal TOR signaling pathways have been conducted in ascomycetes, while data on basidiomycetes other than *C. neoformans* are scarce [13,16]. In *Pleurotus ostreatus* for instance, the TOR gene is duplicated and orthologs of the TOR pathway are present suggesting a conservation of that signaling pathway. Recently, a link between SLT2-MAPK, involved in the cell wall integrity signaling, and the TOR pathway has been reported in the edible mushroom and medicinal fungus *Ganoderma lucidum* [17]. In that case, TOR signaling is involved in the regulation of chitin and β-1,3-glucan synthesis and hence of cell wall thickness in a SLT2-MAPK dependent manner [17].

Among basidiomycetes, white rot fungi are very interesting ecological models because of their ability to grow on dead wood and to mineralize it. Wood is considered as a very specific ecological niche: indeed it contains recalcitrant carbon sources, low nitrogen content and potentially a highly toxic environment due to the presence of wood extractives [18]. To adapt to this environment, white rot fungi secrete a large set of enzymes involved in the degradation of wood polymers (cellulose, hemicelluloses and lignin) and possess an extended intracellular detoxification network [19–22]. These two complex machineries require a fine and coordinated regulation system that is up to date largely unknown in particular due to the lack of genetic tools for white-rot basidiomycetes. To test whether the TOR pathway could be involved in regulating the secretion of enzymes involved in lignocellulose decomposition, we tested the effect of rapamycin on *Phanerochaete chrysosporium* growth and secretome composition. By combining genome mining, structure modeling, we identified in this study the TOR signaling pathway of *P. chrysosporium* and highlighted its role in regulating the extracellular secreted protein composition.

Material and methods

Fungal strain

The homokaryotic strain *P. chrysosporium* RP78 was used in this study. This is the most widely used strain of *P. chrysosporium* in studies posterior to 2000, especially after its genome sequence was published in 2004 [23]. A version 2.2 of genomic database is available on https://genome.jgi.doe.gov/Phchr2/Phchr2.home.html. The mycelium is maintained on solid malt extract agar medium (20g.L^{-1} and 30g.L^{-1} respectively).

Growth curve measurement

Germination of P. chrysosporium RP78 conidia was measured using a nephelometric reader (NEPHELOstar Galaxy, BMG Labtech, Offenburg, Germany). For inoculation, suspensions of spores were obtained from 8 day-old mycelia grown on sporulation medium (Glucose (10 $g.L^{-1}$), malt extract (10 $g.L^{-1}$), peptone from potato (2 $g.L^{-1}$); yeast extract (2 $g.L^{-1}$), asparagine (1 $g.L^{-1}$), KH_2PO_4 (2 $g.L^{-1}$), $MgSO_4$.7H2O (1 $g.L^{-1}$), thiamine HCl (1 $mg.L^{-1}$), Agar (30 $g.L^{-1}$), all chemicals used were purchased from Sigma Aldrich. Spores were collected with gentle scraping of the agar plates and filtration through Miracloth. The number of spores per 1 mL of suspension was determined with optical density (OD) measurement at 650 nm, and calculated as previously described [24]. For each microplate well, 200 µl of sample were prepared: 10,000 spores were resuspended in 198 µL of malt 1 % and 2 µL of rapamycin (LC laboratories, R-5000) were added for treatment or 2 µl of DMSO as mock for control. Equipment was set up with the following parameters: temperature of incubation was 37 °C, cycle time 1 hour and the sum of cycles was 72 hours. Relative nephelometric unit (NRU) values were calculated as previously described [25].

Sample preparation for experiments on extracellular proteins

4×10^5 fungal spores were inoculated in 10 mL Tien & Kirt medium (with and without 1 % glucose) and incubated at 37 °C with shaking (120 rpm). After 4 days of incubation, the fungal biomass was transferred to a new 10 mL of Tien & Kirk medium with 10 µL of DMSO for control, or where 10 µL rapamycin dissolved in DMSO (2 $mg.ml^{-1}$) was added. Samples were then incubated at 37 °C with shaking during 48 hours. Supernatants were harvested and stored at -20 °C for further measurements. For each condition, 6 replicates were prepared. Fungal biomasses were dried for 48 hours under vacuum at -85 °C with a lyophilizer (VirTis BenchTop Pro freeze dryers) and weighed just after drying.

β-glucosidase activity assay

This enzymatic assay is based on the release of methylumbelliferone (MU) via cleavage of compound MU-β-D-glucopyranoside (MU-G) as the substrate of β-glucosidase (EC3.2.1.3). The stock solutions of the substrate (5 mM) and calibration (25 mM) were prepared in 2-methoxyethanol and were kept at -20 °C in the dark. All chemicals were purchased from Sigma Aldrich Chemicals. The working solution of the substrate was prepared by dilution with sterile ultrapure water to the final concentration of 500 µM.

The fluorogenic assay was prepared in a black 96-well microplate. The reaction mixture in each well included 50 µL of acetate sodium buffer (100 mM, pH 4.5), 50µl of culture supernatant and 50 µL of

working solution of the substrate. The plate also included calibration wells to obtain fluorescene signals for concentration of released MU, which was calculated from the resulting regression line. The plate was then incubated at 25 °C and shaken at 600 rpm. 100 µL of stopping buffer (Tris 2.5M, pH 11) was added into mixture of reaction after 15, 30, 45 and 60 minutes of incubation to stop reaction. Measurements were performed in Victor^3 microplate reader (Perkin-Elmer life sciences, France) with excitation wavelength set to 360 nm and emission wavelength set to 450 nm.

Sample preparation and protein quantification

After 20 minutes of centrifugation at 3,000 rpm (model 5810/5810 R, Eppendorf) to remove remaining fungal cells, supernatants from 6 replicates were mixed together and vaporized to remove all liquid under vacuum, at -85°C with a lyophilizer (VirTis BenchTop Pro freeze dryers). Pellets were dissolved with ultrapure sterile water in 0.5 volume of the initial volume. 1 mL of this new supernatant was purified for protein quantification. For purification, proteins were precipitated by mixing 1 mL of secreted sample with 200 µl saturated TCA and incubated overnight at -20 °C. Samples were centrifuged at 13,400 rpm at 4 °C for 20 minutes. Supernatants were discarded and the pellets were washed twice with cold acetone. The Interchim Protein Quantification BC assay kit was used for protein quantification. Purified proteins were dissolved with 50 µL of 0.2% SDS before adding the working solution of the provider. Reaction mixtures were incubated at 37 °C for 30 minutes and at cold room or in a fridge for 5 minutes. To determine protein content, the OD was measured at 562 nm with a spectrophotometer Cary50 (Varian).

Proteomic analyses

Samples were produced from the supernatants of 6 replicates mixed together for each condition tested. Pellet of 20 µg of protein were resuspended in 20 µL Urea, 6 M, Tris, 50 mM, pH 8.0 and samples were processed as follows: Cysteine residues were reduced by addition of 4 mM DTT for 45 minutes, alkylated by addition of iodoacetic acid (IAA) at 40 mM for another 45 min and IAA was blocked by addition of excess DTT (40 mM) for 10 minutes. 180 µL of a solution containing Tris-HCl, 50 mM pH 8.0, $CaCl_2$, 1 mM were added together with 1/100th (weight trypsin/weight protein extract) sequencing grade trypsin and digestion was allowed to occur overnight at 37 °C. Samples were then acidified by addition of 10 µL TFA 10%. Samples were fractionated by NanoHPLC on an Ultimate3000 system equipped with a 20 µL sample loop, a pepMap 100 C18 desalting precolumn and a 15 cm pepMap RSLC C18 fractionation column (all from Dionex). Samples (6.4 µL) were injected using the µlpickup mode and eluted by a 2 to 45% acetonitrile gradient over 60 minutes at 300 nL.min^{-1}. Fractions (340, 9 seconds each) were collected with a ProteineerFcII (Bruker) over 51 minutes and

eluted fractions were directly mixed on MTP-1536 BC target (Bruker) spots with α-cyano-4-hydroxycinnamic acid (Bruker). LC-MALDI runs dedicated to peptide identification were processed using dedicated automatic methods piloted by WARP-LC software on an Autoflex speed MALDI-TOF/TOF mass spectrometer (Bruker), first in MS mode in the 700-3,500 mass range, using next-neighbour external calibration for all MALDI spots. Thereafter, masses with S/N > 6 were processed for MS/MS analysis in LIFT mode. Peptide assignments were performed from TOF/TOF spectra by Mascot interrogation (Matrix Science) of the *P. chrysosporium* database piloted in Mascot and compiled by Proteinscape with a mass tolerance of 50 ppm in TOF mode and 0.8 Da in TOF/TOF mode, with optional cysteine carbamidomethylation, methionine oxidation and without enzyme cut. The minimal mascot score for peptides was set to 20 and that for proteins was set to 80. Results were cross-validated by interrogating an irrelevant database using the same criteria. Proteins were considered found in a given sample only if identified with a score above 80. When confronted to the random decoy strategy, this score resulted in a false discovery rate < 1%. The other way around, proteins were considered missing only if they were not identified at all. We could not calculate the effective lack of discovery rate in this specific experiment, but in other, technically similar contexts, such proteins exhibited levels at least 20-fold lower than those identified with a score of 80, with less than 2% errors.

PCR isolation and sequencing of the PcFKBP12 gene and FRB domains coding sequences

Genomic DNA extractions were performed from 3-day old liquid cultures of WT using QIAGEN DNeasy plant kit according to the manufacturer's instruction.

To analyze the sequences of FKBP12 and of the FRB domain coding sequences, a first step of PCR was done using primers: 5'ACTCAGTCCAACCGTACCTG3' (forward) and 5'CGAATGACCCGTCGACAATC3' (reverse) for FKBP12 and 5'TCAGTCGAGAGCTCATCAGG3' (forward) and 5'ACGGCCAACTGAAGATTACG3' (reverse) to amplify the FRB domain sequences. The PCR reactions were performed using Gotaq Flexi DNA polymerase (Promega) and equipment Mastercycler Nexus41 of Eppendorf. PCR products were visualized on agarose gel then purified using PCR DNA and Gel Band Purification kit (GE Healthcare, UK).

Plasmid pGEMt was used for the ligation of purified PCR products according to manufacturer's protocol (Promega A1360, USA). The reaction mixture includes 5µl of buffer 2X, 1µl of plasmid pGEMt, 3µl of PCR products and 1 µL of T4 DNA ligase. This mixture was incubated overnight at 4°C and used to transform *Escherichia coli* DH5α. Plasmid purification was performed using PureYield ™ Plasmid

Miniprep system kit (Promega) following instructions of the provider. Purified plasmids were stored at -20 °C before being sent to sequencing using T7p and SP6 universal primers (GENEWIZ, UK).

3D modeling of the FKBP12-rapamycin-Tor complex in *P. chrysosporium*

The models of FKBP12 and the FRB domain of Tor 3D from *P. chrysosporium* were generated by homology modeling. The models used were the FK506-binding protein 1A from *Aspergillus fumigatus* (73% identity; pdb entry:5hwb) for FKBP12 and the serine/threonine-protein kinase TOR from *human* (63% identity; pdb entry:4jsp) for Tor. Then, the FKBP12-rapamycin-Tor complex was built by superimposition with the crystal structure of the human complex (pdb entry: 1fap) for Tor1 and Tor2. The side chain and rotamers were optimized using YASARA's refinement protocol [26].

Results and discussion

***P. chrysosporium* is sensitive to rapamycin**

In the model yeast *S. cerevisiae*, the Tor kinase pathway is the central regulator of the cellular response to nutrient limitation and stresses. Rapamycin treatment that inactivates Tor leads to various effects at different levels and results in cell growth arrest. This prompted us to investigate the effect of rapamycin on *P. chrysosporium* growth. First, various amounts of rapamycin were applied to *P. chrysosporium* spores, and conidia germination rates were analyzed using nephelometric experiments (Fig. 1A). In the tested conditions, controls without rapamycin displayed a three-step growth curve, with a lag phase (t= 0h to 7.33h ± 0.5), followed by an exponential phase (t= 7.33h ± 0.5 to 30.9h ± 2.7) and then a stationary phase (after t= 30.9h ± 2.7). The lowest tested concentration of rapamycin (100 ng.mL-1) induced an increase both of the lag (37.7h ± 2.5 instead of 7.33h ± 0.5), and exponential (more than 30 hours instead of 20 hours) phases. Higher concentrations of rapamycin (200 and 500 $ng.mL^{-1}$) induced a similar growth pattern, increasing the lag phase and decreasing the measured growth rates during the exponential phase. At 1 $\mu g.mL^{-1}$ and 2 $\mu g.mL^{-1}$, rapamycin completely inhibited germination.

The effects of rapamycin were also tested on *P. chrysosporium* growing on solid medium. Three different amounts of rapamycin dissolved in DMSO were dropped on Whatman paper dots placed near *P. chrysosporium* growing mycelia to perform a diffusion test (Fig. 1B). During that experiment, growth was observed on control with DMSO but even the lowest amount of rapamycin tested (1 µg) led to growth inhibition (Fig. 1B, S1_movie).

Effect of TOR inhibition on the protein secretion in *P. chrysosporium*

The secretion of extracellular proteins plays an important role *P. chrysosporium* for the degradation of lignocellulosic material and toxic compounds. As TOR is known to control various cellular processes through sensing nutritional factors such as sugar availability, the function of PcTor as a regulator of extracellular protein content was evaluated with or without glucose and rapamycin.

A first experiment was performed to obtain secreted proteins in liquid culture. A wild-type strain was grown for 4 days on synthetic medium with 1% glucose. Then, the mycelium was transferred for 48 hours into fresh medium containing 1 % or 0 % of glucose, with or without 2 $\mu g.mL^{-1}$ of rapamycin.

Analysis of dry weights of collected mycelia shows an effect of glucose on fungal growth. Rapamycin inhibits growth in both cases, but this effect was more pronounced with glucose (Fig. 2A). Quantitatively, the effect of sugar is not visible on extracellular protein content and with or without glucose there is a decrease due to rapamycin treatment in both tested nutritional conditions (Fig 2B). The β-glucosidase activity was also tested on those samples. With glucose, a decrease of β glucosidase activity can be seen (Fig. 2C). Glucose deprivation leads to an increase of that activity and rapamycin could counter act that induction (Fig. 2C). Taken together, those results indicate that in these experimental conditions sugar deprivation is perceived, a response occurs and rapamycin acts on the three tested parameters.

We used these experimental parameters to assess qualitatively the extracellular protein contents. From the four treatments, the protein pattern of the secretomes on SDS-PAGE gels exhibited differences in presence of rapamycin for both glucose and glucose-deprived conditions (Fig. 2D). Proteomic analyses of the secretomes have been performed for each of the four conditions plus or minus glucose in presence or absence of rapamycin. Samples analyzed were obtained from 6 biological repeats for each treatment. A set of 64 proteins has been identified in those experiments (Fig. 2E and S2_table). These results highlight four points: i. there is a set of 16 proteins found in all four conditions. One of the most abundant proteins found in each case is a copper radical oxidase (AGR57_1123) involved in hydrogen peroxide generation [27] and two GMC oxidoreductases (AGR57_4013 and AGR57_9770). ii. Sugar deprivation increases extracellular protein diversity. Interestingly, four proteins are annotated as protease (AGR57_12626, AGR57_14965, AGR57_1477, AGR57_12049), three are glycoside hydrolases (AGR57_11735, AGR57_12854, AGR57_2053) and an amylase (AGR57_990) can also be found. iii. Proteins identified in point ii are not found in response to rapamycin treatment and iv. more surprisingly we found specific proteins secreted in response to rapamycin and one of them, AGR57_8308, was identified as FKBP12 (S2_table).

Identification of Tor and FKBP12 in *P. chrysosporium*

In previously studied organisms, rapamycin effect is due to its interaction with two partners: FKBP12 and the FRB domain of TOR [28] (Fig. 3B), that leads to the inhibition of the TOR kinase activity. These rapamycin interacting proteins have been searched in the available *P. chrysosporium* strain RP78 genome [23]. A homolog of FKBP12 was detected by BLASTp using FKBP12 sequence from S. cerevisiae as bait (ScFKBP12, SGDID: S000005079). The identified protein Pc FKBP12, coded by the gene AGR57_8308 and located at Scaffold 8:545501-546137, exhibits 63.2 % of identity with Sc FKBP12.

The second partner bound by FKBP12-Rapamycin is Tor. The organization of Tor primary sequence is conserved in all eukaryotic organisms, with the presence of several domains from the N terminal part to the C-terminal part: a HEAT repeat domain, a FAT domain, a FRB domain, the Kinase domain and then a FATC domain. The corresponding gene has been found duplicated in fungal lineages (Fig. 3A) [16]. Using the sequences from S. cerevisiae as bait, two sequences were detected in the genome of *P. chrysosporium* using BLASTp. A first sequence encoded by the gene AGR57_15312 is located on Scaffold 42: 6500-13402 (-). The sequence coding for the FRB domain (PcFRB1) is located between the position 11126 and 11579 of this gene. We found a second hit located on scaffold_20:36724-33343. This sequence returned one transcript sequence AGR57_14232TO. From this gene, the 3' part of the gene, with the sequence of the FRB domain, was missing from the genomic sequence and the transcript. PcFRB domain sequence was amplified by PCR from genomic DNA from *P. chrysosporium* RP78 using the identified sequence coding for PcFRB1 to design primers and subsequently cloned. Sequencing of individual clones revealed the presence of two distinct sequences: the sequence encoded by the gene AGR57_15312 (PcFRB1) and another sequence exhibiting 86.8% of identity at nucleotide level and named PcFRB2.

Previous transcriptomic data of *P. chrysosporium* were used [29] (NCBI GEO GSM3381937-39) focusing on the sequencing reads covering the FRB sequence at Scaffold 42. Alignment of those reads revealed the presence of potential SNPs suggesting the presence of two distinct sequences. Using CAP3 sequence assembly program [30], two contigs were obtained, one strictly similar with the sequence coded by AGR57_15312 on scaffold 42 and the other one containing all the mismatches observed in the cloning experiment.

Alignment of FRB sequences from human, *S. cerevisiae*, *S. pombe* and the basidiomycete *P. ostreatus* with PcFRB1 and PcFRB2 from *P. chrysosporium* revealed a high level of conservation (Fig. 3). Amino acids required for interaction with rapamycin (W93 and F100) are conserved in those phylogenetically distant species. Residues involved in phosphatidic acid binding in TOR (L24, F31 and Y97) are also

conserved. S28, the mutation that is involved in rapamycin resistance in mammalian cells can also be found in all the FRB tested even in both PcFRB (Fig. 3A).

The FKBP12-rapamycin-Tor complexes involving FRB1 or FRB2 from *P. chrysosporium* was generated by homology modeling using a human complex (pdb entry:1fap) followed by an energy minimization (Fig. 3B-C). The total energy obtained from the YASARA Energy Minimization Server [26] were -32, 174 kcal/mol (score: -0.12) and -32, 257 kcal/mol (score: -0.12) for the refined complexes involving PcFRB1 or PcFRB2, respectively. None of the 4 different residues between PcFRB1 (F29, H71, V86 and K91) and PcFRB2 (Y29, I71, I86 and R91) are involved in complex formation and closed to the rapamycin binding site. Rapamycin is hydrogen bonded to the D38, G54, K55, I57 and Y83 residues from Pc FKBP12 (Fig; 3D-F) and also interacts through close contacts with aromatic residues as already described [28]. Among these aromatic residues, W93 and F100 residues from both FRB domains (Fig. 3E-F) are required for interaction with rapamycin. This suggests that rapamycin can interact with the two PcFRB domains.

Conservation of the TOR pathway in *P. chrysosporium*

In the fungal kingdom, the TOR pathway has been extensively studied in model yeast *S. cerevisiae*, *S. pombe*, and the pathogenic *Candida albicans*. In other fungal lineages, ortholog proteins involved in the TOR pathway have been identified by gene homology and for the Basidiomycota lineage, only data for *P. ostreatus* were available presently [16]. The TOR pathway can be divided into three parts, the TOR complexes called TORC1 and TORC2, an upstream part composed of proteins involved in signal transduction and a downstream part including direct targets of the TOR kinase activity. Orthologs identified in *P. chrysosporium* by gene homology for these three parts are summarized in Tables 1, 2 and 3 respectively.

TORC1 is known to control translation at different steps and its activity is sensitive to rapamycin treatment while TORC2 is insensitive to rapamycin and coordinate growth with plasma membrane production and cell wall integrity [8,9,31]. TORC1 and TORC2 have 2 proteins in common: the kinase Tor and a binding partner called Lst8 in S. cerevisiae or Wat1 in *S. pombe*. An ortholog, PcLst8, can be found in *P. chrysosporium* (Table 1) with 58% of identity with ScLst8 and 61.5% of identity with SpWat1. TORC1 is also defined by the presence of Kog1. Interacting with Tor, Kog1 recruits targets for TOR kinase activity. The functional homolog of Kog1 in plant and animal cells is RAPTOR [1]. In *P. chrysosporium*, an ortholog called PcKog1 could be identified, this protein exhibiting 30.4% of identity with ScKog1 and 33.3 % with SpKog1. Tco89 is TORC1 specific and can be found in yeasts *S. cerevisiae* and *S. pombe*, but could not be identified in *P. chrysosporium*. This is probably due to the low sequence

conservation of that protein: SpTco89 and ScTco89 share 11.7% of identity and 19.9% of similarity. In *S. cerevisiae*, in addition to Tor and Lst8, TORC2 is composed of Bit61, Bit2, Avo1, Avo2 and Avo3. Bit61 and Bit2 are paralogs and their sequence share 42.9% of identity and 59.7% of similarity. On the other hand, Bit61 ortholog exists in *S. pombe* but ScBit61 and SpBit61 sequences share 17% of sequence identity and 29.5% of similarity. That low level of sequence homology could explain why those sequences lead to the identification of the same gene (AGR57_12865) in *P. chrysosporium*. For Avo2, which has no known ortholog, no match has been found while searching the *P. chrysosporium* database. PcAvo1 has been identified by its homology with Avo1 but also Sin1 from *S. pombe*. Finally, PcAvo3 could also been retrieved based on its sequence homology with Avo3 and Ste20 from *S. pombe*.

Table 1. Identified elements of TOR complexes of *Phanerochaete chrysosporium* in comparison with elements of TOR complexes of *Saccharomyces cerevisiae* and *Schizosaccharomyces pombe.*

	S. cerevisiae or *S. pombe*				*P. chrysosporium*					
complex	Standard name	SGD Systematic name	SGD ID	Pombase	Proposed name	Gene ID	Location	Protein lenght	% of identity	% of similarity
TORC1/C2	Lst8 Wat1/Pop3	YNL006W	S000004951	SPBC21B10.05c	PcLst8	AGR57_579	SC001:1196227-1197784(+)	326	58.1 61.5	74.2 76.5
TORC1	Kog1 Kog1	YHR186C	S000001229	SPAC57A7.11	PcKog1	AGR57_11672	SC013:163355-168458(-)	1561	30.4 33.3	45.3 49.5
	Tco89	YPL180W	S000006101	SPCC162.12	Not detected					
TORC2	Bit2	YBR270C	S000000474	SPAC6B12.03c		AGR57_12865	SC015:519331-521649 (+)	534	13.9 12.7	22.4 21.3
	Bit61	YJL058C	S000003594	SPCC777.08c		AGR57_12865	SC015:519331-521649 (+)	534	13.3 14.4	24.0 24.2
	Avo1 Sin1	YOL078W	S000005438	SPAPYUG7.02c	PcAvo1	AGR57_5388	SC005:594533-598186 (-)	908	19.2 22.4	31.6 37.8
	Avo2	YMR068W	S000000895		Not detected					
	Avo3/Tsc11 Ste20	YER093C	S000000895	SPBC12C2.02c	PcAvo3	AGR57_8271	SC008:473094-478330(-)	1334	18.6 30.2	37.1 50.9

Saccharomyces cerevisiae data from https://www.yeastgenome.org/

Shizosaccharomyces pombe data from https://www.pombase.org/

Blast done at http://fungidb.org/fungidb/

% of identity and similarity at https://www.ebi.ac.uk/Tools/psa/emboss_needle/

Concerning the upstream part of the TOR pathway, in *S. pombe* and animal cells, TSC1 and TSC2 (Tuberous Sclerosis Complex 1 and 2) form a complex that negatively regulates the GTPase-activity of Rheb (Ras homolog enhanced in brain) to activate TORC1. TSC1 and TSC2 orthologs were identified in all fungal species examined to date with the exception of *S. cerevisiae* [16]. As expected, orthologs named PcTsc1 and PcTsc2 have been detected and also a potential PcRhb1 (Table 2). In *S. cerevisiae*, TORC1 integrates different signals reflecting its regulation by different upstream regulators [32]. On the one hand, TORC1 is regulated by RAG GTPases Gtr1/Gtr2 in complex with Ego1/Ego2/Ego3. This complex is regulated by the GTP exchange factor Vam6. As orthologs for Gtr1, Gtr2 and Vam6 can be found in other fungal lineages [16], we were able to find, in *P. chrysosporium*, genes coding for orthologs of Gtr1, Gtr2 and Vam6 but not for Ego1 and Ego3. Gtr1 is also regulated by SEACIT (Seh1 – associated subcomplex inhibiting TORC1) which is bound and negatively regulated by SEACAT (Seh1 – associated subcomplex activating TORC1). SEACIT is composed of Npr2, Npr3 and Iml1 and SEACAT of Sec13, Seh1, Sea2, Sea3, SeA4 (Gonzalez and Hall, 2017). Orthologs of those components can be retrieved in *P. chrysosporium* (Table 2). On the other hand, Gtr2 activity is regulated by Lst4/Lst7 but no orthologs have been found by sequence homology. Finally, TORC1 activity is regulated by Snf1 in response to cytosolic glucose starvation and an ortholog exists in *P. chrysospoiurm*.

Table 2. Identified upstream elements of the TOR signaling pathway of *Phanerochaete chrysosporium* in comparison with upstream elements of TOR pathway of *Saccharomyces cerevisiae* and *Schizosaccharomyces pombe.*

	S. cerevisiae or *S. pombe*				*P. chrysosporium*					
complex	Standard name	SGD Systematic name	SGD ID	Pombase	Proposed name	Gene ID	Location	Protein lenght	% of identity	% of similarity
Tsc1/ Tsc2	Tsc1			SPAC22F3.13	PcTsc1	AGR57_528	SC001:1108704-1111851(-)	925	20.8	36.6
	Tsc2			SPAC630.13c	PcTsc2	AGR57_9302	SC008:783034-788376(+)	1763	18.8	32.1
	Rhb1	YCR027C	S000000622	SPBC428.16c	PcRhb1	AGR57_1568	SC002:138810–139648(+)	194	40.1 56.6	63.2 71.4
Gtr1/ Gtr2	Gtr1	YML121W	S000004590	SPBC337.13c	PcGtr1	AGR57_793	SC001:1652706-1653971(+)	348	40.7 45.6	57.3 64.8
	Gtr2	YGR163W	S000003395	SPCC777.05	PcGtr2	AGR57_4381	SC004:781482-783110(+)	435	25.7 31.4	43.7 44.6
	Ego1/Meh1	YKR007W	S000001715		Not detected					
	Ego3/Slm4	YBR077C	S000000281		Not detected					
	Vam6	YDL077C	S000002235	SPAC23H4.14	PcVam6	AGR57_7116	SC007:84318-88231(-)	1038	17.3 23.3	30.0
SEACIT	Npr2	YEL062W	S000000788	SPAC23H3.03c	PcNpr2	AGR57_425	SC001:882467-884614(-)	632	18.2 23.2	29.8 38.1
	Npr3/Rmd11	YHL023C	S000001015	SPBC543.04	PcNpr3	AGR57_4386	SC004:792751-795311(-)	781	16.5 20.5	29.4 36.8
		YJR138W	S000003899	SPBC26H8.04c	PcIml1	AGR57_11382	SC012:775902-781246(-)	1639	24.0 26.4	41.7 42.1
SEACAT	Seh1	YGL100W	S000003068	SPAC15F9.02	PcSeh1	AGR57_5195	SC005:129083-130804(+)	430	30.5 29.6	45.4 47.0
	Sec13/Anu3	YLR208W	S000004198	SPBC215.15	PcSec13	AGR57_14171	SC019:388062-389213(+)	332	51.6 53.6	64.8 68.3
	Sea2/Rtc1	YOL138C	S000005498	SPAC4F8.11	PcSea2	AGR57_7036	SC006:1979960-1984607(-)	1299	16.4 19.2	28.4 30.9
	Sea4	YBL104C	S000000200	SPAC12G12.01c	PcSea4	AGR57_6153	SC006:62362-66094(-)	1123	22.9 24.4	36.6 38.2
	Sea3/Mtc5	YDR128W	S000002535	SPAC11E3.05	PcSea3	AGR57_731	SC001:1518472-1523186(+)	1238	26.0 23.8	39.9 37.4
Lst4/ Lst7	Lst4	YKL176C/	S000001659	SPAC30C2.07	Not detected					
	Lst7/ Bhd1	YGR057C/	S000003289	SPBC24C6.08c	Not detected					
	Snf1 Ssp2	YDR477W	S000002885		PcSnf1	AGR57_13796	SC018:113339 - 115564 (+)	607	36.8 35.4	50.8 49.2

Saccharomyces cerevisiae data from https://www.yeastgenome.org/

Shizosaccharomyces pombe data from https://www.pombase.org/

Blast done at http://fungidb.org/fungidb/

% of identity and similarity at https://www.ebi.ac.uk/Tools/psa/emboss_needle/

For the downstream part of the TOR pathway in S. cerevisiae, the best known targets of TORC1 are the PP2A phosphatase Sit4, which forms a complex with Tap42 as regulatory subunit and Sch9, an AGC kinase with functional homology to the p70S6 Kinase in animal cells [33]. In *P. chrysosporium*, we were able to find orthologs for those proteins (Table 3). This result is in accordance with results previously obtained in *P. ostreatus* but we were also able to find two orthologs for another target of TORC2, Ypk2, while none of them were found in *P. ostreatus* [16]. The same orthologs were found for Ypk1 and interestingly, the two identified orthologs have an even better identity with Gad8, the target of TORC1 and TORC2 in S. pombe than with Ykp1 (Table 3). Finally, an ortholog has been identified for the TORC2 target Pkc1. All together, these results suggest that TOR pathway from *P. chrysosporium* is more closely related to *S. pombe* than *S. cerevisiae*.

Table 3. Identified downstream elements of the TOR signaling pathway of *Phanerochaete chrysosporium* in comparison with downstream elements of TOR pathway of *Saccharomyces cerevisiae* and *Schizosaccharomyces pombe*.

	S. cerevisiae or *S. pombe*				*P. chrysosporium*					
Target of	Standard name	SGD Systematic name	SGD ID	Pombase	Proposed name	Gene ID	Location	Protein lenght	% of identity	% of similarity
TORC1	**Tap42**	YMR028W	S000004630	SPCC63.05	PcTap42	AGR57_809	SC001:1683869-1685426 (-)	389	24.1 27.1	42.7 43.0
TORC1	**Sit4**	YDL047W	S000002205	SPCC1739.12	PcSit4	AGR57_15090	SC027:124552-125781 (+)	305	55.9 58.2	75.9 79.1
TORC1	**Sch9**	YHR205W	S000001248	SPAC1B9.02c	PcSch9	AGR57_2503	SC002:2055146-2058000 (+)	675	34.6 36.3	46.0 47.9
TORC2	**Ypk1**	YKL126W	S000001609		PcYpk1-2 or PcGad8	AGR57_11425 AGR57_8253	SC012:862786-864920(+) SC008:439512-441528(+)		44.3 56.6	55.9 70.3
TORC2	**Ypk2**	YMR104C	S000004710		PcYpk1-2 or PcGad8	AGR57_11425 AGR57_8253	SC012:862786-864920(+) SC008:439512-441528(+)	547 549	41.9 39.9	53.7 53.8
TORC1/2	**Gad8**			SPCC24B10.07	PcYpk1-2 or PcGad8	AGR57_8253 AGR57_11425	SC008:439512-441528(+) SC012:862786-864920(+)	549 547	51.7 53.6	64.0 68.3
TORC2	**Pkc1**	YBL105C	S000000201			AGR57_14288	SC020: 136736 - 140671 (+)		36.8	51.5

Saccharomyces cerevisiae data from https://www.yeastgenome.org/

Shizosaccharomyces pombe data from https://www.pombase.org/

Blast done at http://fungidb.org/fungidb/

% of identity and similarity at https://www.ebi.ac.uk/Tools/psa/emboss_needle/

Conclusion

With this study, we found that the TOR pathway play a central role in *P. chrysosporium*. Using rapamycin, we show that the TOR pathway is involved in conidia germination, vegetative growth and the secreted protein composition. Interestingly, rapamycin treatment leads to the identification of proteins secreted in response to rapamycin. One of them is PcFKBP12 which is an unusual location for this protein. In *A. fumigatus*, change in localization of AfFKBP12 has been observed in response to the immunosuppressant FK506 but not its secretion [34]. Due to amino acid conservation, the FRB domain of TOR and FKBP12 from *P. chrysosporium* can interact with rapamycin. The other components of the TOR pathway in *P. chrysosporium* have been identified and more components are related to the TOR pathway from *S. pombe* relative to *S. cerevisiae*.

Acknowledgment

We thank Dr. JB Vincourt from the proteomics core facility of UMS2008 IBSLor UL-CNRS-INSERM for performing mass spectrometric analysis.

We thank Professor Jean-Pierre Jacquot for his help and comments during manuscript preparation. This work was supported by a grant overseen by the French National Research Agency (ANR) as part of the "Investissements d'Avenir" program (ANR-11-LABX-0002-01, Lab of Excellence ARBRE). NDV was supported by a Doctoral Fellowship from the Ministry of Agriculture and Rural Development, Vietnam (Agricultural and Fisheries Biotechnology Program) and support from French ministry of foreign affair (program Campus France). FGA was supported by a postdoctoral grant from Region Grand Est.

Appendix. Supplementary material.

S1_movie. The effect of rapamycin on *P. chrysosporium* growth during a diffusion test.

S2_table. Table of data on the proteins identified during proteomic experiment.

Bibliography

1. Wullschleger S, Loewith R, Hall MN. TOR Signaling in Growth and Metabolism. Cell. 2006;124: 471–484. doi:10.1016/j.cell.2006.01.016

2. Bertram PG, Choi JH, Carvalho J, Chan T-F, Ai W, Zheng XFS. Convergence of TOR-Nitrogen and Snf1-Glucose Signaling Pathways onto Gln3. Molecular and Cellular Biology. 2002;22: 1246–1252. doi:10.1128/MCB.22.4.1246-1252.2002

3. Stracka D, Jozefczuk S, Rudroff F, Sauer U, Hall MN. Nitrogen Source Activates TOR (Target of Rapamycin) Complex 1 via Glutamine and Independently of Gtr/Rag Proteins. J Biol Chem. 2014;289: 25010–25020. doi:10.1074/jbc.M114.574335

4. Crespo JL, Daicho K, Ushimaru T, Hall MN. The GATA Transcription Factors GLN3 and GAT1 Link TOR to Salt Stress in *Saccharomyces cerevisiae*. J Biol Chem. 2001;276: 34441–34444. doi:10.1074/jbc.M103601200

5. Niles BJ, Joslin AC, Fresques T, Powers T. TOR Complex 2-Ypk1 signaling maintains sphingolipid homeostasis by sensing and regulating ROS accumulation. Cell Rep. 2014;6: 541–552. doi:10.1016/j.celrep.2013.12.040

6. Weisman R, Choder M. The Fission Yeast TOR Homolog, tor1 +, Is Required for the Response to Starvation and Other Stresses via a Conserved Serine. J Biol Chem. 2001;276: 7027–7032. doi:10.1074/jbc.M010446200

7. Heitman J, Movva NR, Hall MN. Targets for cell cycle arrest by the immunosuppressant rapamycin in yeast. Science. 1991;253: 905–909. doi:10.1126/science.1715094

8. Loewith R, Jacinto E, Wullschleger S, Lorberg A, Crespo JL, Bonenfant D, et al. Two TOR Complexes, Only One of which Is Rapamycin Sensitive, Have Distinct Roles in Cell Growth Control. Molecular Cell. 2002;10: 457–468. doi:10.1016/S1097-2765(02)00636-6

9. Zheng X-F, Fiorentino D, Chen J, Crabtree GR, Schreiber SL. TOR kinase domains are required for two distinct functions, only one of which is inhibited by rapamycin. Cell. 1995;82: 121–130. doi:10.1016/0092-8674(95)90058-6

10. Sehgal SN, Baker H, Vézina C. RAPAMYCIN (AY-22, 989), A NEW ANTIFUNGAL ANTIBIOTIC. J Antibiot. 1975;28: 727–732. doi:10.7164/antibiotics.28.727

11. Cruz MC, Cavallo LM, Görlach JM, Cox G, Perfect JR, Cardenas ME, et al. Rapamycin Antifungal Action Is Mediated via Conserved Complexes with FKBP12 and TOR Kinase Homologs in *Cryptococcus neoformans*. Molecular and Cellular Biology. 1999;19: 4101–4112. doi:10.1128/MCB.19.6.4101

12. Meléndez HG, Billon-Grand G, Fèvre M, Mey G. Role of the Botrytis cinerea FKBP12 ortholog in pathogenic development and in sulfur regulation. Fungal Genetics and Biology. 2009;46: 308–320. doi:10.1016/j.fgb.2008.11.011

13. Bastidas RJ, Shertz CA, Lee SC, Heitman J, Cardenas ME. Rapamycin Exerts Antifungal Activity In Vitro and In Vivo against Mucor circinelloides via FKBP12-Dependent Inhibition of Tor. Eukaryotic Cell. 2012;11: 270–281. doi:10.1128/EC.05284-11

14. Yu F, Gu Q, Yun Y, Yin Y, Xu J-R, Shim W-B, et al. The TOR signaling pathway regulates vegetative development and virulence in *Fusarium graminearum*. New Phytologist. 2014;203: 219–232. doi:10.1111/nph.12776

15. Dementhon K, Paoletti M, Pinan-Lucarré B, Loubradou-Bourges N, Sabourin M, Saupe SJ, et al. Rapamycin Mimics the Incompatibility Reaction in the Fungus *Podospora anserina*. Eukaryot Cell. 2003;2: 238–246. doi:10.1128/EC.2.2.238-246.2003

16. Shertz CA, Bastidas RJ, Li W, Heitman J, Cardenas ME. Conservation, duplication, and loss of the Tor signaling pathway in the fungal kingdom. BMC Genomics. 2010;11: 510. doi:10.1186/1471-2164-11-510

17. Chen D-D, Shi L, Yue S-N, Zhang T-J, Wang S-L, Liu Y-N, et al. The Slt2-MAPK pathway is involved in the mechanism by which target of rapamycin regulates cell wall components in *Ganoderma lucidum*. Fungal Genetics and Biology. 2019;123: 70–77. doi:10.1016/j.fgb.2018.12.005

18. Valette N, Perrot T, Sormani R, Gelhaye E, Morel-Rouhier M. Antifungal activities of wood extractives. Fungal Biology Reviews. 2017;31: 113–123. doi:10.1016/j.fbr.2017.01.002

19. Eastwood DC, Floudas D, Binder M, Majcherczyk A, Schneider P, Aerts A, et al. The Plant Cell Wall–Decomposing Machinery Underlies the Functional Diversity of Forest Fungi. Science. 2011;333: 762–765. doi:10.1126/science.1205411

20. Floudas D, Binder M, Riley R, Barry K, Blanchette RA, Henrissat B, et al. The Paleozoic Origin of Enzymatic Lignin Decomposition Reconstructed from 31 Fungal Genomes. Science. 2012;336: 1715–1719. doi:10.1126/science.1221748

21. Morel M, Meux E, Mathieu Y, Thuillier A, Chibani K, Harvengt L, et al. Xenomic networks variability and adaptation traits in wood decaying fungi. Microbial Biotechnology. 2013;6: 248–263. doi:10.1111/1751-7915.12015

22. Nagy LG, Riley R, Bergmann PJ, Krizsán K, Martin FM, Grigoriev IV, et al. Genetic Bases of Fungal White Rot Wood Decay Predicted by Phylogenomic Analysis of Correlated Gene-Phenotype Evolution. Mol Biol Evol. 2017;34: 35–44. doi:10.1093/molbev/msw238

23. Martinez D, Larrondo LF, Putnam N, Gelpke MDS, Huang K, Chapman J, et al. Genome sequence of the lignocellulose degrading fungus *Phanerochaete chrysosporium* strain RP78. Nature Biotechnology. 2004;22: 695–700. doi:10.1038/nbt967

24. Tien M, Kirk TK. Lignin-Degrading Enzyme from the Hymenomycete *Phanerochaete chrysosporium* Burds. Science. 1983;221: 661–663. doi:10.1126/science.221.4611.661

25. Joubert A, Calmes B, Berruyer R, Pihet M, Bouchara J-P, Simoneau P, et al. Laser nephelometry applied in an automated microplate system to study filamentous fungus growth. BioTechniques. 2010;48: 399–404. doi:10.2144/000113399

26. Krieger Elmar, Joo Keehyoung, Lee Jinwoo, Lee Jooyoung, Raman Srivatsan, Thompson James, et al. Improving physical realism, stereochemistry, and side-chain accuracy in homology modeling: Four approaches that performed well in CASP8. Proteins: Structure, Function, and Bioinformatics. 2009;77: 114–122. doi:10.1002/prot.22570

27. Kersten P, Cullen D. Copper radical oxidases and related extracellular oxidoreductases of wood-decay Agaricomycetes. Fungal Genetics and Biology. 2014;72: 124–130. doi:10.1016/j.fgb.2014.05.011

28. Choi J, Chen J, Schreiber SL, Clardy J. Structure of the FKBP12-Rapamycin Complex Interacting with Binding Domain of Human FRAP. Science. 1996;273: 239–242. doi:10.1126/science.273.5272.239

29. Fernández-González AJ, Valette N, Kohler A, Dumarçay S, Sormani R, Gelhaye E, et al. Oak extractive-induced stress reveals the involvement of new enzymes in the early detoxification response of *Phanerochaete chrysosporium*. Environmental Microbiology. 2018;20: 3890–3901. doi:10.1111/1462-2920.14409

30. Huang X, Madan A. CAP3: A DNA Sequence Assembly Program. Genome Res. 1999;9: 868–877. doi:10.1101/gr.9.9.868

31. Roelants FM, Leskoske KL, Martinez Marshall MN, Locke MN, Thorner J. The TORC2-Dependent Signaling Network in the Yeast *Saccharomyces cerevisiae*. Biomolecules. 2017;7: 66. doi:10.3390/biom7030066

32. González A, Hall MN. Nutrient sensing and TOR signaling in yeast and mammals. EMBO J. 2017;36: 397–408. doi:10.15252/embj.201696010

33. Urban J, Soulard A, Huber A, Lippman S, Mukhopadhyay D, Deloche O, et al. Sch9 Is a Major Target of TORC1 in *Saccharomyces cerevisiae*. Molecular Cell. 2007;26: 663–674. doi:10.1016/j.molcel.2007.04.020

34. Falloon K, Juvvadi PR, Richards AD, Vargas-Muñiz JM, Renshaw H, Steinbach WJ. Characterization of the FKBP12-Encoding Genes in *Aspergillus fumigatus*. PLOS ONE. 2015;10: e0137869. doi:10.1371/journal.pone.0137869

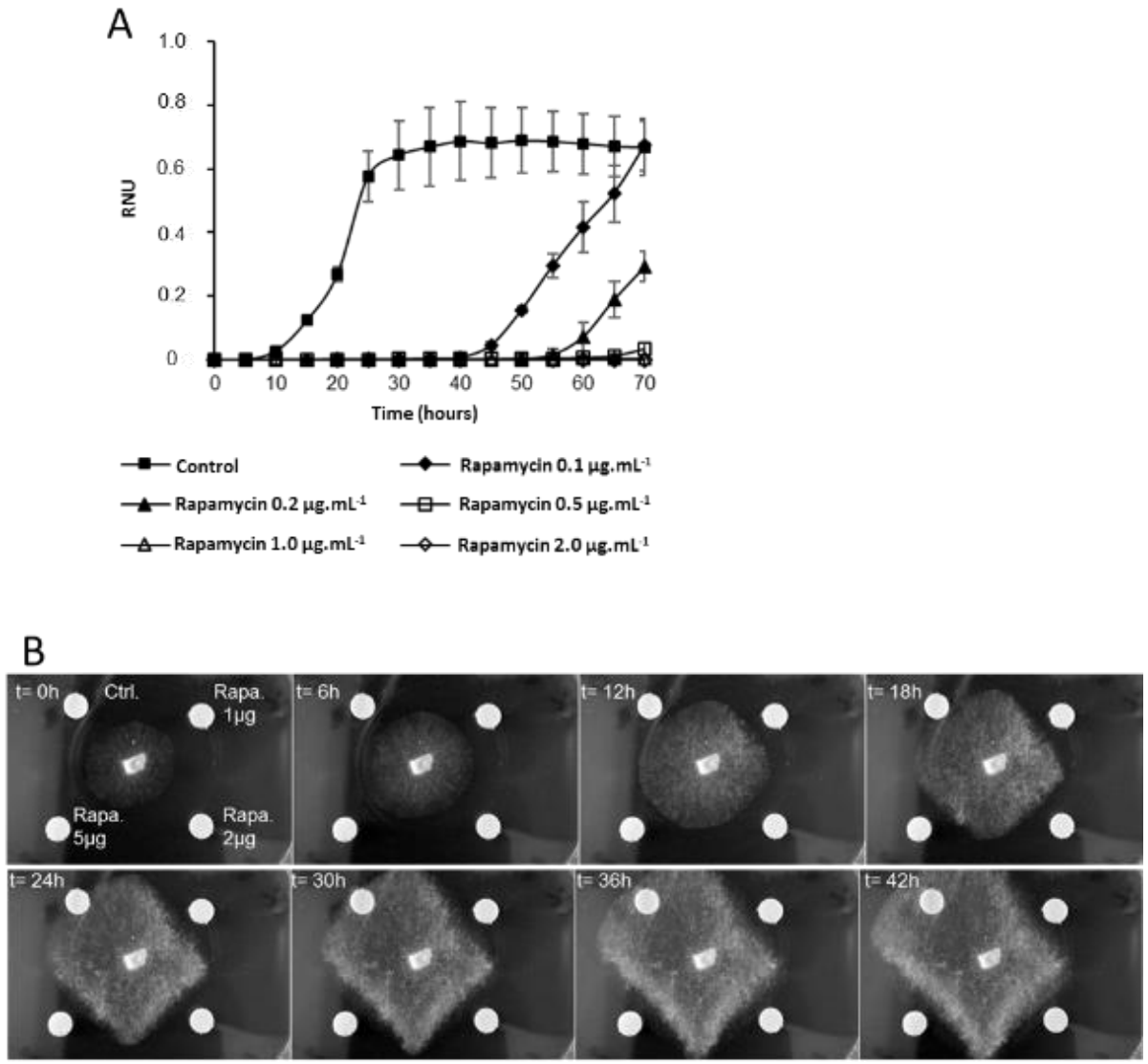

Figure 1. Effect of rapamycin on *P. chrysosporium* growth.

A. Growth curve measured after germination of conidia from *P. chrysosporium* RP78 in liquid medium using nephelometric measurement with different concentrations of rapamycin. Those curves represent means ± SD of n= 3 replicates.

B. Effect of rapamycin on hyphae growth in solid medium (agar plate). Rapamycin dissolved in DMSO was loaded on Whatman filter paper dots, DMSO was used as control, and both were used as in a disk diffusion test. Movie of the corresponding experiment is provided in S1_movie.

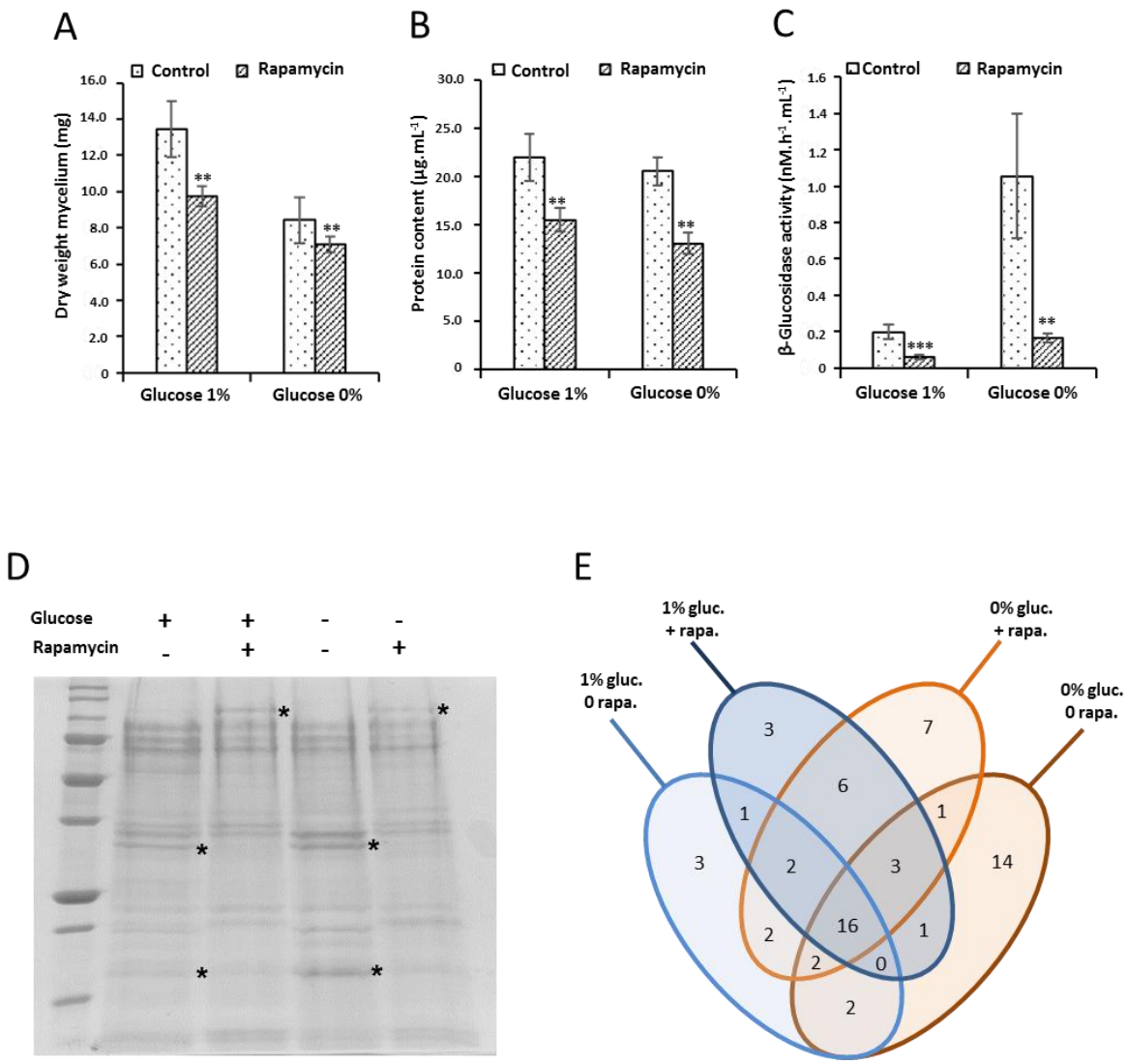

Figure 2. Rapamycin affects the secretome in *P. chrysosporium*.

Five days old liquid cultures of *P. chrysosporium* were transferred to fresh liquid medium for 48 hours with or without glucose and with or without rapamycin.

A. Effect of glucose and rapamycin on dry weight of fungus cultivated in liquid medium. Represented values are means ± SD with n= 6.

B. Effect of glucose and rapamycin on the concentration of proteins secreted in the liquid medium as measured using the BC assay. Values represented are means ± SD with n=3.

Figure 2. Continued.

C. Beta-glucosidase activity observed in the liquid culture medium containing the secreted enzymes. The activity has been measured using fluorogenic assay. Values represented are means ± SD with n=6. Two asterisks (**) denote the statistical difference of the added rapamycin medium compare with the control medium ($p< 0.05$) as determined by the two sample t-test at (A) and (B). Three asterisks (***) and two of them (**) represent ($p<0.001$) and ($p<0.01$) as determined by the two sample t-test at (C), respectively.

D. Representative Coomassie blue stained SDS-PAGE of the proteins secreted by *P. chrysosporium* in the conditions described above. 13 µg of proteins were loaded for each condition. Asterisk marks highlighted the major change observed.

E. Venn diagram representing the number of common and specific proteins found in the four different conditions analyzed. The list of proteins found in each class is provided in S2_table.

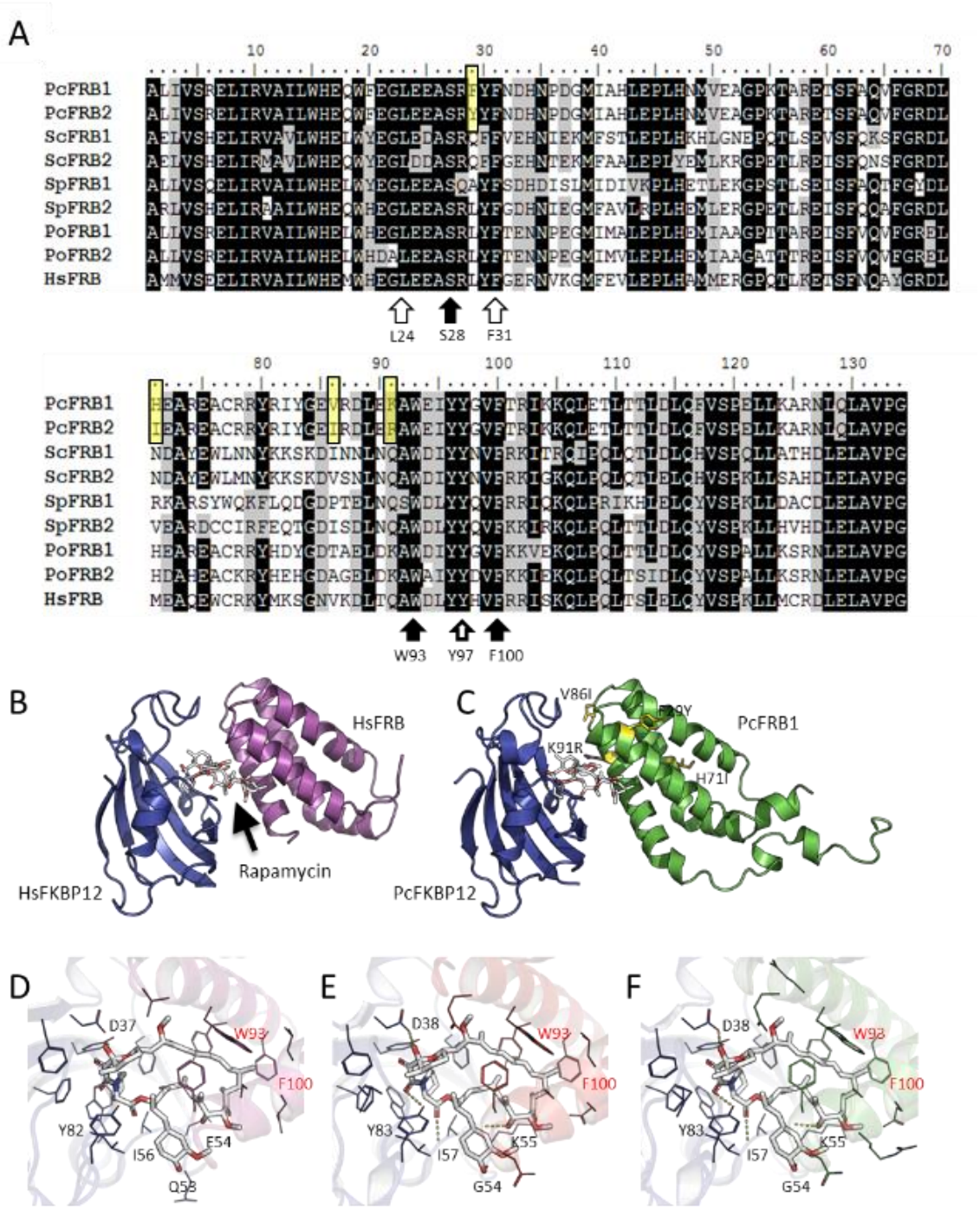

Figure 3. *P. chrysosporium* possesses two FRB domains that can interact with rapamycin and form TOR_{FRB}-Rapamycin-FKBP12 complex.

A. Sequence alignment of the two FRB domains of *P. chrysosporium* with the FRB domain of HsTOR (protein ID: P42345.1), the 2 FRB domains of *S. cerevisiae* (Tor1 SGDID:S000003827 and Tor2: SGDID:S000001686), *S. pombe* (Tor1: SPBC30D10.10c and Tor2: SPBC216.07c from https://www.pombase.org/), *P. ostreatus* (https://mycocosm.jgi.doe.gov/pages/search-for-genes.jsf?organism=PleosPC15_2, TOR1 ID: 1113153 and TOR2 ID: 1051426).

Figure 3. Continued

B. Crystal structure of HsFKBP12-HsFRB-rapamycin ternary complex (pdb entry:1fap).

C. 3D model of the predicted structure for *P. chrysosporium* FKBP12-rapamycin-FRB complexes. FKBP12, FRB and PcFRB1 are colored in blue, purple and green, respectively. Substitutions occurring between PcFRB1 and PcFRB2 are highlighted as yellow sticks. Secondary structures are shown in ribbon representation and the rapamycin is shown as white sticks.

D-F. Close-up views of the rapamycin binding site in the human FKBP12-rapamycin-FRB complex (D) and in *P. chrysosporium* involving PcFRB1 (E) and PcFRB2 (F). Hydrogen bonded residues to the rapamycin are named in black. W93 and F100 aromatic residues are pointed in red, their positions are given from the beginning of the FRB domain.

Supplementary results

Characterization of *P. chrysosporium* mutants resistant to rapamycin

Introduction

With the aim to characterize deeply the functions of TOR in *P. chrysosporium*, a screening experiment was performed to select the mutants resistant to rapamycin. 10 mutants were obtained and their phenotypes were determined via growth characterization. Genes encoding target proteins including FRB domains and FKBP12 were cloned to examine mutations. Interactions between rapamycin with these targets also carried out by modeling experiments to identify the effects of mutations. The genome of *rap8* mutant with a mutation in FKBP12 was sequenced in order to examine if this mutation is causative to the rapamycin resistance phenotype. Additional enzymatic activity assay revealed that this mutant could be used for characterizing PcTOR signaling pathway in *P. chrysosporium*.

Experiment protocols

Mutagenesis procedure: Conidia of wild type strain *P. chrypsoporium* RP78 were obtained by cultivation at 37 °C for 5 days on the sporulation medium. After exposed to UV light for 30 seconds, mutated conidia were suspended in ultrapure water with gentle scraping of the agar plates and filtration through Miracloth. 10,000 spores were plated on Petri dishes containing fresh malt extract agar medium supplemented with 2 $mg.L^{-1}$ of rapamycin (LC laboratories, R-5000). Petri dishes were incubated at 37 °C until the appearance of individual mycelia on the medium surface. Fragment of mycelia were picked up and subcultures were performed on sporulation medium mixed with 2 $mg.L^{-1}$ of rapamycin. 10,000 spores obtained from this medium were transferred into 10 mL of liquid malt extract 1% supplemented with 2 $mg.L^{-1}$ of rapamycin. Single spore progenies growing in liquid medium were fished and grown on the fresh sporulation medium mixed with 2 $mg.L^{-1}$ of rapamycin. Spores growing on this medium were used as mutant lines called *rap* mutants for further experiments.

Growth curve measurement: Germination of *P. chrysosporium* RP78 conidia was measured using a nephelometric reader (NEPHELOstar Galaxy, BMG Labtech, Offenburg, Germany). For inocula, suspensions of spores were obtained from 8 day-old mycelia grown on the sporulation medium. Spores were collected with gentle scraping of the agar plates and filtration through Miracloth. The number of spores per 1 mL of suspension was determined with optical density (OD) measurement at 650 nm, and calculated as previously described (Tien and Kirk, 1983). For each microplate well, 200 µl of sample were prepared: 10,000 spores were resuspended in 198 µL of malt 1% and 2 µL of rapamycin (LC laboratories, R-5000) were added for treatment or 2 µl of DMSO as mock for control. Equipment was set up with the following parameters: temperature of incubation was 37°C, cycle time 1 hour, and the sum of cycles was 72 hours. Relative nephelometric unit (NRU) values were calculated as previously described (Joubert et al., 2010).

PCR isolation and sequencing of the PcFKBP12 gene and FRB domains coding sequences

Genomic DNA extractions were performed from 3-day old liquid cultures of WT and *rap* mutants using QIAGEN DNeasy plant kit according to the manufacturer's instruction.

To analyze the sequences of FKBP12 and of the FRB domain coding sequences from WT and mutant strains, the first step of PCR was done using primers: 5'ACTCAGTCCAACCGTACCTG3' (forward) and 5'CGAATGACCCGTCGACAATC3' (reverse) for FKBP12 and 5'TCAGTCGAGAGCTCATCAGG3' (forward) and 5'ACGGCCAACTGAAGATTACG3' (reverse) to amplify the FRB domain sequences. The PCR reactions were performed using Gotaq Flexi DNA polymerase (Promega) and equipment Mastercycler Nexus41 of Eppendorf. PCR products were visualized on agarose gel then purified using PCR DNA and Gel Band Purification kit (GE Healthcare, UK).

Plasmid pGEMt was used for the ligation of purified PCR products according to the manufacturer's protocol (Promega A1360, USA). The reaction mixture includes 5µl of buffer 2X, 1µl of plasmid pGEMt, 3µl of PCR products, and 1 µL of T4 DNA ligase. This mixture was incubated overnight at 4 °C and used to transform *Escherichia coli* DH5α. Plasmids purification was performed using PureYield ™ Plasmid Miniprep system kit (Promega) following instructions of provider. Purified plasmids were stored at -20 ˚C before being sent to sequencing using T7p and SP6 universal primers (GENEWIZ, UK).

3D modeling of the FKBP12-rapamycin-TOR complex in *P. chrysosporium*

The models of FKBP12 and the FRB domain of TOR 3D from *P. chrysosporium* were generated by homology modeling. The models used were the FK506-binding protein 1A from *Aspergillus fumigates* (73% identity; pdb entry:5hwb) for FKBP12 and the Serine/threonine-protein kinase TOR from *human* (63% identity; pdb entry:4jsp) for TOR. Then, the FKBP12-rapamycin-TOR complex was built by superimposition with the crystal structure of the human complex (pdb entry :1fap) for TOR1 and TOR2. The side chain and rotamers were optimized using YASARA's refinement protocol (Krieger Elmar et al., 2009).

Genome resequencing

DNAseq was performed at the GeT-PlaGe core facility, INRA Toulouse. DNA-seq libraries have been prepared according to Illumina's protocols using the Illumina TruSeq Nano DNA LT Library Prep Kit. Briefly, DNA were fragmented by sonication, and adaptators were ligated to be sequenced. 8 cycles of PCR were applied to amplify libraries. Library quality was assessed using an Advanced Analytical Fragment Analyzer and libraries were quantified by QPCR using the Kapa

Library Quantification Kit. DNA-seq experiments have been performed on an Illumina Miseq using a paired-end read length of 2x250 pb with the Illumina MiSeq Reagent Kits v2.

Sample preparation for experiments on extracellular proteins

4×10^5 fungal spores were inoculated in 10 mL Tien & Kirt medium (with and without 1 % glucose) and incubated at 37 °C with shaking (120 rpm). After 4 days incubation, the fungal biomass was transferred to a new 10 mL of Tien & Kirk medium with 10 µL of DMSO for control, or where 10 µL rapamycin dissolved in DMSO (2 $mg.mL^{-1}$) was added. Samples were then incubated at 37 °C with shaking during 48 hours. Supernatants were harvested and stored at -20 °C for further measurements. For each condition, 6 replicates were prepared. Fungal biomasses were dried for 48 hours under vacuum at -85 °C with a lyophilizer (VirTis BenchTop Pro freeze dryers) and weighed just after drying.

Results

Generating mutants resistant to rapamycin and their characterization

Isolation and growth pattern of *rap* mutants

To validate the identification of the rapamycin interacting proteins, an UV mutagenesis on *P. chrysosporium* conidia was performed. A similar strategy of screening mutants resistant to rapamycin has previously allowing identifying *ScTOR1* and *ScTOR2* in *S. cerevisiae* (Heitman et al., 1991) and more recently *FgTOR* in *F. graminearum* (Yu et al., 2014). Conidia from the homokaryotic strain *P. chrysosporium* RP78 were also UV irradiated as described in methods, then plated on malt agar medium containing 20 $\mu g.mL^{-1}$ of rapamycin. Twenty mutants, named *rap1* to *rap20,* able to grow in the presence of rapamycin at this concentration, were isolated. Only 10 of them were able to produce conidia being resistant to rapamycin (20 $\mu g.mL^{-1}$) and then selected for further analyses.

Spore germination and growth of these *rap* mutants were followed in liquid cultures in presence of rapamycin (20 $\mu g.mL^{-1}$). With the exception of *rap2* and *rap12*, all tested rap mutants were able to grow in these conditions. *rap8*, *rap11*, *rap14*, *rap15,* and *rap17* exhibited a growth pattern similar to WT without rapamycin (Fig. 28A). In comparison with others mutants, exponential phases of *rap1, rap8,* and *rap16* occurred latter: 20h, 48h, and 65h after the inoculation for *rap8*, *rap1,* and *rap16* respectively.

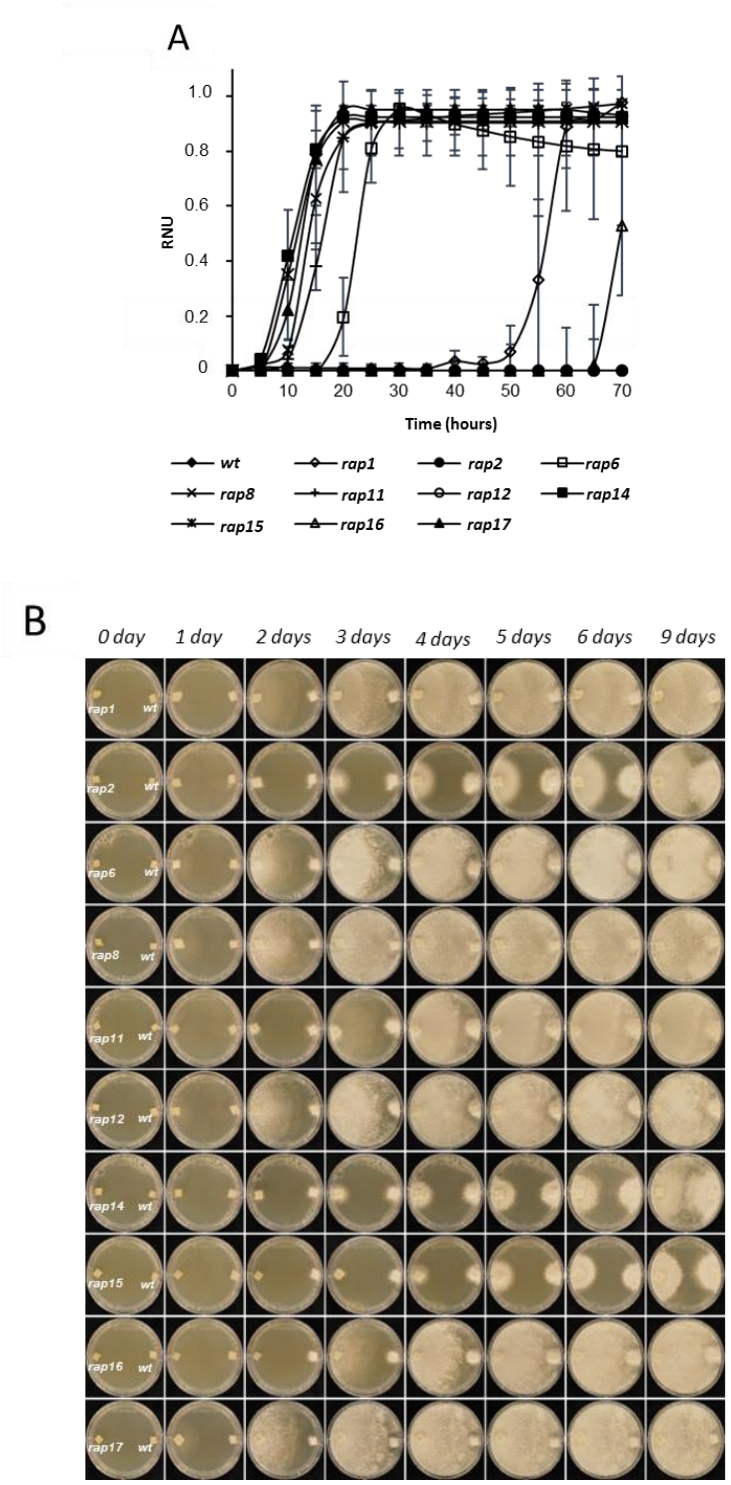

Figure 28. Characterization of *P. chrysosporium rap* mutants resistant to rapamycin.

A. Growth curves observed after germination of *P. chrysosporium* conidia in liquid culture in the presence of 20 µg.mL^{-1} of rapamycin. Those results have been obtained by nephelometric experiment, representative data are means ± SD with n=3 replicates.

B. Growth of *rap* mutants compares to WT on solid medium containing 2 µg.mL^{-1} of rapamycin. Pictures were taken each 24 hours.

On solid medium, two different growth patterns were observed in the presence of rapamycin (2 µg.mL^{-1}) for the *rap* mutants. The growth experiments were designed by inoculation of the tested *rap* mutant and WT in the same plate (Fig 28B). In these conditions, *rap1*, *rap6*, *rap8*, *rap11*, *rap12*, *rap16*, *rap17* were able to colonize the whole plate within 3 days, whereas *rap2*, *rap14* and *rap15* exhibited a dramatically reduced growth rate. In the experiments performed with the three latter *rap* mutants, a weak colonization compared to WT was also observed.

Interestingly, the *rap* mutants were selected on rapamycin and their progeny was able to grow on medium containing rapamycin but different patterns could be observed. The weakest phenotype was observed for *rap2*. It did not grow during the time of the nephelometric experiment and its development on malt agar medium was limited compared to other *rap* mutants but it remained more efficient than WT. Two mutants, *rap1* and *rap16* presented a longer lag phase in the liquid medium and showed a strong resistance to rapamycin on solid medium. *Rap12* was only able to develop on the solid medium. Two other mutants, *rap14* and *rap15* showed a stronger phenotype, compare to WT, in liquid culture than in solid medium. Four mutants, *rap8*, *rap11*, *rap17* were able to grow in both tested conditions. To this last group, belongs also *rap6*, which presented some delay to start the exponential phase but grew strongly on solid medium with rapamycin.

Identification of mutations in *rap* mutants

As it was done for *F. graminearum* (Yu et al., 2014), to identify genes potentially involved in the rapamycin resistance in the selected *rap* mutants, a gene candidate strategy was performed by sequencing for each mutant the PcFKBP12 coding gene, AGR57_8308, and the sequence coding for FRB1 and FRB2 domains from the gene AGR57_15312 and AGR57_14232, respectively.

Obtained results are summarized in Fig. 29 and Table 1. A mutation was found in *rap8 PcFKBP12* leading to an earlier termination of translation (K98Stop). In the same mutant, a second mutation was found in scaffold 42 near the sequence coding for the FRB1 domain. This second mutation leads to the L110P substitution (Fig. 29, Table 1). L110 is conserved between species with the exception of SpFRB1 which possesses an I100 (Fig. 3A, article II).

Four mutants exhibited mutations in the FRB1 coding sequence (Fig. 29, Table 1). In all cases, those mutations led to substitutions on amino acids which are conserved between species (Fig. 3A, article II). This is the case for *rap6* (FRB1 W93L), *rap11* (FRB1 F100L), and *rap14* (FRB1 F62S). For *rap15*, the substitution leads to FRB1 E25V, E25 being well conserved between species except in *S. cerevisiae* where there are D25 in both ScFRB1 and ScFRB2 (Fig. 3A, article II). At this position, an acidic function seems to be required as E to D is a conservative change.

Table 1. Summary of mutations identified in PcFKBP12 and PcFRB in rap mutants.

The *PcFKBP12* gene is localized at Scaffold 8: 545501-546137, the data are provided according to this position. *PcFRB* sequences are part of *PcTOR* genes which are localized on Scaffold 20 and Scaffold 42. For The *FRB* sequence from the *TOR* gene localized on Scaffold 20:33739-38873, the 3' part of that gene is missing from the database (https://genome.jgi.doe.gov/pages/search-for-genes.jsf?organism=Phchr2), position are given according to sequence alignment of the protein sequence shown in Fig. 2. For the *FRB* sequence from the *TOR* gene localized on Scaffold 42:7003-13402, the 5' sequence of the gene is missing but the sequence of the FRB domain was available from the same database.

	Position of the mutations[a]		
Mutant name	PcFKBP12	PcFRB1	PcFRB2
rap1	ND	ND	ND
rap2	ND	ND	H38R C**A**T→C**G**T
rap6	ND	W93L T**G**G→T**T**G:11045	ND
rap8	K→stop codon **A**AG→**T**AG:545654	L110P* C**T**C→C**C**C:11096	ND
rap11	ND	F100L TT**C**→TT**A** :11057	ND
rap12	ND	ND	K120E **A**AG→**G**AG
rap14	ND	F62S T**T**T→T**C**T : 10957	ND
rap15	ND	E25V G**A**A→G**T**A :10841	E13G G**A**A→G**G**A
rap16	ND	ND	ND
rap17	ND	F29Y TTC→TAC :10853	ND

ND : Not Detected
a Alternative residue with position number in FRB, changed codon and position number of equivalent nucleotide in DNA sequence 5'3' of genes.
Mutation are in bold.
* This mutation is not in the FRB domain (but in the kinase domain).

Three mutants, *rap2*, *rap12,* and *rap 15* possess mutations in the FRB2 coding sequence leading to three different substitutions (Fig. 29, table 1). In *rap2*, we found the substitution FRB2 H42R. Interestingly, H42 is only present in PcFRBs and this position is not conserved between species (Fig. 3A, article II). In *rap12*, we detected another substitution FRB2 K124E; K124 can be found in *P. chrysosporium* and *P. ostreatus* but this amino acid is not conserved in other organisms (Fig. 3A, article II). With another substitution, *rap15* cumulates two mutations, one in FRB1 described above, and another one in FRB2 (F58G). Both are in conserved amino acids (Fig. 3A, article II).

Two mutants, *rap1* and *rap16*, did not exhibit any mutations in the examined sequences. These two mutants were able to fully grow on solid medium with rapamycin but the lag phase was increased in liquid medium (Fig. 28A). Those results suggest that other mechanisms of resistance are occurring in those mutants and they will need further investigation.

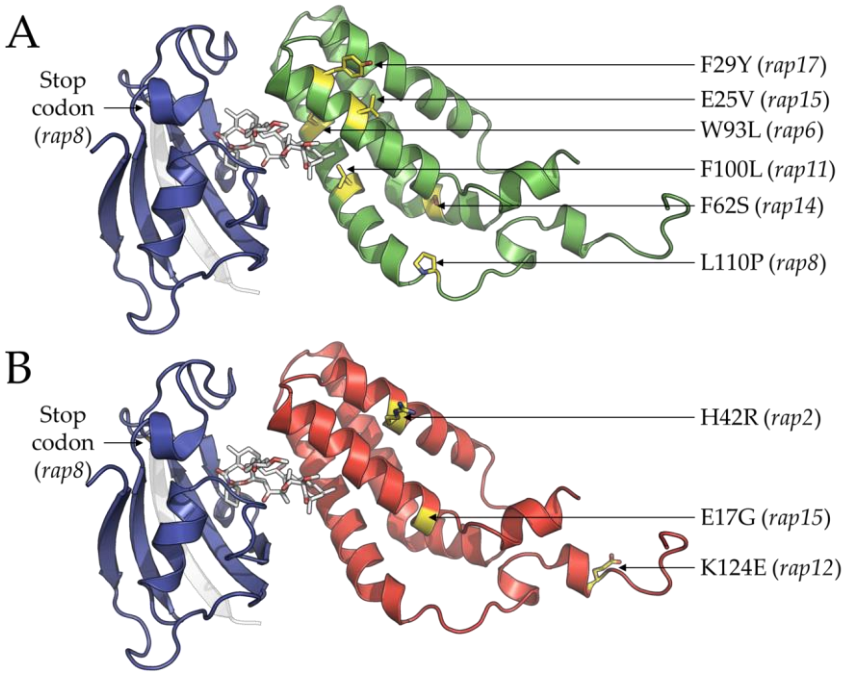

Figure 29. Identified mutations in the *P. chrysosporium* FKBP12-rapamycin-FRB complexes.

3D models of the predicted *P. chrysosporium* FKBP12-rapamycin-FRB1 (A) and of FKBP12-rapamycin-FRB2 (B). FKBP12, FRB1, FRB2 and the rapamycin are colored in blue, green, red and white, respectively. Secondary structures are shown in ribbon representation and the rapamycin is shown as sticks. Point mutations occurring on FRB1 and FRB2 depending on fungal strain are highlighted as yellow sticks. The stop codon found in FKBP12 (*rap8*) is also pointed.

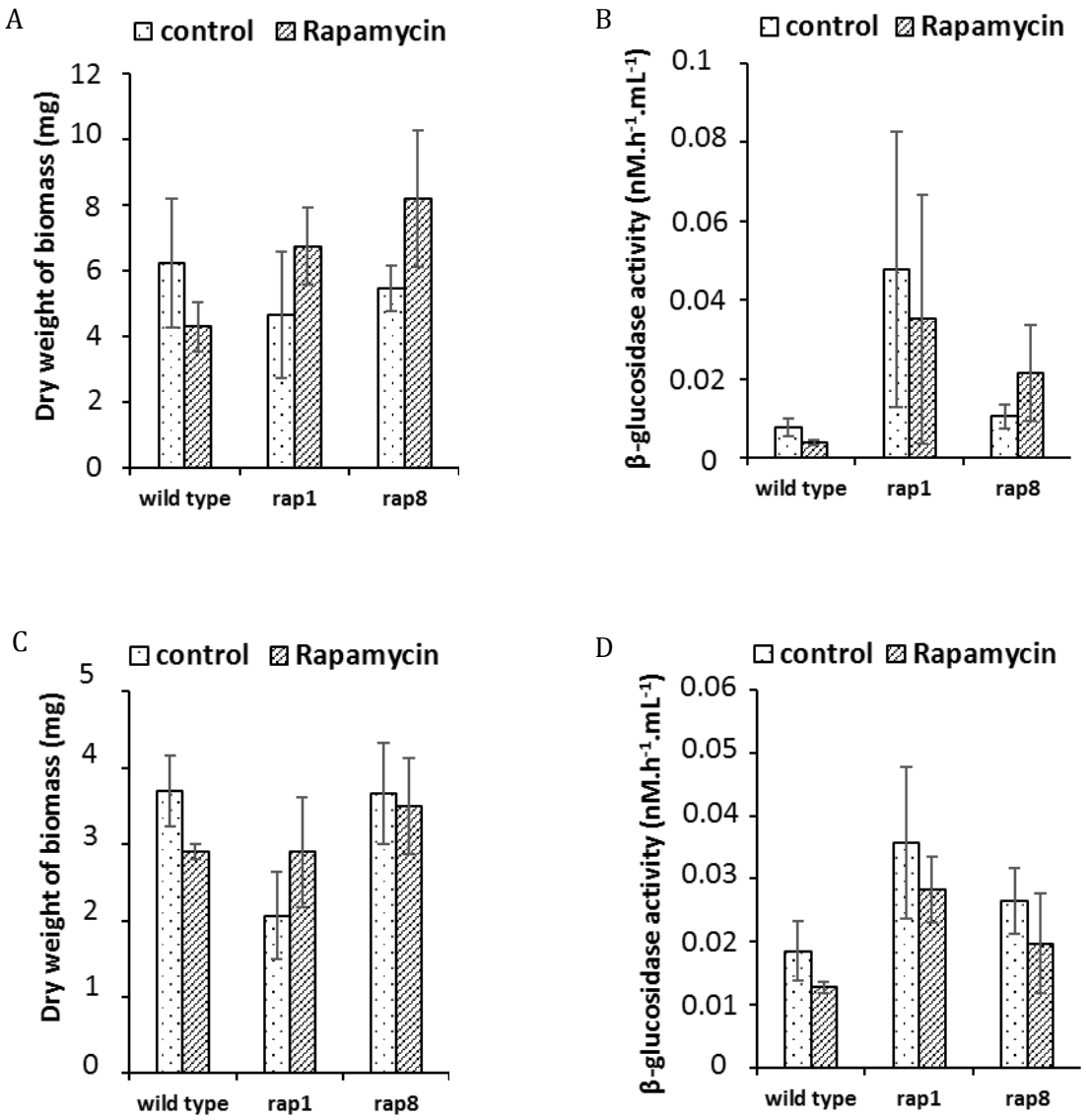

Figure 30. Inhibitory effects of rapamycin on WT fungus, but not on *rap* mutants.

Biomass and secretome are obtained after 24 hours of incubation. Representative values are means ± SD with n=3. (A) and (B) presence of glucose 1%, (C) and (D) glucose 0%.

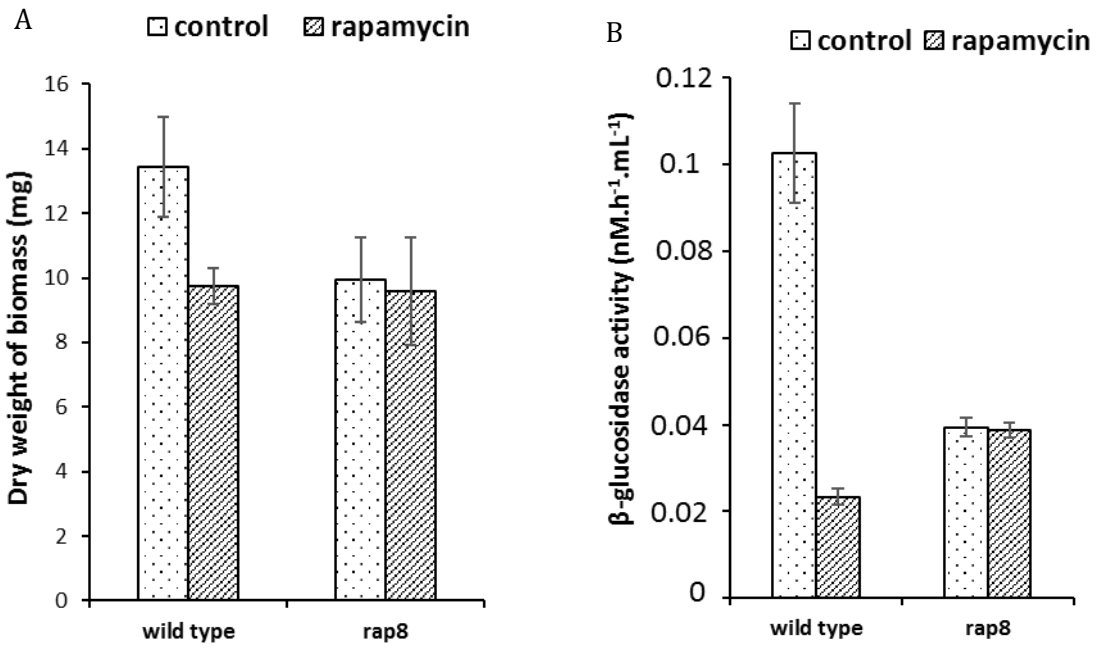

Figure 31. Rapamycin had no significant effects on growth and secretion of mutant *rap8*.

A. Rapamycin affects dry weight of fungus of WT, but not *rap8* cultivated in liquid medium. Representative values are means ± SD with n= 6.

B. β-glucosidase activity observed in the liquid culture medium containing the secreted enzymes. The activity has been measured using fluorogenic assay. Representative values are means ± SD with n=6.

The mutant strain *rap8* as the genetic material for detail characterization of PcTOR

Potential effects of PcTOR on extracellular secretion were estimated using WT, *rap1* lacking mutation in potential investigated targets, and *rap8* with one non-sense mutation in the FKBP12 encoding gene. Cultures were performed in liquid conditions in the presence or absence of glucose (1%) and rapamycin. After 24 hours of incubation, biomass was weighed after drying and β-glucosidase activity was tested from the supernatant. The results are shown in Fig 30. In both conditions, with glucose 1% (Fig. 30 A, B) and in absence of glucose (Fig. 30 C, D), no significant differences in biomass production and enzymatic activity were detected for both mutants. In contrast, as expected, a strong effect of rapamycin on the WT was observed. Besides, higher β-glucosidase activities were measured in mutant supernatants compared to WT supernatants in the absence of rapamycin.

To examine more in detail the role of TOR in the regulation of the extracellular system, an experiment was designed only using WT and *rap8* in presence of glucose 1% (T&K complete medium). Fungal biomass and supernatant were collected after 48 hours of incubation. The results show that rapamycin significantly inhibits biomass production and β-glucosidase activity for WT (Fig. 31A). In contrast, there are not any effects of this molecule on *rap8* (Fig. 31B). These results confirm that rapamycin is not toxic for *rap8* or does not inhibit PcTORC1 in this mutant, and possibly due to the mutation of FKBP12. To examine this possibility, WGS data analysis (Table 2) with the highest allele frequency indicates that this mutation is causative to explain the rapamycin resistance phenotype of this mutant.

In conclusion, these data suggest that *rap8* could be a good model to investigate deeply the role of TOR in *P. chrysosporium* and in particular its involvement in the regulation of extracellular enzyme secretion.

Table 2. Summary of mutations identified in *rap8* mutant.

Gene identifier	Identity of scaffold	Position of a base in the reference sequence	Base in reference sequence	Alternative/ mutant base	Region of DNA which is affected by the change	Amino acid according to reference	Resulting substitution
AGR57_978.1	scaffold_1	2014140	C	T	CDS	S	F
AGR57_184.1	scaffold_1	381847	G	A	CDS	T	I
AGR57_2477.1	scaffold_2	1997151	G	A	intronic/noncoding		
AGR57_2137.1	scaffold_2	1254968	T	C	CDS	I	T
AGR57_2137.1	scaffold_2	1254969	C	G	CDS	I	T
AGR57_3208.1	scaffold_3	603384	G	A	CDS	S	L
AGR57_3812.1	scaffold_3	1940559	T	C	CDS	H	R
AGR57_3380.1	scaffold_3	956228	C	T	3'UTR		
AGR57_3847.1	scaffold_3	2005431	C	A	3'UTR		
AGR57_3027.1	scaffold_3	236361	T	A	CDS	E	V
AGR57_3925.1	scaffold_3	2222969	G	A	CDS	A	V
AGR57_3884.1	scaffold_3	2100647	C	A	intronic/noncoding		
AGR57_4463.1	scaffold_4	938824	G	A	CDS	D	N
AGR57_5703.1	scaffold_5	1296384	G	A	CDS	P	S
AGR57_5462.1	scaffold_5	768560	T	C	CDS	Y	H
AGR57_6330.1	scaffold_6	417493	A	T	intronic/noncoding		
AGR57_7315.1	scaffold_7	489300	C	T	CDS	G	N
AGR57_7315.1	scaffold_7	489301	C	T	CDS	G	N
AGR57_7565.1	scaffold_7	1112691	G	T	CDS	G	V
AGR57_8308.1	scaffold_8	545533	T	A	CDS	K	*
AGR57_8307.1	scaffold_8	545533	T	A	3'UTR		
AGR57_8904.1	scaffold_8	1770197	A	G	intronic/noncoding		
AGR57_9574.1	scaffold_9	1408801	C	T	5'UTR		
AGR57_9574.1	scaffold_9	1408840	C	T	5'UTR		
AGR57_9574.1	scaffold_9	1408842	C	T	5'UTR		
AGR57_9889.1	scaffold_10	244728	C	T	intronic/noncoding		
AGR57_10000.1	scaffold_10	549474	T	G	CDS	V	G
AGR57_10695.1	scaffold_11	688350	T	C	CDS	Q	R
AGR57_10797.1	scaffold_11	883699	T	A	3'UTR		
AGR57_11148.1	scaffold_12	222596	G	A	CDS	P	L
AGR57_11228.1	scaffold_12	476142	G	C	CDS	G	A
AGR57_11169.1	scaffold_12	266479	C	T	intronic/noncoding		
AGR57_11169.1	scaffold_12	266818	T	C	intronic/noncoding		
AGR57_11482.1	scaffold_12	992281	T	G	intronic/noncoding		
AGR57_11797.1	scaffold_13	411797	G	T	CDS	M	I
AGR57_12474.1	scaffold_14	684383	G	A	intronic/noncoding		
AGR57_12502.1	scaffold_14	751208	T	G	intronic/noncoding		
AGR57_13274.1	scaffold_16	415490	T	G	CDS	Y	S
AGR57_14130.1	scaffold_19	281097	A	G	CDS	S	G
AGR57_14379.1	scaffold_20	317897	C	T	CDS	D	N
AGR57_14516.1	scaffold_21	288979	C	T	CDS	A	T
AGR57_14531.1	scaffold_21	313557	T	C	CDS	M	V
AGR57_14627.1	scaffold_22	147569	G	A	CDS	S	L

CDS: coding sequence

UTR: untranslated region

Discussion and conclusions (Article I & II)

As reported in the introduction part of this manuscript, wood decaying fungi have developed efficient detoxification systems allowing them to deal with potential toxic molecules. Studies of these enzymatic networks and in particular their regulation at the molecular level have been limited due to the lack of genetic tools. **To overcome this bottleneck, a forward genetic approach was proposed and tested**. Based on a **Whole Genome Sequencing (WGS) strategy,** we have confirmed that such approach could be efficient for identifying targets of potential antifungal compounds in the model *P. chrysosporium.* Indeed, as presented in the first article dealing with itraconazole as proof of concept, sequencing of pooled DNA genome from a forward genetic screen that produced mutants resistant to itraconazole, was useful to identify the potential target. In the supplementary results of article 2, WGS of *rap8* confirmed that this mutant harbors a mutation which leads to a shorter form of FKBP12, the receptor required for TOR inhibition by rapamycin.

Advances of next-generation sequencing technology enabled to isolate causative mutations from forward genetic screens for model organisms such as *Arabidopsis thaniana* (Schneeberger and Weigel, 2011), zebrafish (*Danio rerio*) (Sanchez et al., 2017). Concerning wood decaying fungi, this approach has been applied only for the white rot fungus *P. ostreatus*, but with a more complex procedure. Indeed, mutant screens were performed after mutagenesis of UV irradiated protoplasts (Nakazawa et al., 2016). Based on the selectable markers involving in 5-fluororotic acid catabolism (this compound becoming toxic after the action of the orotidine 5'-phosphate decarboxylase), and combined with a screening of mutants able to decolorize dyes (Remazol Brilliant Blue R and Orange II), two mutations linked to defects in the ligninolytic system, in particular leading to the complete lack of MnPs activity, were identified (Nakazawa et al., 2017). The first mutation was found in a gene encoding for a putative chromatin modifier, whereas the second one concerned a putative DNA-binding protein, which is specific to agaricomycetes (Nakazawa et al., 2017). For the fungus *P. chrysosporium*, protoplast production remains challenging, therefore, mutagenesis was performed by exposing directly fungal conidia to UV irradiation, a method, which had been previously used in *P. chrysosporium* (Tien and Myer, 1990). To date, mutants obtained in this study remain stable after several rounds of cultivation. These mutants could be a valuable toolkit for future genetic studies.

In the second article, the TOR signaling pathway was identified in *P. chrysosporium*. To characterize PcTOR, a strategy with a combination of bioinformatics, PCR amplification, and sequencing was designed. Indeed, we used the sequence coding the FRB domain that is the part of TOR involved in the binding of the complex FKBP12/rapamycin which leads to TOR inhibition

in *S. cerevisiae*. By blasting with ScFRB as a query on the genomic database of *P. chrysosporium*, only one gene coding TOR was identified in this fungus, so we hypothesized that there is only one gene encoding for TOR in this fungus. However, this hypothesis was not validated via direct sequencing of the PCR product amplified from the identified gene. To examine if *P. chrysosporium* possesses two distinct genes encoding for TOR as in *S. cerevisiae* and *S. pombe*, additional experiments have been performed. By mining previous data from microarray experiments, two different RNA sequences encoding for PcTOR were identified. To confirm this result, an experiment with classical cloning was performed, and two distinct sequences encoding for TOR were retrieved. These data are reported in the article II. In addition, the obtained results suggested that PcTOR could be involved in the regulation of the extracellular protein content.

There are several studies mentioning the functions of TOR signaling in the regulation of secreted protein production, for instance *in A. nidulans* and *N. crassa* (Brown et al., 2013; Xiong et al., 2014). Nevertheless, to date, this link has not been studied, even in filamentous ascomycete species producing secreted enzymes with commercial value for agriculture or industry. This link has only been demonstrated in the pathogenic yeast *C. albicans* (Chen et al., 2012). Indeed, the small GTPase Rhb1 binds to TOR signaling components including TOR1 and its downstream effectors thus helping control the expression of Secreted Aspartic Protease 2 (Sap2), a hydrolytic enzyme that is necessary for cell growth under amino acid availability, and therefore for virulence of this pathogenic yeast on human hosts (Chen et al., 2012). In the latest report, Rhb1 has been identified as having a role in the expression of the efflux pump, thereby affecting fluconazole susceptibility (Chen et al., 2019). From this result, TOR is possibly linked to the intracellular detoxification system through elements of the secretory pathways. To date, there are no reports on such a link in all kingdoms.

In contrast to TOR, Protein Kinase A (PKA) has been shown to be a key regulator of extracellular protein secretion in fungi. This has been shown not only in pathogenic fungi but also in wood decaying fungi such as *P. chrysosporium* (McCotter et al., 2016; Syed and Yadav, 2012). Recently, based on the proteomic data of *P. ostreatus* obtained in response to lignocellulosic components, it has been shown that several ribosomal proteins become more abundant when the fungus is grown in presence of xylan and CMC containing medium, but this was not the case on medium containing lignin (Xiao et al., 2017). The expression of these proteins has been considered to be regulated by TOR as well as by PKA. Therefore, TOR may be involved in sensing carbon nutrients and in the regulation of the secretome composition via a crosstalk with PKA. This relationship has been characterized in *S. cerevisiae* and could be similar in filamentous fungi. From this viewpoint, TOR and PKA have also been recently proposed as parallel regulators of hyphal branching (Harris, 2019).

In fact, characterizing the emerging link between TOR and vesicle trafficking remains to be challenged. In yeast *S. cerevisiae*, there have been several studies focusing on this relationship since several components of TORC1 such as TOR1, TOR2, Lst8, Kog1, and Tco89, are localized to major organelles involved in membrane trafficking (endosomal, Golgi, and vacuolar compartments). Furthermore, the TOR pathway integrates signals from PKA and Snf1p in yeast (Shashkova et al., 2015). PKA and Snf1p are known as secretion regulators in filamentous fungi in response to glucose sensing (Brown et al., 2014; McCotter et al., 2016). In *S. cerevisiae*, Snf1p acts with TOR signaling in response to glucose starvation through the regulation of the TOR targets such as Sch9, Tip41, and Gln3. The interactions between Snf1 and the TOR signaling pathway are not direct but occur via the PKA pathway (Braun et al., 2014; Zhang et al., 2011).

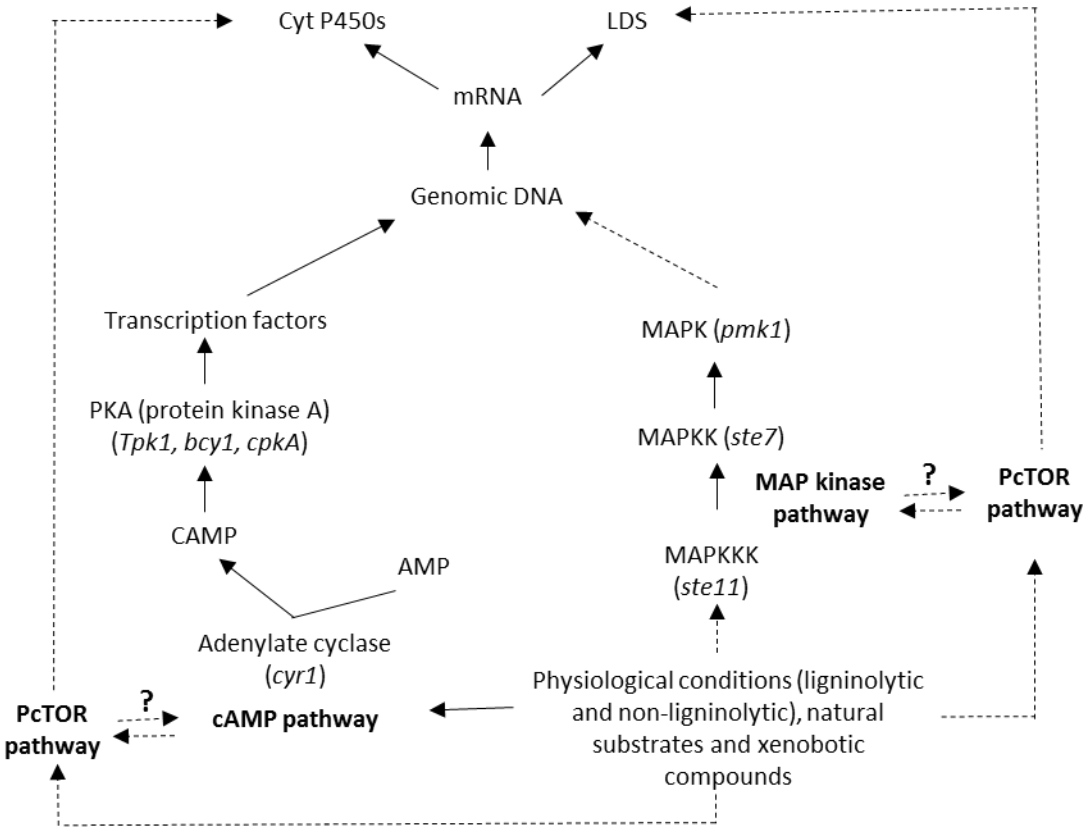

Figure 32. The proposed involvement of signaling pathways in expression of Cyt P450s and extracellular lignin degrading enzyme system (LDS) in *P. chrysosporium*.

Dashed arrows exhibit multiple steps or uncharacterized relationships. From Syed and Yadav with modifications (Syed and Yadav, 2012).

Understanding the regulation of extracellular secretion in fungi is essential for biotechnological applications (Snyman et al., 2019). Thus, the crosstalk between TOR and PKA, or Snf1 should be highlighted more in detail for application to extracellular production, especially for lignin degradation as proposed in Fig. 32. The findings concerning PcTOR described in this thesis are therefore relevant for this purpose.

The mutant strains with mutations in genes of interest are very important materials useful for characterizing genes via the reverse genetic approach. Ten rapamycin resistance mutants have been obtained with UV irradiation as mutagenesis agents. There are two mutants without any mutations in TOR. In the others with mutations in TOR, there are two mutants with mutations at the highly conserved residues essential for the interaction with rapamycin called *rap6* and *rap11*, and only one mutant with a mutation in FKBP12 defined as *rap8* that was confirmed to be used for characterizing PcTOR. To explain the inhibitory effect of rapamycin on WT strain, a docking modeling experiment was used. The molecular modeling result showed similar interactions to that in yeast *S. cerevisiae*. This approach was also applied to evaluate the possible effects of identified mutations on interactions which could explain the resistance phenotype. For these mutants, a study of regulatory components, in particular of TOR, will help characterize the secretome of the wood decaying fungi that has been proposed to be essential to understand the lifestyle and interactions of filamentous with environment (McCotter et al., 2016).

In conclusion, the obtained results including confirmation of the feasibility of WGS for the identification and isolation of causative mutations from a forward genetic screen for *P. chrysosporium* and the regulatory functions of PcTOR on the secretome of this fungus reveal future perspectives for utilizing this fungus, including its detoxification systems. From this study, WGS can indeed be applied to find the causal targets involved in the adaptation of *P. chrysosporium* in the context of wood degradation.

Article III

Isolation and characterization of *Phanerochaete chrysosporium* mutants resistant to wood extractives from *Bagassa guianensis* Aubl.

(This article has been prepared for submitting to journal BMC Genomic)

Introduction: In the wood degradation process, wood decaying fungi are exposed to toxic compounds either already present in wood (extractives) or coming from lignocellulose biotransformation. They have therefore developed efficient detoxification systems that enable them to deal with those compounds. Due to the lack of genetic tools in wood decaying fungi, the detoxification systems have been previously studied via biochemical characterization of several components giving only few insights about the regulation of these complex systems. Previous works confirmed that a forward genetic approach could be used in *P. chrysosporium*. We hypothesized that this approach can be used to find unknown important targets in the detoxification network, that may give new clues to better understand these detoxification systems. This study was therefore designed to identify targets involved in detoxification of *P. chrysosporium* in response to wood extractives of *Bagassa guianensis* Aubl. (bagassa wood extractives (BWE)).

Results: With the same method used to screen mutants resistant to itraconazole and rapamycin, mutants resistant to the acetonic extracts of *Bagassa guianensis* heartwood (*bag* mutants) were obtained. From the analysis of the mutant's growth in presence of BWE, two mutants, *bag4* and *bag31*, were selected to identify genes related to wood extractives resistance phenotype. The result of sequencing showed only one causal target gene with the same mutation position. The mutation was validated after classical cloning. The candidate gene encodes for a DENN domain-containing protein. Homologs are largely distributed in the fungal kingdom, and specific for each species. This protein is closely related to human DENND6B protein. Molecular modeling of the interactions between this DENND protein and the typical Rab GEF could explain the resistance phenotype. Additionally, from comparison with its functionally-related protein Avl9 in the yeast *S. cerevisiae*, potential functions of this protein were proposed.

Isolation and characterization of *Phanerochaete chrysosporium* mutants resistant to wood extractives from *Bagassa guianensis* Aubl.

Authors:

Nguyen D.V, Noel D, Gonzales F, Amusant N, Schwartz M, Morel-Rouhier M, Gelhaye E, Sormani R*

[a] Université de Lorraine, INRAE, IAM, F-54000 Nancy, France

*Corresponding author: Rodnay Sormani

Unité Mixte de Recherches 1136 Université de Lorraine/INRAE

Interactions Arbres / Micro-organismes

Faculté des sciences, entrée 1B, 3éme étage

Bd des aiguillettes

54500 VANDOEUVRE-Lès-NANCY

France

Mail: rodnay.sormani@univ-lorraine.fr

Tel: + 33 3 72 74 51 59

Abstract

Background: The wood decaying fungi of basidyomycetes have been known as the main degraders of lignin as well as lignocellulosic materials which is important for biorefinery industry. In this process, fungi must to cope with the toxic metabolites and stressors as byproducts. They also have to detoxify wood extractives with antifungal molecules. Those works are performed with the detoxification network. The functional characterization of this network has been hampered by the lack of genetic materials and toolkits. The genetic approach with next generation sequencing technology may provides a new strategy to overcome this bottleneck.

Results: We used the model fungus *Phanerochaete chrysosporium* with mutations linked to resitance phenotype against wood extractives from *Bagassa guianensis* Aubl. for the identification of candidate genes. Those mutants were obtained by the mutagenesis of WT strain with UV light and screening on the selective medium in presence of wood extractives at lethal concentration for WT. Two mutants *bag4* and *bag31* were chosen for whole-genome sequencing. By comparing to available genomic database as reference genome, the set of candidate SNPs was called for each mutant. They share one SNP on one same gene. There were not any other SNPs found on this gene even in the sequencing data of the bulked sample. This gene may encode one DENN domain – containing protein. Based on combination of sequencing analysis with molecular modeling, the possible functions were predicted.

Conclusions: In this work, we found the candidate gene encoding possibly a DENND protein as the causative factor underlying the resistance of fungus *P. chrysosporium* against *Bagassa guianensis* wood extractives. This result confirmed that the used sequencing strategy with sequencing both bulked mutants and individual mutant is efficient. It also confirmed that the forward genetic approach based on whole genome sequencing is feasible for characterizing *P. chrysosporium* in adaptation to wood extractives.

Keywords: *Phanerochaete chrysosporium*; *Bagassa guianensis* Aubl.; wood extractives

1. Introduction

The interest for wood decaying fungi has increased those last few years mainly due to their potential use in biomass valorization for the second generation of biofuels, their important function in the global carbon cycle and the damages that they can cause to wood materials. Indeed, these fungi, degrade and use efficiently wood components as carbon and energy sources. However, during these processes, wood decaying fungi have to cope with potential toxic molecules already present (wood extractives) or generate during the oxidative degradation of wood polymers. Wood extractives are non-structural components that can be removed with neutral to polar solvents. Their chemical nature and their composition could vary according to many factors such as the considered species, the wood part, or the tree growth conditions (Kebbi-Benkeder et al. 2014). To adapt to this potential toxic environment, wood decaying fungi have developed efficient detoxification systems (Morel et al., 2013). Comparative genomic approaches have highlighted extensions of multi-genetic families involved in drug metabolism (mainly cytochrome P450 monooxygenases and glutathione transferases (GST)) in wood decaying fungi compared to other fungi. In *Phanerochaete chrysosporium*, a white-rot model fungus, the presence of oak acetonic extract induced the expression of some of these genes (Thuillier et al., 2014). Several glutathione transferases from wood decaying fungi have been biochemically characterized demonstrating their interaction with wood extractives (Mathieu et al., 2012; Perrot et al., 2018). However, proteins involved in wood extractives resistance remains to be identified requiring an approach without *a priori*. The lack of physiological data concerning detoxification pathways in wood decaying basidiomycetes is mainly due to the absence of available genetic tools for these organisms. To bypass this bottleneck, a forward genetic strategy has been recently developed in *P. chrysosporium*, which has been allowed the screening itraconazole resistant mutants (*rit*) and rapamycin resistant mutants (*rap*) and to find each time the causal mutations. Here, we report the use of this approach to generate and characterize mutants resistant to wood extractives of *Bagassa guianensis* Aubl. *B. guianensis,* which is also known as tatajuba, is a large tree found in French Guiana. *B. guianensis* belongs to the Moraceae family that contains species with important economic and medicinal values due to the production of secondary compounds such as flavonoids, stilbenes, triterpenoids and xanthones, which possess antimicrobial activities in particular against wood decaying basidiomycetes (Royer et al., 2010, Perrot et al., 2018).

In this paper, we investigated the inhibitory activity of *B. guianensis* extractives on the germination and growth of *P. chrysosporium* RP78. From generation and characterization of *P. chrysosporium* mutants resistant to these extractives, a gene potentially involved in wood extractives resistance was identified by a forward genetic approach. Possible functions of this gene encoding a DENN-domain containing protein was discussed.

2. Materials and methods

2.1 Fungal strain and wood extractives preparation

The homokaryotic strain *Phanerochaete chrysosporium* RP78 was used in this study. The genomic database version 2.2 of this strain (Martinez et al., 2004) is available on https://genome.jgi.doe.gov/Phchr2/Phchr2.home.html. Wild type and mutated strains were maintained on solid malt extract agar medium (20 $g.L^{-1}$ and 30 $g.L^{-1}$ respectively) for storage.

Heartwood of *Bagassa guianensis* Aubl. was collected from the commercial origin (Degrad Saramaca's sawmill, Kourou, French Guiana). Samples were ground to fine sawdust (0.2 to 0.4 mm) before to be Soxhlet-extracted successively during 24 h using acetone. Acetone was then evaporated and dried extractives were stored at -18 °C before use. The bagassa wood extractives (BWE) were resuspended in DMSO.

2.2 Mutagenesis and screening of conidia from *P. chrysosporium*

Conidia of *P. chrysosporium* RP78 were obtained by cultivation at 37 °C for 5 days on sporulation medium (Glucose (10 $g.L^{-1}$), malt extract (10 g. L^{-1}), peptone from potato (2 $g.L^{-1}$); yeast extract (2 $g.L^{-1}$), asparagine (1 $g.L^{-1}$), KH_2PO_4 (2 $g.L^{-1}$), $MgSO_4.7H_2O$ (1 $g.L^{-1}$), thiamine HCl (1 $mg.L^{-1}$), Agar (30 $g.L^{-1}$)), all chemicals used were purchased from Sigma Aldrich. These conidia were directly irradiated with UV light for 30 seconds. Mutated spores were continuously suspended in water by filtering with Miracloth. A suspension volume with 10.000 spores was plated on the petri dish containing malt extract-agar medium (20 $g.L^{-1}$, 30 $g.L^{-1}$ respectively) mixed with BWE (100 $mg.L^{-1}$ in final concentration). Petri dishes were incubated at 37 °C until the appearance of individual conidia on medium surface. Appeared mycelia were harvested and cultivated on sporulation medium mixed with 100 $mg.L^{-1}$ of wood extractives. 10,000 conidia developed on that medium were moved into Falcon tube containing 10 mL of liquid medium of 1% malt extract in presence of 45 µg. L^{-1} of wood extractives. Single spore progenies growing in liquid medium were fished and grown on sporulation medium mixed with 100 $mg.L^{-1}$ of wood extractives. Spores from this medium were used as mutant lines called *bag* mutants for further experiments.

2.3. Germination

Germination of *P. chrysosporium* RP78 conidia was measured using a nephelometric reader (NEPHELOstar Galaxy, BMG Labtech, Offenburg, Germany). For inocula, spores were obtained from 8 day-old mycelia grown on sporulation medium from a gentle scraping of the agar plates and filtration through Miracloth. The spores concentation was determined) measuring the optical density at 650

nm as previously described (Tien and Kirk, 1983). 10,000 spores were resuspended in 200 µL of malt extract 1% in presence or absence of BWE and incubated in the nephelometer reader at 37 °C for 72 hours. Relative nephelometric unit (NRU) values were calculated as previously described (Joubert et al., 2010).

2.4 Solid cultures

The medium malt extract 2% agar (MA) was supplemented or not by BWE (stock solution (100 mg/ml) in DMSO). Plates were inoculated using one fungal mycelium plug. Additional experiments have been carried out using diffusion tests. Papers impregnated or not by BWE were placed on MA plates before their inoculation. Plates were depicted after 48 hours for analysis.

2.5 Wood degradation testing

P. chrysosporium WT and the studied mutants were cultivated on MA in presence of *B. guianensis* wood chips. After 2 months of incubation at 37°C, wood chips were harvested, dried and weighted in order to determinate their mass loss.

2.5 Genomic DNA purification and sequencing procedure

Genomic DNA extractions were performed from 3-day liquid cultures using QIAGEN DNeasy plant kit. DNAseq was performed at the GeT-PlaGe core facility, INRA Toulouse. DNA-seq libraries have been prepared according to Illumina's protocols using the Illumina TruSeq DNA PCR-free HT Library Prep Kit. Briefly, DNA was fragmented by sonication, size selection was performed using SPB beads (kit beads) and adaptors were ligated to be sequenced. Library quality was assessed using an Advanced Analytical Fragment Analyzer and libraries were quantified by QPCR using the Kapa Library Quantification Kit. DNA-seq experiments have been performed on an Illumina HiSeq3000 using a paired-end read length of 2x150 bp with the Illumina HiSeq3000 Reagent Kits.

2.6 Data analysis for SNPs identification

In the first step, all short reads from high-throughput sequencing were mapped to the reference genome of *Phanerochaete chrysosporium* RP78 v2.2 (Martinez et al., 2004; Ohm et al., 2014), available on https://genome.jgi.doe.gov/Phchr2/Phchr2.home.html, using BWA (Li and Durbin, 2009). In the next step, the VCF file containing the called SNPs was built with SAMtools (Li, 2011). In the final, the SNPs were identified by filtering, frequencies calculation, and visualization with SHOREmap v3.5 (Sun and Schneeberger, 2015).

2.7 Mutation validation of target gene

Polymerase chain reaction (PCR): The PCR was performed using enzyme Gotaq G2 Flexi DNA polymerase with Mg-free 5X Green Gotaq Flexi Reaction Buffer (Promega). The forward primer ATGGGTGTCACTGTCGAGG and the reverse primer CTCGAACTTGAGCGTCGA. A volume of 20 µl reaction mixture was composed of 1X green Gotaq Flexi Buffer, 2 mM $MgCl_2$, 0.16 mM DNTP, 0.1 µM forward and reverse primers, around 2.5 ng/µl of gDNA and 0.01 U/µl Gotaq G2 Flexi in final concentration, sterile water. The reaction program was run according to the following protocol: (1) 2 min at 95°C, (2) repetition cycles composed of 30s at 95°C, 30s at melting temperature 55°C and a step at 72°C with a specific elongation time (1min30s for gDNA, and 1min15s for cDNA). Those steps were repeated 35 times. PCR products were visualized on agarose gel then purified using PCR DNA and Gel Band Purification kit (GE Healthcare, UK).

Sequence cloning and sequencing: Plasmid PGEMt was used for the ligation of purified PCR products according to manufacturer protocol (promega A1360, USA). The reaction mixture includes 5µl of buffer 2X, 1µl of plasmid PGEMt, 3µl of PCR products and 1µl of T4 DNA ligase. This mixture is incubated overnight at 4°C and used to transform *E.coli* DH5α. Plasmid purification was performed after 3ml culture of an isolated transformed colony. Plasmid purification was performed using PureYield ™ Plasmid Miniprep system kit (Promega) following the instructions of provider. Purified plasmids were stored at -20°C before being sent to sequencing using T7p and SP6 universal primers (GENEWIZ, UK).

3. Results

3.1 *B. guianensis* extractives have the inhibitory effect on the growth of *Phanerochaete chrysosporium* RP78

In liquid medium, germination of *P. chrysosporium* RP78 spores was followed in presence of several concentrations of *B. guianensis* extractives (BWE) (Fig. 1A). In absence of BWE, three growth phases have been observed : a lag phase (0 h to 5 h), an exponential phase (5 h to 30 h) and a stationary phase after 30 h of incubation. In presence of 10 $\mu g.mL^{-1}$ BWE, a similar germination pattern was observed. The presence of 20 $\mu g.mL^{-1}$ BWE concentration increased the lag phase (15 h). The exponential phase was also longer, 45 hours instead of 20 hours. At higher BWE concentrations (30 $\mu g.mL^{-1}$ and higher), conidia germination was completely inhibited. The inhibitory effects of BWE (100 $\mu g.mL^{-1}$ and higher) were also confirmed on P. chrysosporium solid cultures (Fig. 1B) and through the diffusion tests (300 $\mu g.mL^{-1}$ and higher) (Fig. 1C).

Altogether, these data confirmed the antifungal properties of acetonic extracts of *B. guianensis* as reported previously (Royer et al., 2010; Perrot et al., 2018) and defined the appropriate extractives concentrations to perform the screening of *P. chrysosporuim* RP78 resistant mutants.

3.2 Isolation and characterization of selected *bag* mutants

P. chrysosporium conidia were exposed to UV light for 30 seconds and then plated on MA supplemented with 100 µg. mL^{-1} *B. guianensis* extractives. After 5 incubation days, 46 individual colonies (*bag* mutants) were picked up and subcultured on sporulation medium containing *B. guianensis* extractives (100 µg. mL^{-1}). 10,000 spores of each mutant were harvested after one week and added to 10 mL of malt extract medium supplemented *B. guianensis* extractives (50 $\mu g.mL^{-1}$). After 3 days, germinated conidia were fished individually and plated. Among the 46 *bag* mutant strains, 31 were able to grow under these conditions. A second round of conidia production and isolation was perfomed using the same culture conditions to generate lines considered as “one spore progeny”.

Solid cultures of the obtained *bag* mutants were performed (Fig. 2A). In presence of 100 µg. mL^{-1} *B. guianensis* extractives, all mutants exhibit a better growth than the wild type in the tested conditions. The growth rate of *bag2* and *bag4* were clearly faster than the other mutants. Based on this first test, liquid cultures were performed using six *bag* mutants selected from the 31 mutants (Fig. 2C, D). *bag2* and *bag4* were selected since they exhibited the highest growth rate in previous experiments. In contrast to the other mutants (data not shown), *bag31* and *bag23* are able to grow in presence of 200 $\mu g.mL^{-1}$ of *B. guianensis* extractives (Fig. 2B) and were also selected. Two other mutants *bag1* and *bag5* were randomly selected.

In absence of *B. guianensis* extractives, similar growth patterns were observed for the tested mutants and the WT. Nevertheless, a slight increase of the lag phase was observed for the mutants in comparison with the WT (Fig. 2C). In presence of BWE (30 $\mu g.mL^{-1}$), WT, *bag5*, *bag23* germination were fully inhibited, whereas conidia germination was observed for *bag1*, *bag2*, *bag4* and *bag31.* As expected*,* germination and growth rates of the tested mutants were dependant of the used concentration of BWE as shown in in supplement data (Fig. S1).

3.3 Identification and validation of causative mutation linked to BWE resistance

From the screening experiment described above, *bag4* and *bag31* were selected for a whole-genome re-sequencing strategy. Genomic DNA from *bag4* and *bag31* were extracted and individually sequenced using Mi-seq technology. At the same time, a bulk of gDNA from all *bag* mutants and from

the WT has been pooled (0.5 µg/mutant). This gDNA mixture, named collection DNA, has been sequenced using the same technology.

For the individual mutant whole genome re-sequencing experiments, the obtained sequencing data have been aligned with the reference genome (Martinez et al., 2004). Using the SHOREmap software (Sun and Schneeberger, 2015) and 0.75 cut-off of allele frequency, mutations were identified in the genomes of the sequenced mutants For the *bag4* sequencing experiment, 1006 SNPs were found in the whole genome. Removing the intergenic mutations and synonymous mutations (nucleotide substitution that did not lead to amino acid substitution), detected SNPs dropped to 50. In other words, 50 SNPs were in non-intergenic regions, not synonymous and they were found in 46 genes (Table 1). Using the same strategy, 1301 SNPs were found in the whole-genome of *bag* 31 and 64 were not intergenic not synonymous and they were found in 54 genes (Table 2). Only one gene was found mutated in both genomes (after the described selection): AGR57_7124 (Fig. 3A), both carrying the same substitution (C to T; scaffold 7 at position 104070). This mutation led to an amino acid substitution, replacing a glutamic acid by a lysine. The presence of this mutation in both mutated (but not in the WT) genomes was confirmed by sequencing PCR product obtained from gDNA from *bag4*, *bag31* and WT (data not shown). This substitution was also found in collection DNA with a frequency of 0.33 (i.e. this SNP is found in 33% of the short reads at this position). However, no additional mutation was observed in encoding sequence for AGR57_7124. Taking together, these data suggest that several bag mutants possess this mutation. However, not all the *bag* mutants carry a mutation in AGR_7124 suggesting that *bag* phenotype can be due to other mutations.

3.5 AGR57_7124 is coding a DUF1630 protein and share homology with DENN domain proteins

Based on automatic annotation and homologs found in FungiDB and Joint Genome Institute databases, AGR_7124 encodes a protein containing a domain with unknown function 1630 (DUF1630). Using a genomic comparative approach, homologs were identified in 28 fungal genomes on 158 genomes tested (in November 2019). Homologs were found in fungi like pathogens, mycorrhizal or saprotrophic fungi from ascomycetes and basidiomycetes groups. When homologs have been found, only one sequence per genome shares homology with PcDUF1630 sequence in the examined genomes. Homologs of PcDUF1630 were also found in plant and animal kingdoms. In human, the closest homolog of PcDUF1630 is the protein DENND6B. The 18 identified human DENND (Differentially Express in Normal and Neoplastic cells Domain) proteins have been classified into eight families. All these DENND proteins harbor the typical feature of Rab GTPases regulators (Marat et al., 2011). PcDUF1630 exhibits 40% of similarity at the protein level with HsDENND6A and HsDENND6B proteins.

To predict more in detail the possible function of PcDUF1630 and consequences from the mutation, a modeling experiment has been done. PcDUF1630 was input to the automatic modeling server SwissModel. The templates identified by SwissModel are the PDB entries 6EKK and 3TW8, which are DENN-domain containing proteins. Based on the structure of HsDENND1B (PDB 3TW8), a predictive model of PcDUF1630 was built. With a sequence identity of only 13.20 % between the template and the sequence of PcDUF1630, the model built has a low confidence QMEAN score of -8.30. However, an acceptable solvation score of -1.79 may indicate a global fold that would be viable. The results of this structural modeling work are interpreted as putative hypothesis for future work. The overall fold of PcDUF1630 could be similar to the one of HsDENND1B (PDB 3TW8), corresponding to a central beta-sheet surrounded by alpha-helices in a bi-lobed fashion. In PDB 3TW8, DENND1B (Fig. 4A, blue-green color) interacts with the Rab35 GTPase (Fig. 4A, yellow color) via several non-covalent interactions including one H-bond between Rab35:R79 and the CO main chain of DENND1B: H192 at the C-terminal end of helix 6 (Fig. 4A). In the modeled PcDUF1630 structure, the equivalent helix bears the motif CLLLC with the second cysteine at the end of the helix and immediately followed by the acidic E335 residue (Fig. 4B). By homology, we suggest that these exposed residues would interact with a protein partner, putatively a GTPase. Interestingly, the mutation found in *bag4* and *bag31* leads to an amino acid substitution at this position. The mutated PcDUF1630^{E335K} exhibits a basic K residue instead of the acidic E335 residue, and the corresponding strains *bag4* and *bag31* are able to grow in presence of the BWE. From those results a putative explanation should be that a molecule from the BWE inhibits the interaction between the two partners PcDUF1630/DENND and a putative GTPase leading to the antifungal BWE effect. In this hypothesis the mutation in AGR57_7124, leading to PcDUF1630^{E335K} substitution, avoid the molecule from BWE to interact with PcDUF1630/DENND, leading to a resistance phenotype.

3.6 Resistance to BWE leads to an increase wood degradation of *B. guianensis* wood

From our previous results we can make the following syllogism: BWE have antifungal activity (Fig. 1) and BWE protects *B. guianensis* wood from fungal driven decaying, so mutants resistant to BWE better decay *B. guianensis* wood than Wild type fungus.

This has been tested. Sequenced *bag* mutants (*bag4* and *bag31*) were grown in presence of *B. guianensis* wood chips, the WT being used as control. After 25 days of incubation at 37 °C, mutants colonized the wood samples unlike WT (Fig. 5A). After 2 months of incubation, wood chips were harvested and mass losses determined (Fig. 5B). *bag4* and *bag31* had a significant higher degradation capacity of *B. guianensis* wood chips than the WT, demonstrating that their resistance to BWE leads to a better ability to decay *B. guianensis* wood.

4. Discussion

Due to their importance in carbon cycle and their potential commercial applications, white rot fungi are organisms of major interest. Among them, *P. chrysosporium* has been considered a model in studies of lignin and xenobiotics degradation. One of the most difficulties which restricts characterizing more deeply this fungus is the lack of genetic materials, especially the lack of effective protocols for generating transformants. There have been several attempts to deal with this problem, one of them is genetic forward screens with support of next generation sequencing (see article 1).

Whole genome sequencing to call the causal gene involved in the acetonic wood extractives of *Bagassa guianensis* Aubl. resistance phenotype

Forward genetics enable identification of mutants with phenotypes of interest which start mechanistic understanding of biological process via reverse genetics in later (Schneeberger, 2014). Recently, Whole Genome Senquencing sequencing method enable to identify powerfully mutations including SNPs and small indels as described in model organisms (Schneeberger and Weigel, 2011). This strategy has been used to identify targets involved in drug resistance strains appearing during clinlic practice (Köser et al., 2014). For instance, it has been very efficient to find mutations involved in itraconazole resistant strains of *Aspergillus fumigatus* (Abdolrasouli et al., 2015; Camps et al., 2012). One big challenge in candidate SNP identification is the availability of high number of SNPs emerged from mutagenesis process by chemical mutagens or radiations. In plant and animal such as *Arabidopsis thaliana* or zebrafish, general strategy is the combination of meiotic mapping with whole genome sequencing to identify the causative mutations. Therefore, backcrossing of mutants with parential strains, or pooling of several mutants with wild type is necessary (Schneeberger and Weigel, 2011; Zuryn et al., 2010). This strategy enable to reduce the possible maximum numbers non-causal SNPs. The major limitation of this way, that is also called re-sequencing, is the requirement of a reference genome sequence. To deal with this limitation, a new mapping protocol was developed based on advances in short-read sequencing analysis algorithms which enable SNPs calling without a reference genome sequence (Nordström et al., 2013). This method, callled the straightforward identification of causative mutation, is carried out by searching for common genes disrupted in two different mutants with the same phenotype isolated from the same screen (Nordström et al., 2013). Genome sequencing also could directly performed for only separated mutant alone, without bulked pooling (Zuryn et al., 2010).

For fungal strains with available genomic databases, directly sequencing a single mutant of interest without backcrossing is feasable thanks to the availability of filtering toolkit that also allow to reduce

the numbers of non-causal SNPs. In our case, since genomic databases is available for *P. chrysosporium*, SAMtools, one of the most reliable toolkits for SNPs calling (Altmann et al., 2012), was applied to call candidate SNPs. This tool also is one of fastest computational tools. At the step of candidate SNP identification, Shoremap, one toolkit which enable to remove intergenic and synonymous mutations, and also support variant filtering, was applied.

Following this identification strategy via direct sequencing, we here show that this method is also powerful for identifcation of causal mutation in the model white rot *P. chrysosporium* via directly sequencing two single mutants that were isolated from the same screen, and were resistant to BWE in comparison to WT strain. Antifungal activities of *B. guianensis* extractives could be mainly due to the presence of moracins but also to other compounds (Royer et al., 2012). Several compounds could then be involved in inhibitory effects. Confirming that, the allele frequency value of the candidate SNP identified from sequencing data of *bag4* and *bag31* decreases but remain at an important level (33%) in sequencing data of the bulked sample. *Bag4* and *bag31* were selected for their resistance towards *B. guianensis* extractives. However *bag4* is able to grow faster that *bag31* in presence of 100 $mg.L^{-1}$ of *B. guianensis* extractives (Fig. 2A) while *bag31* is more resistant to extractives than *bag4* at concentration 200 $mg.L^{-1}$ (Fig. 2B). Both mutants are more efficient than the WT to degrade *B. guianensis* wood, confirming the importance of extractives in wood durability of this species.

Identification of PcDUF1630 as the DENN-domain containing protein reveals perspectives for the characterization of adaptation/detoxification mechanism of *P. chrysosporium* in response to antifungal wood extractives

From the developed approach, a DENN-domain containing protein was identified as a potential gene involved in *B. guianensis* extractives resistance. The resulting protein named PcDUF1630/PcDENND exhibits the highest similarity to HsDENND6B. According to Pfam database classification, DENND family belongs to Avl9 clan comprising members which are involved in vesicle formation and trafficking (Finn et al., 2014). Two structural motifs were well conserved in DENN-like proteins (Levine et al., 2013). The first is a GxxØ motif that is typical of longin domain (LD) protein, and the second is an Asx motif that forms the tight β-turn. They were shown to be specific for tight β-turns and likely critical to the overall structure of DENN-like proteins (Levine et al., 2013). Typical property of DENND proteins is to interact with small GTPases belonging to Rab protein family mediating the exchange of GDP to GTP by GEF activity. HsDENND/Pfam116 has been shown to exhibit a GEF activity toward Rab14(Linford et al., 2012). Through this activity, Pfam116 was shown to regulate the endocytic recycling pathway required for ADAM protease trafficking and regulation of cell-cell junctions (Linford et al., 2012). Based on these data, an involvement of PcDENND/PcDUF1630 in the secretory pathway

and stress response could be proposed. From molecular modeling, the observed mutation in PcDENND could change interactions between PcDENND and Rab GTPase leading to extractive resistance phenotype of *bag4* and *bag31*. Nevertheless, this hypothesis remains to be confirmed by additionnal experiments.

Abbreviations

BWE: Bagassa wood extractives; SNPs: Single nucleotide polymorphisms; WT: wild type; UV: UltraViolet radiation; JGI: DOE Joint Genome Institute; BWA: Burrows-Wheeler Aligner; AF: Allele frequency; DENND: DENN-domain containing protein; GEF: Guanine nucleotide exchange factor

Acknowledgment

This work was supported by a grant overseen by the French National Research Agency (ANR) as part of the "Investissements d'Avenir" program (ANR-11-LABX-0002-01, Lab of Excellence ARBRE). NDV was supported by a Doctoral Fellowship from the Ministry of Agriculture and Rural Development, Vietnam (Agricultural and Fisheries Biotechnology Program) and support from French ministry of foreign affair (program Campus France). FGA was supported by a postdoctoral grant from Region Grand Est.

Bibliography

Abdolrasouli, A., Rhodes, J., Beale, M.A., Hagen, F., Rogers, T.R., Chowdhary, A., Meis, J.F., Armstrong-James, D., Fisher, M.C., 2015. Genomic Context of Azole Resistance Mutations in Aspergillus fumigatus Determined Using Whole-Genome Sequencing. mBio 6. https://doi.org/10.1128/mBio.00536-15

Altmann, A., Weber, P., Bader, D., Preuß, M., Binder, E.B., Müller-Myhsok, B., 2012. A beginners guide to SNP calling from high-throughput DNA-sequencing data. Hum. Genet. 131, 1541–1554. https://doi.org/10.1007/s00439-012-1213-z

Camps, S.M.T., Dutilh, B.E., Arendrup, M.C., Rijs, A.J.M.M., Snelders, E., Huynen, M.A., Verweij, P.E., Melchers, W.J.G., 2012. Discovery of a hapE Mutation That Causes Azole Resistance in Aspergillus fumigatus through Whole Genome Sequencing and Sexual Crossing. PLOS ONE 7, e50034. https://doi.org/10.1371/journal.pone.0050034

Finn, R.D., Bateman, A., Clements, J., Coggill, P., Eberhardt, R.Y., Eddy, S.R., Heger, A., Hetherington, K., Holm, L., Mistry, J., Sonnhammer, E.L.L., Tate, J., Punta, M., 2014. Pfam: the protein families database. Nucleic Acids Res. 42, D222–D230. https://doi.org/10.1093/nar/gkt1223

Harsay, E., Schekman, R., 2007. Avl9p, a Member of a Novel Protein Superfamily, Functions in the Late Secretory Pathway. Mol. Biol. Cell 18, 1203–1219. https://doi.org/10.1091/mbc.e06-11-1035

Joubert, A., Calmes, B., Berruyer, R., Pihet, M., Bouchara, J.-P., Simoneau, P., Guillemette, T., 2010. Laser nephelometry applied in an automated microplate system to study filamentous fungus growth. BioTechniques 48, 399–404. https://doi.org/10.2144/000113399

Köser, C.U., Ellington, M.J., Peacock, S.J., 2014. Whole-genome sequencing to control antimicrobial resistance. Trends Genet. 30, 401–407. https://doi.org/10.1016/j.tig.2014.07.003

Levine, T.P., Daniels, R.D., Gatta, A.T., Wong, L.H., Hayes, M.J., 2013. The product of C9orf72, a gene strongly implicated in neurodegeneration, is structurally related to DENN Rab-GEFs. Bioinformatics 29, 499–503. https://doi.org/10.1093/bioinformatics/bts725

Li, H., 2011. A statistical framework for SNP calling, mutation discovery, association mapping and population genetical parameter estimation from sequencing data. Bioinformatics 27, 2987–2993. https://doi.org/10.1093/bioinformatics/btr509

Li, H., Durbin, R., 2009. Fast and accurate short read alignment with Burrows–Wheeler transform. Bioinformatics 25, 1754–1760. https://doi.org/10.1093/bioinformatics/btp324

Linford, A., Yoshimura, S., Bastos, R.N., Langemeyer, L., Gerondopoulos, A., Rigden, D.J., Barr, F.A., 2012. Rab14 and Its Exchange Factor FAM116 Link Endocytic Recycling and Adherens Junction Stability in Migrating Cells. Dev. Cell 22, 952–966. https://doi.org/10.1016/j.devcel.2012.04.010

Marat, A.L., Dokainish, H., McPherson, P.S., 2011. DENN Domain Proteins: Regulators of Rab GTPases. J. Biol. Chem. 286, 13791–13800. https://doi.org/10.1074/jbc.R110.217067

Martinez, D., Larrondo, L.F., Putnam, N., Gelpke, M.D.S., Huang, K., Chapman, J., Helfenbein, K.G., Ramaiya, P., Detter, J.C., Larimer, F., Coutinho, P.M., Henrissat, B., Berka, R., Cullen, D., Rokhsar, D., 2004. Genome sequence of the lignocellulose degrading fungus Phanerochaete chrysosporium strain RP78. Nat. Biotechnol. 22, 695–700. https://doi.org/10.1038/nbt967

Mathieu, Y., Prosper, P., Buée, M., Dumarçay, S., Favier, F., Gelhaye, E., Gérardin, P., Harvengt, L., Jacquot, J.-P., Lamant, T., Meux, E., Mathiot, S., Didierjean, C., Morel, M., 2012. Characterization of a

Phanerochaete chrysosporium Glutathione Transferase Reveals a Novel Structural and Functional Class with Ligandin Properties. J. Biol. Chem. 287, 39001–39011. https://doi.org/10.1074/jbc.M112.402776

Morel, M., Meux, E., Mathieu, Y., Thuillier, A., Chibani, K., Harvengt, L., Jacquot, J.-P., Gelhaye, E., 2013. Xenomic networks variability and adaptation traits in wood decaying fungi. Microb. Biotechnol. 6, 248–263. https://doi.org/10.1111/1751-7915.12015

Nordström, K.J.V., Albani, M.C., James, G.V., Gutjahr, C., Hartwig, B., Turck, F., Paszkowski, U., Coupland, G., Schneeberger, K., 2013. Mutation identification by direct comparison of whole-genome sequencing data from mutant and wild-type individuals using k -mers. Nat. Biotechnol. 31, 325–330. https://doi.org/10.1038/nbt.2515

Ohm, R.A., Riley, R., Salamov, A., Min, B., Choi, I.-G., Grigoriev, I.V., 2014. Genomics of wood-degrading fungi. Fungal Genet. Biol., Biomass Degradation by Fungi 72, 82–90. https://doi.org/10.1016/j.fgb.2014.05.001

Perrot, T., Schwartz, M., Saiag, F., Salzet, G., Dumarçay, S., Favier, F., Gérardin, P., Girardet, J.-M., Sormani, R., Morel-Rouhier, M., Amusant, N., Didierjean, C., Gelhaye, E., 2018. Fungal Glutathione Transferases as Tools to Explore the Chemical Diversity of Amazonian Wood Extractives. ACS Sustain. Chem. Eng. 6, 13078–13085. https://doi.org/10.1021/acssuschemeng.8b02636

Royer, M., Herbette, G., Eparvier, V., Beauchêne, J., Thibaut, B., Stien, D., 2010. Secondary metabolites of Bagassa guianensis Aubl. wood: A study of the chemotaxonomy of the Moraceae family. Phytochemistry 71, 1708–1713. https://doi.org/10.1016/j.phytochem.2010.06.020

Schneeberger, K., 2014. Using next-generation sequencing to isolate mutant genes from forward genetic screens. Nat. Rev. Genet. 15, 662–676. https://doi.org/10.1038/nrg3745

Schneeberger, K., Weigel, D., 2011. Fast-forward genetics enabled by new sequencing technologies. Trends Plant Sci. 16, 282–288. https://doi.org/10.1016/j.tplants.2011.02.006

Sun, H., Schneeberger, K., 2015. SHOREmap v3.0: Fast and Accurate Identification of Causal Mutations from Forward Genetic Screens, in: Alonso, J.M., Stepanova, A.N. (Eds.), Plant Functional Genomics: Methods and Protocols, Methods in Molecular Biology. Springer New York, New York, NY, pp. 381–395.

Thuillier, A., Chibani, K., Belli, G., Herrero, E., Dumarçay, S., Gérardin, P., Kohler, A., Deroy, A., Dhalleine, T., Bchini, R., Jacquot, J.-P., Gelhaye, E., Morel-Rouhier, M., 2014. Transcriptomic Responses of Phanerochaete chrysosporium to Oak Acetonic Extracts: Focus on a New Glutathione Transferase. Appl Env. Microbiol 80, 6316–6327. https://doi.org/10.1128/AEM.02103-14

Tien, M., Kirk, T.K., 1983. Lignin-Degrading Enzyme from the Hymenomycete Phanerochaete chrysosporium Burds. Science 221, 661–663. https://doi.org/10.1126/science.221.4611.661

Zuryn, S., Gras, S.L., Jamet, K., Jarriault, S., 2010. A Strategy for Direct Mapping and Identification of Mutations by Whole-Genome Sequencing. Genetics 186, 427–430. https://doi.org/10.1534/genetics.110.119230

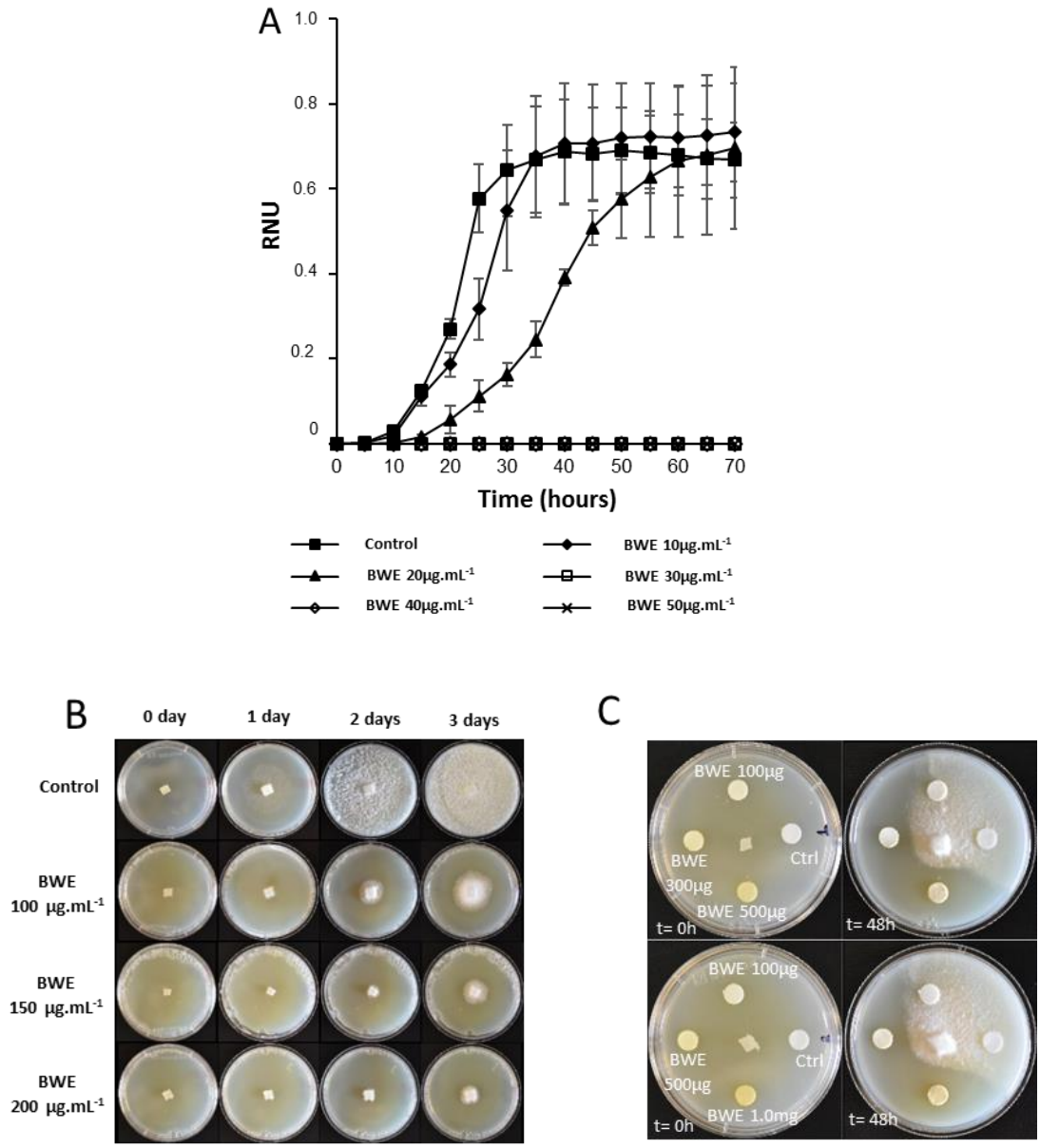

Figure 1. Effect of acetonic bagassa wood extractives (BWE) on germination and hyphal growth of *P. chrysosporium* RP78 conidia.

A. Determination of BWE concentration needed to fully inhibit conidia germination using nephelometric measurement. Freshly collected conidia of *P. chrysosporium* RP78 were cultivated during 72 hours in malt extract 1% liquid medium with different concentration of BWE, DMSO was added in the control of experiment. Testing plate were incubated at 37 °C. RNU represents Ralative Nephelometric Unit. Standard deviation was calculated from 9 and 3 replicates for control and treatments, respectively.

Figure 1. Continued.

B. BWE inhibit hyphal growth of *P. chrysosporium* RP78 conidia. A plug of of *P. chrysosporium* RP78 was placed at the center of Petri dishes of either malt extract 2% agar (Control) or malt extract 2% agar supplemented with extractives at concentrations of 100 µg.mL^{-1}, 150 µg.mL^{-1}, 200 µg.mL^{-1}. Petri dishes were incubated at 37 °C, and pictures were obtained during 3 days of incubation.

C. Inhibition of BWE with the use of Whatman filter paper. On the malt extract 2% agar medium, Whatman papers were impregnated with different contents of extractives, or 10 µl DMSO for control (Ctrl). A plug of *P. chrysosporium* RP78 was placed at the center of petri dish. Pictures were taken at the begining of the test (t=0h) and after 48 hours of incubation at 37 °C.

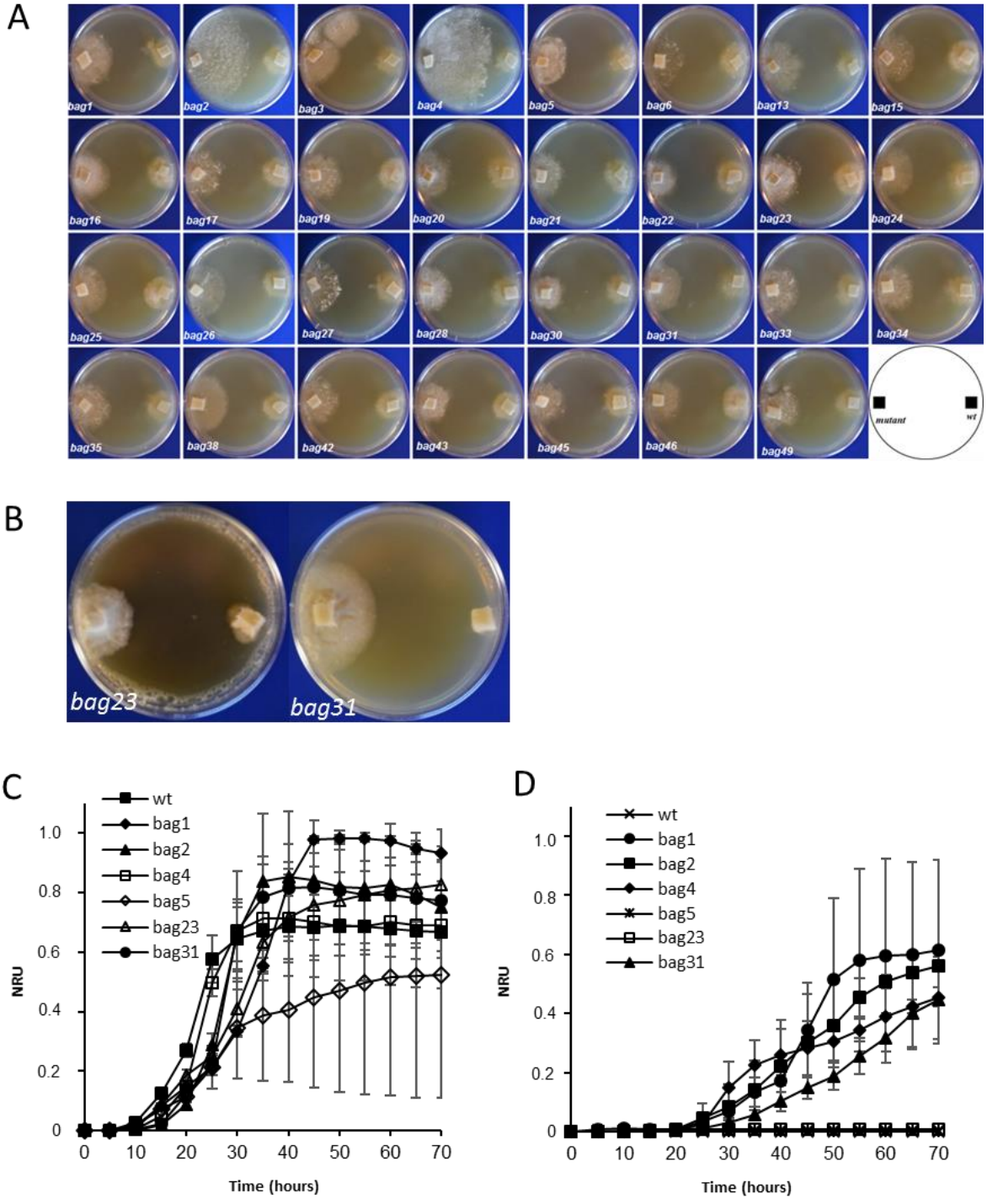

Figure 2: Phenotype of *bag* mutants.

A. Hyphal growth of *bag* mutants in comparison with that of wild type on malt extract 2% agar mixed with BWE at 100 µg. mL^{-1}. B. The resistance against BWE 200 µg. mL^{-1}.

Figure 2: Continued.

C, D. Conidia germination of *WT*, *bag1*, *bag2*, *bag4, bag5, bag23* and *bag31* in control condition (without extractives), and in presence of BWE at 30 µg.mL^{-1} which inhibited completely germination of WT (Fig. 1). Measurement have been done during 70h using nephelometer. Standard deviation was calculated from 3 replicates.

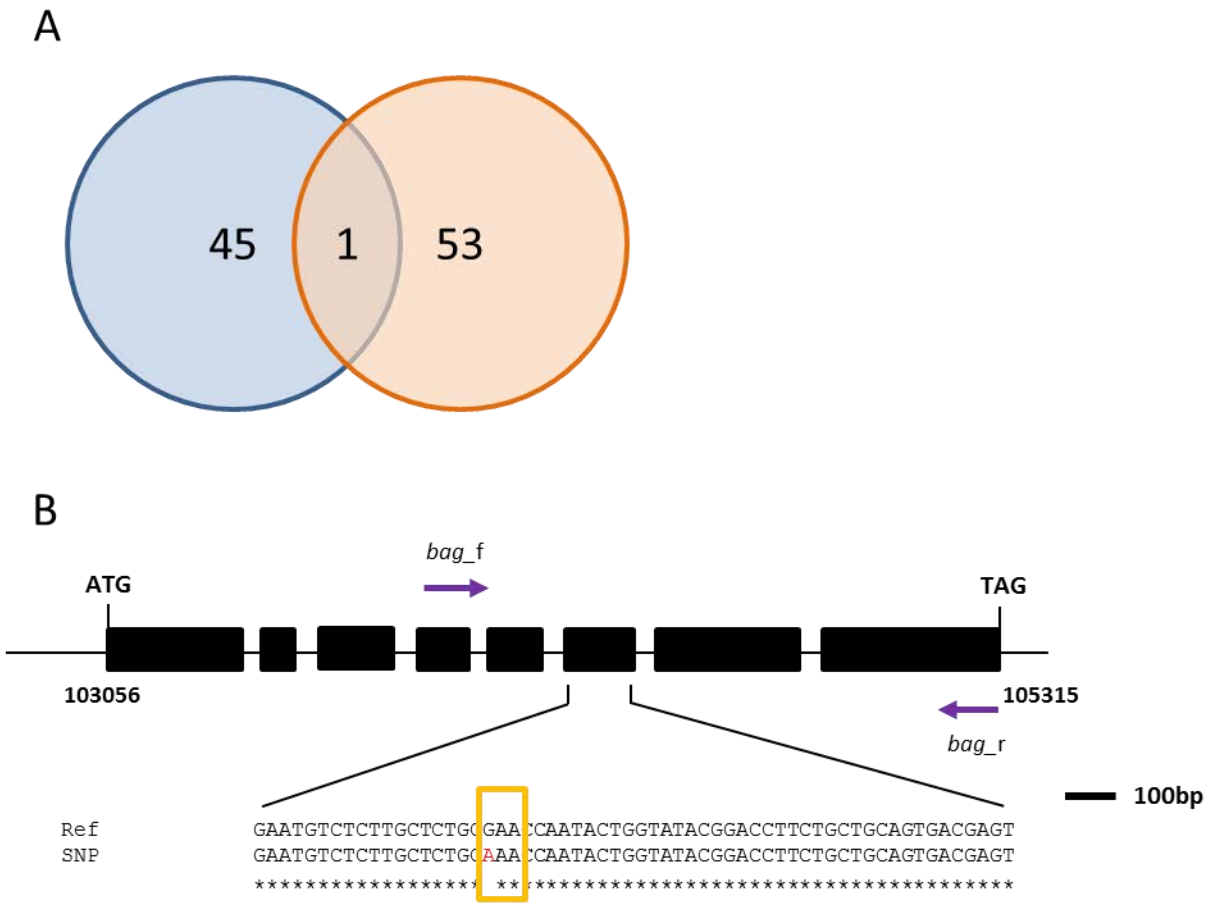

Figure 3. The causal mutation in *bag* mutants.

A. Venn diagram highlighting the common mutations between two distinct sequencing experiments of gDNA of *bag4* and *bag31*.

B. Graphical mapping of gene with the causal mutation that located at Scaffold 7: 104070 G→A.

Table 1. List of genes with identified SNP in the mutant *bag4*.

Gene identifier	Identity of scaffold	Position of a base in the reference sequence	Base in the reference sequence	Alternative/ mutant base	Region of DNA which is affected by the change	Amino acid according to reference	Resulting substitution
AGR57_827	scaffold_1	1737019	G	A	CDS	S	L
AGR57_1241	scaffold_1	2695172	C	A	CDS	R	L
AGR57_1794	scaffold_2	571089	G	T	intronic/noncoding		
AGR57_2419	scaffold_2	1866158	C	T	CDS	S	F
	scaffold_2	1866159	C	T	CDS	S	F
AGR57_1996	scaffold_2	994606	G	T	CDS	G	V
AGR57_2068	scaffold_2	1127968	G	A	CDS	P	S
AGR57_4000	scaffold_3	2364982	C	T	CDS	S	F
AGR57_3251	scaffold_3	696781	G	T	CDS	P	T
AGR57_3368	scaffold_3	926070	C	T	CDS	P	S
AGR57_3812	scaffold_3	1940559	T	C	CDS	H	R
	scaffold_3	1940656	C	T	CDS	E	K
AGR57_4372	scaffold_4	761370	C	A	CDS	Q	K
AGR57_4603	scaffold_4	1202261	C	T	CDS	H	Y
	scaffold_4	106632	C	T	CDS	A	V
AGR57_5668	scaffold_5	1208924	G	A	CDS	S	F
AGR57_5390	scaffold_5	602115	A	G	CDS	V	A
AGR57_5827	scaffold_5	1545859	T	C	CDS	F	L
AGR57_6058	scaffold_5	2008794	G	A	CDS	S	L
AGR57_5947	scaffold_5	1768617	G	A	CDS	S	L
AGR57_6650	scaffold_6	1079424	G	A	CDS	Q	*
AGR57_6349	scaffold_6	462761	A	C	CDS	L	R
AGR57_7118	scaffold_7	92036	A	G	CDS	S	P
AGR57_7124	scaffold_7	104070	C	T	CDS	E	K
AGR57_7162	scaffold_7	182780	G	A	splice_site_change		
AGR57_8406	scaffold_8	725988	G	A	intronic/noncoding		
AGR57_9613	scaffold_9	1490106	G	A	CDS	E	K
AGR57_10338	scaffold_10	1393250	G	A	intronic/noncoding		
AGR57_10340	scaffold_10	1395593	C	A	CDS	A	S
AGR57_10648	scaffold_11	584854	C	T	CDS	T	I
AGR57_10648	scaffold_11	584855	C	T	CDS	T	I
AGR57_11335	scaffold_12	696261	G	A	CDS	L	F
AGR57_11708	scaffold_13	228855	G	A	CDS	P	L
AGR57_11973	scaffold_13	768405	C	T	CDS	T	I
	scaffold_13	768406	C	T	CDS	T	I
AGR57_12000	scaffold_13	838485	C	T	CDS	D	N
AGR57_11998	scaffold_13	833772	G	A	intronic/noncoding		
AGR57_12514	scaffold_14	779288	G	A	five_prime_UTR		
AGR57_12707	scaffold_15	132567	G	A	three_prime_UTR		
AGR57_13158	scaffold_16	186161	C	T	CDS	S	L
AGR57_13368	scaffold_16	610413	G	T	CDS	A	E
AGR57_13650	scaffold_17	429051	C	T	intronic/noncoding		

AGR57_13883	scaffold_18	276623	G	C	CDS	R	G
AGR57_13973	scaffold_18	438733	T	C	intronic/noncoding		
AGR57_13967	scaffold_18	421555	G	T	CDS	G	C
AGR57_14132	scaffold_19	285815	T	C	CDS	C	R
AGR57_14067	scaffold_19	122229	G	A	intronic/noncoding		
AGR57_14256	scaffold_20	76704	A	G	splice_site_change		
AGR57_14583	scaffold_22	43867	G	A	three_prime_UTR		
AGR57_15117	scaffold_28	5479	A	T	CDS	T	S

End of table 1. List of genes with identified SNP in the mutant *bag4*.

Table 2. List of genes with identified SNP in the mutant *bag31*.

Gene identifier	Identity of scaffold	Position of a base in the reference sequence	Base in the reference sequence	Alternative/ mutant base	Region of DNA which is affected by the change	Amino acid according to reference	Resulting substitution
AGR57_346	scaffold_1	700916	C	T	CDS	L	F
AGR57_2818	scaffold_2	2832102	C	T	CDS	R	C
AGR57_1730	scaffold_2	457746	G	A	CDS	E	K
AGR57_1948	scaffold_2	899205	A	G	CDS	L	P
AGR57_2137	scaffold_2	1254971	A	G	CDS	E	G
AGR57_2356	scaffold_2	1731833	C	T	three_prime_UTR		
AGR57_2239	scaffold_2	1463655	C	T	intronic/noncoding		
AGR57_3779	scaffold_3	1867898	G	A	three_prime_UTR		
AGR57_3056	scaffold_3	300900	G	A	five_prime_UTR		
AGR57_2935	scaffold_3	28017	G	A	three_prime_UTR		
AGR57_3937	scaffold_3	2245008	G	T	intronic/noncoding		
AGR57_3881	scaffold_3	2095986	G	C	splice_site_change		
	scaffold_3	2088151	C	T	CDS	A	V
AGR57_4947	scaffold_4	1885717	A	G	CDS	I	T
AGR57_5181	scaffold_5	92331	T	C	CDS	K	R
AGR57_5275	scaffold_5	369658	A	G	CDS	E	G
AGR57_5181	scaffold_5	92318	T	G	CDS	Q	H
AGR57_5744	scaffold_5	1369986	G	A	three_prime_UTR		
AGR57_5203	scaffold_5	144620	G	A	CDS	L	F
AGR57_5274	scaffold_5	361895	T	C	CDS	V	A
AGR57_6776	scaffold_6	1352909	A	G	intronic/noncoding		
	scaffold_6	1352901	A	G	intronic/noncoding		
AGR57_6184	scaffold_6	139687	G	A	CDS	P	L
AGR57_6344	scaffold_6	448209	G	A	CDS	W	*
AGR57_6892	scaffold_6	1709186	G	C	CDS	C	S
AGR57_7124	scaffold_7	104070	C	T	CDS	E	K
AGR57_7090	scaffold_7	39320	A	C	five_prime_UTR		
AGR57_7625	scaffold_7	1260380	G	A	CDS	R	Q
AGR57_8082	scaffold_8	97914	A	G	CDS	F	L
	scaffold_8	95437	C	A	three_prime_UTR		
AGR57_8504	scaffold_8	928136	C	T	five_prime_UTR		
	scaffold_8	928137	C	T	five_prime_UTR		
AGR57_8081	scaffold_8	95018	G	A	intronic/noncoding		
AGR57_8082	scaffold_8	95833	G	T	intronic/noncoding		
	scaffold_8	98020	C	T	intronic/noncoding		
AGR57_8884	scaffold_8	1734171	A	G	intronic/noncoding		
	scaffold_8	1734163	C	T	intronic/noncoding		
AGR57_8081	scaffold_8	94792	T	C	CDS	N	D
AGR57_9417	scaffold_9	1090506	G	A	CDS	S	L
AGR57_9601	scaffold_9	1471159	C	G	three_prime_UTR		
AGR57_9801	scaffold_9	1882978	C	T	CDS	R	C
AGR57_9256	scaffold_9	631412	C	T	CDS	R	Q

AGR57_9457	scaffold_9	1160597	C	T	intronic/noncoding		
AGR57_9982	scaffold_10	520862	G	A	intronic/noncoding		
AGR57_10234	scaffold_10	1117680	G	T	CDS	A	E
AGR57_10326	scaffold_10	1373584	G	T	intronic/noncoding		
AGR57_11410	scaffold_12	837649	G	C	CDS	S	W
	scaffold_12	837660	G	A	CDS	A	V
	scaffold_12	837661	G	A	CDS	A	V
AGR57_11874	scaffold_13	568834	C	T	CDS	A	V
AGR57_12966	scaffold_15	728132	G	A	CDS	L	F
AGR57_13356	scaffold_16	582344	C	T	CDS	E	K
	scaffold_16	582485	C	T	CDS	V	I
AGR57_13376	scaffold_16	632827	C	T	five_prime_UTR		
AGR57_13515	scaffold_17	186862	G	A	intronic/noncoding		
AGR57_14198	scaffold_19	445524	G	A	CDS	T	I
AGR57_14027	scaffold_19	45138	C	T	CDS	P	S
AGR57_14393	scaffold_20	341602	G	A	intronic/noncoding		
AGR57_14705	scaffold_22	294741	G	A	CDS	R	C
AGR57_14728	scaffold_22	338061	C	T	CDS	L	F
AGR57_14764	scaffold_23	108879	C	A	CDS	P	Q
AGR57_14917	scaffold_24	195662	G	A	CDS	R	*
AGR57_15334	scaffold_51	4551	C	G	CDS	E	D

End of table 2. List of genes with identified SNP in the mutant *bag31*.

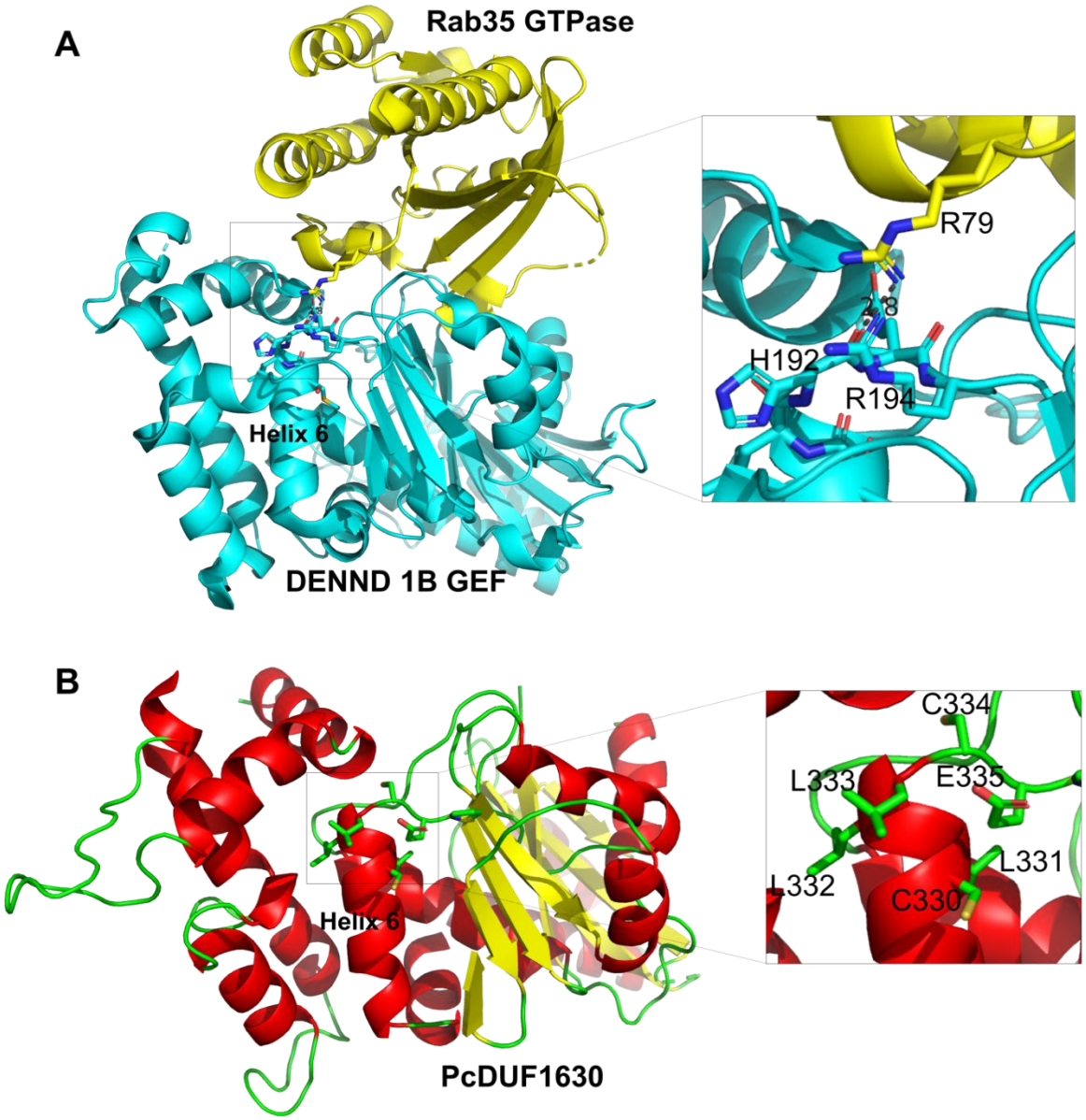

Figure 4. Structural modelling of PcDUF1630 based on the crystal structure of DENND1B in complex with Rab35 GTPase.

A. X-ray structure of DENND1B in complex with Rab35 GTPase. Interactions between the two partners in the region of helix 6 are shown.

B. Modeled structure of PcDUF1630 focused on the putative CLLLC motif at the end of helix 6.

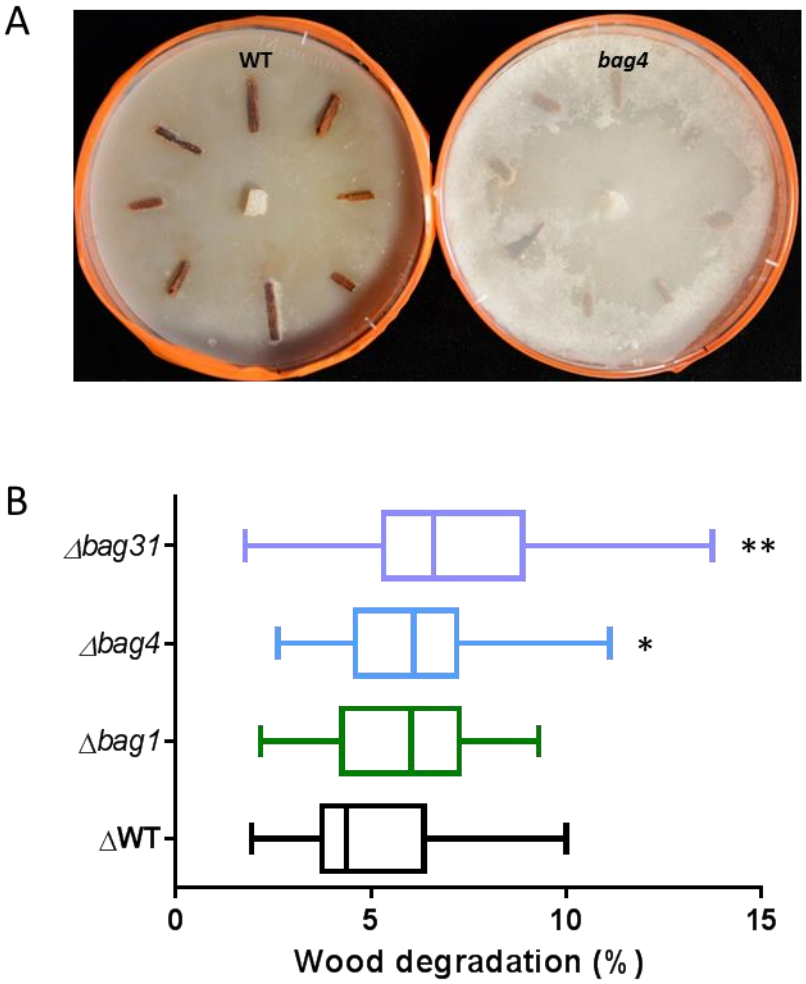

Figure 5. Degradation of wood chips by WT and selected mutant trains of *P. chrysosporium*.

A. On malt agar medium in the petri dish, 8 wood chips were placed appositionally through the central of the plate where one fungal plug was put. The plate with WT is on the left and that with *bag4* on the right were pictured after 25 days of incubation at 37 °C.

B. The weight loss percentage (%) of wood chips represent the wood degradation caused by WT and three selected mutants including *bag1*, *bag4* and *bag31* after two months of incubation at 37 °C. The x-axis is representing the percentage of wood chips degradation and the y-axis is representing the individual genotypes used for the experiment. The result is calculated from 32 replicates for each box plot. One asterisk represents a p-value < 5% and two asterisks represent a p-value < 1%.

Supplementary results

Characterization of *P. chrysosporium* mutants resistant to *Prunus avium* wood extractives

Introduction

Previous results presented in this manuscript demonstrate that the developed forward genetic approach in *P. chrysosporium* RP78 permits to identify mutant resistant to toxic compound and whole genome mutant re-sequencing can be used to identify the target of the toxic compound. This approach has been used to analyze cherry tree wood extractives (CTWE) antifungal activity. CTWE were selected from previous studies. 95 different extractives provided by Pr. Dumarçay from LERMAB have indeed been evaluated for their antifungal activities (Kebbi-Benkeder et al. 2015). Those extractives were obtained from oak, cedar, chestnut, walnut, pine, larch, beech, cherry, and spruce trees. All those trees were collected in the eastern part of France. For each species, different parts of wood have been considered, and four solvents have been used to extract the considered molecules. The antifungal properties of these extracts were then tested to of *P. chrysosporium* germination using nephelometer experiments (Fig. 33). Cherry tree wood dichloromethane extracts exhibited strong antifungal properties (**Fig. 33I**) and then were selected for further analysis.

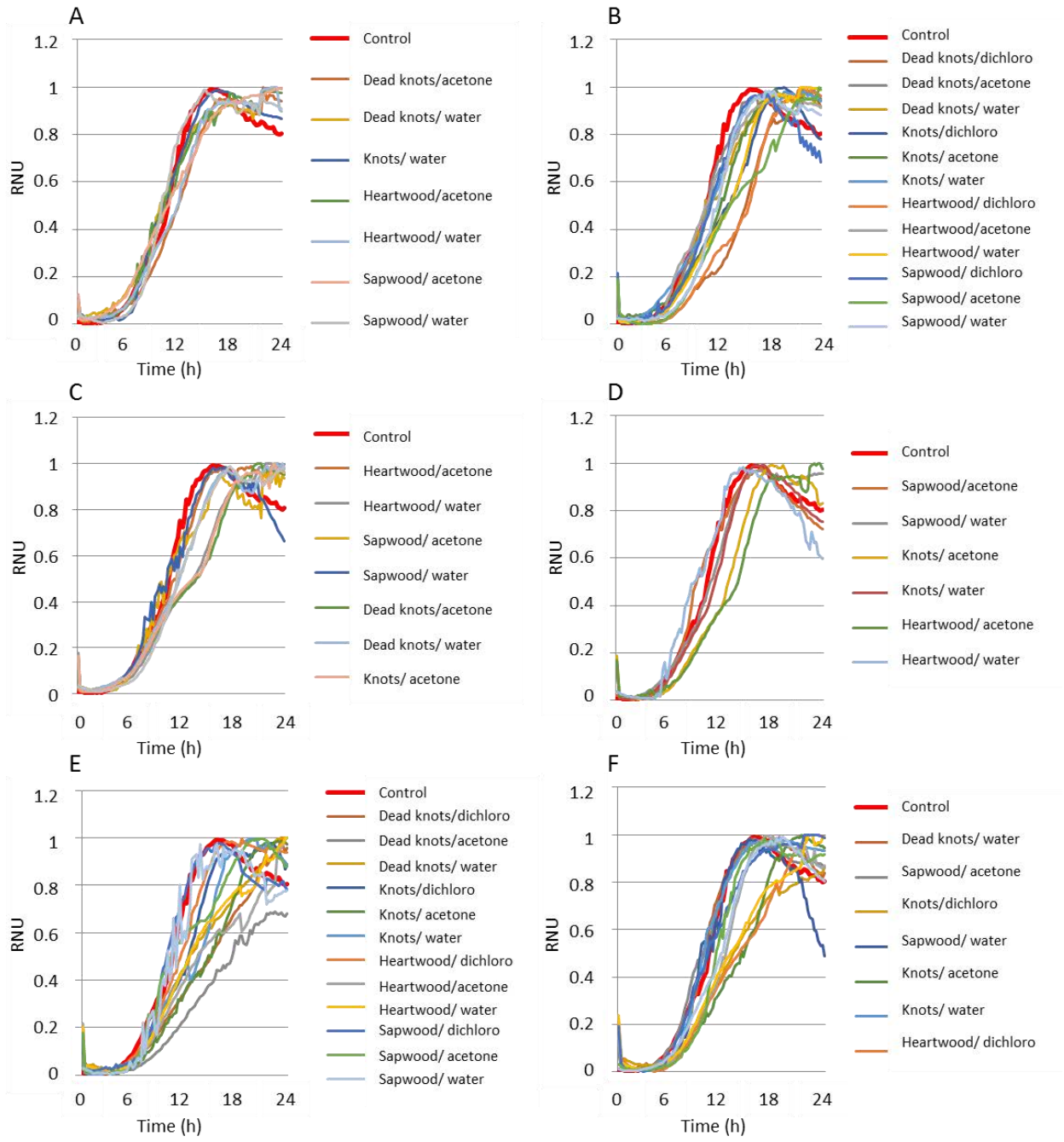

Figure 33. Effect of wood extractives on germination of *P. chrysosporium* RP78 conidia determined by nephelometry.

Measurement have been done in malt extract 2% liquid medium at 37 °C. Wood extractives have been tested at 10 µg.mL^{-1}. DMSO has been used has control and corresponding result is provided on every panel. Representative data are means of n=3 independent experiments.

Extractives tested were obtained from different parts of oak tree (A), cedar tree (B), chestnut tree (C), walnut tree (D), pine tree (E), dawn redwood tree (F) (to be continued)

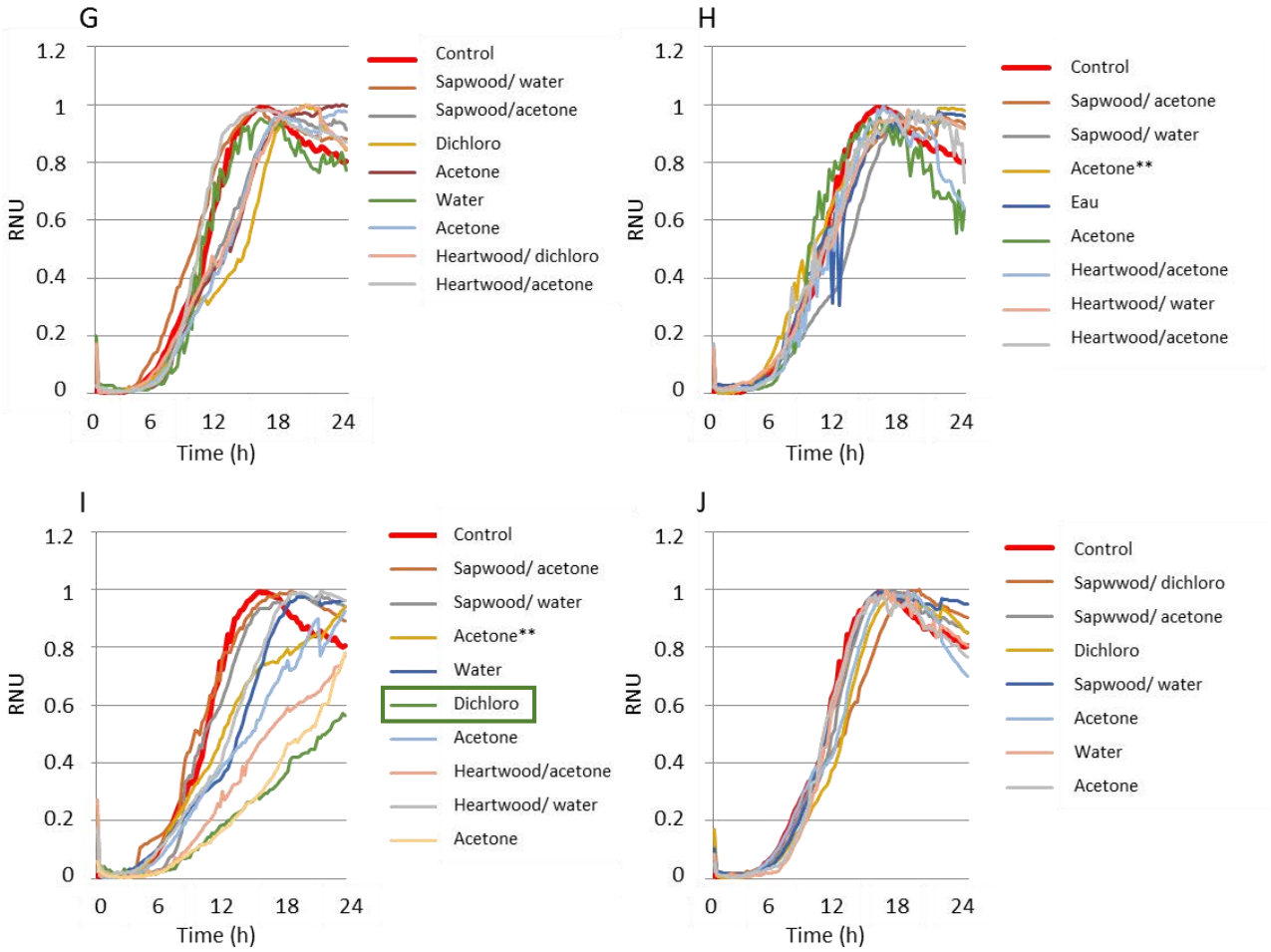

Figure 33. Continued.

Extractives tested were obtained from different parts of larch tree (G), beech tree (H), cherry tree (I), spruce tree (J).

RNU stand for relative nephelometer unit.

Results

Effects of CTWE on *P. chrysosporium* RP78

Several concentrations of CTWE were used to inhibit germination of wild type spores (Fig.34A). In the absence of extractives, three growth phases were detected: a lag phase (from t=0 h to 5 h), an exponential phase (from t=5 h to t=30 h), and a stationary phase after 30 h. In the presence of CTWE at 10 $\mu g.mL^{-1}$, the growth rate decreased during the exponential phase. The increase of the CTWE concentrations confirmed the antifungal effects of these extracts. From 30 $\mu g.mL^{-1}$, spore germination was fully inhibited.

The inhibition of CTWE against hyphal growth also was tested on malt extract agar medium (Fig.34B). A plug of fungus *P. chrysosporium* RP78 was placed on the medium supplemented with different concentrations of CTWE. Control experiments had not extractives but DMSO. Inhibitory activity of CTWE was observed even after the first incubation day. After two incubation days, while the fungus completely covered the plate surface in the control conditions, fungal growth started only in presence of CTWE 40 $\mu g.mL^{-1}$. After three incubation days, results demonstrated that CTWE have an inhibitory effect on the hyphal growth of fungus *P. chrysosporium* RP78.

Additional experiments were performed using Whatman filter paper imbibed with several CTWE concentrations (drops of 10 µL). After 48 hours of incubation at 37 °C, fungal hyphae are observed on control Whatman paper and on Whatman paper imbibed with 100 µg of CTWE. In the other conditions, the fungus avoided Whatman papers.

In conclusion, the results showed that CTWE had an inhibitory effect on germination and hyphal growth of the fungus *P. chrysosporium* RP78. Therefore, CTWE can be a useful candidate to identify potential targets involved in detoxification of *P. chrysosporium* in response to wood extractives.

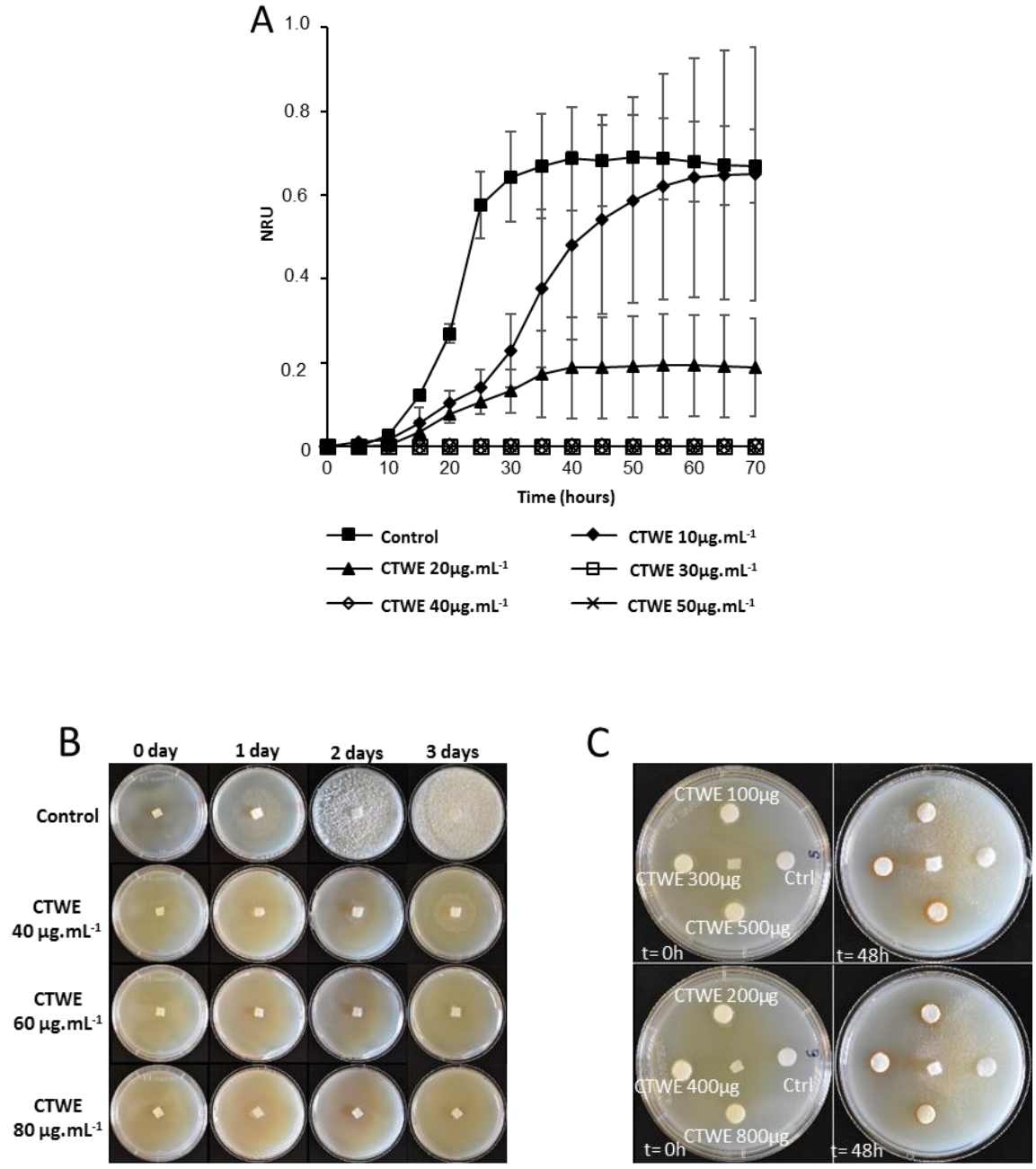

Figure 34. Effect of dichloromethane cherry tree wood extractives (CTWE) on germination and hyphal growth of *P. chrysosporium* RP78 conidia.

A. Determination of CTWE concentration needed to fully inhibit conidia germination using nephelometric measurement. Freshly collected conidia of *P. chrysosporium* RP78 were cultivated during 72 hours in malt extract 1% liquid medium with different concentration of CTWE, DMSO was added in the control experiment. Testing plate were incubated at 37 °C. RNU represent Ralative Nephelometric Unit. Standard deviation was calculated from 9 and 3 replicates for control and treatments, respectively.

Figure 34. Continued.

B. CTWE inhibit hyphal growth of *P. chrysosporium* RP78 conidia. A plug of *P. chrysosporium* RP78 was placed at the center of Petri dishes of malt extract 2% agar (Control), or malt extract 2% agar supplemented with extractives at concentrations of 40 µg.mL^{-1}, 60 µg.mL^{-1}, 80 µg.mL^{-1}. Petri dishes were incubated at 37 °C, and pictures were obtained during three days of the experiment.

C. Inhibition of CTWE with the use of Whatman filter paper. On the malt extract 2% agar medium, Whatman papers were impregnated with different contents of extractives, or 10 µl DMSO for control (Ctrl). A plug of *P. chrysosporium* RP78 was placed at the center of Petri dish. Pictures were taken at the beginning of the test (t=0h) and after 48 hours of incubation at 37 °C.

Mutagenesis and screening mutant resistant to CTWE

For this work, *P. chrysosporium* mutants resistant to CTWE were produced to identify targets of cherry tree wood extractives, and also to serve for understanding the functions of detoxification systems. For the generation of mutants, conidia were exposed to UV light for 30 seconds then plated on malt extract agar plate supplemented with cherry tree extractives 75 µg.mL^{-1}, which were found previously with one experiment to find the threshold for WT spores. After 5 days of incubation at 37 °C, small colonies were observed on the selective mediums. 55 individual colonies were picked up for *chy* mutants resistant to CTWE. These mutants were obtained by direct sub-culture on the fresh new sporulation medium containing wood extractives for one week. 10,000 spores of each mutant were harvested and inoculated into 10 mL of 1% malt extract medium with 75 µg.mL^{-1}. After 5 days of incubation for germinated conidia of *chy*, they were fished individually and plated. There were 38 of 55 *chy* mutant strains able to grow under this condition. A second round of conidia production on sporulation medium with wood extractives and isolation was performed to generate lines considered as “one spore progeny”.

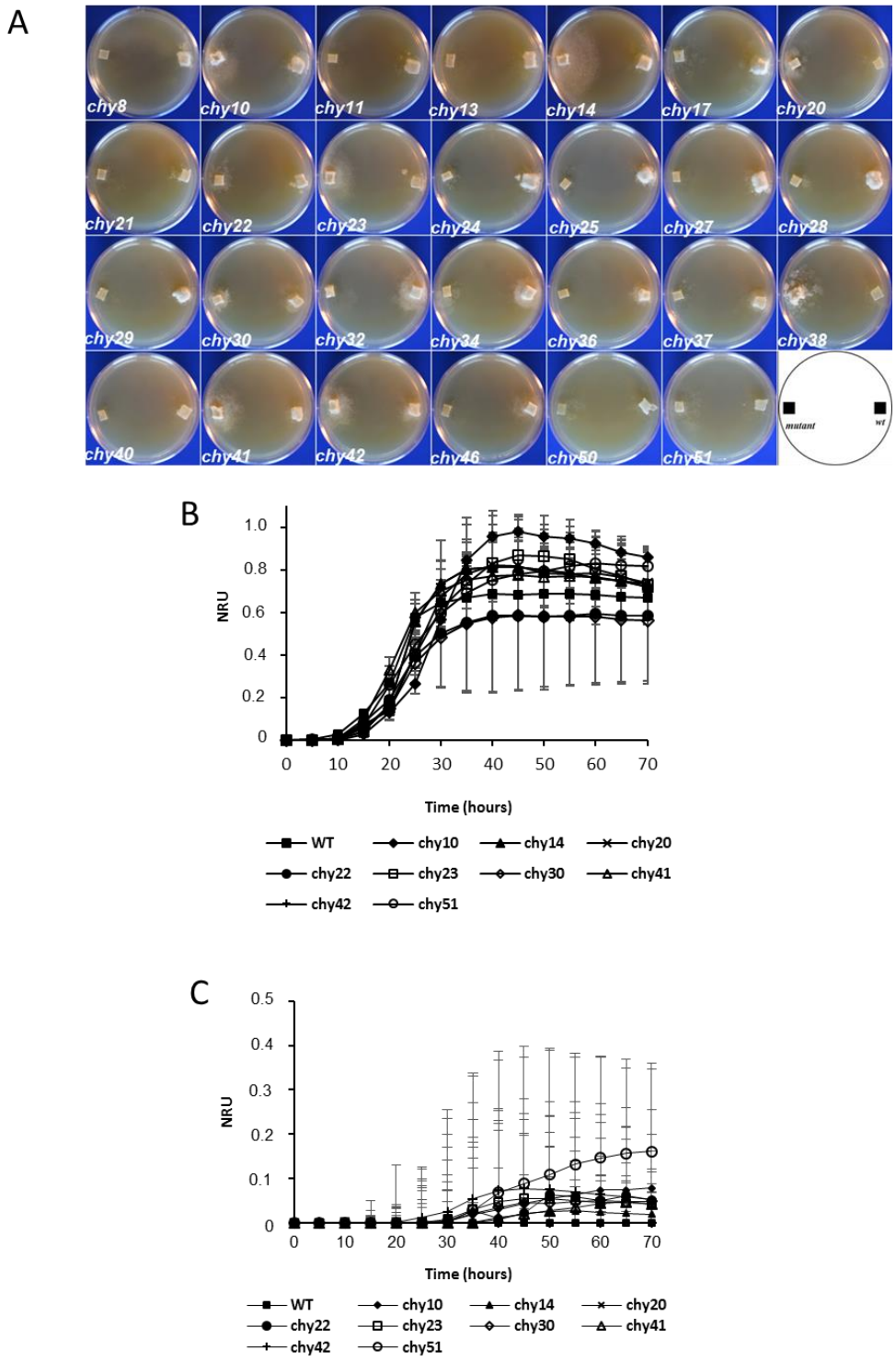

Figure 35. Phenotype of *chy* mutants.

(A) Hyphal growth of *chy* mutants in comparison with that of wild type on malt extract agar 2% mixed with bagassa wood extractives at 80 µg. mL^{-1}. (B, C) Conidia germination *chy10*, *chy14*, *chy20, chy22*, *chy23*, *chy23*, *chy30*, *chy 41, chy42 and chy51* in control condition (without extractives), and in presence of CTWE at 30 µg.mL^{-1} which inhibited completely germination of WT (Fig. 34A). Measurements have been done during 72 h using nephelometer.

Phenotypes of *chy* mutants

For the obtained collection of *chy* mutants, the resistance phenotype against CTWE on malt extract agar medium was examined (Fig.35A). After one week of incubation at 37 °C, 28 *chy* mutants were able to grow on the medium containing CTWE at 80 µg.mL^{-1}, while the WT was inhibited completely. Among these mutants, *chy14* exhibited the highest growth rate. Other mutants including *chy23*, *chy38*, *chy41,* and *chy42* have also interesting phenotype since they were able to grow strongly on the selected medium (Fig.35A).

Nine mutants selected from the library of 28 mutants were used to test their ability to germinate in the presence of cherry extractives using nephelometry assay (Fig.36). Those are mutants with a clearly stronger growth phenotype than the others. In the absence of wood extractives, mutants exhibit the same growth pattern than the WT. In the presence of cherry extractives at 10 µg.mL^{-1}, mutants germinated however after a more or less lag phase. The longer lag phase took place for *chy10*, *chy20*, *chy22*, *chy30*, *chy41*, and *chy51*. At concentration of 30 µg.mL^{-1} by which spores of wild type were completely inhibited (Fig.36), germination of spores was detected for *chy10*, *chy22*, *chy23*, *chy23*, *chy30*, *chy41, chy42 and chy51.* The other mutants, *chy14* and *chy20*, were completely inhibited. The results of the germination of these mutants in the presence of cherry wood extracts 30 µg.mL^{-1} were summarized in Fig.35C.

Identification of the causal mutation(s) leading to CTWE resistance

As previously, a strategy of whole genome re-sequencing experiments was performed. The first step was the extraction of genomic DNA from each of the identified *chy* mutant. The same amount of DNA from all the individual mutant has been pooled, then genomic DNA from WT have been added in a 1/29 ratio of the total amount of DNA. This gDNA mixture has been sequenced using Hi-seq technology. In addition, gDNA from *chy14* has been sequenced individually. The obtained candidate SNPs are given in table 3, and their allele frequencies are presented in Fig. 37.

The results from those experiments have been aligned with the reference genome revealing 2 lists of mutations. All those mutations can be mapped to the reference genome and a frequency value can be given for each of them (Fig. 37A). This value reflects the number of sequenced reads with a mutation in comparison to the total number of sequenced reads for the same position.

SNPs are common between the two experiments (Fig. 37B) and constitute a short list of potential candidates. From the frequency analyses, the standard profile of the mutation should have a high frequency in the experiment of *chy14* resequencing and should be found in the pooled gDNA sequencing experiment.

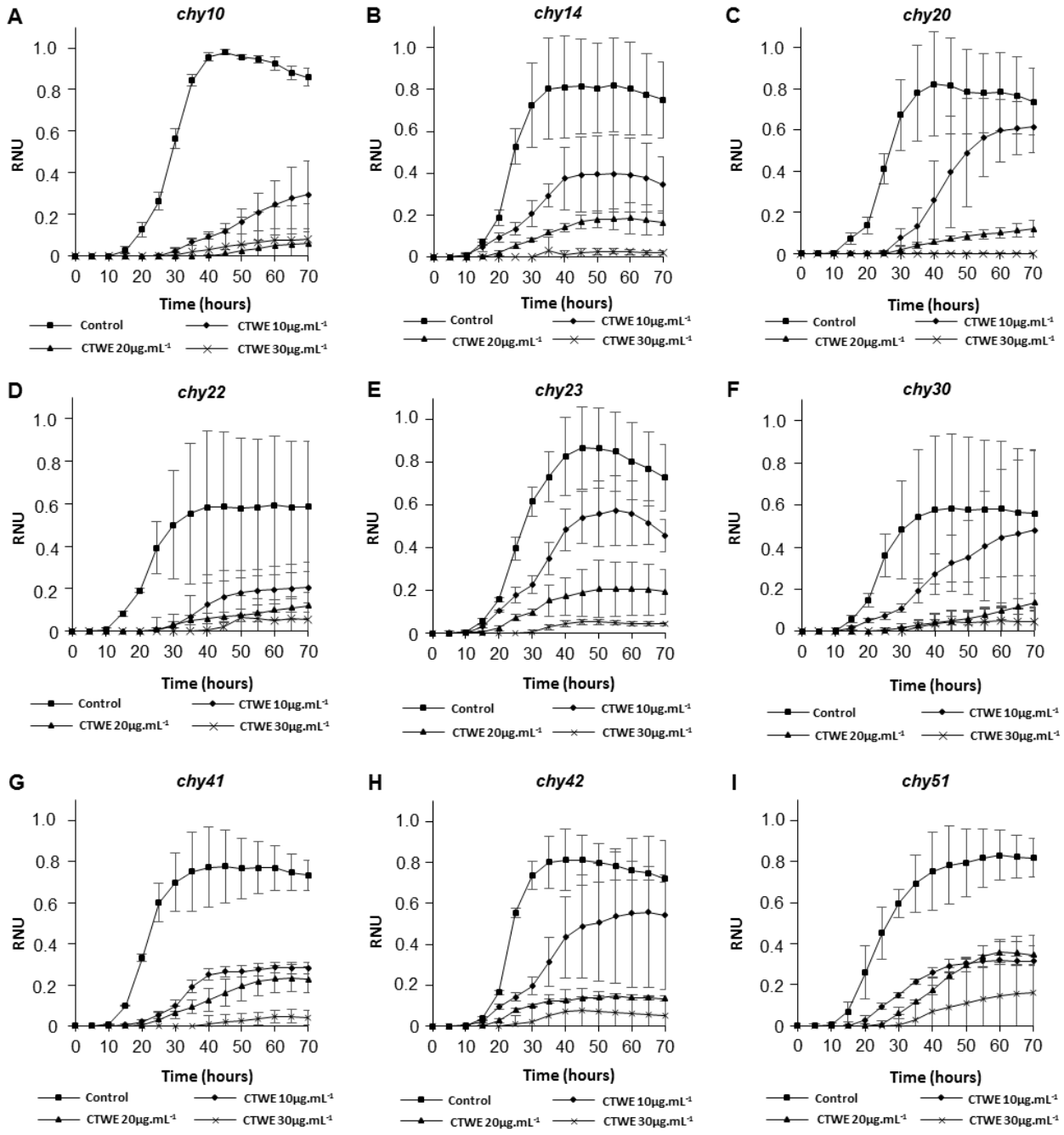

Figure 36. Germination phenotype of selected *chy* mutants in presence of CTWE.

Germination of spores was measured with nephelometer for mutants of *chy10* (A), *chy14* (B), *chy20* (C), *chy22* (D), *chy23* (E), *chy30* (F), *chy41* (G), *chy42* (H), *and chy51* (I). WT spores were inhibited completely at this concentration of extractives. Conidia have been cultivated in 200 µL of malt extract 1% medium for 72h in presence of 0, 10, 20, and 30 $\mu g.mL^{-1}$ of CTWE. Incubator was set up at 37 °C for testing.

Table 3. List of genes with identified SNP in the mutant *chy14*.

Gene identifier	Identity of scaffold	Position of a base in the reference sequence	Base in reference sequence	Alternative/ mutant base	Region of DNA which is affected by the change	Amino acid according to reference	Resulting substitution
AGR57_32.1	scaffold_1	68158	A	T	CDS	L	H
AGR57_717.1	scaffold_1	1491624	C	T	CDS	P	L
AGR57_717.1	scaffold_1	1491627	C	A	CDS	A	D
AGR57_1328.1	scaffold_1	2885189	C	T	CDS	I	I
AGR57_1112.1	scaffold_1	2380739	G	A	CDS	S	F
AGR57_381.1	scaffold_1	793411	A	C	CDS	L	*
AGR57_643.1	scaffold_1	1338431	G	A	CDS	E	K
AGR57_527.1	scaffold_1	1107374	G	A	CDS	S	F
AGR57_9930.1	scaffold_10	414091	C	T	CDS	E	K
AGR57_10022.1	scaffold_10	606482	T	C	CDS	R	G
AGR57_10216.1	scaffold_10	1075321	G	A	CDS	A	V
AGR57_10273.1	scaffold_10	1246130	C	T	CDS	V	I
AGR57_10098.1	scaffold_10	834097	G	T	CDS	L	I
AGR57_10367.1	scaffold_10	1463654	C	T	intronic/noncoding		
AGR57_11004.1	scaffold_11	1335501	C	T	CDS	F	F
AGR57_10436.1	scaffold_11	150059	C	T	CDS	D	N
AGR57_10453.1	scaffold_11	180621	C	T	intronic/noncoding		
AGR57_11199.1	scaffold_12	327277	C	A	CDS	H	K
AGR57_11199.1	scaffold_12	327279	T	A	CDS	H	K
AGR57_11432.1	scaffold_12	889727	T	A	CDS	Y	N
AGR57_11417.1	scaffold_12	850229	T	A	CDS	N	I
AGR57_11487.1	scaffold_12	1000677	G	A	three_prime_UTR		
AGR57_11500.1	scaffold_12	1027890	T	A	three_prime_UTR		
AGR57_11711.1	scaffold_13	240932	G	T	CDS	E	*
AGR57_11966.1	scaffold_13	755761	T	G	CDS	I	M
AGR57_12001.1	scaffold_13	840955	C	A	CDS	P	H
AGR57_12036.1	scaffold_13	908475	G	A	CDS	Q	Q
AGR57_11743.1	scaffold_13	306685	C	T	intronic/noncoding		
AGR57_15435.1	scaffold_136	3211	A	G	intronic/noncoding		
AGR57_15435.1	scaffold_136	3223	G	A	intronic/noncoding		
AGR57_12281.1	scaffold_14	230805	A	G	CDS	L	L
AGR57_12628.1	scaffold_14	987657	G	A	intronic/noncoding		
AGR57_12842.1	scaffold_15	442792	A	C	CDS	H	P
AGR57_12842.1	scaffold_15	442826	T	G	CDS	S	R
AGR57_13026.1	scaffold_15	854705	C	G	CDS	L	L
AGR57_12999.1	scaffold_15	790451	T	C	intronic/noncoding		
AGR57_13817.1	scaffold_18	154413	G	T	CDS	A	S
AGR57_13869.1	scaffold_18	256087	G	A	CDS	V	V
AGR57_13973.1	scaffold_18	438733	T	C	intronic/noncoding		
AGR57_14130.1	scaffold_19	281090	C	A	CDS	V	V
AGR57_1931.1	scaffold_2	871198	T	C	CDS	T	T

AGR57_2480.1	scaffold_2	2006212	T	A	CDS	K	*
AGR57_2597.1	scaffold_2	2261667	C	T	CDS	L	L
AGR57_1972.1	scaffold_2	949928	G	T	intronic/noncoding		
AGR57_2165.1	scaffold_2	1313913	T	G	intronic/noncoding		
AGR57_2753.1	scaffold_2	2693656	C	T	intronic/noncoding		
AGR57_2866.1	scaffold_2	2937329	C	T	three_prime_UTR		
AGR57_14490.1	scaffold_21	216479	A	G	CDS	H	R
AGR57_14531.1	scaffold_21	313652	A	G	CDS	L	P
AGR57_14693.1	scaffold_22	271128	G	T	CDS	P	H
AGR57_14988.1	scaffold_25	166646	A	T	CDS	M	K
AGR57_3205.1	scaffold_3	597747	T	C	CDS	I	V
AGR57_3295.1	scaffold_3	777644	A	G	CDS	K	R
AGR57_3334.1	scaffold_3	870487	A	C	CDS	K	Q
AGR57_3417.1	scaffold_3	1024367	C	A	CDS	W	L
AGR57_3442.1	scaffold_3	1080684	C	A	CDS	T	K
AGR57_3684.1	scaffold_3	1696016	A	G	CDS	L	L
AGR57_3688.1	scaffold_3	1702461	G	A	CDS	R	R
AGR57_3725.1	scaffold_3	1776526	G	A	CDS	F	F
AGR57_4179.1	scaffold_4	349371	A	C	CDS	F	C
AGR57_4386.1	scaffold_4	793343	A	C	CDS	W	G
AGR57_4585.1	scaffold_4	1172217	G	A	CDS	G	D
AGR57_15312.1	scaffold_42	8737	C	G	intronic/noncoding		
AGR57_15312.1	scaffold_42	8741	A	G	intronic/noncoding		
AGR57_15312.1	scaffold_42	8745	T	G	intronic/noncoding		
AGR57_5789.1	scaffold_5	1465862	C	T	CDS	L	L
AGR57_5864.1	scaffold_5	1619450	G	A	CDS	D	D
AGR57_5864.1	scaffold_5	1619464	G	T	CDS	Q	K
AGR57_5871.1	scaffold_5	1638107	G	C	CDS	Q	H
AGR57_5495.1	scaffold_5	855555	G	A	CDS	I	I
AGR57_6295.1	scaffold_6	355407	G	A	CDS	G	S
AGR57_6478.1	scaffold_6	744879	A	G	CDS	H	R
AGR57_6803.1	scaffold_6	1507740	G	T	CDS	T	T
AGR57_6541.1	scaffold_6	873737	G	A	CDS	R	C
AGR57_6612.1	scaffold_6	1011470	G	A	CDS	F	F
AGR57_6725.1	scaffold_6	1241242	A	G	CDS	T	T
AGR57_7120.1	scaffold_7	99620	T	C	CDS	L	P
AGR57_7931.1	scaffold_7	1840330	T	C	CDS	S	P
AGR57_7966.1	scaffold_7	1897789	A	C	CDS	Q	H
AGR57_7950.1	scaffold_7	1864780	C	T	CDS	T	I
AGR57_8109.1	scaffold_8	152868	G	T	CDS	E	*
AGR57_8204.1	scaffold_8	331380	A	C	CDS	F	V
AGR57_8218.1	scaffold_8	365849	G	T	CDS	A	A
AGR57_8327.1	scaffold_8	579838	C	T	CDS	P	L
AGR57_8990.1	scaffold_9	65685	C	A	CDS	Q	K
AGR57_9260.1	scaffold_9	642272	C	G	CDS	D	E
AGR57_9665.1	scaffold_9	1585575	C	T	intronic/noncoding		

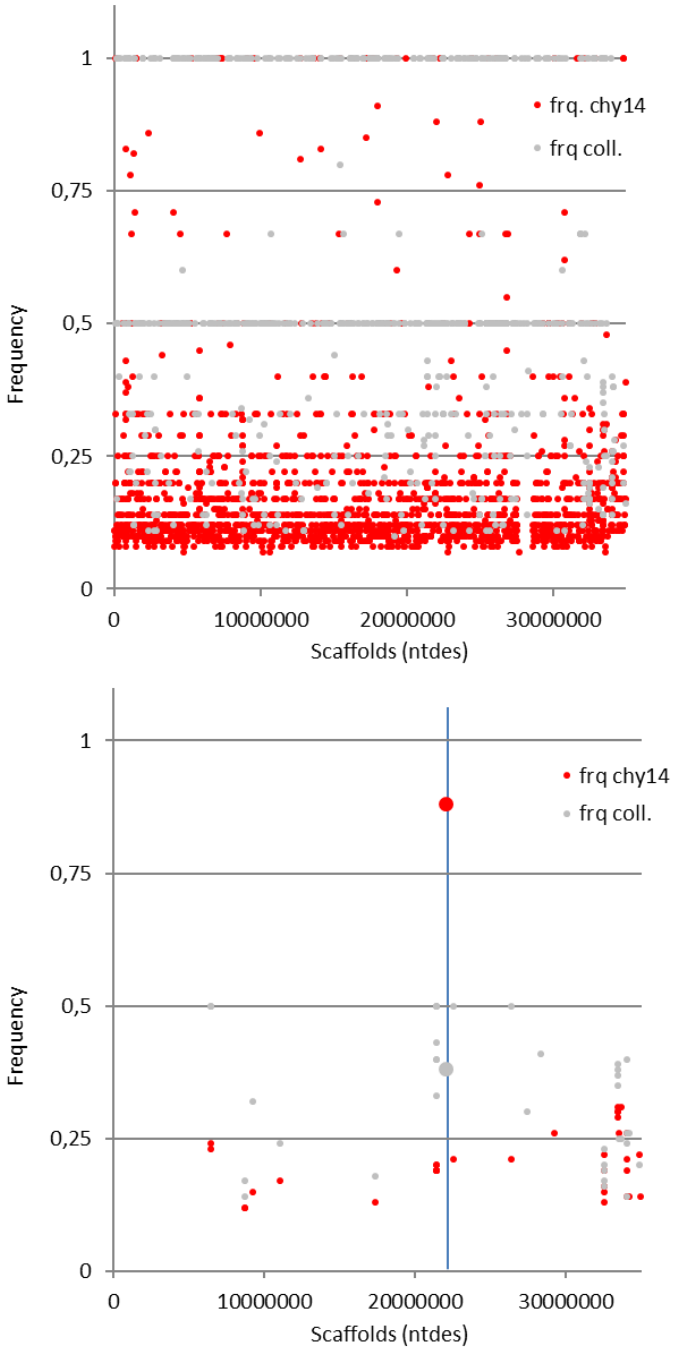

Figure 37. Genomic survey of the mutations in *chy* mutants.

A. Graphical representation of the SNPs list with their frequency identified during the genome sequencing of the gDNA from the collection of *chy* mutants and individual sequencing of *chy14*. The SNP lists and frequencies were obtained as the output of shore map (Sun and Schneeberger, 2015); the corresponding table is provided. The x axis represents the scaffolds: scaffold 1 cover the position from 1- 3273479; Scaffold 2 covers the position from 3273480 to 6317450 and so on until Scaffold 412 which cover the position from 35148491 to 35149519. The y axis is a direct output of shore map and represents the frequency of each SNP.

Figure 37. Continued.

B. Same graphical representation highlighting only the common SNPs found in the bulk sequencing experiment of the collection and *chy14*. The position of the identified mutation of interest is represented by a vertical blue bar. The corresponding dots have an increase in size (from 3pts to 6 pts).

Involvement of AGR57_10098 in resistance against CTWE

The identified gene encodes a protein composed of 739 amino acid residues. By blasting on Fungidb database (Basenko et al., 2018), this protein appears as a NACHT domain-containing protein, the product of *het* gene and its ortholog is HET-e, which was identified as a protein responsible for vegetative incompatibility in the fungus *Podospora anserina* (Saupe et al., 1995). This database also showed that this protein contains a P-loop harboring a Nucleoside Triphosphate Hydrolases (P-loop-NTPase) domain. This protein class has been described to be involved in defense against pathogen invasion in plants (Arya and Acharya, 2018).

het (heterokaryon incompatible) gene has been identified in both Ascomycota and Basidiomycota. In Ascomycota, this gene was described in detail in fungus *P. anserina* (Espagne et al., 2002). For Basidiomycota, distribution and evolution of *het* gene homologs were performed based on the genome of 41 representatives, 35 of them belonging to Agaricomycotina (Van der Nest et al., 2014). Surprisingly, there were no other genes encoding for HET and NACHT domains identified for fungus *P. chrysosporium* (Van der Nest et al., 2014).

NACHT domain-containing proteins mainly have been studied in animals and plants. They belong to two large groups of Nucleotide-binding oligomerization domain (NOD) - like receptors (NLRs). Their diversity has been studied only recently in fungi (Dyrka et al., 2014). Fungal NLRs exhibit similarities to plants and animals which counterparts in possible mechanisms to recognize and respond to heterospecific nonself (Uehling et al., 2017). In fungi, this protein was known as one of mediator for Programmed Cell Death (PCD) in the two model species *N. crassa* and *P. anserina* (Paoletti and Clavé, 2007).

From a structural point of view, HET-e domain protein is a part of the STAND (Signal Transduction Adenosine Triphosphatase) proteins, that contains three modules including HET (effector domain), NACHT domain, and a WD40 repeat domain (ligand-binding domain). To trigger PCD through non-self-recognition, it requires the binding of a ligand to the WD40 domain. This interaction leads to a conformational change in the *het* gen product to release the HET domain, which initiates a signaling cascade for PCD activation (Paoletti and Clavé, 2007). Since the HET domain is fungal specific, it was suggested as a favorable target for the development of specific antifungal drugs (Paoletti and Clavé, 2007).

In filamentous fungi, besides occurring in the development process and non-self-recognition, PCD also occurs in response to exogenic compounds such as antifungal compounds from plants, oxidative radicals, and stress causing molecules (Gonçalves et al., 2017). For the obtained results, it is possible to hypothesize that CTWE exhibits antifungal activity to *P. chrysosporium* through mechanisms involved in PCD pathways.

DISCUSSION AND PERSPECTIVES

One main objective of this work was to develop a forward genetic strategy allowing the identification of master genes involved in the detoxification systems of the model fungus *P. chrysosporium*. Recently, a similar strategy was developed in the fungal phytopathogen *Sclerotinia homoeocarpa* (Sang et al., 2018). The regulation and coordination of intracellular detoxification systems of this fungus in response to xenobiotics was indeed investigated via characterizing mutants resistant to several common fungicides (Sang et al., 2018). In particular, the design of experiments was based on a comparison of differential gene expression between wild type strain and strains which are resistant to fungicides such as propiconazole, iprodione, boscalid, fluprimidol. By RNA-seq analysis combined with genetic modification approaches, one transcriptional factor named ShXDR1 was identified as a key regulator of expression and coordination of CYPs and ABC efflux transporters (Sang et al., 2018). A mutation (M853T) in this factor was confirmed as the causative element leading to resistance phenotype by the use of CRISPR-Cas9 system to delete gene coding ShXDR1 (Sang et al., 2018). Furthermore, to evaluate if the xenobiotic detoxification pathway of ShXDR1 is conserved in other ascomycetes, a gene encoding ShXDR1 harboring the mutation (ShXDR1^{T853}) was introduced into a plant-pathogenic fungus *Botrytis cinerea*. Two transformants containing ShXDR1^{T853} are more resistant to propiconazole and iprodione, but not to boscalid and to fluprimidol. In these two transformants, genes encoding BcCYP65 and for BcatrD (ABC transporter) are overexpressed and highly induced in response to propiconazole treatment in comparison to the wild type strain. This result indicates that the xenobiotic detoxification system is conserved in filamentous ascomycete fungi (Sang et al., 2018). This also indicates that the detoxification system as we know is perhaps the emerged tip of the iceberg.

Due to the absence of genetic tools in *P. chrysosporium*, such an approach could not be used in this fungus. Few data are available on the regulation of detoxification systems in this fungus. During the growth of *P. chrysosporium* on solid spruce wood in which extractives are toxic for fungi, the transcriptomic analysis revealed upregulation of genes encoding for transporters and CYPs, but the expression regulation of these proteins was discussed in the context of functional analysis of extracellular oxidation, but not in the context of involved regulators (Korripally et al., 2015). Previously, cAMP and MAP kinase signaling pathways were identified as having an important role in the regulation of gene expression involved in secondary metabolism and biodegradation process under nutrient-limited conditions (Doddapaneni and Yadav, 2005). Under these conditions, both extracellular peroxidases (LiPs and MnPs) and P450s are upregulated, but there were no proposals concerning potential links between regulatory proteins and expression of these proteins (Doddapaneni and Yadav, 2005). In fact, regulation of P450s gene expression could be mediated via ligand-binding nuclear receptor transcription factors and could involve signaling

components of the cAMP pathway and MAP kinase pathway (Ahlgren et al., 1999; Tan et al., 2004). In addition, another analysis also found that homologs of ScHOG kinases known as components in response to stress are also upregulated under these conditions. Therefore, the MAP kinase pathway signaling was proposed to control P450s expression in *P. chrysosporium* (Syed and Yadav, 2012).

Master genes involved in the coordination and regulation of the detoxification systems in wood decaying fungi and particularly in *P. chrysosporium* remain to be identified and the proposed approach developed during this work could be efficient for that.

Wood extractives as tools to characterize wood decaying fungi

Identification of novel target proteins through clarification of inhibitory or induction activity of a given small molecule has provided breakthroughs in biological studies. One of the most well-known molecules is rapamycin that is produced by bacteria *Streptomyces hygroscopicus*. This compound inhibits TOR, a kinase protein that regulates numerous important pathways in eukaryotic organisms, and also demonstrated to be present in the fungus *P. chrysosporium* in our study.

There have been several studies measuring the antifungal activity of wood extractives either to evaluate their roles in the natural durability of wood or to find molecules which could be used as wood preservatives. Antifungal mechanisms were also discussed for several compounds with characterized chemical structures (Valette et al., 2017).

Previously, based on a postulate that combination of the extracellular peroxidases proteins with the intracellular detoxification proteins have key roles in detoxification of wood extractives, interactions between these proteins and wood extractives have been examined to explain the functions of these proteins. The studies performed from this approach resulted in the discovery of the xenomic networks which help explain adaptation traits of wood decaying fungi (Morel et al., 2013). More recently, wood extractives have been used to study evolution and adaptation of the white rot fungi to their habitat. For instance, interactions of several GSTs of Omega and Ure2p classes from two white rot fungi *T. versicolor* and *P. chrysosporium* with 60 wood extractives isolated from wood and knots of several species in France have been investigated (Deroy et al., 2015). The data not only showed that the specificity of those interactions is closely linked to the chemical composition of the extractives but also indicated that fungal GSTome could reflect the chemical environment related to wood degradation condition (Deroy et al., 2015). Additionally, wood extractives also are very useful materials to identify new important elements of the detoxification systems. Indeed, a RNA-seq analysis of the early detoxification response of *P.*

chrysosporium to oak wood extractives revealed the induction of new enzymes involved in the detoxification systems (Fernández-González et al., 2018). They include seven small secreted proteins of the extracellular system, five CytP450s, and one GST of the intracellular system. The detailed biochemical characterization of this GST results in one hypothetical proposal on the role as a transporter and a solubilizing factor of extractives molecules for this protein (Fernández-González et al., 2018).

With the developed approach which was motivated for searching new solutions to deeply characterize the wood decaying fungi through the model fungus *P. chrysosporium*, two novel target proteins were found in this thesis through isolation of candidate genes from a forward genetic screen of mutants resistant to wood extractives. Interestingly, those targets do not belong to the previously characterized detoxification systems. Nevertheless, additional genetic validation as well as biochemical and/or physiological experiments are required to unravel their roles under wood degradation conditions. In addition to perspectives for understanding the adaptation or the detoxification mechanisms of wood decaying fungi, biochemical and physiological characterization of two targets from *bag* and *chy* mutants can supply new fungal inhibitory molecules. Indeed, from molecular modeling, it is possible that there is a molecule interacting with PcDUF1630/PcDENND protein resulting in dysfunction of this protein that has GEF activity *vs.* Rab GTPases. From this hypothesis, the recombinant protein PcDUF1630/PcDENND need to be produced, and molecular interactions between this protein with fractionated bagassa wood extractives fraction have to be measured. In parallel, the inhibitory effect of each wood extractive fraction on the growth of *P. chrysosporium* is also essential. The combination of these two data will permit to address the proposed hypothesis. A similar framework can be applied for the NACHT domain-containing protein.

From the works performed in this thesis, it is possibly to propose that a similar strategy can be further used to find targets linked to other wood extractives. The obtained results will provide not only data for finding key proteins of detoxification pathways but also the potential molecules from wood extractives with actions as wood preservatives or antifungal agents.

The possible relationships between identified proteins PcTOR and PcDUF1630 protein and secretion

In this thesis, we have identified and confirmed for the first time the presence of several proteins in the white rot fungus *P. chrysosporium*. They are PcTOR and related signaling networks, PcDUF1630/DENND, and NACHT domain containing proteins (PcNACHTD). Are there any potential relationships between them?

As mentioned in the results section, PcDUF1630/PcDENND was identified to relate functionally to Avl9p, a member belonging to protein superfamily Avl9 that has a functional role in the late secretory pathway in the yeast *S. cerevisiae* (Harsay and Schekman, 2007). Avl9p is a conserved protein identified from a genetic screen design to obtain new secretory mutants from a strain where the secretory pathway was defective. In the yeast *S. cerevisiae*, Avl9p is involved in the generation of secretory vesicles, and maybe for the exit from the Golgi compartment. Avl9p plays also a role in vesicle trafficking from early endosomes and has possible functions in deforming membranes for vesicle fusion, and in recruiting cargo proteins (Harsay and Schekman, 2007).

In yeast *S. cerevisiae*, Avl9p maybe linked to Gtr proteins in the regulation of plasma membrane homeostasis or cargo protein sorting (Zhang et al., 2010). Those Gtr proteins are elements belonging to the upstream part of TORC1 signaling pathway (Fig.7). The screening of a library of chemical compounds to find inhibitors of exocytic transport led to the identification of a link between Avl9p and Gtr2p (Zhang et al., 2010). Indeed, a group of inhibitors led to lethal phenotype of ΔAvl9p strain could be suppressed by Gtr2p overexpression (Zhang et al., 2010). This result suggested that there is a coordination between signaling pathways and traffic pathways for the regulation of cell growth and proliferation.

In eukaryotic cells, transporting material between membrane-bound organelles or the plasma membrane is performed via secretory vesicles (Fig. 38) The vesicle transport is closely organized by numerous proteins, among them, GTPases allow delivering vesicular cargo to the correct destination. To date, Rab GTPases have been known to be activated by DENND proteins (Marat et al., 2011). Additionally, the cultivation of *rap1*, which is over-secreting enzymes (Fig. 30), led to mimic the phenotype of *bag*31 when growing on BWE (Fig. 39). For this reason, it could be hypothesized that PcDUF1630/PcDENND may be functionally linked to the secretory pathway. Additional evidence can be brought by a reverse experiment.

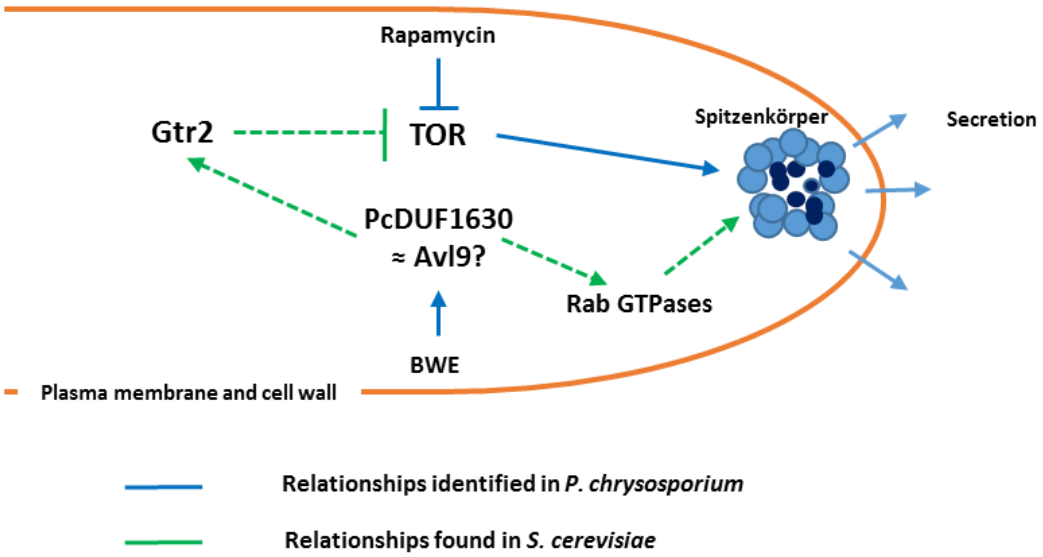

Figure 38. The possible links of PcDUF1630/DENND to TOR signaling and secretory pathway in *P. chrysosporium*.

Proteins are secreted by secretory vesicles that concentrate at the apex of hyphae and control growth of hyphal mycelia in a compartment called Spitzenkörper. TOR is inhibited by rapamycin. This inhibition leads to qualitative modifications of the secreted proteins. From our results, Bagassa wood extractives (BWE) interact with PcDUF1640/DENND. The closest yeast homolog of PcDUF1640/DENND is Avl9. Avl9 regulates the secretory pathway via Rab GTPases. DENND proteins are also known to interact with the Rag GTPases Gtr2. Gtr2 negatively regulates TORC1. Dashed lines represent putative relationships in *P. chrysosporium*.

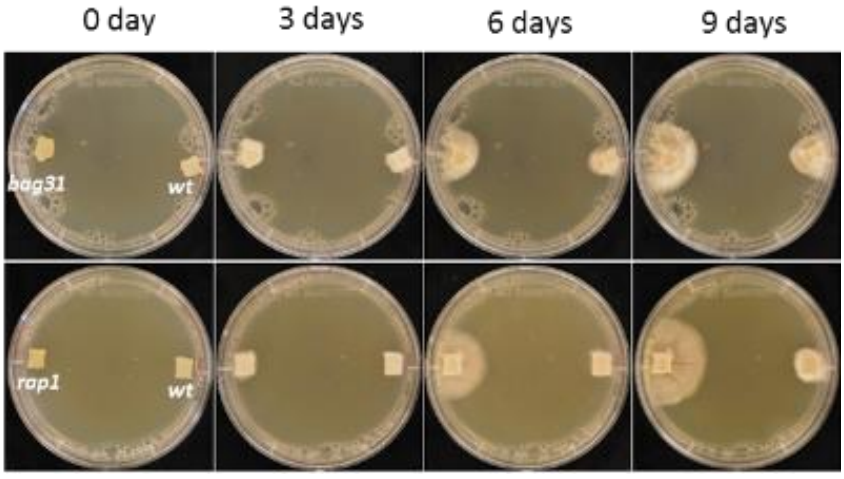

Figure 39. Bagassa wood extractives resistance of *bag31* and *rap1* mutants in comparison to WT strain.

The experiment was designed on malt extract agar medium supplemented with BWE 200 µg.mL^{-1}. Plates were incubated at 37 °C.

There are several instances where Rab GTPases have regulatory roles *vs.* the TOR complex and components of TOR signaling. Indeed, Rab5 GTPase is the key regulator of localization and activation of TORC1 in mammalian cells, and its disruption leads to the decrease of TOR function in yeast. This regulation is controlled through PI(3)P synthesis (Bridges et al., 2012). Furthermore, Ypt53, which is an isoform of Rab5 GTPase, is up-regulated in yeast under nutritional stress conditions (Nakatsukasa et al., 2014). In these conditions, up-regulation of Ypt53 and Vps21, a protein with vacuolar hydrolase activity, enables to prevent the accumulation of ROS and maintain mitochondrial respiration, thereby helping yeast cells adapting to environmental challenges (Nakatsukasa et al., 2014). One hypothesis put forward was that the up-regulation of Ypt53 acts as a positive feedback to modulate TORC1 activity and its downstream signaling cascade (Nakatsukasa et al., 2014). Since PcDUF1630/PcDENND has been predicted as a regulator of Rab14 GTPases, it could also modulate the TORC1 activity in response to BWE.

The possible relationships between PcTOR and PcNACHT protein

As discussed in the result section describing the effect of cherry tree extractives, the NACHT protein which is the product of *het* gene that is known to control the incompatibility reaction. In the incompatibility reaction, there is an induced set of genes named *idi* genes. It comprises 7 genes identified in the fungus *P. aserina*. *Idi-1, idi-2, idi-3* encode small proteins that could be localized in the cell wall or secreted. *Idi-6, idi-7* are both autophagy genes. *Idi-4* is a gene encoding a transcription factor which will be discussed in the following paragraph.

For the fungus *P. aserina*, rapamycin treatment mimics the incompatibility reaction (Dementhon et al., 2003). Indeed, *idi* genes which are triggered by the *het-R* and *het-V* interactions are induced during the cell death promoted by nitrogen and carbon starvation, and by rapamycin treatment. Characterizing one of them, *idi-1* which encodes for a cell wall protein, not only showed a protective function rather than cell death promoting role, but also mimicking between rapamycin treatment and the incompatibility reaction at the cytological level (Dementhon et al., 2003). From this point of view, a hypothesis concerning the influence of *het* genes on the TOR pathway was proposed with two distinct models. The first is that the interaction of *het* gene products perturbates the general cellular metabolism which is then sensed by the TOR pathway leading to inactivation of this pathway and induction of autophagy. The second is that the *het* gene products participate in a signaling cascade feeding the TOR pathway. Particularly, *het* genes interaction may directly inactivate TOR signaling (Dementhon et al., 2003). Analyzing in more detailed *idi*-genes expression indicates that it is under the control of TOR kinase, which confirms the second hypothesis (Dementhon et al., 2004).

Among *idi* genes identified in *P. aserina*, a gene named *idi-4* which encodes for a bZIP transcription factor (IDI-4) was confirmed to be a mediator for control of *idi* genes expression by TOR (Dementhon et al., 2004). Sequence analysis of IDI-4 showed that it was an ortholog of Gcn4 from *S. cerevisiae* (Dementhon et al., 2004). In this yeast, Gcn4 has been known as a key regulator playing an important role in cellular antioxidant defense under oxidative stress and nutrient starvation conditions, and it has been considered to control the expression of 10% of genes (Mascarenhas et al., 2008). Biochemical characterization showed that IDI-4 bZIP domain binds the pseudopalindomic ATGANTCAT sequence like the GCN-4/CPC binding site in yeast (Dementhon and Saupe, 2005).

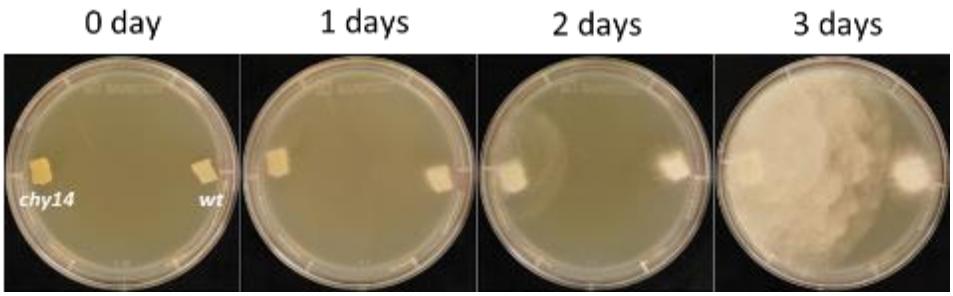

Figure 40. Rapamycin resistance of *chy14* in comparison to WT strain.

The experiment was designed on the medium malt extract agar supplemented with rapamycin 2 $\mu g.mL^{-1}$. Plates were incubated at 37 °C.

In the presence of rapamycin, the *chy14* mutant exhibits a resistance phenotype (Fig. 40). It might hypothesize that PcNACHT acts as an upstream factor of PcTOR, like products of *het* genes in *P. aserina*. In the presence of rapamycin, TOR kinase activity may not reduce leading to the obtained phenotype. Quantification of PcTOR kinase activity in the future work should help clarify the role of TOR and its relationship to PcNACHT.

Using the protein sequences of IDI-4 and Gcn4 as a query, one sequence (ID: 2915724) with the highest close relationship has been retrieved in *P. chrysosporium*. This protein has also been annotated as a bZIP transcription factor, a homolog of Yap1, and Pap1 in *S. cerevisiae* and *S. pombe*, respectively, and was identified for the first time to be up-regulated in presence of oak extractives (Thuillier et al., 2014). Measurements of the expression of this transcription factor in response to cherry tree extractives may provide information about its role in the detoxification of the wood extractives.

In summary, PcNACHT could be linked to TOR signaling as an upstream element and control the cell death program (PCD) through signaling. The involvement of PcAP1 as well as of IDI-4 to this pathway needs to confirmed.

Understanding the functions of TOR signaling in *P. chrysosporium*

Proteomic analysis could be used to characterize deeply the role of TOR in regulating the secretome response of *P. chrysosporium*

P. chrysosporium, like other white rot fungi, is capable of secreting proteins or enzymes that breakdown the lignocellulosic materials into components used for fungal growth and development. Those proteins are liberated into the surrounding environment or remain in contact or bound to the outer cell wall. The secretome reflects then the responses and adaptation of fungi to their environment (McCotter et al., 2016). Detailed investigations of secretome allow a better understanding of the mechanisms involved in the lignocellulose degradation and then the optimal design of enzymatic cocktails used in biomass refinery and for bioremediation purposes. Proteomic is very highly useful for studying protein expression and finding the novel proteins likely to play important roles in wood degradation. To date, this toolkit has significantly contributed to clarifying wood degrading mechanisms of white rot fungi including differentiation of that of brown rot fungi (Alfaro et al., 2014).

Proteomic analysis can be done in two different ways: gel-based or gel-free (Abdallah et al., 2012; Bianco and Perrotta, 2015). In this thesis, the second option was chosen for identifying secretome proteins. This method permits to identify more proteins in comparison with gel-based. Importantly, this technique does not require labeling and therefore avoids undesirable effects linked to this process. Furthermore, it also overcomes the disadvantages of gel-based method which is normally affected by brown extractives that result in smearing the 2-D-page (Bianco and Perrotta, 2015). To date, the free-labeling technique has been applied to characterize the secretome of the lignocellulosic degrading fungus *Thermobifida fusca* in response to different lignocellulosic biomass (Adav et al., 2012). The results indicated the expression of cellulolytic enzymes induced in cellulose degradation, and enzymes degrading hemicellulose, pectin and lignin induced in lignocellulosic conditions (Adav et al., 2012).

In this thesis, proteomic analysis was applied to help identify the regulatory role of PcTOR in secretion (article II). As mentioned in the introduction part, TOR in filamentous fungi has been proposed to have a regulatory role in sensing and adaptation to carbon sources which results in secretome changes, but this relationship, to date, has not been characterized for wood decaying fungi. For available *rap* mutants, proteomics can contribute to clarifying the role of TOR in *P. chrysosporium*, and maybe the role of FKBP12. FKBP12s belong to PPIases that play important roles in various cellular processes including signal transduction, growth, protein secretion, and virulence of pathogens (Delic et al., 2013; Ren et al., 2005).

The possible relationship between TOR and the intracellular detoxification system

As discussed in the introduction part, wood degradation context is linked to stress. TOR plays an important role in cellular regulation responding to stress in all characterized organisms including filamentous fungi. In these conditions, the intracellular detoxification enzymes are also strongly expressed and play a role in cell protection, as shown for wood decaying fungi (Morel et al., 2009a, 2013). This leads to the following question: is there a functional link between PcTOR signaling and intracellular detoxification proteins?

In filamentous fungi, the ortholog of yeast Yap1 (fAp1) is the transcriptional factor regulating the intracellular detoxification enzymes expression in response to stress and xenobiotics (Simaan et al., 2019). In addition to Hog1 and MAPK pathway, Yap1 is involved in an important pathway able to detect oxidants in response to chemical stress signals (Fig. 8). In particular, these elements play an important role in oxidative stress tolerance of fungal phytopathogens caused by phytochemical compounds. Like Yap1 in yeast, fAp1 has been shown to regulate the expression of both antioxidant and drug detoxification systems resulting in fungicide resistance in several pathogens such as *A. flavus* and *C. neoformans* (Paul et al., 2015; Ukai et al., 2018).

In yeast, Yap1 accumulates in the nucleus in response to carbon stress. In particular, when there is a shift from glucose to glycerol medium, Yap1 moves from the cytoplasm to the nucleus(Wiatrowski and Carlson, 2003). Going deeply, this localization is independent of respiration and of the Snf1, PKA, and TOR (Wiatrowski and Carlson, 2003). There is a conserved localization in filamentous fungi under stress condition, and the lack of Yap1 leads to the decrease in expression of genes coding catalases, peroxidases, peroxiredoxins.

For filamentous fungi, in addition to the role as a key regulator of cellular stress protection, Yap1 homologs control a large array of processes such as regulating genes involved in virulence, development, secondary metabolism, and nutrient assimilation (Mendoza-Martínez et al., 2019). It thus plays an extended role in filamentous fungi in comparison to yeast.

In mammalian, Nrf2 has been known as the homolog with a similar function to Yap1 (Gacesa et al., 2015). In human, Nrf2 plays an important role in the coordinated regulation of Phase II drug metabolism enzymes and Phase III drug transporters (Shen and Kong, 2009). The link between Nrf2 and TOR has been identified in recent times (Bendavit et al., 2016). Indeed, Nrf2 can directly regulate mTOR via binding to the ARE region in the mTOR promoter in a manner dependent on phosphatidylinositol 3-kinase (PI3K) (Bendavit et al., 2016). In a very recent study, the activation of the pathway Nrf2-TOR has been confirmed to modulate antioxidant gene transcription and to

enhance cellular protection and survival of *Trachemys scripta elegans* in response to salinity stress (Ding et al., 2019).

In wood decaying fungi, the homolog of Yap1 has hardly been studied even in the model fungus *P. chrysosporium*. Interestingly, the transcript PcAP1 which was identified as the homolog of Yap1, was found to be more than 5-fold induced in response to oak extractives of *P. chrysosporium* (Thuillier et al., 2014). Additionally, it also was found that several genes are induced in this condition. They are linked to intracellular degradative pathways of toxic compounds including 12 genes encoding for CytP450 in phase I detoxification enzymes, and 8 genes coding for the conjugating glycosyl transferases (GT) and glutathione transferases known as phase II detoxification enzymes (Thuillier et al., 2014). Previously, a transcriptomic analysis performed on *P. chrysosporium* treated with Atropine showed repression of genes involved in PKC signaling pathway and glutathione-depending systems. By comparison with the yeast system, a role of PcAP1 was proposed as a regulator of those systems (Minami et al., 2009). To date, there are no direct studies on the role of PcAP1 and its links to the intracellular detoxification system, and PKC in *P. chrysosporium*.

From the above analysis, it is likely that there is a role for TOR signaling connected to AP1 in response to toxic wood extractives of *P. chrysosporium*. Therefore, it may hypothesized that there is possibly a PcAP1-PcTOR pathway (Fig. 41) possessing a similar role as in other filamentous fungi and mammalian that functions as a pathway linked to the detoxification network of this fungus. Confirming this hypothesis may clarify the detoxification mechanism of wood decaying fungi in the context of wood degradation, especially in coping with wood extractives.

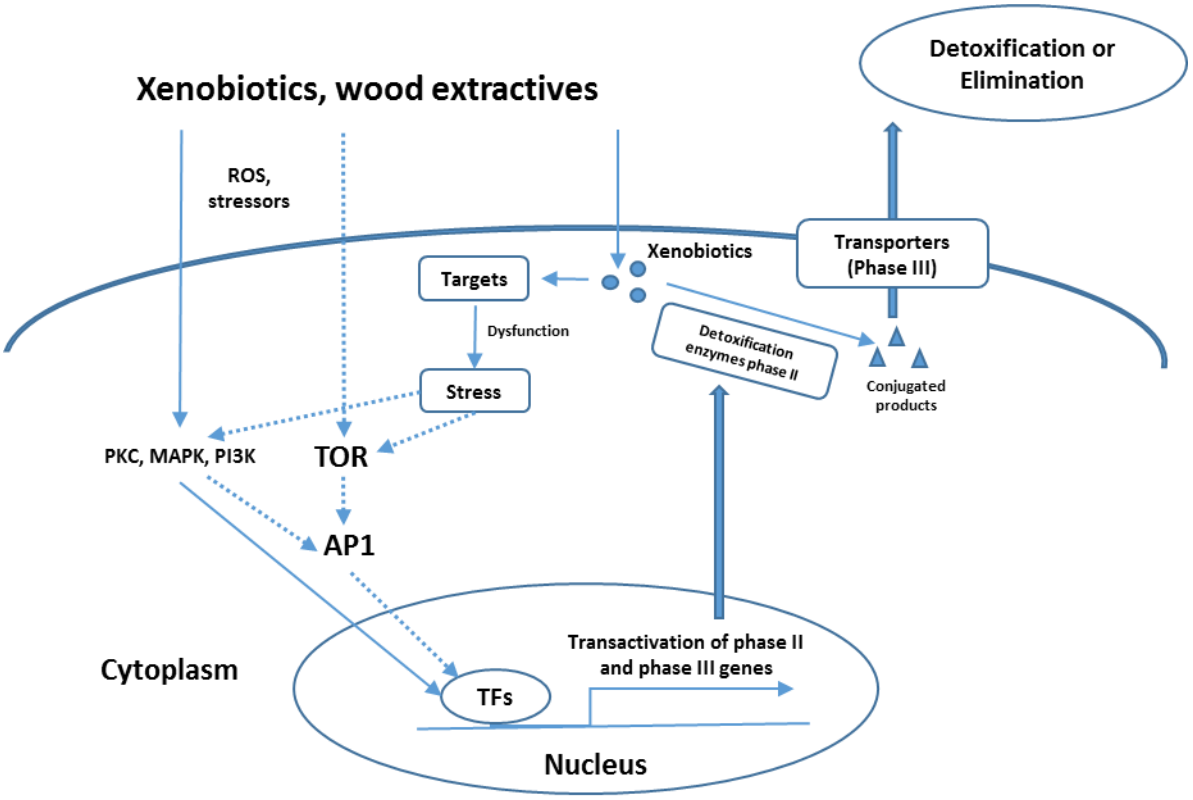

Figure 41. Proposed detoxification pathway for *P. chrysosporium*.

Xenobiotics include toxic molecules from environment, lignin degradation, and wood extractives. They promote PKC and MAPK directly or indirectly as stress agents resulting in the activation of transcription factors of genes encoding phase II enzymes and transporters (phase III). These proteins conjugate xenobiotic molecules to form products. Those products are effluxed outside the cellular environment. Transcription factors (TFs) also could be activated by the TOR-AP1 signaling pathway in *P. chrysosporium*. Dashed lines represent uncharacterized relationships.

Future perspectives

In recent years, lignin degradation has received increasing attention as an environmental process but also as an industrial process for use of byproducts of paper and fuel production. Lignin and its byproducts may contribute as building blocks for chemical products such as bioadhesives for wood product industry. Biotransformation of lignin has been mainly based on white rot fungi of basidiomycetes that therefore may have a significant role in biomass refinery. Due to their extracellular oxidative system, these fungi have also a high potential in the bioremediation of toxic compounds from industrial pollution. In this process of those toxic components, the extracellular system has an important role in breaking down chemical structures into reduced toxic compounds. Additionally, the intracellular protective system plays important functions in deeply reducing compounds modified by the extracellular enzymes. They are also essential in stress adaptation and ROS detoxification. The combination of both two systems generates a very complex system of the detoxification network with diverse actions that enable wood decaying fungi to adapt to their environment.

Identification of TOR in *P. chrysosporium*, one master regulator in eukaryotic organisms, and its possible involvement as a component of the detoxification network in this fungus, may promote new discovery on detoxification mechanisms in wood decaying fungi. As a consequence, **insights of the detoxification networks of wood decaying fungi will allow improving strains or design of optimal environmental conditions in biological detoxification**, that may contribute to advances in detoxification solutions for the industry, especially in lignocellulose biomass processing.

Drug and multi-drug resistance of microbial pathogens is one of the most pressing challenges to human at the present time. In parallel with studies to clarify the drug resistance mechanisms, discoveries of new antifungal compounds are also very important for solving this challenge. **Identification of new target proteins in fungi with inhibitory molecules from wood extractives may provide the scientific basis for developing valuable compounds for new antifungal agents in therapeutic practice or in agriculture**. In this thesis, the identification of PcDUF1630/PcDENND and PcNACHT proteins, which are respectively involved in responses to wood extractives from bagassa and cherry tree, may be of particular interest for this theme. Biochemical characterization of the proteins will help to understand their physiological roles is essential.

General conclusions

The major purpose of this work was to characterize the detoxification systems in wood decaying fungi with the model fungus *Phanerochaete chrysosporium* RP78. The main approach was forward genetics as a possible idea from advances in next-generation sequencing (NGS) technology. In the first work, the whole genome sequencing was confirmed as a reliable technique and could be used for the characterization of *P. chrysosporium* by the genetic approach. In the next work, Target of rapamycin (TOR) was identified and validated. Its signaling pathway components were also identified. This signaling pathway exhibits regulatory roles *vs.* the secretome. Mutations identified in target genes of mutant strains resistant rapamycin were verified, but whole genome sequencing is individually required for each mutant to ensure the causal link between those mutations and the resistance phenotype. In this thesis, the mutant *rap8* was confirmed by this technique. This work is essential for characterizing PcTOR in detail, which may not only give insight into detoxification networks but also contribute to the TOR signaling knowledge in filamentous fungi. For this mutant, it is possible to characterize the role of FKBP12 whose homolog has a vital role in enhancing multiple stress tolerance in plants (Alavilli et al., 2018).

Finally, the whole genome sequencing was applied to find the targets related to the toxicity of wood extractives from bagassa and cherry tree. Candidate genes were identified and are under genetic validation at lab. The obtained results show that the forward-genetic approach followed by mutant whole genome re-sequencing is a feasible strategy for characterizing *P. chrysosporium* in response to antifungal wood extractives. Most importantly, the sequencing strategy to isolate the causal element from phenotype resistant to extractives as a toxic mixture has been shown via these works for the first time. The reverse genetic approach with biochemical and physiological characterization is proposed to highlight the functions of those targets in the detoxification processes of wood decaying fungi. This also enables us to understand more deeply the mechanistic actions of the detoxification systems.

REFERENCES AND BIBLIOGRAPHY

Abdallah, C., Dumas-Gaudot, E., Renaut, J., and Sergeant, K. (2012). Gel-Based and Gel-Free Quantitative Proteomics Approaches at a Glance. International Journal of Plant Genomics, Article ID 494572.

Abdolrasouli, A., Rhodes, J., Beale, M.A., Hagen, F., Rogers, T.R., Chowdhary, A., Meis, J.F., Armstrong-James, D., and Fisher, M.C. (2015). Genomic Context of Azole Resistance Mutations in *Aspergillus fumigatus* Determined Using Whole-Genome Sequencing. mBio *6*.

Adav, S.S., Cheow, E.S.H., Ravindran, A., Dutta, B., and Sze, S.K. (2012). Label free quantitative proteomic analysis of secretome by *Thermobifida fusca* on different lignocellulosic biomass. J. Proteomics *75*, 3694–3706.

Affeldt, K.J., Carrig, J., Amare, M., and Keller, N.P. (2014). Global Survey of Canonical *Aspergillus flavus* G Protein-Coupled Receptors. mBio *5*, e01501-14.

Ahlgren, R., Suske, G., Waterman, M.R., and Lund, J. (1999). Role of Sp1 in cAMP-dependent Transcriptional Regulation of the Bovine CYP11A Gene. J. Biol. Chem. *274*, 19422–19428.

Alarco, A.-M., and Raymond, M. (1999). The bZip Transcription Factor Cap1p Is Involved in Multidrug Resistance and Oxidative Stress Response in *Candida albicans*. J. Bacteriol. *181*, 700–708.

Alfaro, M., Oguiza, J.A., Ramírez, L., and Pisabarro, A.G. (2014). Comparative analysis of secretomes in basidiomycete fungi. J. Proteomics *102*, 28–43.

Alic, M., Mayfield, M.B., Akileswaran, L., and Gold, M.H. (1991). Homologous transformation of the lignin-degrading basidiomycete *Phanerochaete chrysosporium*. Curr. Genet. *19*, 491–494.

Altmann, A., Weber, P., Bader, D., Preuß, M., Binder, E.B., and Müller-Myhsok, B. (2012). A beginners guide to SNP calling from high-throughput DNA-sequencing data. Hum. Genet. *131*, 1541–1554.

Alvarez, B., and Moreno, S. (2006). Fission yeast Tor2 promotes cell growth and represses cell differentiation. J. Cell Sci. *119*, 4475–4485.

Anouhe, J.-B.S., Niamké, F.B., Faustin, M., Virieux, D., Pirat, J.-L., Adima, A.A., Kati-Coulibaly, S., and Amusant, N. (2018). The role of extractives in the natural durability of the heartwood of *Dicorynia guianensis* Amsh: new insights in antioxydant and antifungal properties. Ann. For. Sci. *75*, 15.

Anttila, A.-K., Pirttilä, A.M., Häggman, H., Harju, A., Venäläinen, M., Haapala, A., Holmbom, B., and Julkunen-Tiitto, R. (2013). Condensed conifer tannins as antifungal agents in liquid culture. Holzforschung *67*, 825–832.

Arantes, V., and Goodell, B. (2014). Current Understanding of Brown-Rot Fungal Biodegradation Mechanisms: A Review. In Deterioration and Protection of Sustainable Biomaterials, (American Chemical Society), pp. 3–21.

Arbenz, A., and Avérous, L. (2015). Chemical modification of tannins to elaborate aromatic biobased macromolecular architectures. Green Chem. *17*, 2626–2646.

Arya, P., and Acharya, V. (2018). Plant STAND P-loop NTPases: a current perspective of genome distribution, evolution, and function. Mol. Genet. Genomics *293*, 17–31.

Bahn, Y.-S., Xue, C., Idnurm, A., Rutherford, J.C., Heitman, J., and Cardenas, M.E. (2007). Sensing the environment: lessons from fungi. Nat. Rev. Microbiol. *5*, 57–69.

Basenko, E.Y., Pulman, J.A., Shanmugasundram, A., Harb, O.S., Crouch, K., Starns, D., Warrenfeltz, S., Aurrecoechea, C., Stoeckert, C.J., Kissinger, J.C., et al. (2018). FungiDB: An Integrated Bioinformatic Resource for Fungi and Oomycetes. J. Fungi *4*, 39.

Bastidas, R.J., Shertz, C.A., Lee, S.C., Heitman, J., and Cardenas, M.E. (2012). Rapamycin Exerts Antifungal Activity In Vitro and In Vivo against Mucor circinelloides via FKBP12-Dependent Inhibition of Tor. Eukaryot. Cell *11*, 270–281.

Bayram, Ö., and Braus, G.H. (2012). Coordination of secondary metabolism and development in fungi: the velvet family of regulatory proteins. FEMS Microbiol. Rev. *36*, 1–24.

Belt, T., Keplinger, T., Hänninen, T., and Rautkari, L. (2017). Cellular level distributions of Scots pine heartwood and knot heartwood extractives revealed by Raman spectroscopy imaging. Ind. Crops Prod. *108*, 327–335.

Bendavit, G., Aboulkassim, T., Hilmi, K., Shah, S., and Batist, G. (2016). Nrf2 Transcription Factor Can Directly Regulate mTOR linking cytoprotective gene expression to a major metablolic regulator that generates redox activity. J. Biol. Chem. *291*, 25476–25488.

Bertram, P.G., Choi, J.H., Carvalho, J., Chan, T.-F., Ai, W., and Zheng, X.F.S. (2002). Convergence of TOR-Nitrogen and Snf1-Glucose Signaling Pathways onto Gln3. Mol. Cell. Biol. *22*, 1246–1252.

Bertrand Teponno, R., Kusari, S., and Spiteller, M. (2016). Recent advances in research on lignans and neolignans. Nat. Prod. Rep. *33*, 1044–1092.

Besnard, F., Koutsovoulos, G., Dieudonné, S., Blaxter, M., and Félix, M.-A. (2017). Toward Universal Forward Genetics: Using a Draft Genome Sequence of the Nematode *Oscheius tipulae* To Identify Mutations Affecting Vulva Development. Genetics *206*, 1747–1761.

Bianco, L., and Perrotta, G. (2015). Methodologies and Perspectives of Proteomics Applied to Filamentous Fungi: From Sample Preparation to Secretome Analysis. Int. J. Mol. Sci. *16*, 5803–5829.

Biasini, M., Bienert, S., Waterhouse, A., Arnold, K., Studer, G., Schmidt, T., Kiefer, F., Cassarino, T.G., Bertoni, M., Bordoli, L., et al. (2014). SWISS-MODEL: modelling protein tertiary and quaternary structure using evolutionary information. Nucleic Acids Res. *42*, W252–W258.

Blanchette, R.A. (2000). A review of microbial deterioration found in archaeological wood from different environments. Int. Biodeterior. Biodegrad. *46*, 189–204.

Boeckstaens, M., André, B., and Marini, A.M. (2007). The yeast ammonium transport protein Mep2 and its positive regulator, the Npr1 kinase, play an important role in normal and pseudohyphal growth on various nitrogen media through retrieval of excreted ammonium. Mol. Microbiol. *64*, 534–546.

Braun, K.A., Vaga, S., Dombek, K.M., Fang, F., Palmisano, S., Aebersold, R., and Young, E.T. (2014). Phosphoproteomic analysis identifies proteins involved in transcription-coupled mRNA decay as targets of Snf1 signaling. Sci. Signal. *7*, ra64-ra64.

Braunsdorf, C., Mailänder-Sánchez, D., and Schaller, M. (2016). Fungal sensing of host environment. Cell. Microbiol. *18*, 1188–1200.

Bridges, D., Fisher, K., Zolov, S.N., Xiong, T., Inoki, K., Weisman, L.S., and Saltiel, A.R. (2012). Rab5 proteins regulate activation and localization of target of rapamycin complex 1. J. Biol. Chem. *287*, 20913–20921.

Brocco, V.F., Paes, J.B., Costa, L.G. da, Brazolin, S., and Arantes, M.D.C. (2017). Potential of teak heartwood extracts as a natural wood preservative. J. Clean. Prod. *142*, 2093–2099.

Brosch, G., Loidl, P., and Graessle, S. (2008). Histone modifications and chromatin dynamics: a focus on filamentous fungi. FEMS Microbiol. Rev. *32*, 409–439.

Brown, A.J.P., Cowen, L.E., Pietro, A. di, and Quinn, J. (2017). Stress Adaptation. Microbiol. Spectr. *5*.

Brown, N.A., de Gouvea, P.F., Krohn, N.G., Savoldi, M., and Goldman, G.H. (2013). Functional characterisation of the non-essential protein kinases and phosphatases regulating *Aspergillus nidulans* hydrolytic enzyme production. Biotechnol. Biofuels *6*, 91.

Brown, N.A., Ries, L.N.A., and Goldman, G.H. (2014). How nutritional status signalling coordinates metabolism and lignocellulolytic enzyme secretion. Fungal Genet. Biol. *72*, 48–63.

Brown, N.A., Reis, T.F. dos, Ries, L.N.A., Caldana, C., Mah, J.-H., Yu, J.-H., Macdonald, J.M., and Goldman, G.H. (2015). G-protein coupled receptor-mediated nutrient sensing and developmental control in *Aspergillus nidulans*. Mol. Microbiol. *98*, 420–439.

Cai, P., Wang, B., Ji, J., Jiang, Y., Wan, L., Tian, C., and Ma, Y. (2015). The Putative Cellodextrin Transporter-like Protein CLP1 Is Involved in Cellulase Induction in *Neurospora crassa*. J. Biol. Chem. *290*, 788–796.

Cameron, M.D., Timofeevski, S., and Aust, S.D. (2000). Enzymology of *Phanerochaete chrysosporium* with respect to the degradation of recalcitrant compounds and xenobiotics. Appl. Microbiol. Biotechnol. *54*, 751–758.

Camps, S.M.T., Dutilh, B.E., Arendrup, M.C., Rijs, A.J.M.M., Snelders, E., Huynen, M.A., Verweij, P.E., and Melchers, W.J.G. (2012). Discovery of a hapE Mutation That Causes Azole Resistance in *Aspergillus fumigatus* through Whole Genome Sequencing and Sexual Crossing. PLOS ONE *7*, e50034.

Casado, C., González, A., Platara, M., Ruiz, A., and Ariño, J. (2011). The role of the protein kinase A pathway in the response to alkaline pH stress in yeast. Biochem. J. *438*, 523–533.

Castro, P.A. de, Reis, T.F. dos, Dolan, S.K., Manfiolli, A.O., Brown, N.A., Jones, G.W., Doyle, S., Riaño-Pachón, D.M., Squina, F.M., Caldana, C., et al. (2016). The Aspergillus fumigatus SchASCH9 kinase modulates SakAHOG1 MAP kinase activity and it is essential for virulence. Mol. Microbiol. *102*, 642–671.

Celimene, C.C., Micales, J.A., Ferge, L., and Young, R.A. (2005). Efficacy of Pinosylvins against White-Rot and Brown-Rot Fungi. Holzforschung *53*, 491–497.

Céspedes, C.L., Avila, J.G., Garcıá, A.M., Becerra, J., Flores, C., Aqueveque, P., Bittner, M., Hoeneisen, M., Martinez, M., and Silva, M. (2014). Antifungal and Antibacterial Activities of *Araucaria araucana* (Mol.) K. Koch Heartwood Lignans. Z. Für Naturforschung C *61*, 35–43.

Chang, S.-T., Wang, S.-Y., Wu, C.-L., Su, Y.-C., and Kuo, Y.-H. (2005). Antifungal Compounds in the Ethyl Acetate Soluble Fraction of the Extractives of Taiwania (Taiwania cryptomerioides Hayata) Heartwood. Holzforschung *53*, 487–490.

Chen, D., Wang, Y., Zhou, X., Wang, Y., and Xu, J.-R. (2014). The Sch9 Kinase Regulates Conidium Size, Stress Responses, and Pathogenesis in *Fusarium graminearum*. PLOS ONE *9*, e105811.

Chen, D.-D., Shi, L., Yue, S.-N., Zhang, T.-J., Wang, S.-L., Liu, Y.-N., Ren, A., Zhu, J., Yu, H.-S., and Zhao, M.-W. (2019). The Slt2-MAPK pathway is involved in the mechanism by which target of rapamycin regulates cell wall components in *Ganoderma lucidum*. Fungal Genet. Biol. *123*, 70–77.

Chen, Y.-H., Yeh, T.-F., Chu, F.-H., Hsu, F.-L., and Chang, S.-T. (2015). Proteomics Investigation Reveals Cell Death-Associated Proteins of Basidiomycete Fungus *Trametes versicolor* Treated with Ferruginol. J. Agric. Food Chem. *63*, 85–91.

Chen, Y.-T., Lin, C.-Y., Tsai, P.-W., Yang, C.-Y., Hsieh, W.-P., and Lan, C.-Y. (2012). Rhb1 Regulates the Expression of Secreted Aspartic Protease 2 through the TOR Signaling Pathway in Candida albicans. Eukaryot. Cell *11*, 168–182.

Chen, Y.-W., Yeh, Y.-C., Chen, H.-F., Chen, R.-C., Lin, G.-Y., Chen, Y.-T., and Lan, C.-Y. (2019). The small GTPase Rhb1 is involved in the cell response to fluconazole in *Candida albicans*. FEMS Yeast Res. *19*.

Choi, J., Chen, J., Schreiber, S.L., and Clardy, J. (1996). Structure of the FKBP12-Rapamycin Complex Interacting with Binding Domain of Human FRAP. Science *273*, 239–242.

Crespo, J.L., Daicho, K., Ushimaru, T., and Hall, M.N. (2001). The GATA Transcription Factors GLN3 and GAT1 Link TOR to Salt Stress in *Saccharomyces cerevisiae*. J. Biol. Chem. *276*, 34441–34444.

Cruz, M.C., Cavallo, L.M., Görlach, J.M., Cox, G., Perfect, J.R., Cardenas, M.E., and Heitman, J. (1999). Rapamycin Antifungal Action Is Mediated via Conserved Complexes with FKBP12 and TOR Kinase Homologs in *Cryptococcus neoformans*. Mol. Cell. Biol. *19*, 4101–4112.

De Koker, T.H., Nakasone, K.K., Haarhof, J., Burdsall, H.H., and Janse, B.J.H. (2003). Phylogenetic relationships of the genus *Phanerochaete* inferred from the internal transcribed spacer region. Mycol. Res. *107*, 1032–1040.

Delic, M., Valli, M., Graf, A.B., Pfeffer, M., Mattanovich, D., and Gasser, B. (2013). The secretory pathway: exploring yeast diversity. FEMS Microbiol. Rev. *37*, 872–914.

Dementhon, K., and Saupe, S.J. (2005). DNA-Binding Specificity of the IDI-4 Basic Leucine Zipper Factor of *Podospora anserina* Defined by Systematic Evolution of Ligands by Exponential Enrichment (SELEX). Eukaryot. Cell *4*, 476–483.

Dementhon, K., Paoletti, M., Pinan-Lucarré, B., Loubradou-Bourges, N., Sabourin, M., Saupe, S.J., and Clavé, C. (2003). Rapamycin Mimics the Incompatibility Reaction in the Fungus *Podospora anserina*. Eukaryot. Cell *2*, 238–246.

Dementhon, K., Saupe, S.J., and Clavé, C. (2004). Characterization of IDI-4, a bZIP transcription factor inducing autophagy and cell death in the fungus *Podospora anserina*. Mol. Microbiol. *53*, 1625–1640.

Deroy, A., Saiag, F., Kebbi-Benkeder, Z., Touahri, N., Hecker, A., Morel-Rouhier, M., Colin, F., Dumarcay, S., Gérardin, P., and Gelhaye, E. (2015). The GSTome Reflects the Chemical Environment of White-Rot Fungi. PLOS ONE *10*, e0137083.

Diaz-Guerra, T.M., Mellado, E., Cuenca-Estrella, M., and Rodriguez-Tudela, J.L. (2004). A Point Mutation in the 14α-Sterol Demethylase Gene cyp51A Contributes to Itraconazole Resistance in *Aspergillus fumigatus*. Antimicrob. Agents Chemother. *48*, 1071–1071.

Dijck, P.V., Brown, N.A., Goldman, G.H., Rutherford, J., Xue, C., and Zeebroeck, G.V. (2017). Nutrient Sensing at the Plasma Membrane of Fungal Cells. Microbiol. Spectr. *5*.

Ding, L., Li, W., Li, N., Liang, L., Zhang, X., Jin, H., Shi, H., Storey, K.B., and Hong, M. (2019). Antioxidant responses to salinity stress in an invasive species, the red-eared slider (*Trachemys scripta elegans*) and involvement of a TOR-Nrf2 signaling pathway. Comp. Biochem. Physiol. Part C Toxicol. Pharmacol. *219*, 59–67.

Doddapaneni, H., and Yadav, J.S. (2005). Microarray-based global differential expression profiling of P450 monooxygenases and regulatory proteins for signal transduction pathways in the white rot fungus *Phanerochaete chrysosporium*. Mol. Genet. Genomics *274*, 454–466.

van der Does, H.C., and Rep, M. (2017). Adaptation to the Host Environment by Plant-Pathogenic Fungi. Annu. Rev. Phytopathol. *55*, 427–450.

Donaton, M.C.V., Holsbeeks, I., Lagatie, O., Zeebroeck, G.V., Crauwels, M., Winderickx, J., and Thevelein, J.M. (2003). The Gap1 general amino acid permease acts as an amino acid sensor for activation of protein kinase A targets in the yeast *Saccharomyces cerevisiae*. Mol. Microbiol. *50*, 911–929.

Dyrka, W., Lamacchia, M., Durrens, P., Kobe, B., Daskalov, A., Paoletti, M., Sherman, D.J., and Saupe, S.J. (2014). Diversity and Variability of NOD-Like Receptors in Fungi. Genome Biol. Evol. *6*, 3137–3158.

Eastwood, D.C., Floudas, D., Binder, M., Majcherczyk, A., Schneider, P., Aerts, A., Asiegbu, F.O., Baker, S.E., Barry, K., Bendiksby, M., et al. (2011). The Plant Cell Wall–Decomposing Machinery Underlies the Functional Diversity of Forest Fungi. Science *333*, 762–765.

Enjalbert, B., Smith, D.A., Cornell, M.J., Alam, I., Nicholls, S., Brown, A.J.P., and Quinn, J. (2005). Role of the Hog1 Stress-activated Protein Kinase in the Global Transcriptional Response to Stress in the Fungal Pathogen *Candida albicans*. Mol. Biol. Cell *17*, 1018–1032.

Espagne, E., Balhadère, P., Penin, M.-L., Barreau, C., and Turcq, B. (2002). HET-E and HET-D belong to a new subfamily of WD40 proteins involved in vegetative incompatibility specificity in the fungus *Podospora anserina*. Genetics *161*, 71–81.

Falcone Ferreyra, M.L., Rius, S., and Casati, P. (2012). Flavonoids: biosynthesis, biological functions, and biotechnological applications. Front. Plant Sci. *3*.

Falloon, K., Juvvadi, P.R., Richards, A.D., Vargas-Muñiz, J.M., Renshaw, H., and Steinbach, W.J. (2015). Characterization of the FKBP12-Encoding Genes in *Aspergillus fumigatus*. PLOS ONE *10*, e0137869.

Fernández-González, A.J., Valette, N., Kohler, A., Dumarçay, S., Sormani, R., Gelhaye, E., and Morel-Rouhier, M. (2018). Oak extractive-induced stress reveals the involvement of new enzymes in the early detoxification response of *Phanerochaete chrysosporium*. Environ. Microbiol. *20*, 3890–3901.

Finn, R.D., Bateman, A., Clements, J., Coggill, P., Eberhardt, R.Y., Eddy, S.R., Heger, A., Hetherington, K., Holm, L., Mistry, J., et al. (2014). Pfam: the protein families database. Nucleic Acids Res. *42*, D222–D230.

Fitzgibbon, G.J., Morozov, I.Y., Jones, M.G., and Caddick, M.X. (2005). Genetic Analysis of the TOR Pathway in Aspergillus nidulans. Eukaryot. Cell *4*, 1595–1598.

Floudas, D., Binder, M., Riley, R., Barry, K., Blanchette, R.A., Henrissat, B., Martínez, A.T., Otillar, R., Spatafora, J.W., Yadav, J.S., et al. (2012). The Paleozoic Origin of Enzymatic Lignin Decomposition Reconstructed from 31 Fungal Genomes. Science *336*, 1715–1719.

Flowers, S.A., Colón, B., Whaley, S.G., Schuler, M.A., and Rogers, P.D. (2015). Contribution of Clinically Derived Mutations in ERG11 to Azole Resistance in *Candida albicans*. Antimicrob. Agents Chemother. *59*, 450–460.

Fulekar, M.H., Pathak, B., Fulekar, J., and Godambe, T. (2013). Bioremediation of Organic Pollutants Using *Phanerochaete chrysosporium*. In Fungi as Bioremediators, E.M. Goltapeh, Y.R. Danesh, and A. Varma, eds. (Berlin, Heidelberg: Springer Berlin Heidelberg), pp. 135–157.

Gacesa, R., Dunlap, W.C., and Long, P.F. (2015). Bioinformatics analyses provide insight into distant homology of the Keap1–Nrf2 pathway. Free Radic. Biol. Med. *88*, 373–380.

García, I., Mathieu, M., Nikolaev, I., Felenbok, B., and Scazzocchio, C. (2008). Roles of the *Aspergillus nidulans* homologues of Tup1 and Ssn6 in chromatin structure and cell viability. FEMS Microbiol. Lett. *289*, 146–154.

García-Salcedo, R., Lubitz, T., Beltran, G., Elbing, K., Tian, Y., Frey, S., Wolkenhauer, O., Krantz, M., Klipp, E., and Hohmann, S. (2014). Glucose de-repression by yeast AMP-activated protein kinase SNF1 is controlled via at least two independent steps. FEBS J. *281*, 1901–1917.

Gonçalves, A.P., Heller, J., Daskalov, A., Videira, A., and Glass, N.L. (2017). Regulated Forms of Cell Death in Fungi. Front. Microbiol. *8*, 1837.

Gong, P., Guan, X., and Witter, E. (2001). A rapid method to extract ergosterol from soil by physical disruption. Appl. Soil Ecol. *17*, 285–289.

González, A., and Hall, M.N. (2017). Nutrient sensing and TOR signaling in yeast and mammals. EMBO J. *36*, 397–408.

González, A., Shimobayashi, M., Eisenberg, T., Merle, D.A., Pendl, T., Hall, M.N., and Moustafa, T. (2015). TORC1 Promotes Phosphorylation of Ribosomal Protein S6 via the AGC Kinase Ypk3 in *Saccharomyces cerevisiae*. PLoS ONE *10*.

Hagiwara, D., ASANO, Y., YAMASHINO, T., and MIZUNO, T. (2008). Characterization of bZip-Type Transcription Factor AtfA with Reference to Stress Responses of Conidia of *Aspergillus nidulans*. Biosci. Biotechnol. Biochem. *72*, 2756–2760.

Hagiwara, D., Asano, Y., Marui, J., Yoshimi, A., Mizuno, T., and Abe, K. (2009). Transcriptional profiling for *Aspergillus nidulans* HogA MAPK signaling pathway in response to fludioxonil and osmotic stress. Fungal Genet. Biol. *46*, 868–878.

Hagiwara, D., Sakamoto, K., Abe, K., and Gomi, K. (2016). Signaling pathways for stress responses and adaptation in Aspergillus species: stress biology in the post-genomic era. Biosci. Biotechnol. Biochem. *80*, 1667–1680.

Hammel, K.E., Kapich, A.N., Jensen, K.A., and Ryan, Z.C. (2002). Reactive oxygen species as agents of wood decay by fungi. Enzyme Microb. Technol. *30*, 445–453.

Hargrove, T.Y., Wawrzak, Z., Lamb, D.C., Guengerich, F.P., and Lepesheva, G.I. (2015). Structure-Functional Characterization of Cytochrome P450 Sterol 14α-Demethylase (CYP51B) from *Aspergillus fumigatus* and Molecular Basis for the Development of Antifungal Drugs. J. Biol. Chem. *290*, 23916–23934.

Harju, A.M., and Venäläinen, M. (2002). Genetic Parameters Regarding the Resistance of *Pinus sylvestris* Heartwood to Decay Caused by *Coniophora puteana*. Scand. J. For. Res. *17*, 199–205.

Harris, S.D. (2019). Hyphal branching in filamentous fungi. Dev. Biol. *451*, 35–39.

Harsay, E., and Schekman, R. (2007). Avl9p, a Member of a Novel Protein Superfamily, Functions in the Late Secretory Pathway. Mol. Biol. Cell *18*, 1203–1219.

Hatakka, A., and Hammel, K.E. (2011). Fungal Biodegradation of Lignocelluloses. In Industrial Applications, M. Hofrichter, ed. (Berlin, Heidelberg: Springer Berlin Heidelberg), pp. 319–340.

Hayes, B.M.E., Anderson, M.A., Traven, A., van der Weerden, N.L., and Bleackley, M.R. (2014). Activation of stress signalling pathways enhances tolerance of fungi to chemical fungicides and antifungal proteins. Cell. Mol. Life Sci. *71*, 2651–2666.

Heitman, J., Movva, N.R., and Hall, M.N. (1991). Targets for cell cycle arrest by the immunosuppressant rapamycin in yeast. Science *253*, 905–909.

Hirosue, S., Tazaki, M., Hiratsuka, N., Yanai, S., Kabumoto, H., Shinkyo, R., Arisawa, A., Sakaki, T., Tsunekawa, H., Johdo, O., et al. (2011). Insight into functional diversity of cytochrome P450 in the white-rot basidiomycete *Phanerochaete chrysosporium*: Involvement of versatile monooxygenase. Biochem. Biophys. Res. Commun. *407*, 118–123.

Huang, X., and Madan, A. (1999). CAP3: A DNA Sequence Assembly Program. Genome Res. *9*, 868–877.

Huberman, L.B., Liu, J., Qin, L., and Glass, N.L. (2016). Regulation of the lignocellulolytic response in filamentous fungi. Fungal Biol. Rev. *30*, 101–111.

Huberman, L.B., Coradetti, S.T., and Glass, N.L. (2017). Network of nutrient-sensing pathways and a conserved kinase cascade integrate osmolarity and carbon sensing in *Neurospora crassa*. Proc. Natl. Acad. Sci. *114*, E8665–E8674.

Irmler, S., Rogniaux, H., Hess, D., and Pillonel, C. (2006). Induction of OS-2 phosphorylation in *Neurospora crassa* by treatment with phenylpyrrole fungicides and osmotic stress. Pestic. Biochem. Physiol. *84*, 25–37.

Jacobs, A., Lundqvist, J., Stålbrand, H., Tjerneld, F., and Dahlman, O. (2002). Characterization of water-soluble hemicelluloses from spruce and aspen employing SEC/MALDI mass spectroscopy. Carbohydr. Res. *337*, 711–717.

James, T.Y., Lee, M., and Diepen, L.T.A. van (2011). A Single Mating-Type Locus Composed of Homeodomain Genes Promotes Nuclear Migration and Heterokaryosis in the White-Rot Fungus *Phanerochaete chrysosporium*. Eukaryot. Cell *10*, 249–261.

Javelle, A., Morel, M., Rodríguez-Pastrana, B.-R., Botton, B., André, B., Marini, A.-M., Brun, A., and Chalot, M. (2003). Molecular characterization, function and regulation of ammonium transporters (Amt) and ammonium-metabolizing enzymes (GS, NADP-GDH) in the ectomycorrhizal fungus *Hebeloma cylindrosporum*. Mol. Microbiol. *47*, 411–430.

Jeon, J., Choi, J., Lee, G.-W., Dean, R.A., and Lee, Y.-H. (2013). Experimental Evolution Reveals Genome-Wide Spectrum and Dynamics of Mutations in the Rice Blast Fungus, *Magnaporthe oryzae*. PLOS ONE *8*, e65416.

Joubert, A., Calmes, B., Berruyer, R., Pihet, M., Bouchara, J.-P., Simoneau, P., and Guillemette, T. (2010). Laser nephelometry applied in an automated microplate system to study filamentous fungus growth. BioTechniques *48*, 399–404.

Jourdes, M., Pouységu, L., Deffieux, D., Teissedre, P.-L., and Quideau, S. (2013). Hydrolyzable Tannins: Gallotannins and Ellagitannins. In Natural Products: Phytochemistry, Botany and Metabolism of Alkaloids, Phenolics and Terpenes, K.G. Ramawat, and J.-M. Mérillon, eds. (Berlin, Heidelberg: Springer Berlin Heidelberg), pp. 1975–2010.

Kameshwar, A.K.S., and Qin, W. (2017). Metadata Analysis of *Phanerochaete chrysosporium* Gene Expression Data Identified Common CAZymes Encoding Gene Expression Profiles Involved in Cellulose and Hemicellulose Degradation. Int. J. Biol. Sci. *13*, 85–99.

Kasai, N., Ikushiro, S., Hirosue, S., Arisawa, A., Ichinose, H., Wariishi, H., Ohta, M., and Sakaki, T. (2009). Enzymatic properties of cytochrome P450 catalyzing 3′-hydroxylation of naringenin from the white-rot fungus *Phanerochaete chrysosporium*. Biochem. Biophys. Res. Commun. *387*, 103–108.

Kasai, N., Ikushiro, S., Hirosue, S., Arisawa, A., Ichinose, H., Uchida, Y., Wariishi, H., Ohta, M., and Sakaki, T. (2010). Atypical kinetics of cytochromes P450 catalysing 3′-hydroxylation of flavone from the white-rot fungus *Phanerochaete chrysosporium*. J. Biochem. (Tokyo) *147*, 117–125.

Kawamura, F., Ohara, S., and Nishida, A. (2005). Antifungal activity of constituents from the heartwood of Gmelina arborea: Part 1. Sensitive antifungal assay against Basidiomycetes. Holzforschung *58*, 189–192.

Kersten, P., and Cullen, D. (2007). Extracellular oxidative systems of the lignin-degrading Basidiomycete Phanerochaete chrysosporium. Fungal Genet. Biol. FG B *44*, 77–87.

Kersten, P., and Cullen, D. (2014). Copper radical oxidases and related extracellular oxidoreductases of wood-decay Agaricomycetes. Fungal Genet. Biol. *72*, 124–130.

Khanbabaee, K., and Ree, T. van (2001). Tannins: Classification and Definition. Nat. Prod. Rep. *18*, 641–649.

Kirk, T.K. (1975). Effects of a Brown-Rot Fungus, Lenzites trabea, on Lignin in Spruce Wood. Holzforsch. - Int. J. Biol. Chem. Phys. Technol. Wood *29*, 99–107.

Kirker, G.T., Blodgett, A.B., Arango, R.A., Lebow, P.K., and Clausen, C.A. (2013). The role of extractives in naturally durable wood species. Int. Biodeterior. Biodegrad. *82*, 53–58.

Klasson, H., Fink, G.R., and Ljungdahl, P.O. (1999). Ssy1p and Ptr3p Are Plasma Membrane Components of a Yeast System That Senses Extracellular Amino Acids. Mol. Cell. Biol. *19*, 5405–5416.

Kodama, Y., Omura, F., Takahashi, K., Shirahige, K., and Ashikari, T. (2002). Genome-wide expression analysis of genes affected by amino acid sensor Ssy1p in *Saccharomyces cerevisiae*. Curr. Genet. *41*, 63–72.

Korripally, P., Hunt, C.G., Houtman, C.J., Jones, D.C., Kitin, P.J., Cullen, D., and Hammel, K.E. (2015). Regulation of Gene Expression during the Onset of Ligninolytic Oxidation by *Phanerochaete chrysosporium* on Spruce Wood. Appl. Environ. Microbiol. *81*, 7802–7812.

Köser, C.U., Ellington, M.J., and Peacock, S.J. (2014). Whole-genome sequencing to control antimicrobial resistance. Trends Genet. *30*, 401–407.

Krah, F.-S., Bässler, C., Heibl, C., Soghigian, J., Schaefer, H., and Hibbett, D.S. (2018). Evolutionary dynamics of host specialization in wood-decay fungi. BMC Evol. Biol. *18*, 119.

Krieger Elmar, Joo Keehyoung, Lee Jinwoo, Lee Jooyoung, Raman Srivatsan, Thompson James, Tyka Mike, Baker David, and Karplus Kevin (2009). Improving physical realism, stereochemistry, and side-chain accuracy in homology modeling: Four approaches that performed well in CASP8. Proteins Struct. Funct. Bioinforma. *77*, 114–122.

Kües, U., Nelson, D.R., Liu, C., Yu, G.-J., Zhang, J., Li, J., Wang, X.-C., and Sun, H. (2015). Genome analysis of medicinal Ganoderma spp. with plant-pathogenic and saprotrophic life-styles. Phytochemistry *114*, 18–37.

Kulik, T., Buśko, M., Pszczółkowska, A., Perkowski, J., and Okorski, A. (2014). Plant lignans inhibit growth and trichothecene biosynthesis in *Fusarium graminearum*. Lett. Appl. Microbiol. *59*, 99–107.

Kulmburg, P., Mathieu, M., Dowzer, C., Kelly, J., and Felenbok, B. (1993). Specific binding sites in the alcR and alcA promoters of the ethanol regulon for the CREA repressor mediating carbon cataboiite repression in *Aspergillus nidulans*. Mol. Microbiol. *7*, 847–857.

Kurtzman, C.P., and Piškur, J. (2015). Taxonomy and phylogenetic diversity among the yeasts. In Comparative Genomics: Using Fungi as Models, (Springer Berlin Heidelberg), pp. 29–46.

Kusuma, I.W., and Tachibana, S. (2008). Antifungal secoabietane dialdehyde and bisabolane-type terpenoids from the heartwood of *Cryptomeria japonica* D. Don. Holzforschung *62*, 624–626.

Kusumoto, N., Ashitani, T., Murayama, T., Ogiyama, K., and Takahashi, K. (2010). Antifungal Abietane-Type Diterpenes from the Cones of *Taxodium distichum* Rich. J. Chem. Ecol. *36*, 1381–1386.

Laothanachareon, T., Tamayo-Ramos, J.A., Nijsse, B., and Schaap, P.J. (2018). Forward Genetics by Genome Sequencing Uncovers the Central Role of the Aspergillus niger goxB Locus in Hydrogen Peroxide Induced Glucose Oxidase Expression. Front. Microbiol. *9*.

Latva-Mäenpää, H., Laakso, T., Sarjala, T., Wähälä, K., and Saranpää, P. (2013). Root neck of Norway spruce as a source of bioactive lignans and stilbenes. Holzforschung *68*, 1–7.

Lee, H., Lamichhane, A.K., Garraffo, H.M., Kwon-Chung, K.J., and Chang, Y.C. (2012). Involvement of PDK1, PKC and TOR signalling pathways in basal fluconazole tolerance in *Cryptococcus neoformans*. Mol. Microbiol. *84*, 130–146.

Lee, H.V., Hamid, S.B.A., and Zain, S.K. (2014). Conversion of Lignocellulosic Biomass to Nanocellulose: Structure and Chemical Process.

Leistner, E. (1985). CHAPTER 11 - Occurrence and Biosynthesis of Quinones in Woody Plants. In Biosynthesis and Biodegradation of Wood Components, T. Higuchi, ed. (Academic Press), pp. 273–290.

Lekounougou, S., Mounguengui, S., Dumarçay, S., Rose, C., Courty, P.E., Garbaye, J., Gérardin, P., Jacquot, J.P., and Gelhaye, E. (2008). Initial stages of Fagus sylvatica wood colonization by the white-rot basidiomycete *Trametes versicolor*: Enzymatic characterization. Int. Biodeterior. Biodegrad. *61*, 287–293.

Levine, T.P., Daniels, R.D., Gatta, A.T., Wong, L.H., and Hayes, M.J. (2013). The product of C9orf72, a gene strongly implicated in neurodegeneration, is structurally related to DENN Rab-GEFs. Bioinformatics *29*, 499–503.

Li, H. (2011). A statistical framework for SNP calling, mutation discovery, association mapping and population genetical parameter estimation from sequencing data. Bioinformatics *27*, 2987–2993.

Li, H., and Durbin, R. (2009). Fast and accurate short read alignment with Burrows–Wheeler transform. Bioinformatics *25*, 1754–1760.

Li, L., and Borkovich, K.A. (2006). GPR-4 Is a Predicted G-Protein-Coupled Receptor Required for Carbon Source-Dependent Asexual Growth and Development in *Neurospora crassa*. Eukaryot. Cell *5*, 1287–1300.

Li, B., Rotsaert, F.A.J., Gold, M.H., and Renganathan, V. (2000). Homologous Expression of Recombinant Cellobiose Dehydrogenase in *Phanerochaete chrysosporium*. Biochem. Biophys. Res. Commun. *270*, 141–146.

Li, B., Carey, M., and Workman, J.L. (2007a). The Role of Chromatin during Transcription. Cell *128*, 707–719.

Li, L., Wright, S.J., Krystofova, S., Park, G., and Borkovich, K.A. (2007b). Heterotrimeric G Protein Signaling in Filamentous Fungi. Annu. Rev. Microbiol. *61*, 423–452.

Li, L., Zhu, T., Song, Y., Luo, X., Feng, L., Zhuo, F., Li, F., and Ren, M. (2019). Functional Characterization of Target of Rapamycin Signaling in *Verticillium dahliae*. Front. Microbiol. *10*.

Linford, A., Yoshimura, S., Bastos, R.N., Langemeyer, L., Gerondopoulos, A., Rigden, D.J., and Barr, F.A. (2012). Rab14 and Its Exchange Factor FAM116 Link Endocytic Recycling and Adherens Junction Stability in Migrating Cells. Dev. Cell *22*, 952–966.

Liu, X.-L., Hao, Y.-Q., Jin, L., Xu, Z.-J., McAllister, T.A., and Wang, Y. (2013). Anti-Escherichia coli O157:H7 Properties of Purple Prairie Clover and Sainfoin Condensed Tannins. Molecules *18*, 2183–2199.

Loewith, R., and Hall, M.N. (2011). Target of Rapamycin (TOR) in Nutrient Signaling and Growth Control. Genetics *189*, 1177–1201.

Loewith, R., Jacinto, E., Wullschleger, S., Lorberg, A., Crespo, J.L., Bonenfant, D., Oppliger, W., Jenoe, P., and Hall, M.N. (2002). Two TOR Complexes, Only One of which Is Rapamycin Sensitive, Have Distinct Roles in Cell Growth Control. Mol. Cell *10*, 457–468.

López-Berges, M.S., Rispail, N., Prados-Rosales, R.C., and Pietro, A.D. (2010). A Nitrogen Response Pathway Regulates Virulence Functions in *Fusarium oxysporum* via the Protein Kinase TOR and the bZIP Protein MeaB. Plant Cell *22*, 2459–2475.

Lu, J., Venäläinen, M., Julkunen-Tiitto, R., and Harju, A.M. (2015). Stilbene impregnation retards brown-rot decay of Scots pine sapwood. Holzforschung *70*, 261–266.

Lundell, T.K., Mäkelä, M.R., de Vries, R.P., and Hildén, K.S. (2014). Chapter Eleven - Genomics, Lifestyles and Future Prospects of Wood-Decay and Litter-Decomposing Basidiomycota. In Advances in Botanical Research, F.M. Martin, ed. (Academic Press), pp. 329–370.

Lyr, H. (1962). Detoxification of Heartwood Toxins and Chlorophenols by Higher Fungi. Nature *195*, 289–290.

Ma, B., Mayfield, M.B., and Gold, M.H. (2001). The Green Fluorescent Protein Gene Functions as a Reporter of Gene Expression in *Phanerochaete chrysosporium*. Appl Env. Microbiol *67*, 948–955.

MacDonald, J., Suzuki, H., and Master, E.R. (2012). Expression and regulation of genes encoding lignocellulose-degrading activity in the genus *Phanerochaete*. Appl. Microbiol. Biotechnol. *94*, 339–351.

MacRae, W.D., and Towers, G.H.N. (1984). Biological activities of lignans. Phytochemistry *23*, 1207–1220.

Maidan, M.M., Thevelein, J.M., and Van Dijck, P. (2005). Carbon source induced yeast-to-hypha transition in *Candida albicans* is dependent on the presence of amino acids and on the G-protein-coupled receptor Gpr1. Biochem. Soc. Trans. *33*, 291–293.

Manavalan, T., Manavalan, A., and Heese, K. (2015). Characterization of Lignocellulolytic Enzymes from White-Rot Fungi. Curr. Microbiol. *70*, 485–498.

Marat, A.L., Dokainish, H., and McPherson, P.S. (2011). DENN Domain Proteins: Regulators of Rab GTPases. J. Biol. Chem. *286*, 13791–13800.

Mark, R., Lyu, X., Lee, J.J.L., Parra-Saldívar, R., and Chen, W.N. (2019). Sustainable production of natural phenolics for functional food applications. J. Funct. Foods *57*, 233–254.

Marriott, P.E., Gómez, L.D., and McQueen-Mason, S.J. (2016). Unlocking the potential of lignocellulosic biomass through plant science. New Phytol. *209*, 1366–1381.

Marroquin-Guzman, M., and Wilson, R.A. (2015). GATA-Dependent Glutaminolysis Drives Appressorium Formation in *Magnaporthe oryzae* by Suppressing TOR Inhibition of cAMP/PKA Signaling. PLOS Pathog. *11*, e1004851.

Martín, J.F., van den Berg, M.A., Ver Loren van Themaat, E., and Liras, P. (2019). Sensing and transduction of nutritional and chemical signals in filamentous fungi: Impact on cell development and secondary metabolites biosynthesis. Biotechnol. Adv. *37*, 107392.

Martínez, A.T., Speranza, M., Ruiz-Dueñas, F.J., Ferreira, P., Camarero, S., Guillén, F., Martínez, M.J., Gutiérrez, A., and del Río, J.C. (2005). Biodegradation of lignocellulosics: microbial, chemical, and enzymatic aspects of the fungal attack of lignin. Int. Microbiol. Off. J. Span. Soc. Microbiol. *8*, 195–204.

Martinez, D., Larrondo, L.F., Putnam, N., Gelpke, M.D.S., Huang, K., Chapman, J., Helfenbein, K.G., Ramaiya, P., Detter, J.C., Larimer, F., et al. (2004a). Genome sequence of the lignocellulose degrading fungus *Phanerochaete chrysosporium* strain RP78. Nat. Biotechnol. *22*, 695–700.

Mascarenhas, C., Edwards-Ingram, L.C., Zeef, L., Shenton, D., Ashe, M.P., and Grant, C.M. (2008). Gcn4 Is Required for the Response to Peroxide Stress in the Yeast *Saccharomyces cerevisiae*. Mol. Biol. Cell *19*, 2995–3007.

Mathieu, Y., Prosper, P., Buée, M., Dumarçay, S., Favier, F., Gelhaye, E., Gérardin, P., Harvengt, L., Jacquot, J.-P., Lamant, T., et al. (2012). Characterization of a *Phanerochaete chrysosporium* Glutathione Transferase Reveals a Novel Structural and Functional Class with Ligandin Properties. J. Biol. Chem. *287*, 39001–39011.

Mathieu, Y., Prosper, P., Favier, F., Harvengt, L., Didierjean, C., Jacquot, J.-P., Morel-Rouhier, M., and Gelhaye, E. (2013). Diversification of Fungal Specific Class A Glutathione Transferases in Saprotrophic Fungi. PLOS ONE *8*, e80298.

McCotter, S.W., Horianopoulos, L.C., and Kronstad, J.W. (2016). Regulation of the fungal secretome. Curr. Genet. *62*, 533–545.

Meléndez, H.G., Billon-Grand, G., Fèvre, M., and Mey, G. (2009). Role of the *Botrytis cinerea* FKBP12 ortholog in pathogenic development and in sulfur regulation. Fungal Genet. Biol. *46*, 308–320.

Mendoza-Martínez, A.E., Cano-Domínguez, N., and Aguirre, J. (2019). Yap1 homologs mediate more than the redox regulation of the antioxidant response in filamentous fungi. Fungal Biol.

Meux, E., Morel, M., Lamant, T., Gérardin, P., Jacquot, J.-P., Dumarçay, S., and Gelhaye, E. (2013). New substrates and activity of *Phanerochaete chrysosporium* Omega glutathione transferases. Biochimie *95*, 336–346.

Mierziak, J., Kostyn, K., and Kulma, A. (2014). Flavonoids as Important Molecules of Plant Interactions with the Environment. Molecules *19*, 16240–16265.

MINAMI, M., SUZUKI, K., SHIMIZU, A., HONGO, T., SAKAMOTO, T., OHYAMA, N., KITAURA, H., KUSAKA, A., IWAMA, K., and IRIE, T. (2009). Changes in the Gene Expression of the White Rot Fungus *Phanerochaete chrysosporium* Due to the Addition of Atropine. Biosci. Biotechnol. Biochem. *73*, 1722–1731.

Monk, B.C., Tomasiak, T.M., Keniya, M.V., Huschmann, F.U., Tyndall, J.D.A., O'Connell, J.D., Cannon, R.D., McDonald, J.G., Rodriguez, A., Finer-Moore, J.S., et al. (2014). Architecture of a single membrane spanning cytochrome P450 suggests constraints that orient the catalytic domain relative to a bilayer. Proc. Natl. Acad. Sci. *111*, 3865–3870.

Morel, M., Ngadin, A.A., Jacquot, J.-P., and Gelhaye, E. (2009a). Chapter 6 Reactive Oxygen Species in *Phanerochaete chrysosporium* Relationship Between Extracellular Oxidative and Intracellular Antioxidant Systems. In Advances in Botanical Research, (Academic Press), pp. 153–186.

Morel, M., Ngadin, A.A., Droux, M., Jacquot, J.-P., and Gelhaye, E. (2009b). The fungal glutathione S-transferase system. Evidence of new classes in the wood-degrading basidiomycete *Phanerochaete chrysosporium*. Cell. Mol. Life Sci. CMLS *66*, 3711–3725.

Morel, M., Meux, E., Mathieu, Y., Thuillier, A., Chibani, K., Harvengt, L., Jacquot, J.-P., and Gelhaye, E. (2013). Xenomic networks variability and adaptation traits in wood decaying fungi. Microb. Biotechnol. *6*, 248–263.

Nagy, L.G., Riley, R., Bergmann, P.J., Krizsán, K., Martin, F.M., Grigoriev, I.V., Cullen, D., and Hibbett, D.S. (2017). Genetic Bases of Fungal White Rot Wood Decay Predicted by Phylogenomic Analysis of Correlated Gene-Phenotype Evolution. Mol. Biol. Evol. *34*, 35–44.

Nakatsukasa, K., Kanada, A., Matsuzaki, M., Byrne, S.D., Okumura, F., and Kamura, T. (2014). The Nutrient Stress-induced Small GTPase Rab5 Contributes to the Activation of Vesicle Trafficking and Vacuolar Activity. J. Biol. Chem. *289*, 20970–20978.

Nakazawa, T., Tsuzuki, M., Irie, T., Sakamoto, M., and Honda, Y. (2016). Marker recycling via 5-fluoroorotic acid and 5-fluorocytosine counter-selection in the white-rot agaricomycete *Pleurotus ostreatus*. Fungal Biol. *120*, 1146–1155.

Nakazawa, T., Izuno, A., Kodera, R., Miyazaki, Y., Sakamoto, M., Isagi, Y., and Honda, Y. (2017). Identification of two mutations that cause defects in the ligninolytic system through an efficient forward genetics in the white-rot agaricomycete *Pleurotus ostreatus*. Environ. Microbiol. *19*, 261–272.

Nerg, A.-M., Heijari, J., Noldt, U., Viitanen, H., Vuorinen, M., Kainulainen, P., and Holopainen, J.K. (2004). Significance of Wood Terpenoids in the Resistance of Scots Pine Provenances Against the Old House Borer, *Hylotrupes bajulus*, and Brown-Rot Fungus, *Coniophora puteana*. J. Chem. Ecol. *30*, 125–141.

Niamké, F.B., Amusant, N., Charpentier, J.-P., Chaix, G., Baissac, Y., Boutahar, N., Adima, A.A., Kati-Coulibaly, S., and Jay-Allemand, C. (2011). Relationships between biochemical attributes (non-structural carbohydrates and phenolics) and natural durability against fungi in dry teak wood (*Tectona grandis* L. f.). Ann. For. Sci. *68*, 201–211.

Niamké, F.B., Amusant, N., Stien, D., Chaix, G., Lozano, Y., Kadio, A.A., Lemenager, N., Goh, D., Adima, A.A., Kati-Coulibaly, S., et al. (2012). 4′,5′-Dihydroxy-epiisocatalponol, a new naphthoquinone from *Tectona grandis* L. f. heartwood, and fungicidal activity. Int. Biodeterior. Biodegrad. *74*, 93–98.

Niles, B.J., Joslin, A.C., Fresques, T., and Powers, T. (2014). TOR Complex 2-Ypk1 signaling maintains sphingolipid homeostasis by sensing and regulating ROS accumulation. Cell Rep. *6*, 541–552.

Noguchi, R., Banno, S., Ichikawa, R., Fukumori, F., Ichiishi, A., Kimura, M., Yamaguchi, I., and Fujimura, M. (2007). Identification of OS-2 MAP kinase-dependent genes induced in response to

osmotic stress, antifungal agent fludioxonil, and heat shock in *Neurospora crassa*. Fungal Genet. Biol. *44*, 208–218.

Nordström, K.J.V., Albani, M.C., James, G.V., Gutjahr, C., Hartwig, B., Turck, F., Paszkowski, U., Coupland, G., and Schneeberger, K. (2013). Mutation identification by direct comparison of whole-genome sequencing data from mutant and wild-type individuals using k -mers. Nat. Biotechnol. *31*, 325–330.

O'Brien, H.E., Parrent, J.L., Jackson, J.A., Moncalvo, J.-M., and Vilgalys, R. (2005). Fungal Community Analysis by Large-Scale Sequencing of Environmental Samples. Appl. Environ. Microbiol. *71*, 5544–5550.

Odds, F.C., Brown, A.J.P., and Gow, N.A.R. (2003). Antifungal agents: mechanisms of action. Trends Microbiol. *11*, 272–279.

Ogawa, S., Matsuo, Y., Tanaka, T., Yazaki, Y., Ogawa, S., Matsuo, Y., Tanaka, T., and Yazaki, Y. (2018). Utilization of Flavonoid Compounds from Bark and Wood. III. Application in Health Foods. Molecules *23*, 1860.

Ohm, R.A., Riley, R., Salamov, A., Min, B., Choi, I.-G., and Grigoriev, I.V. (2014). Genomics of wood-degrading fungi. Fungal Genet. Biol. *72*, 82–90.

Ohmura, W., Doi, S., Aoyama, M., and Ohara, S. (2000). Antifeedant activity of flavonoids and related compounds against the subterranean termite *Coptotermes formosanus* Shiraki. J. Wood Sci. *46*, 149–153.

Otsubo, Y., and Yamamoto, M. (2010). 12 - TOR and Sexual Development in Fission Yeast. In The Enzymes, (Academic Press), pp. 229–250.

Pan, J.-Y., Chen, S.-L., Yang, M.-H., Wu, J., Sinkkonen, J., and Zou, K. (2009). An update on lignans: natural products and synthesis. Nat. Prod. Rep. *26*, 1251–1292.

Paoletti, M., and Clavé, C. (2007). The Fungus-Specific HET Domain Mediates Programmed Cell Death in *Podospora anserina*. Eukaryot. Cell *6*, 2001–2008.

Park, G., Servin, J.A., Turner, G.E., Altamirano, L., Colot, H.V., Collopy, P., Litvinkova, L., Li, L., Jones, C.A., Diala, F.-G., et al. (2011). Global Analysis of Serine-Threonine Protein Kinase Genes in *Neurospora crassa*. Eukaryot. Cell *10*, 1553–1564.

Paul, S., Doering, T.L., and Moye-Rowley, W.S. (2015). *Cryptococcus neoformans* Yap1 is required for normal fluconazole and oxidative stress resistance. Fungal Genet. Biol. *74*, 1–9.

Pereira H, Graça J, and Rodrigues JC (2009). Wood chemistry in relation to quality. In Wood Quality and Its Biological Basis, (Blackwell & CRC Press, London & Boca Raton, FL), pp. 53–56.

Perrot, T., Schwartz, M., Saiag, F., Salzet, G., Dumarçay, S., Favier, F., Gérardin, P., Girardet, J.-M., Sormani, R., Morel-Rouhier, M., et al. (2018). Fungal Glutathione Transferases as Tools to Explore the Chemical Diversity of Amazonian Wood Extractives. ACS Sustain. Chem. Eng. *6*, 13078–13085.

Pfirrmann, T., Heessen, S., Omnus, D.J., Andréasson, C., and Ljungdahl, P.O. (2010). The Prodomain of Ssy5 Protease Controls Receptor-Activated Proteolysis of Transcription Factor Stp1. Mol. Cell. Biol. *30*, 3299–3309.

Pietarinen, S.P., Willför, S.M., Vikström, F.A., and Holmbom, B.R. (2006). Aspen Knots, a Rich Source of Flavonoids. J. Wood Chem. Technol. *26*, 245–258.

Pinan-Lucarré, B., Iraqui, I., and Clavé, C. (2006). *Podospora anserina* target of rapamycin. Curr. Genet. *50*, 23–31.

Polish, J.A., Kim, J.-H., and Johnston, M. (2005). How the Rgt1 Transcription Factor of *Saccharomyces cerevisiae* Is Regulated by Glucose. Genetics *169*, 583–594.

Qian, B., Liu, X., Jia, J., Cai, Y., Chen, C., Zhang, H., Zheng, X., Wang, P., and Zhang, Z. (2018). MoPpe1 partners with MoSap1 to mediate TOR and cell wall integrity signalling in growth and pathogenicity of the rice blast fungus *Magnaporthe oryzae*. Environ. Microbiol. *20*, 3964–3979.

Ralph, J., Lapierre, C., and Boerjan, W. (2019). Lignin structure and its engineering. Curr. Opin. Biotechnol. *56*, 240–249.

Ramanujam, R., Calvert, M.E., Selvaraj, P., and Naqvi, N.I. (2013). The Late Endosomal HOPS Complex Anchors Active G-Protein Signaling Essential for Pathogenesis in *Magnaporthe oryzae*. PLOS Pathog. *9*, e1003527.

Ratnayake, L., Adhvaryu, K.K., Kafes, E., Motavaze, K., and Lakin-Thomas, P. (2018). A component of the TOR (Target Of Rapamycin) nutrient-sensing pathway plays a role in circadian rhythmicity in *Neurospora crassa*. PLOS Genet. *14*, e1007457.

Ren, P., Rossettini, A., Chaturvedi, V., and Hanes, S.D. (2005). The Ess1 prolyl isomerase is dispensable for growth but required for virulence in *Cryptococcus neoformans*. Microbiology, *151*, 1593–1605.

Ries, L.N.A., Beattie, S.R., Espeso, E.A., Cramer, R.A., and Goldman, G.H. (2016). Diverse Regulation of the CreA Carbon Catabolite Repressor in *Aspergillus nidulans*. Genetics *203*, 335–352.

Riley, R., Salamov, A.A., Brown, D.W., Nagy, L.G., Floudas, D., Held, B.W., Levasseur, A., Lombard, V., Morin, E., Otillar, R., et al. (2014). Extensive sampling of basidiomycete genomes demonstrates inadequacy of the white-rot/brown-rot paradigm for wood decay fungi. Proc. Natl. Acad. Sci. *111*, 9923–9928.

Rodríguez, A.R., Koch, G., Richter, H.-G., Fuentes, T.F.J., Silva, G.J.A., and Satyanarayana, K.G. (2019). Formation of heartwood, chemical composition of extractives and natural durability of plantation-grown teak wood from Mexico. Holzforschung *73*, 547–557.

Rodríguez-Romero, J., Hedtke, M., Kastner, C., Mueller, S., and Fischer, R. (2010). Fungi, hidden in soil or up in the air: light makes a difference. Annu. Rev. Microbiol. *64*, 585–610.

Roelants, F.M., Leskoske, K.L., Martinez Marshall, M.N., Locke, M.N., and Thorner, J. (2017). The TORC2-Dependent Signaling Network in the Yeast *Saccharomyces cerevisiae*. Biomolecules *7*, 66.

Rohlfs, M., Albert, M., Keller, N.P., and Kempken, F. (2007). Secondary chemicals protect mould from fungivory. Biol. Lett. *3*, 523–525.

Royer, M., Rodrigues, A.M.S., Herbette, G., Beauchêne, J., Chevalier, M., Hérault, B., Thibaut, B., and Stien, D. (2012). Efficacy of *Bagassa guianensis* Aubl. extract against wood decay and human pathogenic fungi. Int. Biodeterior. Biodegrad. *70*, 55–59.

Rutherford, J.C., Bahn, Y.-S., van den Berg, B., Heitman, J., and Xue, C. (2019). Nutrient and Stress Sensing in Pathogenic Yeasts. Front. Microbiol. *10*.

Saijo, H., Kofujita, H., Takahashi, K., and Ashitani, T. (2015). Antioxidant activity and mechanism of the abietane-type diterpene ferruginol. Nat. Prod. Res. *29*, 1739–1743.

Sanchez, N.E., Harty, B.L., O'Reilly-Pol, T., Ackerman, S.D., Herbert, A.L., Holmgren, M., Johnson, S.L., Gray, R.S., and Monk, K.R. (2017). Whole Genome Sequencing-Based Mapping and Candidate Identification of Mutations from Fixed Zebrafish Tissue. G3 Genes Genomes Genet. *7*, 3415–3425.

Sang, H., Hulvey, J.P., Green, R., Xu, H., Im, J., Chang, T., and Jung, G. (2018). A Xenobiotic Detoxification Pathway through Transcriptional Regulation in Filamentous Fungi. mBio *9*, e00457-18.

Saupe, S., Turcq, B., and Bégueret, J. (1995). A gene responsible for vegetative incompatibility in the fungus Podospora anserina encodes a protein with a GTP-binding motif and Gβ homologous domain. Gene *162*, 135–139.

Scalbert, A. (1991). Antimicrobial properties of tannins. Phytochemistry *30*, 3875–3883.

Scalbert, A. (1992). Tannins in Woods and Their Contribution to Microbial Decay Prevention. In Plant Polyphenols: Synthesis, Properties, Significance, R.W. Hemingway, and P.E. Laks, eds. (Boston, MA: Springer US), pp. 935–952.

Schlötterer, C., Tobler, R., Kofler, R., and Nolte, V. (2014). Sequencing pools of individuals — mining genome-wide polymorphism data without big funding. Nat. Rev. Genet. *15*, 749–763.

Schneeberger, K. (2014). Using next-generation sequencing to isolate mutant genes from forward genetic screens. Nat. Rev. Genet. *15*, 662–676.

Schneeberger, K., and Weigel, D. (2011). Fast-forward genetics enabled by new sequencing technologies. Trends Plant Sci. *16*, 282–288.

Schultz, T.P., and Nicholas, D.D. (2000). Naturally durable heartwood: evidence for a proposed dual defensive function of the extractives. Phytochemistry *54*, 47–52.

Schultz, T.P., and Nicholas, D.D. (2002). Development of environmentally-benign wood preservatives based on the combination of organic biocides with antioxidants and metal chelators. Phytochemistry *61*, 555–560.

Schultz, T.P., Hubbard, T.F., Jin, L., Fisher, T.H., and Nicholas, D.D. (1990). Role of stilbenes in the natural durability of wood: Fungicidal structure-activity relationships. Phytochemistry *29*, 1501–1507.

Sehgal, S.N., Baker, H., and Vézina, C. (1975). Rapamycin (AY-22,989), a new antifungal antibiotic. II. Fermentation, isolation and characterization. J. Antibiot. (Tokyo) *28*, 727–732.

Sekine, N., Ashitani, T., Murayama, T., Shibutani, S., Hattori, S., and Takahashi, K. (2009). Bioactivity of Latifolin and Its Derivatives against Termites and Fungi. J. Agric. Food Chem. *57*, 5707–5712.

Sharma, K.K., and Kuhad, R.C. (2010). Genetic transformation of lignin degrading fungi facilitated by *Agrobacterium tumefaciens*. BMC Biotechnol. *10*, 67.

Shashkova, S., Welkenhuysen, N., and Hohmann, S. (2015). Molecular communication: crosstalk between the Snf1 and other signaling pathways. FEMS Yeast Res. *15*.

Shen, G., and Kong, A.-N. (2009). Nrf2 plays an important role in coordinated regulation of Phase II drug metabolism enzymes and Phase III drug transporters. Biopharm. Drug Dispos. *30*, 345–355.

Shen, T., Wang, X.-N., and Lou, H.-X. (2009). Natural stilbenes: an overview. Nat. Prod. Rep. *26*, 916–935.

Shertz, C.A., Bastidas, R.J., Li, W., Heitman, J., and Cardenas, M.E. (2010). Conservation, duplication, and loss of the Tor signaling pathway in the fungal kingdom. BMC Genomics *11*, 510.

Shin, C.-S., Kim, S.Y., and Huh, W.-K. (2009). TORC1 controls degradation of the transcription factor Stp1, a key effector of the SPS amino-acid-sensing pathway in *Saccharomyces cerevisiae*. J. Cell Sci. *122*, 2089–2099.

Shnaiderman, C., Miyara, I., Kobiler, I., Sherman, A., and Prusky, D. (2013). Differential Activation of Ammonium Transporters During the Accumulation of Ammonia by *Colletotrichum gloeosporioides* and Its Effect on Appressoria Formation and Pathogenicity. Mol. Plant. Microbe Interact. *26*, 345–355.

Simaan, H., Lev, S., and Horwitz, B.A. (2019). Oxidant-Sensing Pathways in the Responses of Fungal Pathogens to Chemical Stress Signals. Front. Microbiol. *10*.

Singh, B., and Sharma, R.A. (2015). Plant terpenes: defense responses, phylogenetic analysis, regulation and clinical applications. 3 Biotech *5*, 129–151.

Singh, T., and Singh, A.P. (2012). A review on natural products as wood protectant. Wood Sci. Technol. *46*, 851–870.

Sionov, E., Chang, Y.C., Garraffo, H.M., Dolan, M.A., Ghannoum, M.A., and Kwon-Chung, K.J. (2012). Identification of a Cryptococcus neoformans Cytochrome P450 Lanosterol 14α-Demethylase (Erg11) Residue Critical for Differential Susceptibility between Fluconazole/Voriconazole and Itraconazole/Posaconazole. Antimicrob. Agents Chemother. *56*, 1162–1169.

Smith, D.A., Morgan, B.A., and Quinn, J. (2010). Stress signalling to fungal stress-activated protein kinase pathways. FEMS Microbiol. Lett. *306*, 1–8.

Snyman, C., Theron, L., and Divol, B. (2019). Understanding the regulation of extracellular protease gene expression in fungi: a key step towards their biotechnological applications. Appl. Microbiol. Biotechnol. *103*, 5517–5532.

Souza, W.R. de, Morais, E.R., Krohn, N.G., Savoldi, M., Goldman, M.H.S., Rodrigues, F., Caldana, C., Semelka, C.T., Tikunov, A.P., Macdonald, J.M., et al. (2013). Identification of Metabolic Pathways Influenced by the G-Protein Coupled Receptors GprB and GprD in Aspergillus nidulans. PLOS ONE *8*, e62088.

Spencer, C.M., Cai, Y., Martin, R., Gaffney, S.H., Goulding, P.N., Magnolato, D., Lilley, T.H., and Haslam, E. (1988). Polyphenol complexation—some thoughts and observations. Phytochemistry *27*, 2397–2409.

Steinberg, G. (2007). Hyphal Growth: a Tale of Motors, Lipids, and the Spitzenkörper. Eukaryot. Cell *6*, 351–360.

Stewart, P., Gaskell, J., and Cullen, D. (2000). A Homokaryotic Derivative of a *Phanerochaete chrysosporium* Strain and Its Use in Genomic Analysis of Repetitive Elements. Appl Env. Microbiol *66*, 1629–1633.

Stracka, D., Jozefczuk, S., Rudroff, F., Sauer, U., and Hall, M.N. (2014). Nitrogen Source Activates TOR (Target of Rapamycin) Complex 1 via Glutamine and Independently of Gtr/Rag Proteins. J. Biol. Chem. *289*, 25010–25020.

Sun, H., and Schneeberger, K. (2015). SHOREmap v3.0: Fast and Accurate Identification of Causal Mutations from Forward Genetic Screens. In Plant Functional Genomics: Methods and Protocols, J.M. Alonso, and A.N. Stepanova, eds. (New York, NY: Springer New York), pp. 381–395.

Sun, J., and Glass, N.L. (2011). Identification of the CRE-1 Cellulolytic Regulon in *Neurospora crassa*. PLOS ONE *6*, e25654.

Syed, K., and Yadav, J.S. (2012). P450 monooxygenases (P450ome) of the model white rot fungus *Phanerochaete chrysosporium*. Crit. Rev. Microbiol. *38*, 339–363.

Syed, K., Shale, K., Pagadala, N.S., and Tuszynski, J. (2014). Systematic Identification and Evolutionary Analysis of Catalytically Versatile Cytochrome P450 Monooxygenase Families Enriched in Model Basidiomycete Fungi. PLOS ONE *9*, e86683.

Tan, Z., Huang, M., Puga, A., and Xia, Y. (2004). A Critical Role For MAP Kinases in the Control of Ah Receptor Complex Activity. Toxicol. Sci. *82*, 80–87.

Tayeb, A.H., Amini, E., Ghasemi, S., and Tajvidi, M. (2018). Cellulose Nanomaterials—Binding Properties and Applications: A Review. Molecules *23*, 2684.

Taylor, A.M., Gartner, B.L., and Morrell, J.J. (2007). Heartwood Formation and Natural Durability—A Review. Wood Fiber Sci. *34*, 587–611.

Teichert, S., Wottawa, M., Schönig, B., and Tudzynski, B. (2006). Role of the *Fusarium fujikuroi* TOR Kinase in Nitrogen Regulation and Secondary Metabolism. Eukaryot. Cell *5*, 1807–1819.

Teichert, S., Rutherford, J.C., Wottawa, M., Heitman, J., and Tudzynski, B. (2008). Impact of Ammonium Permeases MepA, MepB, and MepC on Nitrogen-Regulated Secondary Metabolism in *Fusarium fujikuroi*. Eukaryot. Cell *7*, 187–201.

Thevelein, J.M., Geladé, R., Holsbeeks, I., Lagatie, O., Popova, Y., Rolland, F., Stolz, F., Van de Velde, S., Van Dijck, P., Vandormael, P., et al. (2005). Nutrient sensing systems for rapid activation of the protein kinase A pathway in yeast. Biochem. Soc. Trans. *33*, 253–256.

Tholl, D. (2015). Biosynthesis and Biological Functions of Terpenoids in Plants. In Biotechnology of Isoprenoids, J. Schrader, and J. Bohlmann, eds. (Cham: Springer International Publishing), pp. 63–106.

Thuillier, A., Chibani, K., Belli, G., Herrero, E., Dumarçay, S., Gérardin, P., Kohler, A., Deroy, A., Dhalleine, T., Bchini, R., et al. (2014). Transcriptomic Responses of *Phanerochaete chrysosporium*

to Oak Acetonic Extracts: Focus on a New Glutathione Transferase. Appl Env. Microbiol *80*, 6316–6327.

Tien, M., and Kirk, T.K. (1983). Lignin-Degrading Enzyme from the Hymenomycete *Phanerochaete chrysosporium* Burds. Science *221*, 661–663.

Tien, M., and Kirk, T.K. (1984). Lignin-degrading enzyme from *Phanerochaete chrysosporium*: Purification, characterization, and catalytic properties of a unique H2O2-requiring oxygenase. Proc. Natl. Acad. Sci. *81*, 2280–2284.

Tien, M., and Myer, S.B. (1990). Selection and characterization of mutants of *Phanerochaete chrysosporium* exhibiting ligninolytic activity under nutrient-rich conditions. Appl. Environ. Microbiol. *56*, 2540–2544.

Treitel, M.A., and Carlson, M. (1995). Repression by SSN6-TUP1 is directed by MIG1, a repressor/activator protein. Proc. Natl. Acad. Sci. *92*, 3132–3136.

Uehling, J., Deveau, A., and Paoletti, M. (2017). Do fungi have an innate immune response? An NLR-based comparison to plant and animal immune systems. PLOS Pathog. *13*, e1006578.

Uemura, T., Kashiwagi, K., and Igarashi, K. (2005). Uptake of putrescine and spermidine by Gap1p on the plasma membrane in *Saccharomyces cerevisiae*. Biochem. Biophys. Res. Commun. *328*, 1028–1033.

Ukai, Y., Kuroiwa, M., Kurihara, N., Naruse, H., Homma, T., Maki, H., and Naito, A. (2018). Contributions of yap1 Mutation and Subsequent atrF Upregulation to Voriconazole Resistance in *Aspergillus flavus*. Antimicrob. Agents Chemother. *62*.

Urban, J., Soulard, A., Huber, A., Lippman, S., Mukhopadhyay, D., Deloche, O., Wanke, V., Anrather, D., Ammerer, G., Riezman, H., et al. (2007). Sch9 is a major target of TORC1 in *Saccharomyces cerevisiae*. Mol. Cell *26*, 663–674.

Valette, N., Perrot, T., Sormani, R., Gelhaye, E., and Morel-Rouhier, M. (2017). Antifungal activities of wood extractives. Fungal Biol. Rev. *31*, 113–123.

Van der Nest, M.A., Olson, Å., Lind, M., Vélëz, H., Dalman, K., Durling, M.B., Karlsson, M., and Stenlid, J. (2014). Distribution and evolution of het gene homologs in the basidiomycota. Fungal Genet. Biol. *64*, 45–57.

Vanholme, R., Demedts, B., Morreel, K., Ralph, J., and Boerjan, W. (2010). Lignin Biosynthesis and Structure. Plant Physiol. *153*, 895–905.

Vasiliauskas, R., Menkis, A., Finlay, R.D., and Stenlid, J. (2007). Wood-decay fungi in fine living roots of conifer seedlings. New Phytol. *174*, 441–446.

Venäläinen, M., Harju, A.M., Saranpää, P., Kainulainen, P., Tiitta, M., and Velling, P. (2004). The concentration of phenolics in brown-rot decay resistant and susceptible Scots pine heartwood. Wood Sci. Technol. *38*, 109–118.

Wang, S.-Y., Wu, J.-H., Shyur, L.-F., Kuo, Y.-H., and Chang, S.-T. (2005). Antioxidant Activity of Abietane-Type Diterpenes from Heartwood of *Taiwania cryptomerioides* Hayata. Holzforschung *56*, 487–492.

Wariishi, H., Valli, K., and Gold, M.H. (1991). In vitro depolymerization of lignin by manganese peroxidase of *Phanerochaete chrysosporium*. Biochem. Biophys. Res. Commun. *176*, 269–275.

Warrilow, A., Ugochukwu, C., Lamb, D., Kelly, D., and Kelly, S. (2008). Expression and Characterization of CYP51, the Ancient Sterol 14-demethylase Activity for Cytochromes P450 (CYP), in the White-Rot Fungus *Phanerochaete chrysosporium*. Lipids *43*, 1143.

Weisman, R., and Choder, M. (2001). The fission yeast TOR homolog, tor1+, is required for the response to starvation and other stresses via a conserved serine. J. Biol. Chem. *276*, 7027–7032.

Wiatrowski, H.A., and Carlson, M. (2003). Yap1 Accumulates in the Nucleus in Response to Carbon Stress in *Saccharomyces cerevisiae*. Eukaryot. Cell *2*, 19–26.

Willför, S., Hemming, J., Reunanen, M., Eckerman, C., and Holmbom, B. (2005). Lignans and Lipophilic Extractives in Norway Spruce Knots and Stemwood. Holzforschung *57*, 27–36.

Winkel-Shirley, B. (2001). Flavonoid Biosynthesis. A Colorful Model for Genetics, Biochemistry, Cell Biology, and Biotechnology. Plant Physiol. *126*, 485–493.

Wong, D.W.S. (2009). Structure and Action Mechanism of Ligninolytic Enzymes. Appl. Biochem. Biotechnol. *157*, 174–209.

Wullschleger, S., Loewith, R., and Hall, M.N. (2006). TOR Signaling in Growth and Metabolism. Cell *124*, 471–484.

Xiao, Q., Ma, F., Li, Y., Yu, H., Li, C., and Zhang, X. (2017). Differential Proteomic Profiles of *Pleurotus ostreatus* in Response to Lignocellulosic Components Provide Insights into Divergent Adaptive Mechanisms. Front. Microbiol. *8*.

Xiong, Y., Coradetti, S.T., Li, X., Gritsenko, M.A., Clauss, T., Petyuk, V., Camp, D., Smith, R., Cate, J.H.D., Yang, F., et al. (2014). The proteome and phosphoproteome of *Neurospora crassa* in response to cellulose, sucrose and carbon starvation. Fungal Genet. Biol. *72*, 21–33.

Xue, C., Bahn, Y.-S., Cox, G.M., and Heitman, J. (2005). G Protein-coupled Receptor Gpr4 Senses Amino Acids and Activates the cAMP-PKA Pathway in *Cryptococcus neoformans*. Mol. Biol. Cell *17*, 667–679.

Yazaki, Y. (2015). Utilization of flavonoid compounds from bark and wood: a review. Nat. Prod. Commun. *10*, 513–520.

Yelle, D.J., Ralph, J., Lu, F., and Hammel, K.E. (2008). Evidence for cleavage of lignin by a brown rot basidiomycete. Environ. Microbiol. *10*, 1844–1849.

Young RA and Akhtar M (1998). Taxonomy of Industrially Important White-Rot Fungi. In Environmentally friendly technologies for the pulp and paper industry. Wiley, New York, pp. 259 -272.

Yu, F., Gu, Q., Yun, Y., Yin, Y., Xu, J.-R., Shim, W.-B., and Ma, Z. (2014). The TOR signaling pathway regulates vegetative development and virulence in *Fusarium graminearum*. New Phytol. *203*, 219–232.

Yun, C.-W., Tamaki, H., Nakayama, R., Yamamoto, K., and Kumagai, H. (1998). Gpr1p, a Putative G-Protein Coupled Receptor, Regulates Glucose-Dependent Cellular cAMP Level in Yeast *Saccharomyces cerevisiae*. Biochem. Biophys. Res. Commun. *252*, 29–33.

Zaman, S., Lippman, S.I., Zhao, X., and Broach, J.R. (2008). How *Saccharomyces* Responds to Nutrients. Annu. Rev. Genet. *42*, 27–81.

Zeilinger, S., Schmoll, M., Pail, M., Mach, R.L., and Kubicek, C.P. (2003). Nucleosome transactions on the *Hypocrea jecorina* (*Trichoderma reesei*) cellulase promoter cbh2 associated with cellulase induction. Mol. Genet. Genomics MGG *270*, 46–55.

Zhang, J., Vaga, S., Chumnanpuen, P., Kumar, R., Vemuri, G.N., Aebersold, R., and Nielsen, J. (2011). Mapping the interaction of Snf1 with TORC1 in *Saccharomyces cerevisiae*. Mol. Syst. Biol. *7*, 545.

Zhang, L., Huang, M., and Harsay, E. (2010). A Chemical Genetic Screen for Modulators of Exocytic Transport Identifies Inhibitors of a Transport Mechanism Linked to GTR2 Function. Eukaryot. Cell *9*, 116–126.

Zhang, W., Kou, Y., Xu, J., Cao, Y., Zhao, G., Shao, J., Wang, H., Wang, Z., Bao, X., Chen, G., et al. (2013). Two Major Facilitator Superfamily Sugar Transporters from *Trichoderma reesei* and Their Roles in Induction of Cellulase Biosynthesis. J. Biol. Chem. *288*, 32861–32872.

Zheng, X.-F., Fiorentino, D., Chen, J., Crabtree, G.R., and Schreiber, S.L. (1995). TOR kinase domains are required for two distinct functions, only one of which is inhibited by rapamycin. Cell *82*, 121–130.

Znameroski, E.A., Li, X., Tsai, J.C., Galazka, J.M., Glass, N.L., and Cate, J.H.D. (2014). Evidence for Transceptor Function of Cellodextrin Transporters in *Neurospora crassa*. J. Biol. Chem. *289*, 2610–2619.

Zurita-Martinez, S.A., and Cardenas, M.E. (2005). Tor and Cyclic AMP-Protein Kinase A: Two Parallel Pathways Regulating Expression of Genes Required for Cell Growth. Eukaryot. Cell *4*, 63–71.

Zuryn, S., Gras, S.L., Jamet, K., and Jarriault, S. (2010). A Strategy for Direct Mapping and Identification of Mutations by Whole-Genome Sequencing. Genetics *186*, 427–430.

Résumé : Les champignons lignivores sont des organismes qui utilisent les composants du bois, la cellulose, les hémicelluloses et la lignine comme sources de carbone et d'énergie. Cependant, les processus oxydatifs utilisés par ces champignons pour décomposer le bois libèrent une myriade de molécules potentiellement toxiques, les extractibles. Ces extractibles sont des composants non structurels du bois. Ils sont responsables des propriétés du bois telles que sa couleur, son odeur et sa durabilité car ils peuvent avoir des propriétés antifongiques.

Pour s'adapter à cet environnement toxique, les champignons responsables de la décomposition du bois ont développé diverses stratégies de détoxication des molécules antifongiques. Afin d'étudier cette détoxication, nous avons développé une stratégie de génétique directe chez le champignon modèle *Phanerochaete chrysosporium*. Après avoir réalisé des mutagènèses aux UV, des mutants résistants à deux molécules, l'itraconazole et la rapamycine, antifongiques aux mécanismes d'action connus ont été sélectionnés et caractérisés. De même, des extractibles provenant de deux essences de bois (*Bagassa guianensis* et *Prunus avium*) et présentant des activités antifongiques ont également été utilisés pour produire deux collections de mutants résistants à ces extractibles. Ces mutants ont été partiellement caractérisés ouvrant ainsi la voie à une meilleure compréhension des systèmes impliqués dans la détoxication des extractibles.

La possibilité de réaliser de telles études chez les champignons lignivores ouvre de nouvelles perspectives. En effet, ces champignons suscitent un intérêt croissant ces dernières années, principalement en raison de leur utilisation potentielle dans la valorisation de la biomasse afin de produire des biocarburants, de leur fonction importante dans le cycle global du carbone mais également en raison des dommages qu'ils peuvent causer au matériau bois.

Mots clés: *Phanerochaete chrysosporium*, extractibles de bois, rapamycine

Abstract: Ligninolytic fungi are wood-degrading organisms that use cellulose, hemicelluloses, and lignin as sources of carbon and energy. However, the oxidative processes used by these fungi to decompose wood release a myriad of potentially toxic extractable molecules. These extractives are non-structural components of wood. They are involved in wood properties such as color, odor, and natural durability as they have antifungal properties.

In order to adapt to this toxic environment, the fungi which are responsible for decomposing wood have developed various strategies to detoxify the antifungal molecules. In order to study this detoxification, we have developed a direct genetic strategy in *Phanerochaete chrysosporium* known as the wood-decomposing fungus model. After performing UV mutagenesis, screens allowing the identification of fungal strains resistant to different antifungal agents were carried out. Two selected molecules, including itraconazole and rapamycin with known mechanisms of antifungal action, made it possible to obtain two first mutant collections that were characterized. Next, extractives from two wood species (*Bagassa guianensis* and *Prunus avium*) with antifungal activities were used to produce two collections of mutants resistant to these extractives. The characterization of these mutants should allow us to understand why these extractives are toxic and how the fungus is able to detoxify them.

The possibility of occurring studies on ligninolytic fungi opens new perspectives. Indeed, these fungi have been the subject of growing interest in recent years, mainly because of their potential use in the valorization of biomass to produce biofuels, their important function in the global carbon cycle, and also because of their wood material damage.

Keywords: *Phanerochaete chrysosporium*, wood extractives, rapamycin